SURFACE MODIFICATION OF DIENE ELASTOMERS VIA RADIATION GRAFTING OF FUNCTIONAL MONOMERS

A Thesis submitted to the

UNIVERISTY OF PUNE

for the degree of

DOCTOR OF PHILOSOPHY

in

CHEMISTRY

by

SHROJAL MOHITKUMAR DESAI

Division of Polymer Chemistry
National Chemical Laboratory
Pune – 411008, India

July 2002

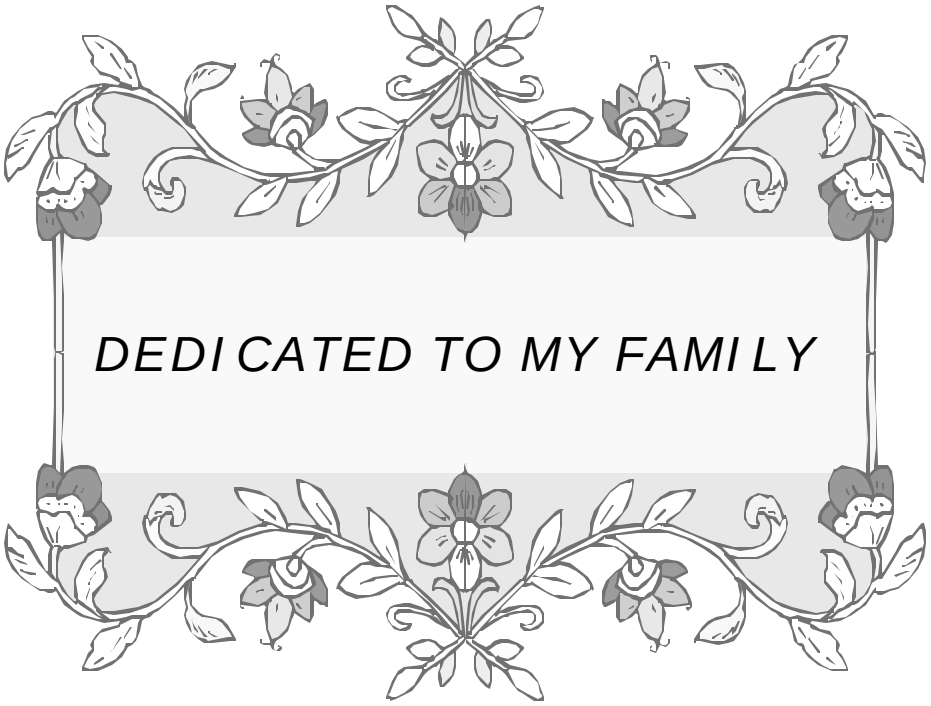
DEDICATED TO MY FAMILY

MAA KRIPA

DECLARATION

Certified that the work incorporated in thesis **"Surface Modification of Diene Elastomers via Radiation Grafting of Functional Monomers"** submitted by Mr. Shrojal Mohitkumar Desai was carried out by the candidate under my supervision. Such material as has been obtained from other source has been duly acknowledged.

(R. P. Singh)
Research guide

ABSTRACT

This thesis presents the results of the surface modification study of the elastomers that have been feebly addressed. Our study was mainly focused on the surface modification using mild techniques viz. photo-grafting and plasma-grafting. The influence of surface modification on the properties of elastomers was deduced from their dyeability, biocompatibility and photo-stability. The influence of various reaction parameters on the surface grafting efficiency has been thoroughly investigated. Amongst the monomers studied, the reactivity was in the order HEMA > AA > GMA > AAm > NVP. Other reaction parameters also have a significant influence on the photo-grafting efficiency. A favorable effect of elevated reaction temperature (i.e. 50 ºC) was observed for low reactivity monomers like NVP whereas highly reactive monomers like HEMA produced thick grafted layer of approximately 5 microns. When surface grafting was carried out using reactive monomers at elevated temperature, subsequent homopolymerization also took place, which is the primary shortcoming of photografting technique. By using the multi functional acrylates, homopolymer formation was substantially reduced. Solvent with high chain transfer constant did not offer good grafting efficacy. Acetone for this purpose is the most suitable solvent. Interestingly, we found that additions of a small amount of H-donating solvent, toluene in our case, significantly reduced the homopolymerization and facilitated efficient surface grafting. Amongst the photoinitiators employed, the efficacy was in the order XT > BP > Bz > BPO > AIBN. The degree of grafting also increased linearly with the increase in the reaction time but only upto a critical point, beyond which it either leveled off or decreased. The modifications attained at the elastomer surfaces were substantiated using different surface sensitive analytical techniques like contact angle measurement, ATR-FTIR, XPS, AFM, SEM and Optical microscopy. The biocompatibility of the surface modified films was examined by *in vitro* human cell adhesion tests.

Another technique that was utilized for achieving surface functionality was plasma induced surface modification. The surfaces of the elastomers were modified by plasma treatment and plasma induced grafting. Oxygen and carbon dioxide were used as reactive gases to generate functional groups onto the surface of elastomer films. It was found that the oxygen plasma treated films generated hydroxy/ hydroperoxy groups, along with a small amount of carbonyl functionalities whereas the carbon dioxide plasma treated films predominantly produced carbonyl and carboxyl species on the modified surfaces. The plasma treatment conditions and reaction parameters greatly influence the degree of surface modification. The substrates PP, PE, EPDM, SBS and SR were taken up for these studies. It

was found that the hydrophilicity of the plasma treated films increased with an increase in the plasma power and plasma treatment time upto a critical point. Treatment at high plasma power and treatment time led to a loss in the attained hydrophilicity. Moreover, it was also observed that the functionality attained at the air polymer interface is lost with the storage time. The mechanism for this behavior has been discussed in details and hypothesis being proposed. The orientation of the functional groups towards the subsurface was very fast in elastomers compared to other thermoplastics. Moreover, upon hydrating the elastomer surface, the lost hydrophilicity is readily retained. Thus, this orientation and reorientation process is very fast in the elastomers. From our study, we learnt that the presence of surface cross-links hinders the migration/orientation of the functional groups. We utilized this demerit of cross-linked surfaces to achieve long-term hydrophilic surfaces by deliberately cross-linking functional monomers with functional cross-linkers onto the surface of EPDM films under the influence of oxygen plasma.

The application of the modified surfaces was determined by performing the biocompatibility tests. The surface hydrophilicity and functionality were found to play major role in determining the biocompatibility of the polymer films. The type of functional groups implanted also determined the success of the bio-material. The non-homogeneously grafted films led to poor cell adhesion. In the present study we have also synthesized some novel vinylic stabilizers and evaluated their photostability against conventional melt blended stabilizers by grafting them onto the surface of PP, PE and SBS films. It was found that the PMPA, a vinylic HALS, performs best, when located at the surface of polymer film. This is for the reason that degradation of any polymer initiates from the surface and proceeds into the matrix. Photostabilizer, when located at the surface, effectively retards the degradation process. It is well known that polymers with hydrocarbon backbone are highly hydrophobic and difficult to stain but we could attain a very good dyeability of these polymer surfaces after surface modification. Thus, our work focuses on both fundamental and applied aspects of surface chemistry.

ABBREVIATIONS

Å	Angstrom
θ	Contact angle
λ	Wavelength
AA	Acrylic acid
AAm	Acrylamide
AFM	Atomic force microscopy
AIBN	Azo bis(isobutyro nitrile)
ATR-FT-IR	Attenuated total refraction Fourier Transform Infrared
BP	Benzophenone
BPO	Benzoyl peroxide
cm^{-1}	Wavenumber
EDX	Energy-dispersive X-ray spectroscopy
EGDMA	Ethylene glycol dimethacrylate
EPDM	Ethylene propylene diene elastomer
EPR	Ethylene propylene rubber
ESCA	Electron spectroscopy for chemical analysis
EVA	Ethyl vinyl alcohol
GMA	Glycidyl methacrylate
HALS	Hindered amine light stabilizer
HEMA	Hydroxy ethyl methacrylate
M	Molar
MA	Maleic anhydride
MFA	Multi functional acrylate
nm	Nanometer
NMR	Nuclear Magnetic Resonance
NR	Natural rubber
NVP	N-vinyl pyrrolidone
PBD	Polybutadiene
PE	Polyethylene
PMMA	Polymethyl methacrylate
PMPA	Penta methyl piperidinyl acrylate
PS	Polystyrene
R.T.	Room temperature
SBS	Styrene butadiene styrene
sccm	Standard cubic centimeter
SEM	Scanning electron microscope
SFM	Scanning force microscopy
SR	Silicone rubber
SSIMS	Static secondary ion mass spectroscopy
STM	Scanning tunneling microscope
UV	Ultra violet
XPS	X-ray photoelectron spectroscopy

ABSTRACT

ABBREVIATIONS

CHAPTER I

SURFACE MODIFICATION AND CHARACTERIZATION OF POLYMERS

CHAPTER VI

SURFACE MODIFICATION OF SILICON RUBBER AND STYRENE BUTADIENE STYRENE FILMS

CHAPTER VII
DESIGN, SYNTHESIS AND PERFORMANCE EVALUATION OF NOVEL POLYMER STABILIZERS

List of Figures

List of Tables

CHAPTER I

SURFACE MODIFICATION AND CHARACTERIZATION OF POLYMERS

1.1 INTRODUCTION

Polymers are important commercial materials and constitute one of the fast moving frontiers of the daily life. Polymers enjoy their importance in a wide range of applications, conventionally from packaging, protective coatings, adhesion, friction & wear, composites, home-appliances, to the most recent ones in bio-materials, micro-electronic devices, high performance membranes, micro-lithography etc. Although, polymers have excellent bulk physical/chemical properties, are cost-effective and easy to process, yet they do not gain any considerable importance as speciality products, except few, due to their inert surface[1-5]. Thus, special surface properties which polymers do not possess, such as chemical resistance, hydrophilicity, roughness, lubricity, selective permeability, adhesion of micro-organisms are required for their success for specific applications [6-11].

Surface properties are of especial concern because the interaction of a polymer with its environment chiefly occurs at the surface[12-15]. Tailoring of these properties using surface modification techniques have become an important tool to convert the inexpensive polymers into valuable commercial products. The generation of technologically useful surface with tailor-made interfaces has generated considerable interest in the scientific and industrial community. Advances have been made in recent years to render polymer surfaces with desired chemical and morphological properties with negligible changes in the polymer bulk properties[16-18]. Many recent studies in the field of polymers have emphasized the need of material compatibility in multiphase systems to provide new materials with improved properties. The modification of the polymer surfaces is thus proposed. Modification of polymer surface with desired properties could be brought about depending upon the type of its application[7, 19-22]. The following changes at the polymer surface are desired to enhance the surface properties:

- Generation of secondary functionalizable reactive groups at the surface.
- Increase the surface free energy of polymers.
- Increase hydrophilicity thereby improving the dyeability, bondability and paintability.
- Improve adhesion of cells and micro-organisms to obtain bio-functional surfaces.
- Improve surface electrical conductivity.
- Improve the chemical and wear resistance.

Tailoring of these surface properties would open an avenue to the most lucrative market.

1.2 DIFFERENT METHODS OF SURFACE MODIFICATION

The necessity of surface modification is underscored by the above-mentioned pre-requisites of the polymer for speciality applications. Moreover, it is very difficult to synthesize polymers with distinct bulk and surface properties. The ability to tailor surface properties has therefore, become an important and challenging area of research. Technologies such as surface engineering and surface coating, which convert inexpensive materials into valuable finished goods have become even more important in the present scenario, as the material cost has become a significant factor in determining the success of any industry. Advances in the surface modification of the polymeric substrate can be brought about by overcoming the drawbacks of conventional methods and devising neoteric tools, depending upon the desired morphological properties and their potential applications. An in-depth understanding and a close survey of the physical and chemical properties of polymer surface are required to bring about surface modification of the polymers. Polymers like polyolefins with versatile physio-chemical properties would be an obvious choice for tailoring surface properties.

Most of the commodity polymers exhibit inert and hydrophobic surfaces restricting their applcations. During the last two decades, researchers have extensively studied radiation induced graft copolymerization[23-30]. However, these techniques still suffer from shortcomings such as damage to the substrate, non-homogeneous grafting, high degree of subsequent homopolymerization and practical inconvenience. As a result of this, the area of surface modification still remains a matter of curiosity. *Oster and coworkers*[31-33] have reported several chemical and photo-physical methods of surface modification fom their pioneering work in this area.

Some of the traditional as well as modern techniques of surface modification with their merits and demerits are briefly discussed in the following sections. Since, some of these techniques are still in their infancy, they need to be thoroughly explored.

1.2.1 Flame treatment

Flame is probably the oldest plasma known to the humanity and is one of the most traditional methods used by the industries for the modification of the polymeric surfaces. It is mainly employed to enhance the hydrophilicity of the polymer surface. Though it consists of a very simple set-up (comprising of a burner and a fuel tank), a very high degree of craftsmanship is needed to produce consistent results. Oxidation at the polymer surface brought about by the flame treatment leads to the formation of functional groups like hydroxyl (-OH), carbonyl (>C=O) and carboxyl (-COOH and -COOR). This surface

oxidation is attributed to interaction of the polymer with different excited species in the flame. For an efficient flame treatment, the variables like air-to-gas ratio, air and gas flow rates, distance between the tip of the flame and the object to be treated, treatment time and the nature of the gas should be optimised[34]. Flame treatment of different polymers has been widely reported in the literature[35-37]. The associated shortcomings of this technique are its limitation to small objects, dependence of its success on the worker's skill and ambient treatment conditions.

1.2.2 Metal deposition

Metal coatings can also help to achieve many desirable surface properties such as electrical conductivity and optical characteristics. This method was initially developed in the early 70's and still continues to fascinate the industries[38-40]. Typically, there are two major industrial techniques for metalization of the polymer surface: *electroless plating* and *vacuum deposition*. Metal coating by electroless plating is different from electroplating in the sense that the electrons required for reduction are supplied by a chemical reducing agent present in the solution whereas in the case of electroplating, the electrons are supplied by an external source like battery or generator. Moreover, electroless plating can be applied to non-conductors like polymers and ceramics.

The most widely used vacuum deposition techniques are evaporation and sputtering. In the evaporation process, heating the metal by an electron beam or by direct resistance produces metal vapors, which gets deposited on the polymer surface. This system is operated at very high vacuum (between 10^{-5} and 10^{-6} torr) and the rate of metal deposition varies from 100 to 250,000 A°/min. Though the possibility of converting this process to a batch or continuous scale is its prime merit, the excellent vacuum requirement makes this process expensive and impractical for large-scale commercial applications.

1.2.3 Chemical treatment

It is the most conventional method known to bring about the surface modification of polymers. This method involves the use of chemical enchants to render the smooth hydrophobic polymer surfaces to rough hydrophilic ones by surface oxidation/ dissolution of amorphous regions as shown in **Figure 1.1**. This treatment has been widely used to treat large objects that would be difficult to treat by any other prevalent industrial techniques. The choice of echant strictly depends on the type of polymer. Usually strong acids like chromic acid are used for such treatment. *McCarthy and coworkers*[41-50] claim to have developed etching reactions that change only the chemical structure of different polymer surfaces. However, the

main shortcoming of chemical treatment is the lack of control over the process, leading to excessive bulk degradation.

Figure 1.1. Sulphuric acid treated **a)** poly(sulfone) **b)** poly(ether ketone)

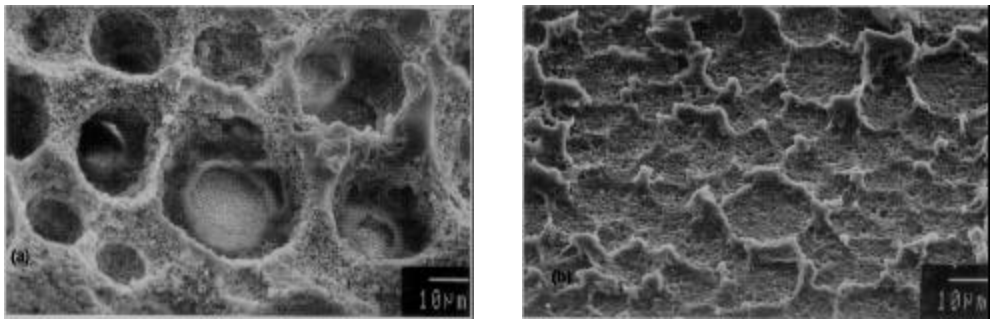

1.2.4 Corona discharge

Corona discharge is a well accepted, relatively simple and most widely used industrial surface treatment for continuous polyolefin films[46-51]. This technique is used mainly in the plastic industry to improve the printability[52] and adhesion[53,54] of the polyolefin films and articles. The corona treatment device, which is very simple and cost effective, consists of a high voltage and high-frequency generator, an electrode and a grounded metal roll covered with an insulating material, as shown in the **Figure 1.2**. The whole system works as a large capacitor with the electrode and the grounded roll as the plates of the capacitor and the roll covering and air as the dielectric. In this system a high voltage applied across the electrodes ionizes the air producing plasma (often identified by the formation of a blue glow in the air gap).

Figure 1.2. Corona treatment assembly.

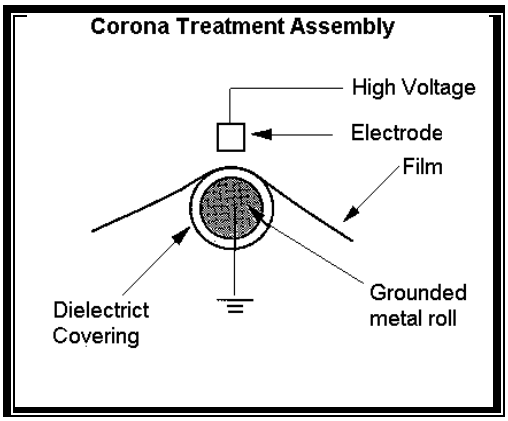

This atmospheric pressure plasma, popularly known as *corona discharge* brings about physical and chemical changes on the polymer surface for improved bondability and dyeability. A number of chemical reactions are bound to take place at the polymer surface as a result of corona treatment. Electrons, ions, excited neutrals and photons that are present in a discharge react with the polymer surface to form radicals. These radicals react with atmospheric oxygen[55] yielding products shown in **Scheme 1.1** and **Scheme 1.2**. The decomposition of the hydroperoxide groups produce >C-OH, >C=O, -COOH on the corona-treated polymer surface[53]. Moreover, the chain-scission produces low-molecular weight oxidized products[56].

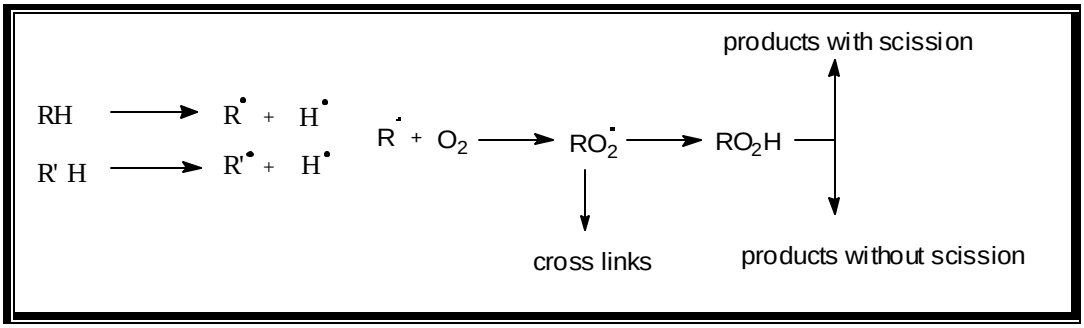

Scheme 1.1 **Scheme 1.2**

This technique has its distinct advantages like, very simple equipment and cost effective treatment. It can be used in continuous operation. However, this method associates some limitations like, non-consistent treatment due to the variation in ambient conditions (such as temperature and humidity), a high possibility of contamination due to the treatment carried out in air and the lack of homogeneity / uniformity of surface modification.

1.2.5 Irradiation

Radiations can be basically differentiated into three different categories on the basis of their energy. High-energy radiation, mainly delivered by X-rays, γ-rays and electron beam from the cobalt (^{60}Co) and magnesium (^{58}Mg) sources, are often known as *ionizing radiation*. Mid-energy radiation usually obtained from the UV rays[57], pulsed / excimer laser[58,59] and plasma sources[60,61] (employing microwave / radio-frequency) and low-energy radiation delivered by infra-red, ultrasonic, microwave and visible sources can bring about desired changes in the polymer backbone depending upon the irradiation time and energy of radiation. The primary role of any of these radiations is to activate the molecules on the polymer backbone, which in-turn reacts with the functional species present in its vicinity to render a functional surface. *Toth et al.*[62] studied surface modification of polyethylene by low keV ion beams where, ultra high molecular weight polyethylene (UHMWPE) and linear

polyethylene (LPE) were treated by low keV H_2^+, He^+ and N_2^+ ion beams and the chemical changes induced on the surface were investigated by FTIR and XPS. Upon treatment by N_2^+ ions, incorporation of nitrogen (N) took place on the surface. The N-content of the surface layer reached the saturation value, ~11 atm % at $m \sim 10^{17}$ ions/cm^2. *Ranby*[63] has briefly reviewed photoinitiated surface modification of PE in the recent past. *Kavc and coworkers*[64] accomplished surface modification of polyethylene by photochemical introduction of sulfonic acid groups. Polyethylene samples were irradiated with UV light in a gas atmosphere containing SO_2 and air to achieve photosulfonation of the surface. The modification, degradation and stability of different polymeric surfaces treated by reactive plasmas[65] were investigated in terms of surface morphology, etching rate and fluid holding capacity. The wetting instability reflected the hydrophobic recovery, which was attributed to the surface configurational changes. Reversible hydrophobic recovery was caused by configurational changes whereas permanent hydrophobic recovery was the result of surface cross-linking and formation of oligomers.

1.2.6 Graft copolymerization

This is the most popular and fundamental method of surface modification[66-71] in the recent time. A graft copolymer is a polymer comprising of molecules with one or more species of blocks connected as side chains to the backbone having configurational features different from those in the main chain.

Graft copolymerization can be represented by:

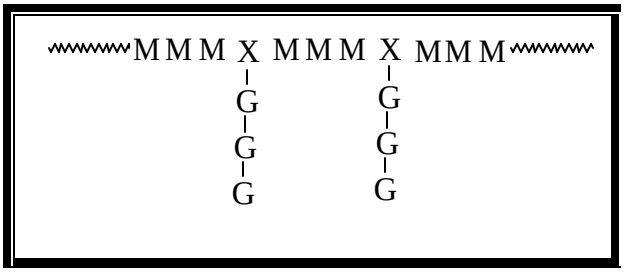

where, M is the monomer unit in the backbone polymer and G is the pendant grafted chain and X is the unit in the backbone to which the graft is attached. Graft copolymerization can be brought about mainly through free-radical mechanism[72-76] and ionic mechanism[77-81]. The former mechanism includes ionization radiation-induced grafting, photografting and plasma grafting whereas the later involves grafting via redox systems using various transition metal ions. A detailed discussion of these methods is given in the following sections:

1.3 DIFFERENT METHODS OF SURFACE GRAFTING

Although, graft copolymerization is a fundamental method of surface grafting, there is a large variety of techniques to obtain graft copolymers[82-84]. Normally, graft copolymerization involves diffusion across a phase boundary between a monomer and the polymeric material. With the advancement of technology and as an outcome of extensive research, it is possible to obtain graft copolymer with definite chain length and lateral spacing on the polymer backbone[85,86]. In the following sections we have described the different techniques of surface grafting.

1.3.1 Ionic mechanism

Ionic polymerization is a well-known technique for the preparation of graft copolymers but the fate of these reactions is determined by the reaction conditions. Since the discovery of *'living polymerization'*, anionic polymerization[87,88] has become an excellent method for obtaining block and graft copolymers. In anionic polymerization, the graft copolymerization is initiated from the anion generated by the reaction of bases with the acidic protons in the polymer chain as shown in the **Scheme 1.3**:

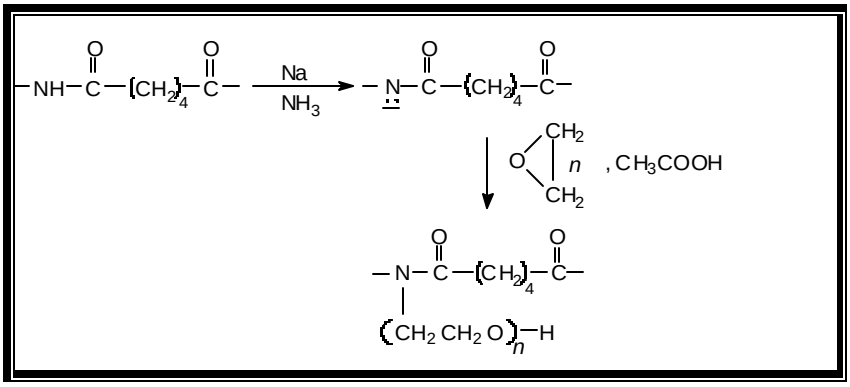

Scheme 1.3

Similarly, in the case of *cationic* method, the initiation reaction between labile alkyl halide[89] and Lewis acid have been utilized for cationic grafting onto halogenated polymers (**Scheme 1.4**): These reactions can be further employed for achieving desired surface modification.

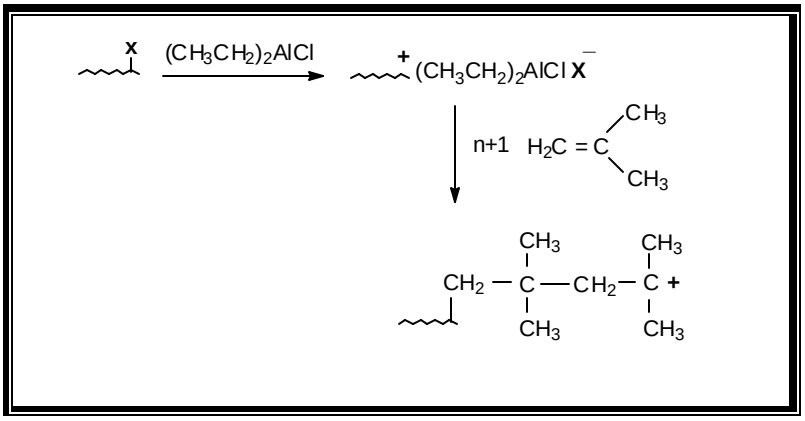

Scheme 1.4

1.3.2 Coupling mechanism

In this method the active hydrogens on the polymer surface are utilized to form graft copolymers. Polyamide is grafted with poly(ethylene oxide) as shown below: The same method is applicable for the polyamide surface modification.

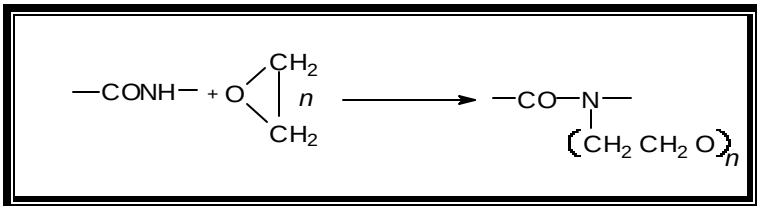

1.3.3 Free-radical mechanism

Free-radical mechanism can be divided into three main categories, which are described in details as under:

1.3.3.1 Chemical grafting

This method involves graft copolymerization using redox initiators[90-92] or free radical initiators[93-97] usually in the solution phase, occasionally under the influence of temperature in the later case. Redox systems have extensively been used to generate active sites especially on the natural polymers[98-101] (like cellulose). Transition metals viz. Cr^{+6}, V^{+5}, Ce^{+4}, Co^{+3}, Mn^{+2} and Fe^{+2} effectively produce free radical sites on the cellulose backbone through the alcohol groups present on them. In a similar approach, several vinylic monomers viz. acrylates, vinyl acetates, methyl acrylates and acrylic acid have been grafted onto chitosan via redox initiation[102]. In an alternative method, the free radical initiators like BP, XT, BZ, BPO and AIBN are thermally activated to give rise to macro-radical sites on polymer backbone to initiate grafting of desired vinylic monomers. *David et al.*[103] in a similar experiment studied the

graft copolymerization of maleic anhydride, methyl methacrylate and acrylamide onto SBS, using AIBN and BPO as radical initiators. The efficiency of these initiators was found to be predominantly dependent on the nature of monomer while, the course of reaction depended on the relative reactivates of monomer versus that of the macro-radical.

Mario et al.[104] have reported grafting of maleic anhydride onto [bis-(4-ethylphenoxy) phosphazene] a new versatile polymer with outstanding properties of heat and flame resistance. The following reactions are assumed to operate during the initiation processes involving redox systems (**Scheme 1.5 (a)** and **(b)**). The resultant radicals ($S^{\bullet}$, $HO^{\bullet}$ and $SO_4^{-\bullet}$) were assumed to interact with the polymer, producing macroradicals (via H abstraction) and initiating grafting in the presence of monomer[105,208,211].

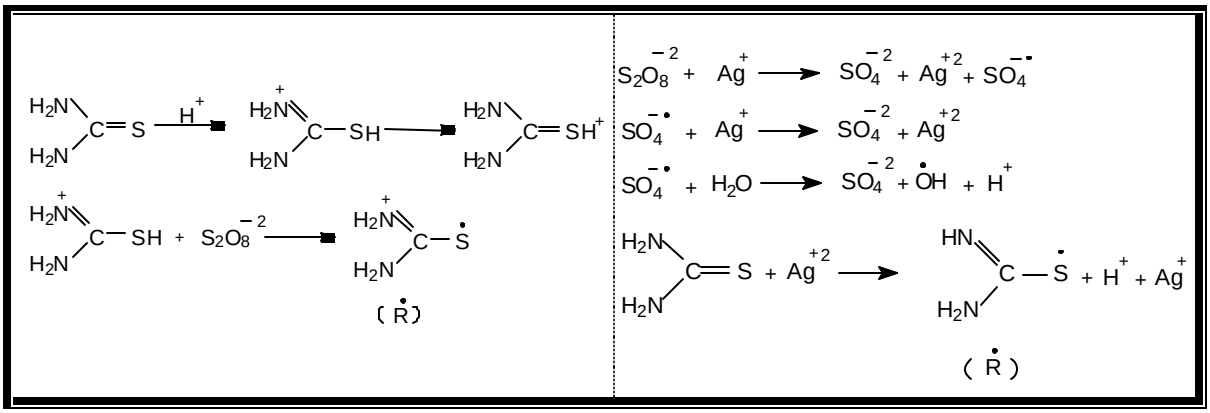

(a) **Scheme 1.5** **b)**

1.3.3.2 Radiation-induced grafting

Radiation grafting[106-114] is a very versatile technique by which surface properties of almost all polymers can be tailored through the choice of different monomers. In this method the most commonly used radiation sources are high- energy electrons, γ-radiation, X-rays, UV-Vis radiation, plasma radiation and more recently used pulsed lasers[115], infra-red[116], microwave[117] and ultrasonic radiation[118]. Grafting is performed either by pre-irradiation or simultaneous irradiation technique[119-122]. In the former technique, free radicals are trapped in the polymer surface/ matrix in an inert atmosphere and a monomer is then introduced into the system to graft it onto the polymer backbone. In the later case, the polymer is irradiated in the presence of a solvent containing a monomer and a photoinitiator. In both these methods, graft copolymerization starts from the radical sites generated along the polymer backbone due to the high-energy radiation. The major

disadvantage of these techniques is homopolymerization and is now successfully overcome by adding varying amount of homopolymer inhibitors. The modifications brought about at the polymer surface as a result of irradiation are schematically presented in the **Figure 1.3**.

Figure 1.3. The surface modifications brought about by irradiation.

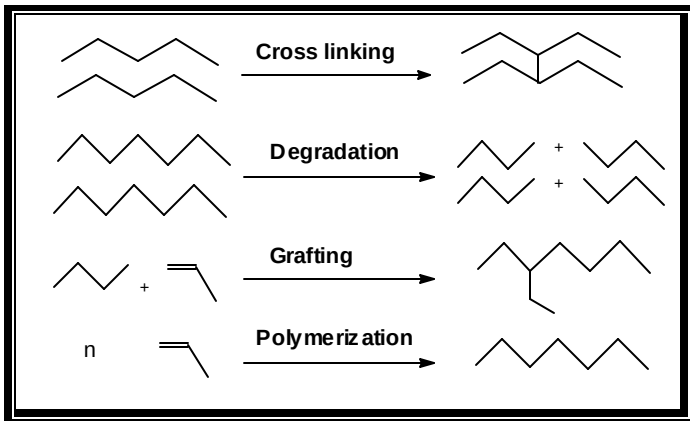

.

The grafting carried out under irradiation conditions can be broadly divided into three main categories:

1.3.3.2.1 High-energy induced grafting

High-energy radiations[123-125] viz. high-energy electrons, X-rays and γ-rays are often known as *ionization radiation* since they displace electrons from the atoms and molecules, producing ions. These radiations deliver a large amount of energy to the substrate, much greater than those associated with their chemical bonds. Ionization radiation can be classified into two categories: direct ionization radiation, which include electrically charged α / β-particles, electrons and protons of kinetic energy sufficient enough to produce ionization with electrons of the irradiated material through Coulombic interaction. Indirect ionization radiation constituting of X-rays and γ-rays do not produce ionization upon interaction with the irradiated material but interact in a way that produces direct ionizing radiation. The commonly used industrial ionization radiation sources are high-energy electrons (0.1-10 MeV) and cobalt-60 (^{60}Co) source (~1.25 MeV). Irradiation of polymers with ionization radiation produces several chemical effects[126,127] such as degradation, cross-linking as well as co-polymerization and grafting in the presence of monomer. As previously mentioned, grafting of vinylic monomers onto a polymer can be achieved by simultaneous or pre-irradiation techniques.

In the early stages, radiation induced grafting was lavishly employed for the bulk grafting. *Claramma et al*.[28] has prepared acrylonitrile-g-NR using γ-rays at different rubber and monomer concentrations and compared the properties of the modified rubbers with those of natural rubber and nitirile rubber. The reaction procedure is described in deatils[128,129]. Methyl methacrylate grafted natural rubber was prepared by initiating the polymerization using γ-radiation. The combined effect of radiation and chemical initiation was also studied and the properties of graft rubbers were compared with those prepared exclusively using redox catalyst[130]. *Bhin et al.*[131] studied the kinetic aspects of acrylic acid grafting onto natural rubber using cobalt-60 source. *Kurbanov and coworkers*[132] studied the radiation grafting of different nitrogen-containing monomers onto polyolefins and Lavsan articles for medical use. Here, the grafting was initiated by γ-irradiation and the effect of grafting conditions on the yield of the product and activity of various alkylating agents towards the modified surfaces was established. *Yamamoto et al.*[133] carried out vapor-phase mutual grafting of methyl acrylate onto polyethylene at high dose rates from electron accelerator and found that the reaction yields the same surface graft structure as those obtained upon grafting at low dose rates from ^{60}Co sources. The same research group[134] also studied the kinetics of the *g*-radiation induced surface grafting of methyl acrylate onto polyethylene using quartz helix micro-balances and found that under typical graft conditions, the grafting rate increased, leveled off, and then accelerated with irradiation time. *Saidov et al.*[135] carried out the grafting of UV absorber N-methylacryloyl benzoxazolinone onto the PE films using γ-radiation in acetone solution in the absence of oxygen. *Ameya et al.*[136] prepared polyethylene films showing electric surface-conductivity by radio-chemically grafting functional monomers onto the polymer surface. *Wang*[137] studied γ-radiation and electron beam radiation-induced graft copolymerization of acrylic acid and methacrylic acid on PVC in the presence of homopolymerization inhibitors. The graft percentage increased with increasing dose rate. The study of γ-radiation and electron beam induced grafting revealed almost similar results, however, the later favored the mass graft-process on PVC films and induced a big improvement in tensile strength and excellent printing ink adhesion[138]. A series of polyether-urethane films were grafted with hydrophilic monomers by the means of γ-radiation. The water uptake of the grafted films increased with the grafting yield and the contact angle studies revealed that all the grafted films had more hydrophilic surfaces than the un-grafted trunk polymer[139]. The γ-radiation induced grafting of N-vinylpyrrolidone was performed by pre-swelling techniques onto segmented polyetherurethane and the grafting was found to occur only in the alkaline

medium. The modified films were found to be thrombo-resistant[140]. *Sommer et al.*[141] brought about hydrophilization of the surface of plastic packaging materials viz. LDPE and PP with γ-rays and X-rays in an inert atmosphere with acrylic acid to give surfaces with reduced contact angles. Thus, an immense literature is now available on the high radiation induced surface grafting.

1.3.3.2.2 Photo grafting

The different energy sources commonly used in radiation grafting are high-energy radiation or ionization radiation (electron beam, X-rays and γ-rays) medium energy (UV and Plasma radiation) and low energy radiation (IR, microwave and ultrasonic radiation). The basic difference between ionization radiation and photo-radiation is that the energy of ionization radiation is much higher than that of the light source employed in photo radiation[142]. The phenomenon of photografting is initiated by the UV radiation obtained from various sources[143] including the most commonly used mercury vapor lamps. Although, wavelength of UV light ranges from 100-400 nm, the working range for surface photografting is 200-400 nm. The wavelength below 200 nm bears very high energy and leads to undesirable degradation of the polymer. It is known that in a photochemical process, absorption of a photon by organic molecule (commonly called chromophore) results in the excitation of the molecule from its ground state giving rise to n-π^* and π-π^* transitions. The extra energy associated with the excited molecule is then dissipated by various processes, amongst which *energy transfer* is the most desirable process for grafting reactions. Absorption of UV light produces an excited singlet (S^{1*}) transition; which then releases a part of its absorbed energy to form a excited triplet (T^{1*}). Before the excited triplet undergoes decay, the absorbed energy is used for photochemically-induced reactions[144].

The two main advantages of photo grafting over ionization radiation grafting are: 1) the modification produced by this technique is virtually restricted to the surface and is then helpful in generating properties like adhesion, antifogging, wear resistance, antistaticness, printability, dyeability and biocompatibility at the polymer surfaces 2) the energy associated with UV light is in competence with the chemical bond energies associated with any two atoms[145]. Hence, UV radiation often has the potential for retention of the properties of monomers and polymers while, the other surface grafting techniques, which use ionization radiation cause damage to the substrate polymer due to excessive degradation. Organic ketones, peroxides and their derivatives are well known photo-initiators for surface photografting. Benzophenone (BP) and its derivatives are most commonly used

photoinitiators. Benzophenone, when absorbs a UV photon, is excited to the short-lived singlet state and then relaxes to a more stable triplet state. Benzophenone in the triplet state abstracts a hydrogen atom from the polymer backbone generating a polymer macro-radical, which then becomes the active site for the surface grafting. The mechanism of surface photographing is represented in the **Scheme 1.6.** Polyethylene and polypropylene films with hydrophilic surfaces were obtained by grafting functional monomers like acrylamide, vinyl pyrrolidone and methacrylic acid using benzophenone as a photoinitiator[146]. ABS films with uniformly grafted acrylamide were prepared by exposing the monomer sandwiched films to UV radiation (400 Watt) for short period. A significant decrease in the water contact angle was observed for the grafted films[147]. The hydrophobic surface of an oriented polypropylene was modified to a hydrophilic surface by grafting it, photochemically with acrylamide. The influence of solvent, additives and sensitizer showed that graft copolymerization was initiated by hydrogen abstraction from the polymer surface by the triplet excited state of the sensitizer. The water contact angle of the modified PP films decreased from 100° to ~ 40° after grafting[148]. Polystyrene films were coated with maleic anhydride in acetone and exposed to UV light to get films with improved wettability[149]. *Kinstle et al*.[150] carried out gas phase photochemical surface modification of polyethylene with chlorine and nitrogen dioxide. The reactive sites thus generated enhanced the photo-induced radical formation in the presence of benzophenone to initiate graft copolymerization of methyl methacrylate and 2-ethylhexyl methacrylate onto the PE surface.

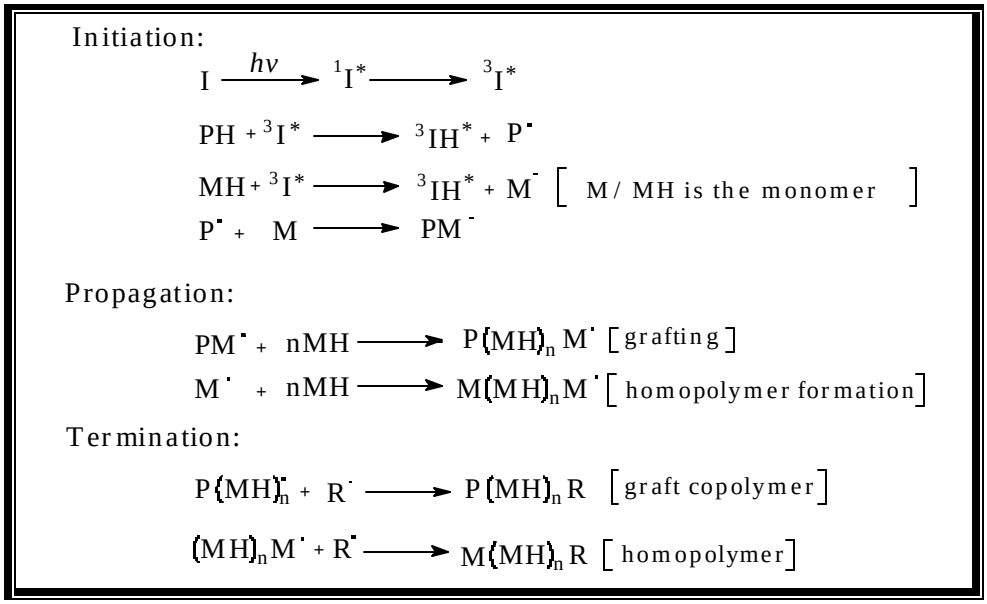

Scheme 1.6

Tazuke and coworkers[151] deduced that when photografting onto polypropylene was initiated by H-abstraction by an excited sensitizer, the rate of surface grafting and the surface structure of the grafted polymer depended on the solvent used. In the case where the solvent to polymer interaction was strong, the grafted surface was not sufficiently hydrophilic, although the rate of grafting was fast. This was attributed to the bulk grafting. The use of a solvent with the appropriate affinity to the base polymer is essential to compromise the rate of grafting and the degree of surface modification. The introduction of vinyl monomer (viz acrylic acid, methacrylic acid, methyl methacrylate, acrylonitrile) onto LDPE and PP plates by photografting in liquid/ vapor phase resulted in the formation of grainy and flat structures, respectively, on the surface of the plates. The irradiation in the photografting process was carried out with a high-pressure mercury lamp at 60 ºC using photochemical reactor. The surface structure when analyzed by SEM revealed that the LDPE grafted with acrylic acid and methacrylic acid developed grainy surface structures while, flat surface structures were observed for methyl methacrylate and acrylonitrile grafted PP. It was then concluded that the strong hydrogen bonding in the case of former two monomers was responsible for the formation of the grainy structure on the plates[152]. *Decker*[153] carried out the coating of photocurable epoxy-acrylate on the PVC surface, to protect the superficial degradation of PVC. Adhesion of the coating to the PVC could be improved by photochemical grafting using photoinitiator viz hydroxy acetophenone. *Gosh et al.*[154] studied photografting of poly(methyl methacrylate) chains on natural rubber backbone in benzene using quinoline-Br charge transfer catalyst as photoinitiator and methyl methacrylate as monomer at 35 ºC under visible light. The effects of variation of different reaction parameters are discussed. *Ikada et al.*[155] prepared poly(ethylene terepthalate) film with improved hydrophilicity by coating the surface of the film with Irgacure 651 and treating it with 10% aqueous solution of N,N-dimethyl acrylamide followed by irradiation of UV light for 20 minutes. The contact angle of the surface-treated film with water declined from 80º to 10º. *Uyama and Ikada*[156] carried out graft copolymerization of acrylamide onto nylon 6, PP, PE and ethyl vinyl acetate films. The grafting yield was affected by thermal and photo-irradiation applied simultaneously during the reaction. Vapor phase photografting of methyl methacrylate on nylon 6 was carried out and the effects of solvent mixed with monomer on benzophenone-sensitized grafting were investigated. The grafting on nylon 6 was promoted by adding a pertinent quantity of the solvent, such as phenol, m-cresol and formic acid. Such an accelerating effect was supposed to originate due to the swelling of substrate film by the solvent. It was also observed that adding small quantity of solvents such as decalin or *p*-xylene retarded grafting on LDPE and

PP films. The differences in the solvent effects on the different types of film substrates are discussed in terms of photo-induced radical formation on the substrates in the presence of different solvents[157]. *Ranby and coworkers*[158] have developed two new processes for surface photografting on sheets, films and fibers of PE, PP and PET. In the first method, *vapor phase transfer* of sensitizer and monomer from a volatile solution brought about uniform grafting of the monomer on the substrate upon UV irradiation. The second method describes UV induced surface grafting of a polymer sheet in a continuous operation. The photochemical grafting of HEMA onto LDPE film was carried out by simultaneous grafting technique[159] wherein, a solution of HEMA, acetone and benzophenone spread between two LDPE films was irradiated by UV light to give grafted surfaces with water contact angle of the films reduced to 50º from initial 90º. Surface photo-grafting of acrylamide onto the ethylene-vinyl alcohol copolymer film was investigated at 60 ºC in aqueous medium, where photoinitiators were previously coated on the film. The effect of different photoinitiators (benzophenone, xanthone, benzoylperoxide and anthraquinone) was also evaluated and it was found that xanthone gave the highest grafting yield. Based on the results of electron probe microanalysis, it was substantiated that for the samples prepared by photo-grafting the grafted, chains were distributed below the surface of the film, while for those samples prepared by ceric salt initiation, the grafted homopolymer chains were located mainly at the surface[160]. A two-step heterogeneous polymer surface modification of poly(acrylonitrile) (PAN) ultra filtration membrane was developed, involving photo-bromination as an activation step and subsequent UV-induced grafting with acrylic acid and methyl acrylate monomers. For relatively low degrees of modification, thin and smooth graft polymer layers were generated which specially altered the membrane-surface hydrophilic[161]. Graft copolymerization of methacrylic acid and acrylamide from an aqueous solution onto acrylonitrile-butadiene-styrene terploymer (ABS) was initiated by the thermal decomposition of polymeric hydroperoxides, which were formed upon UV irradiation of ABS containing anthracene. The graft copolymerization was found to occur above 100 ºC at the endo-peroxide decomposition temperature. The effect of other reaction parameters was also investigated[162].

1.3.3.2.3 Plasma grafting

In the present scenario *plasma modification* is the most accepted technique for the surface modification of polymers in their different physical forms on a laboratory scale[163]. A plasma can be broadly defined as *a gas containing charged and neutral species which include, electrons, + ve ions, - ve ions, radicals, atoms and molecules.* Plasmas are generally categorized on the basis of

electron densities and electron energies. The low electron energy plasma, often called *cold plasma* is most commonly used for surface modification of polymers. The other plasmas known are interstellar plasma, alkaline vapor plasma and the hot plasma and are often used for controlled fusion. In glow discharge plasma, the temperature of the ions and molecules is often ambient whereas that of electrons is higher by a factor almost up to 100. Thus, plasmas produced by glow discharges are called *non-equilibrium* plasmas because the electron temperature is much higher than the gas temperature. A typical plasma reactor is shown in the **Figure 1.4**.

The energy required to form and to sustain a plasma used for surface modification/ polymerization is obtained by an electric field which is produced either by *ac* or *dc* supply. The different *ac* frequencies employed for the excitation are 100 kHz, 13.56 MHz in the radio frequency (RF) range and 2.45 GHz in the microwave (MW) range. The frequency in the range of 10-20 MHz is most commonly used for industrial applications. The externally applied electric field brings about the ionization process whereby; an electron gains sufficient energy and becomes a free electron leaving behind a positive ion. This excited state usually stays for a very short period of time (< 100 ns) and falls to a lower energy level or ground state by *radiative decay*. This relaxation process is known as "*glow discharge*" and a typical nitrogen glow in the plasma reactor is shown in the **Figure 1.5**. The general mechanism of ionization taking place in a plasma chamber is represented in the **Scheme 1.7**.

Scheme 1.7:

The ionization of an atom can be brought about under the influence of external energy source:

$$A + e \rightarrow A^{+} + 2e$$

The atoms in the ground state can be promoted to excited state by electron impact:

$$A + e \rightarrow A^{*} + e$$

The excited state usually stays for a very short period of time normally less than 100ns and then falls to the lower energy level or ground state by radiative decay:

$$A^{*} \rightarrow A + h\nu$$

This relaxation produces a glow discharge.

When a metastable atom (energy-rich chemical reagent with a longer radiative time) collides with a neutral, it causes ionization of the later if the ionization energy of the neutral is less than that of the excited atom:

$$A^{*} + B \rightarrow A + B^{+} + e \quad (A^{*} \text{ is metastable atom})$$

or

$$A^* + B \rightarrow B^* + A$$

Some other reaction like electron impact dissociation, secondary ionization, symmetrical resonant transfer, asymmetrical charge transfer, electron-ion recombination and ion-ion recombination also takes place under the influence of the plasma conditions.

Figure 1.4: Plasma-grafting reactor.

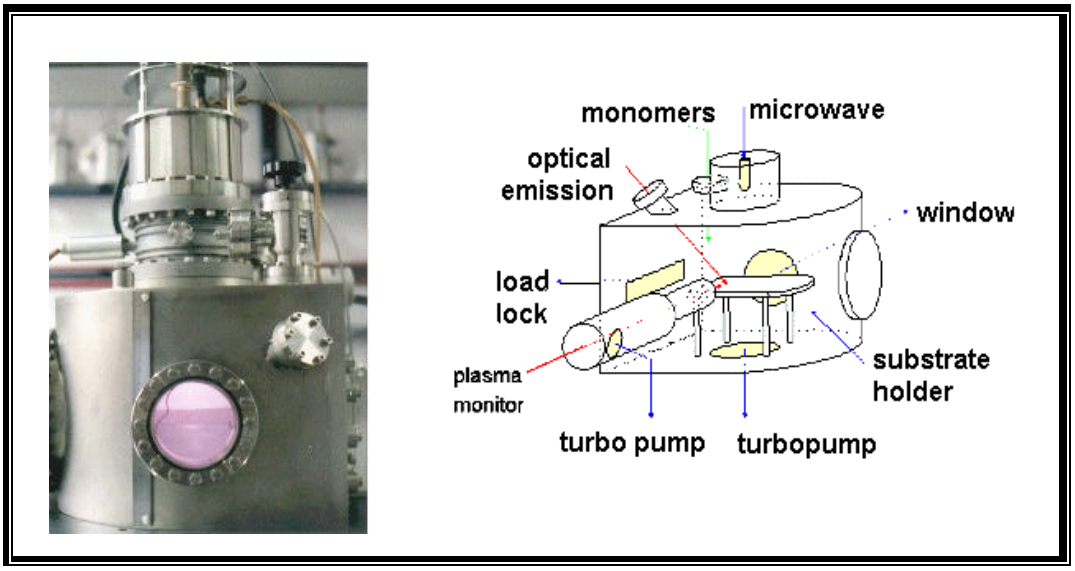

Figure 1.5 Nitrogen glow discharge.

Jacna and coworkers[164] carried out plasma treatment and plasma initiated grafting of acrylic acid onto polypropylene and polyester fibers. The grafting was found to be most successful with polypropylene, giving wettable fibers with a large change in the water contact angle. Surface modification of polyethylene for improved adhesion to epoxy resins, was

attained by plasma-induced grafting of methyl acrylate. The grafted polyethylene joints showed much high bond durability than that shown by surface oxidized polyethylene[165]. *Gil'man et al.*[166] studied the effects of a glow discharge plasma on the properties of natural rubber surface. The glow discharge in air was found to induce weight loss and an increase in surface wettability of the sample. The weight loss and the increase in wettability were directly proportional to the exposure time. *Sakamoto and coworkers*[167] observed that grafting ratio increased by first-treating the surface of the polyester fiber with a low–temperature plasma (110 KHz frequency and 0.64 W/cm^2) for 40 sec in a non-oxidative medium, followed by grafting the material with a radically polymerizable monomer (50 % acrylamide solution) with 0.0001-1.0 % of a transition metal salt [$(NH_4)_2Fe(SO_4)_2$] for 30 min at 60 ºC.

Epaillard and coworkers[168] accomplished the plasma modification of cellulose acetate by applying cold plasma of tetrafluoromethane and sulfur hexafluoride. The interaction of these cold plasmas and cellulose acetate rendered the later with fluorinated surface. As a consequence, the surface energy decreased leading to the surface with significant biocompatibility. Recently, *Epaillard et al*.[85] have also reported the post-grafting of NVP onto a plasma modified PP surface. The equipment used to generate plasma, consisted of microwave generator (433 MHz) with a variable power out-put (0-250 W) which was coupled to a resonant cavity. Before each run, the system was evacuated to 10^{-6} mbar and maintained for 2h. The plasma treated films were dipped into a solution of NVP /distilled water/NH_4OH (60/38/2 wt %) for different time duration and the grafting yield was estimated using ESCA, ATR-FTIR and contact angle measurements. The comparison of the O/C and N/C elemental ratios determined by XPS analysis given in **Table 1.1** shows that the increase in the carbon to oxygen and carbon to nitrogen ratio was due to the grafting of poly(vinyl pyrrolidone) onto PP. The new band corresponding to the carbonyl valance vibration of PVP

Table 1.1 The comparison of the O/C and N/C ratios for PVP-g-PP determined by XPS.

Sample	Elemental ratios (× 100)	
	O/C	N/C
Virgin film	5.3	0
Control sample	21.7	2.3
Plasma modified	14.3	28.6
Extracted after Plasma modification	26.8	3.9
Grafted sample	10.9	10.3
Polyvinylpyrrolidone	16.5	16.5

generated at 1683 cm^{-1} in the ATR-FTIR spectrum also confirmed that the grafting had taken place onto the PP film. Plasma treatment and plasma-grafting has been extensively studied for polymers, but elastomers.

1.4 RECENT ADVANCES IN SURFACE GRAFTING

1.4.1 Use of novel initiators

Initiators play a prime role in any polymerization reaction[90-92]. Organic ketones and peroxides are well accepted as free radical initiators[93-97]. Under the influence of light/heat of suitable amplitude, they undergo sensitized decomposition followed by generation of a free radical site on the polymer backbone (P ·) which subsequently reacts with the monomers in their vicinity of yield grafted polymers. A variety of free radical initiators viz. benzophenone, xanthone, benzoyl peroxide, dicumyl peroxide, azo bis-isobutyronitrile etc. and their mode of action are well documented in the literature[169-174] Scientists world wide, as a result of their extensive research, have developed a range of novel macro and micro-initiators, which outperform the conventional ones. *Katot et al.*[175] developed novel micro-initiators, which use IR irradiation/ microwave/ high voltage for their excitation; modifying the surface of materials such as metals, polymers, fibers etc to impart lubrication, hydrophilicity and/or bio-functionality. In order to overcome the hassles associated with solvent handling during copolymerization and to meet the environmental norms of the global scenario, the free radical graft copolymerization of several functional monomers on the polyolefins was studied under melt processing conditions[176,177]. In a recent trend, graft copolymerization during reactive processing and in extrusion reactor, is accomplished using organic peroxide initiators[178]. In a similar experiment *Naqvi et al.*[179] studied the graft copolymerization of acrylic acid and ethyl methacrylate on LDPE under simulated melt-processing conditions.

Photoactivation of the heterocyclic azides to generate highly reactive nitrenes have been demonstrated as a novel route for the photomodification of metal, glass and polymer surfaces[180]. The use of these novel photoinitiators led to the insertion of organic functional groups into C-H, N-H, O-H bonds. Surface macromolecular architecture with dimensional precision, control of the thickness of grafted layer/ blocks of grafted chains was achieved by using the surface photo-graft copolymerization method. UV irradiation of a benzyl *N,N*-dimethyldithiocarbamyl group-immobilized polymer surface in the presence of vinyl mono mers viz. methacrylic acid and/or styrene at room temperature, allowed precise control of the macromolecular architecture of the grafted chains on the polymer surfaces. The

patterned surfaces thus synthesized by irradiation through a projected mask were visualized by dye staining and cell-culturing[181]. *Anders et al*.[182] developed an unusual method of surface modification based on dip-coating of a substrate with a macro initiator and subsequent free-radical polymerization of functional monomer viz. poly(acrylic acid) hydrogel to give surface with relevant biological properties. The synthesis and application of the novel water insoluble macro initiator poly(octadecene-co-maleic anhydride-tert.-butyl perester) is reported in the literature[183].

1.4.2 Use of advanced initiation techniques

During the past three decades, radiation induced graft copolymerization of monomers onto the surface of polymeric materials by the use of energy source such as UV, γ-irradiation and e-beam has provided convenient means to impart desired surface properties[7-10]. However, these techniques still suffer from some shortcomings such as subsequent homopolymerization and possible damage to the substrate[16-18]. Hence, low energy initiation techniques (viz. near infrared, line tuneable pulse laser and ultrasonic radiations have emerged to be better alternatives[184186].

Laser induced polymerization of monomers have attracted significant attention in the recent years, generating a considerable literature published on both, pulsed and continuous lasers to initiate polymerization[187,188]. However, a little work has been done on laser induced graft copolymerization of monomers onto the surface of polymeric substrates. Lasers have several distinct advantages over other light sources, including narrow wavelength band, which could be tuned to the maximum absorption of the photoinitiator thus, making laser treatment an energy efficient process. Moreover, high energy could be concentrated over a small area, which allows polymerization to be initiated from a remote position within a very short time and with low beam penetration. Pulsed lasers allow short exposure times and less thermal damage by optimizing the time intervals between the pulses. Pulsed CO_2 lasers have large beam sizes, large pulse energy, uses nontoxic gases, have high laser efficiency, are cheap and easy to operate. *Hamid et al.* [189] generated peroxides on the surface of polymer using CO_2 pulsed laser through peroxidation mechanism. Decomposition of these peroxides successfully initiated the graft copolymerization of acrylic acid onto the surface of ethylene-propylene rubber (EPR). The graft level was found to increase with the pulse and then declined above 25 pulses. The CO_2 laser induced surface grafting of HEMA, NVP and acrylamide (Am) onto EPR surface, to achieve biocompatibility was studied by *Mirzadeh et al.* [190].

The efficiency of ultrasonic vibration to induce the graft copolymerization is known since the mid 70s'. But, this versatile technique has hardly been explored[191-195]. Surprisingly only *Yoshida et al* [196]. prepared synthetic resin moldings with improved adhesion to a coating by grafting the surface with vinyl monomers by the means of ultrasonic waves. Thin PVC films containing plasticizer, stabilizer and lubricant were exposed to ultrasonic waves for 3 hours at 60 °C in the presence of styrene to give a grafted copolymer sheet with 5.6 % increase in weight. Grafting of maleic anhydride on PP was carried out using ultrasound as energy source and 80 % grafting was attained with a 3.2 % decrease in the molecular weight under 62 W ultrasound irradiation for 30 min at 60 °C indicating controlled degradation[197]. A highly hydrophilic surface of contact lenses was achieved by grafting [g-methacryloxypropyl-tris(trimethylsiloxy)silane-2,2,2-triflouroethyl methacrylate-1,3-bis(g-methacryloxypropyl)-1,3,3-tertrakis(trimethylsiloxy) disiloxane] onto SR under ultrasound irradiation[198] for 10 – 600 sec. Effect of ultrasonic irradiation on ceric salt (Ce^{+4}) initiated aqueous grafting of methyl methacrylate on regenerated cellulose film was investigated at 60 °C. The reaction of cellulose with Ce^{+4} was found to accelerate under ultrasonic irradiation. However, no accelerated effect of grafting due to the ultrasonic irradiation was observed for the system under reduced pressure[186] of 5 torr.

1.5 SURFACE GRAFTING ONTO DIFFERENT ELASTOMERS

Elastomers by virtue of their flexibility hold a very special position amongst all the existing polymers and are thus employed for a wide range of applications[153, 199,200]. Extensive research has been carried out to achieve bulk modification of various elastomers[153,154, 201-203]. But, the literature on the surface modification of elastomers is still scarce. The inert surface of elastomers restricts them from many potential applications. This shortcoming of the elastomers raises an opportunity for their surface modification. For the last three decades, scientists are engaged in developing functional elastomers using different techniques.

Kowalski et al.[204] performed radiation induced surface modification onto nitrile, butadiene, neoprene and EPDM rubber via sulphochlorination, chlorination and fluorination. The study of the reaction kinetics revealed that all these reactions followed the free-radical mechanism with sulphochlorination having the highest reaction rate. The initiation step was found to depend on the irradiation intensity. *Misra and Kaul* [205] explored the solution grafting of methyl acrylate onto NR using benzoyl peroxide (BPO), azo-bisisobutyronitrile (AIBN) and potassium persulphate ($K_2S_2O_8$). The results of the study revealed that significant grafting

took place in the presence of BPO in benzene at 60 °C whereas using AIBN and $K_2S_2O_8$ in the same reaction medium at 65 °C and 70 °C, respectively, gave only homopolymer. NR latex containing CCl_4 and methyl methacrylate was treated with ionizing radiation to give grafted rubber with good transparency and crack resistance[206]. If it is closely noticed, in all these attempts researchers have focused on the bulk modification of elastomers via graft copolymerization. This leaves a room for the surface modification of elastomers, developing novel applications of this useful material.

1.5.1 Natural rubber and Natural rubber latex

Natural rubber is one of the most versatile natural polymers with excellent elasticity, which is attributed to its highly irregular and coiled structure. Enormous work has been done on redox initiator induced bulk grafting of functional monomers onto the elastomers[207-211]. The graft copolymerization of methyl methacrylate onto natural rubber[212] was carried out using the potassium peroxydisulphate-thiourea redox system in the presence of silver nitrate solution. The resultant generated radicals (R•, •OH and SO_4^{-}•) were assumed to interact with the rubber, producing rubber macro radical (via H abstraction) and then initiated grafting in the presence of monomer. The grafting was found to increase with the monomer concentration and reaction time when the initiator concentration was kept constant. The grafting reaction was studied in the presence of different solvents and the order of reactivity was found to be in the order DMF > DMSO > CCl_4 > $CHCl_3$. In an attempt to improve the tensile strength, GMA, HEMA and diethyl aminoethylmethacrylate (DEAEM) were co-polymerized with NR by γ-irradiation[213].

Burfield et al.[214] studied potassium persulphate initiated graft copolymerization of methacrylamide on the surface of NR latex particles. The grafting efficiency (G.E.) of the monomer was found to be independent of initiator and latex concentration and increased with reaction temperature. The grafting onto the rubber particles was confirmed from the SEM analysis. From the study of the reaction kinetics, it was found that the rate of polymerization was inversely proportional to the induction time. Moreover, the overall activation energy decreased with an increase in the rubber concentration at constant monomer as well as initiator concentrations. The grafting efficiency investigated over a temperature range of 50-70 °C at constant monomer, initiator and rubber concentrations was found to increase markedly with the temperature, reaching 61% at 70 °C. In one of the few attempts of surface modification, *Razzak et al.*[215] carried out radiation-induced simultaneous grafting of *N,N*-dimethyl-acrylamide (DMAA) onto natural rubber (NR) tubes and studied

their blood compatibility. Thoroughly cleaned NR tubes of definite dimension and monomer with/without solvent were taken in specially designed glass reactor. The reactor was repeatedly degassed under reduced pressure and then warmed upto the room temperature and irradiated with γ-radiation from a ^{60}Co-source at a fixed position. The grafted NR tubes were thoroughly cleaned to remove the adhered homopolymer and then dried under vacuum at room temperature. The studied effect of different solvents on the grafting yield clearly suggested that CCl_4 was the best solvent for this system. Moreover, a maximum grafting yield was obtained with 30 vol.% of DMAA in CCl_4. At constant temperature, the degree of grafting increased with irradiation time and a similar trend was observed when dose rate was kept constant upon increasing reaction temperature as shown in **Figure 1.6 (a) and (b),** respectively. The blood compatibility of the grafted NR tubes were determined using the *ex vivo* test developed by *Ikada et al.*[216].

Figure 1.6 (a) Here at 27 ºC, dose rates are (▲) 1.50 kGy/h (▼) 0.33 kGy/h (◆) 0.1 kGy/h **(b)** Here at, 1.50 kGy/h, reaction temperatures are (■) 42 ºC (●) 27 ºC (▲) 0 ºC.

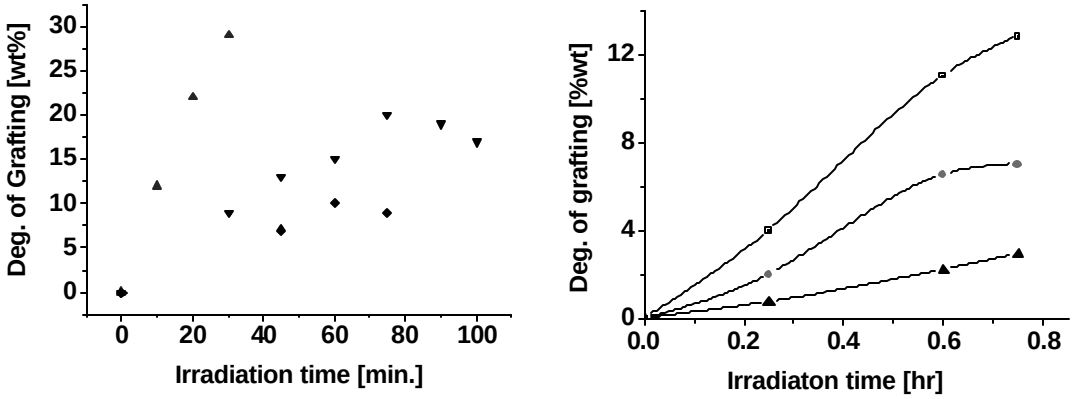

1.5.2 EPDM and EPR elastomers

Rubbers based on ethylene-propylene copolymer are widely used due to their good mechanical properties, very low unsaturation and associated resistance to aging and ozone deterioration. However, they suffer the shortcomings of low hydrophilicity and therefore, low biocompatibility. This limitation of EP rubbers could be overcome by introducing functional groups onto their surface via different methods of surface modification[217-219]. The literature survey shows that bulk grafting has been preferentially attempted over surface grafting for reasons not known. *Wang and coworkers*[220] have recently reported *atom transfer radical polymerization* (ATRP) as a novel method to graft methyl methacrylate onto EPDM backbone via controlled free radical grafting. In an another attempt glycidyl methacrylate (GMA), maleic

anhydride (MA) and acrylic acid (AA) were grafted onto EPDM and EPR using 2,5-di-methyl-2,5-di-(tert-butyl peroxyhexane) as the initiator. The increase in the diene content of the EPDM was found to improve the grafting yield. The chemical titration method was used to measure the degree of grafting[221]. *Barra et al.*[222] studied the chemical modification of EPDM in solution phase using dibenzoyl peroxide as an initiator and maleic anhydride (MA) as a monomer with attempts to optimize the grafting conditions by varying the reaction parameters. The graft copolymerization of N-vinylpyrrolidone (NVP) onto ethylene-propylene-ethylidenenorbornene terpolymer (EPDM) was carried out in toluene using benzoyl peroxide (BPO) as an initiator[223].

Haddadi-asl and coworkers[217] studied radiation grafting of biomonomers (HEMA, NVP, Acrylamide and Acrylonitrile) onto ethylene-propylene elastomers of varying molecular weight with ethylene content ranging from 40 to 70%. The grafting was carried out by *simultaneous method* at room temperature in sealed ampoules containing monomer and rubber samples irradiated at 0.4 to 7.5 kGy/h and yielded best results for highest ethylene content and highest molecular weight of the sample. The same trend has been reported by *Katbab et al.*[224] during the grafting of functional monomers onto EPDM rubber. This result was attributed to the steric effect of side groups of pure PP in EPDM. Another simple explanation of this behavior could be based on the stability [tertiary > secondary] and density [secondary > tertiary] of both the tertiary and secondary macroradicals generated due to the hydrogen abstraction from the polymeric substrate[225]. Although, the macroradicals produced by PP are more stable than those produced by PE, the higher *G*-value[226] of radicals produced by PE, resulted in higher grafting yield on EPM (with higher ethylene content). In the continuation of this work *Haddadi-asl and coworkers*[227] have also studied the effect of novel multifunctional acrylates on surface grafting yield. *Bhowmick and coworkers*[228] investigated the bulk and surface modification of ethylene propylene diene monomer (EPDM) rubber and fluoroelastomer by electron beam irradiation. The resultant properties of the modified EPDM were correlated with the structural alterations.

1.5.3 Styrene butadiene styrene

SBS is also one of the few versatile commodity elastomers that deserve wide range of applications. An application-oriented research has been taking place since almost two decades to improve the surface properties of this useful polymer[229-232]. Surface perfluorofunctionalization of polystyrene and styrene-butadiene-styrene block copolymer by perfluorodiacyl peroxides was carried out to improve the stabitity of SBS in the outdoor

applications[233] Ultraviolet-initiated photografting of glycidyl methacrylate onto styrene-butadiene rubber with influence of monomer concentration, irradiation time and the carbon black content has been studied by *Yu et al.*[234]. Vinylpyridine (VP) was photo-grafted onto styrene-butadiene-styrene (SBS) triblock copolymer membrane by UV-radiation. The membrane was then treated with heparin to prepare heparin-containing VP-g-SBS copolymer membrane for biomaterial usage[229]. Surface modification of different elastomers including SBS and EPDM was attempted to improve their tribological properties[230]. Halogenation of styrene-butadiene rubber to improve its adhesion to polyurethanes is also reported[231]. Flame retardancy of methacrylic acid grafted SBS was investigated by *Wilkie and coworkers*[232]. A two-step mechanism of surface modification of SBS is reported in the literature where photooxidation of SBS containing anthracene was carried out, followed by grafting initiated by photo generated hydroperoxides[235].

1.5.4 Silicone rubber

Silicone rubber (SR) known for its inertness, stability and excellent flexibility, is the most widely studied elastomer from the point of view of its biocompatibility and protective coating applications[236-243]. *Chapiro*[244] carried out grafting of NVP onto SR for biomedical applications. *Boelens et al.* [245] assessed the perseverance of the antibacterial activity of shunts made out of conventional silicone rubber (SR) and SR-g-poly(vinyl pyrrolidone) hydrogel, which had been soaked in various antibiotics before their *in vitro* applications. It was detected that when the SR-g-PVP shunts pretreated with antimicrobials were implanted in the human body for the relief of hydrocephalus, the incidences of shunt-associated infections (SAI) were significantly reduced. For any antibiotic or combination using an arbitrary breakpoint, SR-g-PVP remained anti-bacterially active for longer periods than neat SR. *Chang and coworkers*[246] fabricated heterobifunctional membranes of SR by plasma induced graft polymerization as an artificial organ for penetration keratoprosthesis. These heterobifunctional SR membranes were prepared by grafting different functional polymers on each side of the membrane which possessed upper-side favoring cell attachment and growth, and the lower-side suppressing cell adhesion. Surface characterization and biological properties of plasma grafted phospholipid, poly(2-methacryloyloxyethyl phosphorylcholine) (*p*MPC), onto the silicone rubber membrane was studied by *Hsiue et al.*[247]. The SR membrane onto which the *p*MPC was grafted was activated by argon plasma. ATR-FTIR, ESCA and SEM techniques were employed to characterize the effect of different plasma grafting parameters on the surface properties of SR whereas the blood compatibility was examined by platelet adhesion. Many more studies on

surface modification of SR by graft copolymerization of hydrophilic monomers have been reported in the recent past[248,249]. *Oppermann et al.*[250] investigated the photochemical surface modification of SR and found that photocoupling of water-soluble polymers onto the surface of SR led to greatly enhanced bond strengths even with conventional adhesives. Surface modification of PDMS based vulcanizate by CO_2-pulsed laser was studied as a novel technique for the preparation of blood compatible materials[251]. The data from *in vitro* blood compatibility assessments indicated a significant reduction of platelet adhesion and aggregation for the modified surfaces whereas those platelets which were adherent remained unspread. The extent of platelet adhesion was correlated to the number of laser pulses. Laser-induced surface modification of polydimethylsiloxane as a super-hydrophobic material was also carried in the recent past[252].

RF plasma treatment of polydimethyl siloxane (PDMS) is a useful way of increasing wettability for its enhanced adhesion[253]. Moreover, the plasma treated films undergo hydrophobic recovery with storage time. The behavior of mild flourinated and neat PDMS was compared directly using air, O_2, He, and Ar plasma gases, monitoring hydrophobic recovery by water contact angle changes. Hydrophobicity recovery of PDMS upon storage after exposure to plasma and corona discharges has been studied by contact angle measurements[254]. Initially after the treatment, the samples showed a low surface hydrophobicity but upon storage in dry air, a continuous increase in hydrophobicity was observed. The hydrophobic recovery in all the above-mentioned studies can be attributed to the thermodynamically favorable orientation of the functional groups. *Umaya et al.*[255] observed that hydrophilized SR films by Ar plasma became hydrophobic after storage for a long period of time. This behavior was explained as gradual overturn or the reorientation of polar groups into the hydrophobic bulk due to temperature and environmental effects. They found that the contact angle of plasma-treated SR film increased from 5 to 53° due to storage in air at 25° for 7 days, while it increased to 59° after a storage in air at 105° within 1 h. Many more researchers have studied the effects of reactive gas plasma and corona treatment on the surface of SR films[256-259]. The depth profiling of functional groups was investigated by *Stewart et al.*[260]. The study have shown that Ar plasma treatment using 2-200 W of power produced carbonyl groups on the surface with the maximum concentration of carbonyl species at 50 W of power. The CO_2 plasma treatment led to the formation of both C=O and C=C species on pendant groups attached to the silicone backbone whereas NH_3 plasma treatment resulted in the formation of primary amide groups on the rubber surface.

Although, enormous literature on SR surface modification is available today, a

systematic study on the simultaneous effect of various reaction parameters on the surface properties of SR is still lacking.

1.6 SURFACE ANALYSIS

An in-depth understanding and a close survey of the physical and chemical properties of polymer surface are required in order to bring about surface modification of polymers. It is therefore, necessary to characterize the neat and modified polymer surfaces at their molecular level. Depending upon the type of information required, a variety of sophisticated analytical techniques are available, which provide results with a high degree of accuracy.

The term "surface" though seems to be generalized, changes its definition with respect to various surface analytical techniques. A surface defined by one technique may be the bulk defined by another. Thus, the most appropriate definition of a surface is *the sampling depth of a surface measured by a particular technique*. The sampling depth usually varies from merely few angstroms (A°) to a micrometer (μm) or more. A large variety of analytical techniques, based upon the information desired, are well documented in the literature[262-266] for the characterization of polymer surface. **Figure 1.7** presents a comparative chart of the sampling depth offered by different surface analysis techniques. The choice of the surface analysis technique must be made, keeping in mind; the sample suitability, sample depth, analysis environment and surface-information desired. The information supplied by each technique is often different and complementary. The techniques like scanning electron microscopy (SEM), atomic force microscopy (AFM), tunneling electron microscopy (TEM) and confocal laser scanning microscopy (CLSM) are employed when high resolution, three-dimensional images of the surfaces are desired[267-269].

Figure 1.7 The sampling depth offered by different surface analysis techniques.

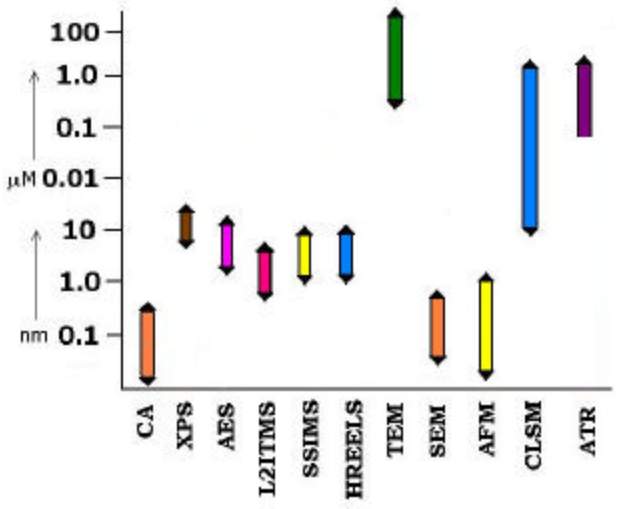

Contact angle measurement and static/dynamic secondary ion mass spectroscopy (SSIMS) are the best choice, when the most surface-sensitive analysis[270-271] is desired. X-ray photo-electron microscopy (XPS), Auger electron spectroscopy (AES), Rutherford back scattering (RBS) and the most recent Two-laser ion trap mass spectrometry (L2ITMS) techniques are utilized when quantification and chemical-state information are required[272-274]. L21TMS is usually employed in conjugation with XPS. One of the most recent techniques for the explicit nanoscopic surface analysis is scanning force microscopy[275]. Angle-resolved surface sensitive soft X-ray absorption spectroscopy[276,277] (NEXAFS) can be used to observe preferential orientations of segments of macromolecules at the surface of polymer by varying the angle between the linearly polarized synchrotron light beam and the surface normal to the investigated sample.

Emoto et al.[278] have recently developed two methods involving determination of partition coefficient and determination of electroosmosis or particle electrophoretic mobility for evaluating polymer (such as polyethylene glycol)-coated surfaces, including surface grafting chemistry, thickness, stability and surface alteration or "masking". Surface plasmon resonance[279] (SPR) and AFM helps in the determination of kinetics and three-dimensional visualization of the alterations on the polymer surface[280]. *Murgasova et al.*[281] have developed the application of liquid chromatography at the critical adsorption point (LC CAP) to analyze PEO-g-PS with short side chains. Using this technique, same authors have determined the apparent molecular weight of polystyrene backbone, the number graft chains per unit backbone and the amount of poly(ethylene oxide) in the graft copolymers. The data obtained by LC CAP were compared with results of static light scattering (SLS), differential refractometry and conventional SEC.

1.6.1 Contact Angle Measurement

This technique helps to reveal the contact angle of a liquid with a solid surface. It is the most simple and sensitive technique to determine the changes in the surface energy and hence hydrophilicity or hydrophobicity of a surface[282,283]. Since, it is very difficult to obtain exquisite information of the outermost few angstroms of a solid surface by any other technique, solid/liquid/ vapor (S/L/V) contact angle measurement emerges to be one of the most surface sensitive probes. The basis of the contact angle technique is the three-plane equilibrium, which exists at the contact point at solid/ liquid/ vapor interface shown in **Figure 1.8**. This equilibrium is normally considered in terms of the surface and interfacial tension or surface and interfacial free energies present in the system.

Figure 1.8 The coexisting solid / liquid/ vapor interface for a water droplet on a non-deformable polymer film.

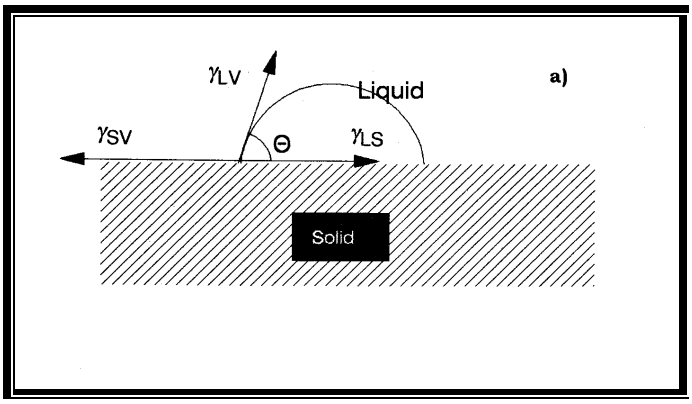

The contact is governed by the force balance at the three-phase boundary and is defined by Young's equation[284].

$$\gamma^{LV} \cos\theta = \gamma^{SV} - \gamma^{SL}$$

γ_{LV} = surface tension of the liquid in equilibrium with its saturated vapor.

γ_{SV} = surface tension of the solid in equilibrium with the saturated vapor of the liquid

γ_{SL} = interfacial tension between the solid and liquid.

Stable equilibrium is obtained only if the following conditions are met:

- The solid surface is rigid, immobile and non-deformable.
- As shown in Figure 1.8, the vertical component of the liquid surface tension $\gamma_{LV} \sin\theta$ is balanced by the elastic stress induced in the solid.
- The solid surface is highly considerably smooth and homogenous. i.e. the surface does not consist of regions, which vary greatly in surface free energy
- The liquid does not swell the solid surface.
- The liquid vapor does not get adsorbed onto the solid surface.
- The polymer surface dynamics does not exist during the time course of the measurement.

Contact angle hysteresis

Equilibrium contact angle is rarely observed and the measured contact angle shows different extent of hysteresis because, one or more of the conditions mentioned above are not met. It is commonly observed that if one measures the contact angle of a liquid drop being advanced slowly over a polymer surface, known as *advancing contact angle* and then makes the measurement with the drop receding over the previously wetted contact surface, known as

receding contact angle, the two contact angles are different. The difference between the advancing and the receding contact angle is commonly known as *contact angle hysteresis*. *Langmuir*[285] was perhaps the first person to suggest that the contact angle hysteresis was caused by the rearrangement of functional groups on the surface.

Some of the commonly used techniques to measure contact angle[286-288] are *Sessile drop method*, *Captitive bubble method* and *Wilhelmy plate method* as shown in **Figure 1.9 (a), (b) and (c)**.

Figure 1.9 (a) Sessile drop method **(b)** Captive bubble method **(c)** Wilhelmy plate method.

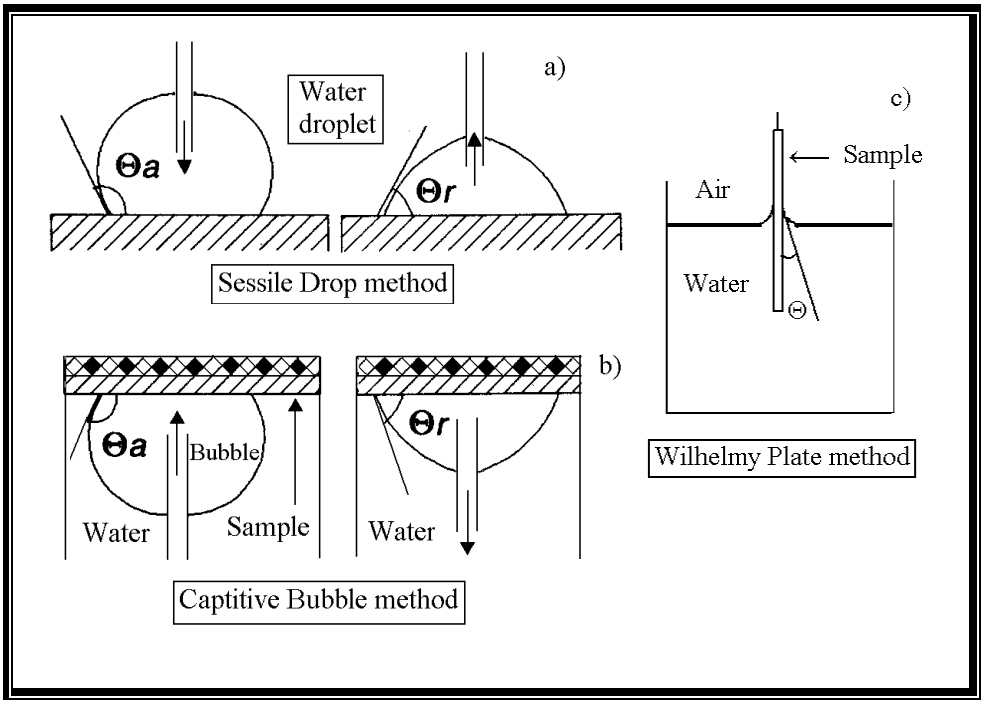

Water is the most versatile liquid probe in contact angle measurement. The water contact angle on the surface is an inverse measure of surface hydrophilicity[289]. Water and diiodomethane are commonly used as liquid probes to estimate surface energies of the solids in terms of polar and non-polar component. Aqueous solutions of different pH are useful to study the acid-base properties of surface ionic groups and also used to determine effective *pKa* values.

1.6.2 Attenuated Total Reflectance Infrared Spectroscopy (ATR-IR)

Infra-red (IR) spectroscopy is a well-established and widely used technique for the identification of functional groups. *Harrick and Fahrenfort*[290,291] with their pioneering efforts, developed a technique, called attenuated total reflectance spectroscopy in which IR spectra of the thin films/ plates can be obtained from near surface region. In ATR-IR, the IR light passes through the optically denser crystal and reflects at the surface of the sample as shown in the **Figure 1.10**. An ample literature[292-297] is now available on the characterization of polymer surface using ATR-FTIR. According to Maxwell's theory, "when the propagation of light takes place through an optically thin, non absorbing medium, it forms a standing wave perpendicular to the total reflecting surface. If the sample absorbs a fraction of this radiation, the propagating wave interacts with the sample and becomes attenuated, giving rise to a reflection spectra, very similar to the absorption spectra".

Figure 1.10. Working of ATR-FTIR.

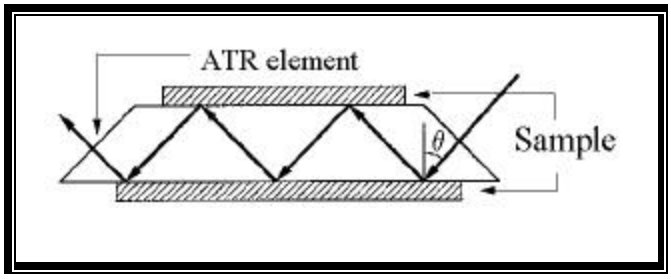

The depth of penetration (d_p) of ATR-FTIR, can be determined using the following equation.

$$d_p = \frac{\lambda_0}{2\pi n (\mathrm{Sin}^2\theta - n_{21}^2)^{1/2}}$$

where θ = angle of incidence between the radiation beam and the normal to the surface.

λ = wave length of the radiation.

$n_{21} = n_2 / n_1$ = refractive index of the sample/refractive index of the optical element.

From the above equation it is obvious that the depth of penetration is linearly dependent on the wavelength of the radiation. Moreover, d_p also depends on the angle of incidence of the radiation, the refractive index of the ATR crystal and the refractive index of the sample. In order to undergo total internal reflection, the IR light should be incident on the ATR crystal at an angle θ, greater than the critical angle θ_c, where $\theta_c = \text{arc sin } (n_2 / n_1)$.

1.6.3 Scanning Electron Microscopy (SEM)

This technique is essentially employed when high resolution-three-dimensional images of the surface morphology are desired [298-301]. When an electron beam impinges on a sample, back scattered electrons, secondary electrons and x-rays are produced as seen in the **Figure 1.11**. A scintillation detector detects secondary electrons, which are emitted from a surface with low energy 50 eV. They are primarily produced within the top few nanometers of the sample. Back-scattered electrons are of high energy and come from the depth of 1µm or more.

Figure 1.11 shows the outline and working of SEM.

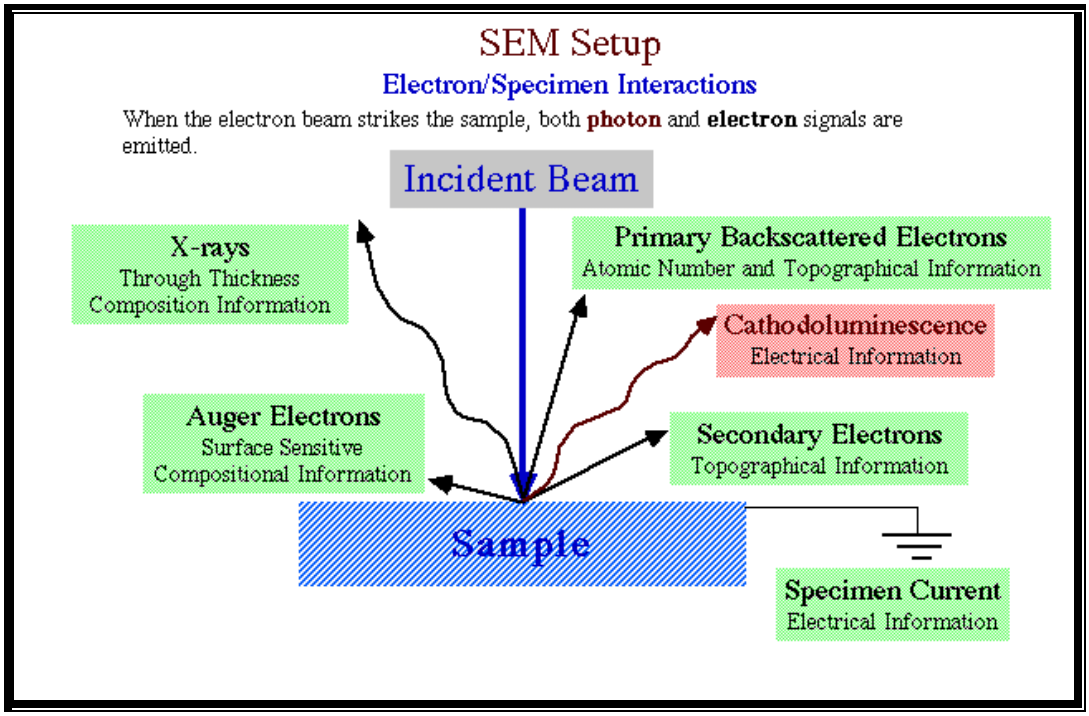

If the system is equipped with an X-ray detector, which measures either the wavelength or the energy of the X-rays, elemental analysis can also be performed [302,303]. The primary electron beam can be focused down to nanometer scale. High-energy electrons are used to obtain high spatial resolution, whereas low-energy electrons are used to increase surface details. To attain a conducting surface and to minimize the beam damage, polymer samples are usually coated with a metal such as gold.

1.6.4 Atomic Force Microscopy

Atomic force microscopy (AFM) is a neoteric tool designed to achieve a high degree

of sensitivity while investigating surfaces of conductors as well as insulators on an atomic scale[304,305]. AFM is based on the concept of scanning tunneling microscope (STM) and is a combination of the principles of the STM and the stylus profilometer[306] (SP). AFM incorporates a probe that does not damage the sample surface and imparts a lateral-resolution of 30 A° and vertical resolution less than 1 A°. The SEM and SP have emerged to be powerful microscopic techniques for studying the surfaces of conductors at an atomic level. The lust of a similar technique for the bulk insulators is now fulfilled by AFM. Using this technique, it is possible to measure all types of forces from inter-atomic to electromagnetic forces[307].

AFM images are obtained by measurement of the force on the tip of the scanner (usually diamond), which is generated by its proximity to the surface of the sample. When the tip is moved horizontally, it follows the path along the surface contours represented by the trace B in the **Figure 1.12**. From the experimental setup[308] shown in the **Figure 1.12** it can be noticed that the cantilever with the attached stylus, is sandwiched between the AFM sample and tunneling tip, which is fixed to a small piezoelectric element called the *modulating piezo*, which drives the cantilever beam at its resonant frequency.

Figure 1.12 The experimental setup of AFM and the path of tip along the surface contours.

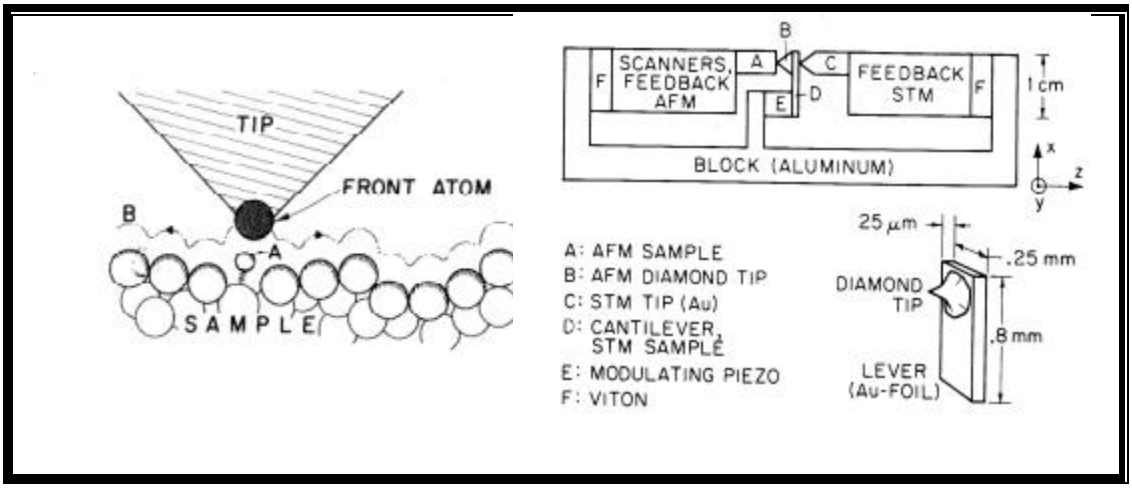

Recently, this technique is often used to detect the interaction of biological systems with organic/polymeric surfaces [341]. AFM with chemically modified tips is more recently used to study the pH dependent changes in the + ve and – ve charges on the substrate surface[310].

1.6.5 X-ray Photoelectron Spectroscopy (XPS)

XPS is perhaps the foremost and widely accepted method for organic surface analysis since, it can identify and quantify elements/functional groups on a surface[311-313]. When a material is irradiated with electromagnetic radiation of sufficient energy, the core electron from the atom is knocked out. This knocked out electron is called *photoelectron* and this effect is called *photoelectric effect*. The excess energy of the irradiation is converted to the kinetic energy of the ejected photoelectron. The binding energy (E_b) of the inner shell electron is determined by the difference between the X-ray photon energy and the kinetic energy, (E_k) of the ejected photoelectron:

$$E_b = h\nu - E_k$$

XPS involves irradiation of the material surface with soft X-rays and measurement of the E_k of the photoelectron. Since the binding energy of the particular shell of an atom is unique for each element; measurement of kinetic energy and hence the binding energy allows the identification of the element[314].

An XPS instrument consists of an X-ray source, an electron analyzer to measure the kinetic energy of photoelectrons, and a data acquisition and processing system[315]. Just as many other surface analysis techniques, XPS is also conducted in an ultra-high-vacuum environment (< 10^{-9} torr). This is essential because the mean elastic path of the photoelectrons is just few centimeters. High vacuum enables to increase this mean elastic path of the photoelectrons in order to cover the distance between the sample and the analyzer. Moreover, it also helps to minimize the contamination from the atmosphere and to avoid the formation of the monolayers of adsorbed material, which affects the quantitative and qualitative analysis of the sample.

In most commercial spectrometers, Al and Mg are used as X-ray target materials, because they produce an X-ray with narrow line width and have sufficient energy to excite the core level electrons of most of the atoms. Many researchers have extensively studied surface modifications using XPS[316-319].

1.6.6 Static secondary ion mass spectroscopy (SSIMS)

SSIMS is another surface selective technique for the characterization[320-322] of modified surfaces. The information obtained from SSIMS complements XPS because, SSIMS can differentiate those polymers that give very similar XPS spectra. Moreover, it offers higher surface selectivity than XPS. The typical sampling depth of SSIMS is approximately 1 nm. This method has sensitivity, sufficient enough to detect amounts less than a monomolecular

layer, particularly, when a high-resolution time-of-flight (ToF) mass analyzer is used [323].

In this technique, a primary noble gas atom or ion (e.g. Ar^0, Ar^+, Xe^0, Xe^+) beam is bombarded on the sample under ultra high vacuum, penetrating to a depth of 30-100 A°. The kinetic energy of the particle is assumed to dissipate via a collision cascade process, which causes the emission of electrons, neutral species and secondary ions, the yields of which vary with polymer surface composition and obviates the possibility of quantitative SIMS information. The positively and negatively charged ions are analyzed in terms of their mass-to-charge ratio by a quadruple or (ToF) mass spectrometer, yielding a positive and negative secondary ion mass spectrum.

The sampling depth of the SSIMS analysis of polymers under these 'static' conditions is of the order 10-12 A^0. Since, the irradiation of the samples may induce sample charging, which will suppress secondary ion yields, the optimum conditions for surface potential are controlled by the simultaneous irradiation of the sample with a flood of low-energy electrons. More recently, ToF SIMS instruments with improved transmission characteristics, good mass discrimination and high working mass ranges (m/z = 0-10000 Da) have been developed [324,325]. The immobilization of unsaturated surfactant; sodium 10-undecenoate and the saturated surfactant sodium dodecanoate carried out on PE surfaces was recently studied by SSIMS[326].

1.6.7 Two Laser Ion Trap Mass Spectroscopy (L2ITMS)

Secondary ion, secondary neutral and laser desorption/ photoionization mass spectrometries are increasingly being applied to organic surface analysis[327-329]. L2ITMS is used for the detection of microscopic amounts of organic materials on the sample surfaces. Many methods of organic surface analysis are although best in their present form provide either insufficient or ambiguous data. For example, XPS has a limited chemical resolution and usually cannot distinguish the sequence of functional groups in a molecule. On the other hand, techniques like high resolution electron energy loss (HREEL), resonance Raman and infrared reflection spectroscopies can identify functional groups and their orientation at the surface but limit themselves to the molecular complexity, optical selection rule and film thickness, giving rise to surface vibrational spectra often, difficult to interpret. Although, ion trap mass spectrometer is less sensitive than the TOF-SIMS, its advantage lies in its tandem mass spectrometry (MS^2) capability[330]. The relative simplicity and low cost of the ion trap are particularly the attractive features of this surface analysis technique.

Principle

The recently developed Two laser ion trap mass spectroscopy uses one laser to desorb

intact molecules from the surface, a second laser for photo-ionization, and an ion trap for single or tandem mass spectrometric analysis.

Instrumental details

The schematic diagram of the apparatus is shown and it's working can be understood from **Figure 1.13**. This modern apparatus possesses separate lasers for desorption and post-ionization, a 170 L/s turbo molecular pump and a MS^2 analyzer. Sample desorption is achieved with the 1064 or 355 nm pulses of Nd: YAG laser. The distance between the probe's surface and the first end cap is 29 ± 2 mm. Laser ionization is achieved with 266 nm pulses. The ion trap experimental conditions are optimized to obtain maximum ion current at minimum peak broadening. The ion trap is operated in rf-mode only, with occasional addition of SWIFT pulses to eject unwanted low-mass ions.

Figure 1.13 The L2ITMS apparatus and it's working.

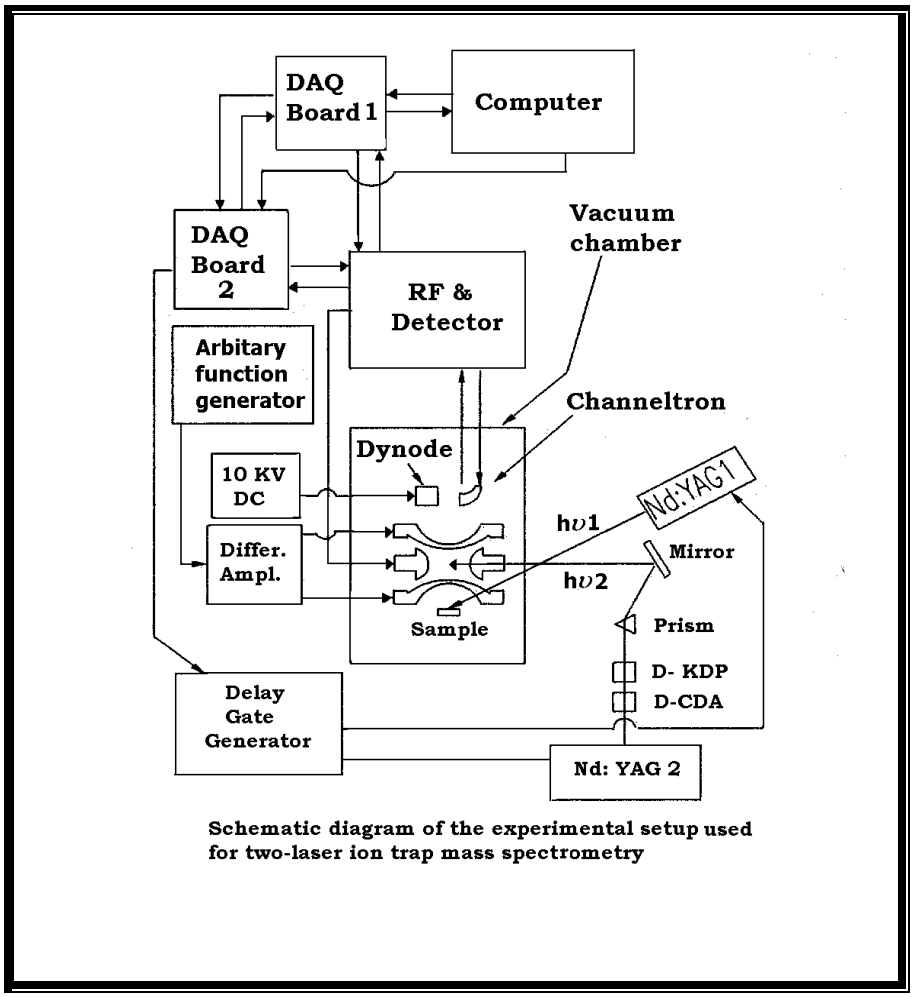

Application

L2ITMS is increasingly being used to analyze the organic mixtures/ complex molecules on the polymer surfaces[331]. Since, the mass spectra of these mixtures are often difficult to interpret, *Kornienko et al.*[328] used L2ITMS in conjunction with XPS to chemically analyze the surface of an ion-bombarded polystyrene thin film.

1.6.8 Scanning Kelvin Microprobe (SKM)

The scanning Kelvin microprobe is one of the most recent tools for investigating the surface-related processes due to its high sensitivity towards structural variations[332], surface modification[333] and contamination[334]. This technique involves the measurement of the *work functions* of the surfaces. Work function can be measured either directly, by the emission of electrons from the surface (i.e. via photoelectric or thermionic methods) or indirectly, by the measurement of the potential difference, which appear upon keeping the materials with different work functions in close proximity. Since, there is no contact between the two plates, this technique is one of the few nondestructive methods of investigating sample surface. For this technique lateral resolution is 1μm and the contact potential difference is in the millivolt range. The instrument is capable of simultaneously imaging the contact potential difference and topography of a scanned surface. Thus, this tandem characterization provides unique information regarding material properties and yields high-resolution topographical images.

Principle

The SKM is based on a parallel plate capacitor model[335]. This historical development of a scanning microscope is based upon the principles proposed by Lord Kelvin[336] where one plate with known work function is used as a reference and the sample with unknown work function represents the other plate. SKM measures the potential difference between the vibrating tip and the sample surface.

Instrumentation

Figure 1.14 represents schematic diagram and working of the instrument, with technical details described elsewhere[337]. The system consists of five units; a distance control unit, scanner, a current to voltage converter, a signal collection unit and a measurement system. The cardinal component of the instrument is its sensing tip. The tip is made from a material with a known work function, usually tungsten. Recently, SKM with voltage modulation has been developed to obtain the discrete surface potentials[338].

Application

Scanning Kelvin Microprobe is a new valuable tool to study the surface chemistry of different conducting, semiconducting and insulating materials[339]. The application of SKM to a non-conducting surface of polymer-based-breast implants[340] is recently reported.

Figure 1.14 represents schematic diagram and working of the SKM.

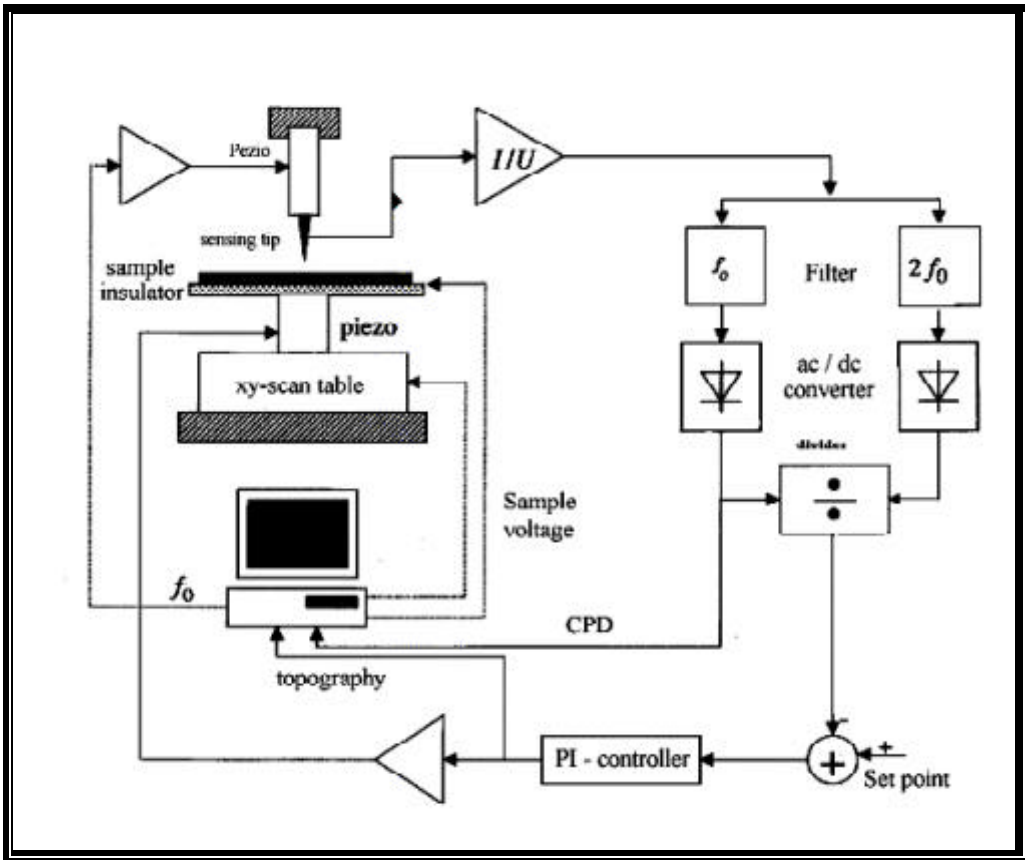

1.7 INFLUENCE OF SURFACE ANCHORED STABILIZERS ON POLYMER DEGRADATION AND STABILIZATION

1.7.1 Polymer Degradation

Degradation is an irreversible change, resembling the phenomenon of the metal corrosion. Degradation of the polymers is a very crucial aspect, which affects their performance in daily life. Throughout the life of a polymer, it encounters different kinds of degradation at various stages, starting from the reactor where a polymer is synthesized, in

extruder where it is processed, during service life and after its failure when it is discharged into the environment. The degradation of polymers involves several chemical and physical processes accompanied by small structural changes, which lead to significant deterioration in useful properties of the polymeric materials[341]. Most of the oxidative degradations[342] take place at the surface of polymeric material because oxidative processes are more intense at surface due to greater availability of oxygen and high temperature. Thus, a brittle outer layer is formed on the polymer surface due to its weathering. Polymer degradation can be manifested from the changes in their chemical structure, reduction in their molecular weight due to chain scission, yellowing, embrittlement and the loss of transparency.

Based on the factors causing the degradation, various types of degradations are as follows:

(a) Thermal degradation: by heat and oxygen
(b) Photo-oxidative degradation: by UV light and oxygen
(c) Mechano-chemical degradation: mechanical energy in shear during melt processing
(d) Chemical degradation: by corrosive chemicals and gases
(e) Radiation induced degradation: by high-energy radiations viz. X-rays and γ-rays
(f) Degradation due to natural weathering: by combination of agents such as wind, rain & light

1.7.2 General mechanism of degradation

Bolland and Gee[343] discovered that the photo- and thermo-oxidative degradation are radical chain processes initiated by the functional groups present in the polymer chain. The degradation mechanism is divided into three main steps, (a) Initiation (b) Propagation (c) Termination

1.7.2.1 Initiation

When polymers are exposed to UV radiation, ionizing radiation, heat etc., they generate free radicals in the polymer backbone as shown in the **Scheme 1.8 (a)**:

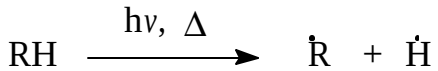

Scheme 1.8 (a)

1.7.2.2 Propagation

In the propagation reaction, the degradative chain is prolonged by the following reactions:

(a) *Formation of polymeric hydroperoxides*

The polymeric radicals and atmospheric oxygen react very fast to form alkoxy and alkylperoxy macroradicals. These macroradicals often, abstract H atom from their vicinity generating many more radicals in the polymer backbone to further react with the atmospheric oxygen (**Scheme 1.8** (b)):

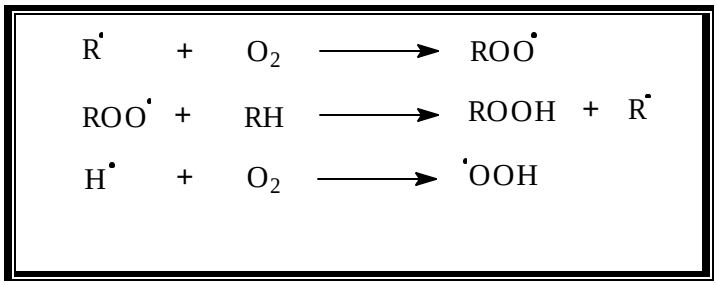

Scheme 1.8 (b)

(b) *Decomposition of polymeric hydroperoxides:*

The free hydroperoxides under the influence of heat and light undergo decomposition to form either homolysis or heterolysis products as shown in the **Scheme 1.8** (c):

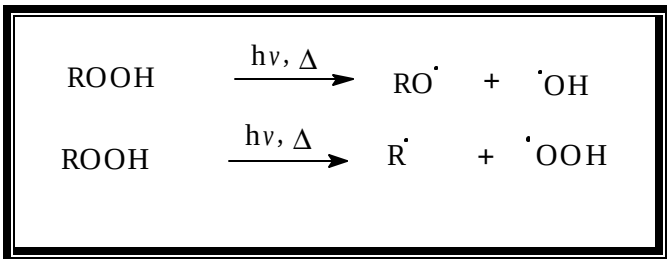

Scheme 1.8 (c)

The Scheme 1.8 (d) and (e) shows that hydroxyl groups are formed as a result of the reaction between alkoxy macro radicals and other polymer molecules. Reaction between two polymer alkoxy radicals by disproportionation method results in the formation of C=O and O-H species.

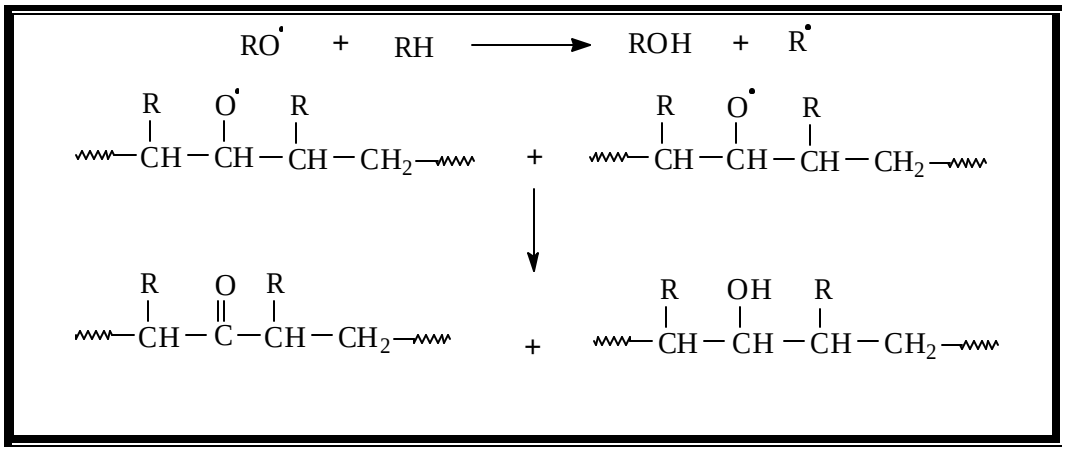

Scheme 1.8 (d) and (e)

1.7.2.3 Termination

The termination of the radical chain takes place by the recombination of the free radicals with the other molecules, forming inactive products **Scheme 1.8** (f):

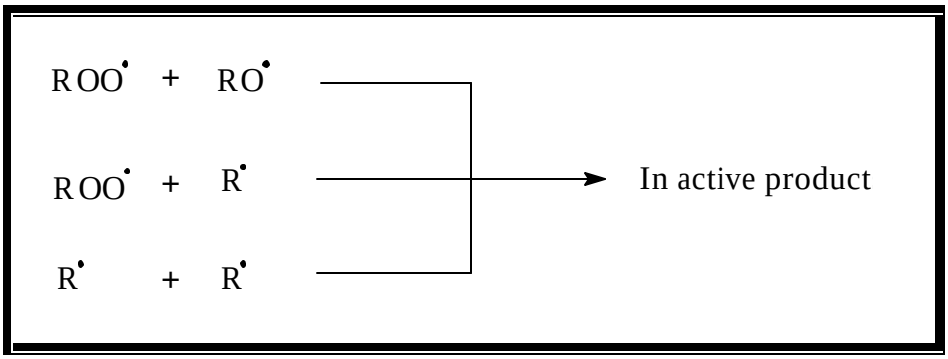

Scheme 1.8 (f)

The polymer radicals usually undergo coupling or crosslinking, depending upon the steric factors. The type of inactive products formed, depends upon the chemical and physical structure of the exposed polymers.

1.7.2 General mechanism of stabilization

As described earlier, the polymers undergo degradation at various stages of their production and service life. Exposure of most polymers to the natural and induced environmental conditions, UV radiation, either alone or in combination with oxygen, profoundly deteriorates their mechanical and optical properties. Small quantities of additives called stabilizers are added into the polymer matrix to retard degradation or depolymerization and impart long-term outdoor stability to the polymers. The stabilizers quench the electronic

excitation energy associated with specific chromophores as a result of photon absorption. It has been established that light screeners, UV absorbers, antioxidants, peroxide decomposers, radical scavengers and excited-state quenchers effectively help in achieving polymer stabilization. The commonly used polymer stabilizers are listed below.

1.7.3.1 Light screeners

The light screeners are interposed as shields between the radiation and the polymer. They function either (1) by absorbing the radiation before it reaches the photoactive species in the polymer or (2) by limiting the damaging radiations penetration into the polymer matrix. Reflection of radiation can be achieved by the selection of suitable paints, coatings or pigments or by metallizing the surface[344]. The pigments used in dispersed form in the polymer matrix show protective activity as screeners due to their low surface energy. Carbon black is commonly used as a pigment because it is the most-effective light screener[344], especially at high temperatures.

1.7.3.2 UV absorbers

The function of the ultraviolet absorber is the absorption and harmless dissipation of ultraviolet radiation, which would otherwise initiate degradation of polymer material. . The *o*-hydroxybenzophenones and *o*-hydroxybenzotriazoles are important groups of UV absorbers since both the groups absorb strongly in the UV region. The photostabilization mechanism[345] of *o*-hydroxybenzophenone and *o*-hydroxybenzotriazoles are believed to be a rapid tautomerism of the excited state as it is shown in **Scheme 1.9**.

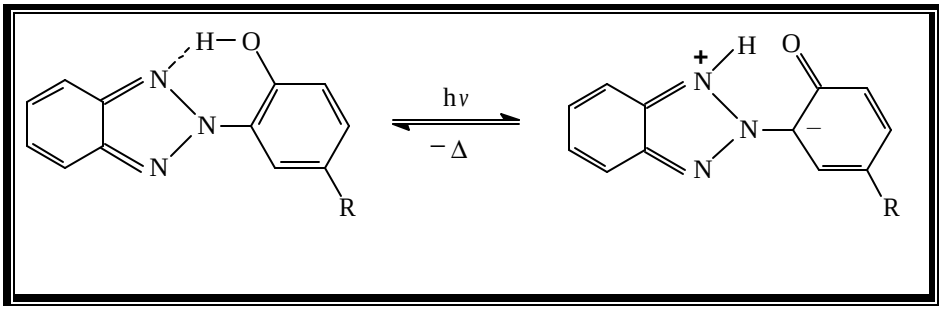

Scheme 1.9

The more basic the hetero-atom (O) in the ground state, the more photo stable is the compound. It is assumed that, in the ground state, the *enol* form is energetically preferred, whereas the reverse is true for the first excited singlet. An argument for this viewpoint lies in the fact that, in the excited state, phenol becomes much more acidic, whereas the hetero-atom O becomes more basic than in the ground state[346].

1.7.3.3 Antioxidants

Antioxidants act as a chain-terminating agent. They stabilize the polymer through the well-known electron delocalization or resonance methods. The unique merit of antioxidant radical is that it does not react with the polymer to initiate a new radical. The antioxidants react faster with peroxide radical (ROO•) then with macro radical (R•) and the activity depends upon their structure[347]. The low molecular weight derivatives of BHT (2,6-ditert butyl-4-methyl phenol) though being effective antioxidants, are highly volatile due to the labile CH_3 group. The secondary arylamine antioxidants are more effective compared to the hindered phenolic antioxidants and they are often used as antiozonants.

1.7.3.4 Hindered amine light stabilizers

Tetramethyl piperidines are commonly known as hindered amines. The hindered amine light stabilizers (HALS) are multifunctional photostabilizers. Ever since their discovery, HALS has gained enormous importance as photostabilizers. The interest in this area was developed because of stable 2,2,6,6-tetramethyl-4-oxopiperidine-N-oxyl free radical[348], which showed an excellent radical scavenging property. They showed UV stabilization in polypropylene, polyethylene, polystyrene and nylon with excellent regenerative radical scavenging capability. The mechanism and mode of action of HALS is well documented by many researchers[349,350]. In the stabilization process HALS can function as:

(a) Decomposer of hydroperoxides and peracids

(b) Deactivators of the charge transfer complexes

(c) Quenchers of singlet oxygen and ketones

(d) Decomposer of ozone

1.7.4 Polymer bound stabilizers

Protection of polymer against thermal and photo-oxidative degradation is achieved by blending the stabilizers in the polymer matrix. Compatible and mobile stabilizers usually give the best protection, but low molecular weight stabilizers are easily lost from the polymer through evaporation or leaching. In order to avoid this loss, polymeric stabilizers have been devised, but their low mobility and poor compatibility often decrease their efficiency. To further improve the performance of the stabilizers, polymerizable stabilizers[351] have been employed with successful results of stabilization compared to the previous methods. These stabilizers generally have a vinyl group or a condensable functional group as a side arm, which can be copolymerized during processing.

1.7.4.1 In-chain copolymerized stabilizers

This class of copolymers mainly comprise of the vinylic stabilizers, which are either added to the feed reactor (in an additive proportion) along with the monomer to yield random block copolymers containing active stabilizers in their backbone or are added during the polymer processing to yield *insitu* grafted copolymers (**Scheme 1.10 (a) and (b**).

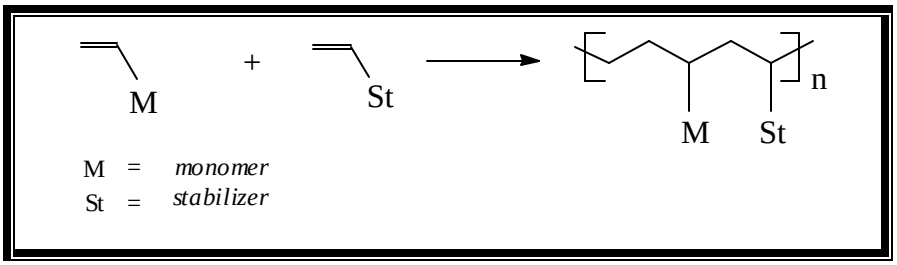

Scheme 1.10 (a)

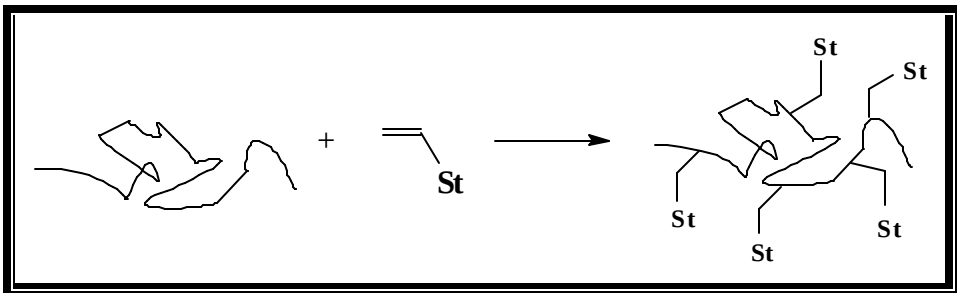

Scheme 1.10 (b)

This class of stabilizers has recently generated a lot of industrial applications. The striking examples of these stabilizers are acryloyloxy HALS and acryloyloxy benzotriazole derivatives[352].

A similar class of stabilizers have also been devised where copolymers with definite proportion of succinic anhydride were first synthesized, followed by secondary reactions between the anhydride group and functionalized HALS to yield polymer with pendant HALS moieties. The secondary reaction takes place via anhydride ring opening mechanism [353].

1.7.4.2 Surface-grafted polymer stabilizers

The thorough understanding of the mechanism of polymer degradation and stabilization has brought about many changes in the design and application of polymer stabilizers[354, 355]. Since, the degradation of any polymer commences from the surface and proceeds towards the bulk, stabilizers are expected to be more efficient when they are also located at the surface. The concept of surface grafted stabilizers has thus emerged. Surface

grafting of stabilizers can be brought about either by directly grafting the vinylic stabilizers to the polymer surface[356] or by first grafting a functional monomer followed by coupling the stabilizer with its functional groups via condensation reactions. However, it should be noted that unreacted functional groups on the polymer surface may act as chromophores leading to unfavorable reactions. Hence, quantitative transformation of the functional groups is the key to the successful stabilization in the later case.

1.8 APPLICATIONS OF SURFACE MODIFIED POLYMERS

Automotive Applications

PP-bumper-paintability

Thermoplastic olefin polymers such as PP and HDPE are used in the manufacture of numbers of automotive parts such as bumpers, window shield, handle and other accessories. However, they have a poor paintability to match the finishing of other automobile body parts. In order to overcome this shortcoming, the polymer surface is either treated by nitrogen plasma or flame treatment. During this treatment, the functional groups are generated on the polymer surface, which enhances its adhesion to paints.

HDPE-fuel tank-permeability

High-density polyethylene is used to make fuel tanks of the automotives, which is an alternative material for steel tanks. HDPE has many advantages over steel, especially the design freedom to utilize unused space and low weight but the shortcoming of HDPE is its permeability to the gasoline. Since, the permeability of a liquid in the polymer depends both on the nature of the bulk as well as surface of the polymer, the surface modification of this polymer by fluorinating it using plasma/corona treatment could successfully overcome the shortcoming.

Conductivity applications

Metallization of plastic surface

Polymer/metal interfaces are encountered in many applications of polymers such as electronic devices, packaging application, electrical appliances etc. Many desirable surface properties, such as electrical conductivity and optical characteristics can be achieved with metal coating. Typically, there are two major techniques for the deposition of metal coating on polymer surface–sputtering and electroless plating. Third and most recent approach for metallization of PE surface is the surface grafting of conducting polymers[357] viz.

polythiophene. PE surface was modified in a three-step process to obtain surface conductivity of 10-6 S/cm^2. A similar attempt to fabricate conducting polymer surface was made by *Neoh et al.*[358].

Membranes

Selective permeability

Polymeric membranes are frequently used to control selective flow of mixtures of gases and liquids. The transport of material through a membrane depends on the chemical and physical characteristics of both the bulk and the surface. Cation-exchange membranes[359] modified with the carboxylic acid groups for battery separator were prepared by radiation-induced grafting of acrylic acid (AA) and methacrylic acid (MA) onto a polyethylene (PE) film. Ion-exchange membranes[360] modified with sulfonic ($-SO_3H$) and phosphonic acid ($-PO_3H$) groups were prepared by radiation-induced grafting of glycidyl methacrylate (GMA) onto polyethylene (PE) films and subsequent sulfonation and phosphonation of poly(GMA) graft chains. The PE membrane modified with $-PO_3H$ group had a lower specific electrical resistance than that of PE membrane modified with $-SO_3H$ group.

Adhesion

Due to their inert surface, polyethylene suffers from a large number of adhesion problems, which can be overcome by well-known surface modification techniques. For example, the auto adhesion of PE films, to enhance the "heat sealing" of PE films can be improved considerably by plasma, corona discharge and oxidation by inorganic oxidants. *Ishihara and coworkers*[361] have recently reported photoinduced graft polymerization of a phospholipid, (2-methacryloyloxyethyl phosphorylcholine) on polyethylene membrane surface, which improved its resistance towards blood cell adhesion. This shows that resistance to adhesion is equally important for some specialty applications. Surface modification of HDPE by DC glow discharge significantly improved its adhesive bonding to steel. Surface modification of polymer films by graft copolymerization led to adhesive-free adhesion. Excimer laser induced surface modification of ultra-high-strength polyethylene fibers enhanced their adhesion with epoxy resins. Polyethylene-polypropylene core materials upon subsequent surface modification with peelable laminated films can be used for confidential postcards[362]. The PE-wood interfacial bonding strength was improved by using the surface modified PE[363] in the composite material. Plasma-pretreated and graft copolymerized HDPE films significantly improved their adhesion with evaporated copper.

Stabilization against degradation

The oxidation and degradation of polymers begin from the surface and slowly proceeds into the bulk. Stabilizers are therefore expected to be the most effective if they are concentrated at the surface, where oxidation takes place. *Singh et al.*[356] have reported single and two-step grafting procedures to covalently link photostabilizer onto the surface of polyolefins including PE. This novel stabilizer is found to be extremely efficient in preventing the photo-oxidation compared to the conventional melt blended stabilizers[364].

Biomedical applications

Together with the advances made in structural and functional substances over the last few decades, there have been an increasing number of developments in materials for use in biomedical technology. Amongst these were the first artificial heart valves, pacemakers, vascular grafts and kidney dialysis. In the following years, advance in materials engineering made possible the use of orthopeadic devices such as knee and hip joint replacement as well as intraocular lenses in the treatment of cataract patients. A true bio-compatible material should certainly possess surface merits like blood compatibility, antibacterial activity, cell/ immuno adhesivity, tissue binding etc. Due to the freedom of design, inert and non-corrosive nature, polymers have proved to be the most favorable alternative for biomedical applications[365]. Temperature responsive controlled drug delivery using biodegradable polymers is presently under extensive study worldwide. Biocompatible materials have been prepared by various methods since their discovery. Efforts were made to improve the surfaces of silicon rubber, polyethylene and polypropylene via graft copolymerization of vinyl functional monomers for their biomedical applications. Biocompatibility and antithrombogeneity of several plastic materials have been improved by radiation-induced grafting of functional monomers like HEMA and AAm. Surface modification of polyethylene balloon catheters for local drug delivery has been recently reported. Surface modification of poly(ethylene-co-vinyl alcohol) (EVA) films via carboxyl group introduction and subsequent immobilization of collagen form excellent biocompatible films. The **Table 1.2** shows the polymers and their potential biomedical applications.

Table 1.2 shows the polymers and their potential biomedical applications.

Polymers	**Applications**
Polyethylene	Articular replacement
Polypropylene	Suture material
Polytetrafluoroethylene	Vascular grafts
Polyester	Resorbable systems
Polyurethane	Blood contact device
Polyvinyl chloride Polymethyl methacrylate	Tubes and Bags Intraocular lenses
Polyacrylate	Dental implants
Silicone rubber	Soft tissue replacement, Ophthalmology

1.9 REFERENCES

1. G. Koo, *Flouropolymers*, Ed. L. A. Wall; Wiley-Interscience, NewYork (1972).
2. A. Baskkin, M. Deyme, M.Nishino, L. Ter-Minassian-Sagara, *Prog. Colloid Polym. Sci.*, **61**, 97 (1976).
3. P. Wang, K. L. Tan and E. T. Kang, *J. Biomater. Sci., Polym. Ed.*, **11**, 169 (2000).
4. J. M. Courtney and T. Gilchrist, *Med. Bio. Eng. Comput.*, **18**, 538 (1980).
5. Z. Feng and B. Ranby, *Die Angew. Makromol. Chemie*, **195**, 17 (1992).
6. A. Baigozhin, *Usp Khim* (Russian), **49**, 2241 (1980).
7. M. Suzuki, A. Kishida, H. Iwata and Y. Ikada, *Macromolecules*, **19**, 1804 (1986).
8. H. Iwata and T. Matsuda, *J. Membrane Sci.*, **38**, 185 (1988).
9. H. Kubota and A. Sugiura, *Polym. Inter.* **34**, 313 (1994).
10. A. M. Mayes, D. J. Irvine and L. G. Griffith, *Mater. Res. Soc. Symp. Proc.*, **530**, 73 (1998).
11. M. Biesalski and J. Ruehe, *Macromolecules*, **32**, 2309 (1999).
12. Y. Ikada, *Macromol. Symp.*, **101**, 455 (1996).
13. A. S. Hoffman, *Macromol. Symp.*, **101**, 443 (1996).
14. J. Lucki, J. F. Rabek and B. Ranby, *Polymer*, **31**, 1772 (1990).
15. D. Klee, R. V. Villari, H. Hocker, B. Dekker, C. Mittermayer, *J. Mater. Sci.: Mater. in Medicine*, **5**, 592 (1994).
16. M. Tatiana and J. Paul, *Mater. Plast.* (Romania), **19**, 87 (1982).
17. H. K. Yasuda, Ed. Plasma Polymerization and Plasma Interactions with Polymeric Material, *J. Appl. Polym. Sci. Appl. Polym. Symp.* **46** (1990).
18. K. Russell, *J. Poly. Sci., Part A, Poly. Chem.*, **33**, 555 (1995).
19. T. Hirotsu and N. Asai, *J. Macromol. Sci-Chem.*, A **28**, 461 (1991).
20. V. S. Pashova, G. S. Georgiev and V. A. Dakov, *J. Appl. Polym. Sci.*, **51**, 807, (1994).
21. N. Inagaki, S. Tasaka and T. Inoue, *J. Appl. Polym. Sci*, **69**, 1179 (1998).
22. E. T. Kang, K. G. Neoh, J. L. Shi, K. L. Tan and D. J. Liaw, *Polym. Adv. Technol.*, **10**, 20 (1999).
23. S. L. Kinstle and J. F. Watson, *J. Polym. Sci. Technol.*, **10**, 461 (1977).
24. S. Yamakawa and F. Yamamoto, *J. Appl. Polym. Sci.*, **22**, 2459 (1978).
25. S. Tazuke and H. Kimura, *J. Polym. Sci., Polym. Lett. Ed.*, **16**, 497 (1978).

26. B. J. Ringrose and E. Kronfli, *Eur. Polym. J*., **36**, 591 (2000).
27. H. Inoue and S. Kohama, *J. Appl. Polym. Sci*., **29**, 877 (1984).
28. N. M. Claramma, N. M. Mathew, E. V. Thomas, *Radiat. Phys. Chem.*, **33**, 87 (1989).
29. M. Giurginca, G. Ivan, J. M. Herdan, *Polym. Degrad. Stab.*, **44**, 79 (1994).
30. J. L. Garnett, L. T. Ng and V. Viengkhou, *Radiat. Technol. Conserv. Environ., Proc. Symp.*, International Atomic Energy Agency: Vienna, Austria, *p.561*, (1998).
31. G. Oster, G. K. Oster and H. J. Moroson, *J. Polym. Sci.*, **34**, 671 (1959).
32. A. Chapiro, *J. Polym. Sci.*, **34**, 439 (1959).
33. A. Chapiro, *J. Polym. Sci.*, **48**, 109 (1960).
34. J. J. Levitzsky, F. J. Lindsey and W. S. Kaghan, *SPE J*, 1305 (1964).
35. I. Sutherland, D.W.Brewis, R. J. Heath and E. Sheng, *Surface Interface Anal*. **17**, 507 (1991).
36. D. Briggs, D. M. Brewis and M. B. Konieczko, *J. Mater. Sci*. **14**,1344 (1979).
37. F. Garbassi, E. Occhiello and F. Polato, *J. Mater. Sci.*, **22**, 207 (1987).
38. I. A. Abu-Isa, *Polym.- Plast. Technol. Eng.*, **2**, 29 (1973).
39. K. L. Mittal and J. R. Susko, Ed. *Metallized Plastics, Vol. 1, Fundamental and Applied Aspects*, Plenum Press, New York (1991).
40. M. Romand, M.Charbonnier, M. Alani and J. Baborowski, [Proc. Symp] Ed. K. L. Mittal VSP: Utrecht, Netherland , *Met. Plast.*, **5** 6, 3 (1998).
41. P. Blaiss, D. J. Carlsson, G. W. Csullog and D. M. Wiles, *J. Colloid Interface Sci*., **47**, 636 (1974).
42. K. Kato, *Polymer*, **9**, 419 (1968).
43. K. W. Lee and T. J. McCarthy, *Macromolecules*, **21**, 2318 (1988).
44. K. W. Lee and T. J. McCarthy, *Macromolecules*, **21**, 3353 (1988).
45. N. L. Franchina and T. J. McCarthy, *Macromolecules*, **24**, 3045 (1991).
46. H. L. Spell and C. P. Christenson, *TAPPI*, **62**, 77 (1979).
47. J. A. Lanauze and D. L. Myers, *J. Appl. Polym. Sci*., **40**, 595 (1990).
48. M. Stradal and D. A. I. Goring, *Polym. Eng. Sci.*, **8**, 57 (1976).
49. M. Stradal and D. A. I. Goring, *Polym. Eng. Sci.*, **17**, 38 (1977).
50. D. Briggs and C.R. Kendall, *Polymer*, **20**, 1053 (1979).
51. T. Hjertberg, B. A. Sultan, and E. M. Sorvik, *J. Appl. Polym. Sci.*, **37**, 1183 (1989).
52. D. Briggs and D. M. Brewis, *Polymer*, **22**, 7 (1981).
53. D. Briggs and C. R. Kendall, *Int. J. Adhesion Adhesives.*, **2**, 13 (1982).
54. D. K. Owens, *J. Appl. Polym. Sci.*, **19**, 265 (1975).

55. M. Strobel, C. Dunatov, J. M. Strobel, C. S. Lyons, S. J. Perron and M. C. Morgen, *J. Adhesion Sci. Technol*., **3**, 321 (1989).
56. L. J. Gerenser, J. F. Elman, M.G. Mason and A. B. Wootton, *Polymer*, **24**, 47 (1983).
57. B. Ranby and J.F. Rabek, *Photodegradation, Photo-oxidation and Photostabilization of Polymers*., Chap1, Interscience, New York, p 2 (1975).
58. D.J. Doyle, *Proc. SPIE-Int. Soc. Opt. Eng.*, p.260 (1993).
59. M. Okoshi and M. Murahara, *J. Photopolym. Sci. Technol.*, **7,** 381 (1994).
60. J.E. Klemberg-Sapieha, L.K. Martinu and M.R. Wertheimer, *Met. Plast.*, **2,** 315 (1992).
61. A. Hollaender, J. Behnisch and H. Zimmermann, *J. Appl. Polym. Sci.*, **49,** 1857 (1993).
62. A. Toth, T. Bell, I. Bertoti, M. Mohai and B. Zelei, *Nucl. Instrum. Methods. Phys. Res. Sect. B.*, **148,** 1131 (1999).
63. B. Ranby, *Mater Res Innovations* **2**, 64 (1994).
64. T. Kavc, W. Kern, M.F. Ebel, R. Svagera and P. Poelt, *Chem. Mater.*, **12,** 1053 (2000).
65. C.M. Weikart and H.K. Yasuda, *J. Polym. Sci. Part A Polym. Chem.*, **38,** 3028 (2000).
66. S. Lenka, P. L. Nayak and A. Basak, *J. Polym. Sci*., *Polym. Chem. Ed*., **24**, 3139 (1986).
67. C. H. Bamford and J. C. Ward, *Polymer*, **22**, 277 (1961).
68. A. Chapiro, *J. Polym. Sci*, *Polym. Symp*. **50**, 181 (1975).
69. A. Baszkin, M. Deyme, M. Nishino and L. Ter-Minassian-Saraga, *Prog. Colloid Polym. Sci.*, **61**, 97 (1976).
70. R. Gaczynski and B. Krajewska, *Polimery* (Polish) **30**, 349 (1985).
71. M. T. Razzak, Y. Tabata and K. Otsuhata, *Radiat. Phys. Chem*., **42**, 57 (1993).
72. A. W. Adamson and A. H. Sporer, *J. Inorg. Nucl. Chem.* **8**, 209 (1958).
73. M. Lutfor, S. Silong, W. Yunus, M. Zaki Ab Rahman,; M. Ahmad and M. Haron, *J. Appl. Polym. Sci.*, **77**, 784 (2000).
74. M. K. Mishra, *J. Macromol. Sci. - Rev. Macromol. Chem*., **C 22**, 409 (1982).
75. S. N. Mishra, S. Lenka and P. L. Nayak, *Eur. Polym. J.*, **27**, 1319 (1991).
76. R. S. Lehrle and S. L. Willis, *Polymer*, **38**, 5937 (1997).
77. B. D. Ratner, T. Balisky and A. S. Hoffman, *J. Bioeng*., **1**, 115 (1977).

78. H. A. Kashani, J. A. Barrie and M. H. George, *J. Polym. Sci., Polym. Chem. Ed*. **16**, 533 (1978).
79. Lehman and P. Dreyfuss, *Adv. Chem. Ser*., **176**, 587 (1979).
80. N. Tsubokawa and A. Naitoh, *Shikizai Kyokaishi*, **72**, 475 (1999).
81. M. Takayanagi and T. Kayatose, *J. Polym. Sci., Polym. Chem. Ed*., **21**, 31 (1983).
82. H. L. Needles and K. W. Alger, *J. Appl. Polym. Sci.,* **19**, 2207 (1975).
83. H. Yasuda, in *Plasma Polymerization*, Academic Press, New York (1985).
84. H. Ichijima, T. Okada, Y. Uyama and Y. Ikada, *Makromol. Chem.*, **192**, 1213 (1991).
85. F. P. Epaillard, J. C. Brosse and T. Falher, *Macromol. Chem. Phys.*, **199**, 1613 (1998).
86. H. J. Lee, Y. Nakayama and T. Matsuda, *Macromolecules*, **32**, 6989 (1999).
87. M. Szwarc, *Nature* **178**, 1168 (1956).
88. D. Mecerreyes, P. Dubois, R. Jenrome and J. L. Hedrick; *Macromol. Chem. Phys.*, **222**, 156 (1999).
89. J. Lehman and P. Dreyfuss, *Adv. Chem. Ser*., **176**, 587 (1979).
90. T. Sato, M. Takada and T. Otsu, *Makromol. Chem*., **148**, 239 (1971).
91. T. Sato and T. Otsu, *Makromol. Chem*., **125**, 1 (1969).
92. S. Lenka, P. L. Nayak and I. B. Mohanty, *J. Appl. Polym. Sci*., **30**, 2711 (1985).
93. L. Horner and K. H. Knapp, *Makromol. Chem*., **93**, 69 (1966).
94. C. S. Sheppard and, R. E. MacLeay, US 4045427, 20 pp. (1977).
95. G. Bouquet, W. C. Kentie, P. J. G. de Theije and F. V. Damme, *Polym. Prep*., **37**, 536 (1996).
96. Y. Li, J. M. Desimone, C. D. Poon and E. T. Samuski, *J. Appl. Polym. Sci*., **64**, 883 (1997).
97. N. S. Allen, T. Corrales, M. Edge, F. C. C. Peinado, M. B. Pinar and A. Green, *Eur. Polym. J*., **34**, 303 (1998).
98. A. Bendak, M. I. Khalil, M. H. El-Rafie and A. Hebeiss, *J. Appl. Polym. Sci.*, **19**, 335 (1975).
99. S. N. Bhattacharya and D. Maldas, *Prog. Polym. Sci.*, **10**, 171 (1984).
100. O. Y. Mansour and A. Nagaty, *Prog. Polym. Sci*., **11**, 91 (1985).
101. H. S. Blair, J. Guthrie, T. K. Law and P. Turkington, *J. Appl. Polym. Sci*., **33**, 641 (1984).
102. C. Hamit, H. Hatice, Y. Osman and R. Y. Elvan, *Eur. Polym. J*., **34**, 493 (1998).
103. D. D. Jiang and C. A. Wilkie, *Eur. Polym. J*., **34**, 997 (1998).

104. G. Mario, F. Minto, G. Fontana, R. Bertani and G. Facchin, *Macromolecules*, **28**, 4399 (1995).
105. D. R. Burfield and S. C. Ng, *Eur. Polym. J.*, **14**, 793 (1978).
106. A. Moshonov and Y. Auny, *J. Appl. Polym. Sci*., **25**, 771 (1980).
107. H. Nakayama and T. Nezu, GB 2025433 (1980).
108. E. A. De Los Santos Gonzalez, M. J. L. Gonzalez and M. C. Gonzalez, *J. Appl. Polym. Sci*., **68**, 45 (1998).
109. M. L. Sanduja, C. Horowitz and P. Thottathil, US 5763557, 5 pp (1998).
110. M. D. Hohol and M. W. Urban, *Polymer*, **35**, 5560 (1994).
111. W. Minghong, B. Bao, J. Chen, Y. Xu, S. Zhou and Z. Ma, *Radiat. Phys. Chem*., 56, 341 (1999)
112. D. Knittel and E. Schollmeyer, *Polym. Int*., **45**, 103 (1998).
113. E. T. Ada, O. Kornienko and L. Hanley, *J. Phys. Chem. B*, **102**, 3959 (1998).
114. C. P. Ho and H. Yasuda, *J. Appl. Polym. Sci*., **39**, 1541 (1990).
115. H. Mirzadeh, A. A. Katbab, M. T. Khorasani and R. P. Burford, *Radiat. Tech Asia'93 UV/EB Conf. Expo., Conf. Proc*., **661**, Rad. Tech., Japan (1993).
116. H. Muratake and Y. Shigemitsu, *Kawamura Rikagaku Hokoku*(Japanese), 67-75 (1997).
117. F. P. Epaillard, B. Chevet and J. C. Brosse, *Eur. Polym. J*., **26**, 333 (1990).
118. H. Aoyama and H. Kiguchi, JP 04295818 A2 (1992).
119. S. Yamakawa, *J. Appl. Polym. Sci*., **20**, 3057 (1976).
120. M. P. Carreon, R. Aliev, R. Ocampo and G. Burillo, *Polym. Bull.*, **44**, 331(2000).
121. S. Tazuke, T. Matoba, H. Kimura and T. Okada, *ACS Symp. Ser*., **121**, 217 (1980).
122. F. Yamamoto, S. Yamakawa and Y. Kato, *J. Polym. Sci. Polym. Chem. Ed*., **16**, 1833 (1978).
123. P. D. Kale and H. T. Lokhande, *J. Appl. Polym. Sci*., **22**, 3335 (1975).
124. A. Hebeish, S. E. Shalaby and A. M. Bayazeed, *J. Appl. Polym. Sci*., **22**, 3335 (1978).
125. Y. L. Hsieh, M. Shinawarta and M. D. Castillo, *J. Appl. Polym. Sci*., **31**, 509 (1986).
126. A. Charlesby, *Nature*, **171**, 167 (1953).
127. E. J. Lawton, A. M. Bueche and J. S. Balwit, *Nature*, **172**, 76 (1953).
128. V. Stannett, W. K. Walsh, E. Bittencourt, R. Liepins and J. R. Surles, *Appl. Polym. Symp.*, **31**, 201 (1977).
129. E. M. El-Nesr, A. M. Dessouki and E. M. Abdel-Bary, *Polym. Int*. **46**, 150 (1998).
130. F. Sundardu and S. Kadariah, *J. Appl. Polym. Sci*., **29**, 1515 (1984).

131. D. Bhin and H. T. Huy, *Radiat. Phys. Chem*., **53**, 177 (1998).
132. S. A. Kurbanov, U. N. Musaev, B. S. Khakimdzhanov, E. V. Smurova, S. P. Novikova, N. B. Dobrova and T. Nauchn, *Tashk. Gos. Univ.* (Russian), **502**, 129 (1976).
133. F. Yamamoto, S. Yamakawa and Y. Kato, *J. Polym. Sci., Polym. Chem. Ed*., **16**, 1897 (1978).
134. F. Yamamoto and S. Yamakawa, *J. Polym. Sci., Polym. Chem. Ed.*, **18**, 2257 (1980).
135. B. D. Saidov and U. G. Gaadurov, Uzb. Khim. Zh. (Russian), **5**, 57 (1980).
136. K. Ameya, *Nenpo-Tokkyo-toritsu Aisotopu Sogo Knekyusho* (Japanese), Vol. **43**, (1982).
137. U. P. Wang, *Radiat. Phys. Chem*. **25**, 491 (1985).
138. W. R. Thalman, *Adv. Print. Sci. Technol*., **14**, 302 (1979).
139. B. Jasen and G. Ellinghorst, *J. Biomed. Mat. Res*., **18**, 655 (1984).
140. H. Ha, Y. Pan, J. Wu, F. Yang and X. Feng, *Rad. Phys. Chem*., **25**, 501 (1985).
141. H. Sommer, E. Leuthold and U. Rausch, Ger. Offen., DD 215474 A2 (1984).
142. B. Ranby, J. F. Rabek *Photodegradation, Photo-oxidation and Photostabilization of Polymers*., Interscience, New York, Chap. 1, p. 45 (1975).
143. Catalog: Immersion lamps for Laboratory Experiments, Original Hanau GmbH, German.
144. Chi Ming Chan, *Surface Modification and Characterization of Polymers*., Hanser Publishers (1994).
145. Photodegradation, *Photooxidation and Photostabilization of Polymers*., B. Ranby and J. F. Rabek, John Wiley Publishers, p. 45 (1973).
146. S. Tazuke and H. Kimura, *J. Polym. Sci. Poly. Lett. Ed.*, **16**, 497 (1978).
147. S. Tazuke, H. Kimura and H. Nakayama, Jpn. Kokai Tokkyo koho Jpn 54063178 (1979).
148. S. Tazuke and H. Kimura, *Makromol. Chem*., **179**, 2306 (1978).
149. S. Tazuke, H. Kimura and H. Nakayama, Ger. Offen., DE 78-2725477 (1977).
150. J. F. Kinstle and S. L. Watson, *Poly. Sci. Technol*., **10**, 461 (1977).
151. S. Tazuke, T. Matoba, H. Kimura and T. O. Kada, *ACS Symp. Ser*. **121**, 217 (1980).
152. Y. Ogiwara, H. Kubota and Y. Hata, *J. Poly. Sci. Poly. Lett. Ed., J. Polym. Sci., Polym. Lett. Ed.*, **23**, 365 (1985).
153. C. Decker, *J. Appl. Polym. Sci*., **28**, 97 (1983).
154. P. Gosh and M. Banerjee, *J. Macromol. Chem. Part A*, **17**, 1273 (1982).
155. Y. Ikada and Y. Umaya, Jpn Kokai Tokkyo Koho JP 62104843 A2 (1987).

156. Y. Umaya and Y. Ikada, *J. Appl. Polym. Sci*., **36**, 1087 (1988).
157. H. Kobuta and Y. Ogiwara, *J. Appl. Polym. Sci*., **38**, 717 (1989).
158. B. Ranby, Z. M. Gao, A. Hult and P. Y. Zhang, *ACS Symp. Ser.*, **364**, 168 (1988).
159. S. Edge, S. Walker, W. James Feast and W. F. Pacynko, *J. Appl. Polym. Sci*., **47**, 1075 (1993).
160. H. Kubota, A. Sugiura and Y. Hata, *Polym. Int.*, **34**, 313 (1994).
161. M. Ulbritch and A. Oechel, *Eur. Polym. J*., **32**, 1045, (1996).
162. M. Suzuki and C. Wilkie, *J. Polym. Sci. Part A*, *Polym. Chem*. **33**, 1025 (1995).
163. K. L. Tang, L. L. Woon, H. K. Wong E. T. Kang and K. G. Neoh, *Macromolecules*, **26**, 2832 (1993).
164. J. Janaca, P. Malcik and J. Petrovsky, *Folia Fac. Sci. Nat. Univ. Purkynianoe Brun.*, **18**, 77 (1977).
165. S. Yamakawa and F. Yamamoto, *J. Appl. Polym. Sci*., **25**, 41 (1980).
166. A. B. Gil`man, A. A. Khan, R. R. Shifrina, V. M. Kolotyrkin, V. T. Kozlov and V. A. Orlov, *Vysokomol. Soedin. Ser*. (Russian), **B 21**, 220 (1979).
167. I. Sakamoto, T. Akagi and S. Yamaguchi, JP 61089236 (1986).
168. F. P. Epaillard, G. Legeay and J. C. Bross *J. Appl Poly. Chem*., **44**, 1513 (1992).
169. M. K. Mishra, *J. Macromol. Sci. -Rev. Makromol. Chem.,* **C 20**, 149 (1981).
170. S. E. Shalaby, A. M. Bayzeed and A. Hebeish, *Ibid,* **22**, 1359 (1978).
171. A. Liebersohn and D. H. Kohn, *Ibid,* **12**, 2435 (1974).
172. G. G. Haber and J. M. Weiss, *Naturwissenschaften*, **20**, 94 (1932); *Proc. R. Soc.*, London; **147 A**, 332 (1934).
173. A. Hebeish and P.C. Meheta, *Ibid,* **37**, 911 (1967).
174. S. R. Patil and R. S. Konar, *J. Polym. Sci.*, **57**, 609 (1962).
175. Katot et al.
176. L. Gu, A. N. Hrymak and S. Zhu, *J. Appl. Polym. Sci.*, **76**, 1412 (1999).
177. Huang and N. C. Liu. *J. Appl. Polym. Sci*., **67**, 1957 (1998).
178. S. S. Pesetskii, Y. M. Krivoguz and A. P. Yuvchenko, *Zh. Prikl. Khim* (Russian), **71**, 1364 (1998).
179. M. K. Naqvi and R. Reddy, *Polym. - Plast. Technol. Engg*. **36**, 585 (1997).
180. M. A. Harmer, *Langmiur*, **7**, 2010 (1991).
181. Y. Nakayama and T. Matsuda, *Macromolecules*, **29**, 8622 (1996).
182. C. Anders, R. Gratner, V. Steinert, B. I. Voit and S. Zschoche, *J. M. S.-Pure and Appl Chem.,* **A 36**, 1017 (1999).

183. V. Steinert, M. Ratzsch and S. Reinhardt, DE 4034 902 A1 (1990).
184. M. W. Katoot, PCT Int. Appl. WO 9739838 A1, p. 49 (1997).
185. M. Dadsetan, H. Mirzadeh and N. Sharifi-Sanjani, *J. Appl. Polym. Sci.*, **76**, 401 (2000).
186. T. Kondo, H. Kubota and R. Katakai, *J. Appl. Polym. Sci*., **71**, 251 (1999).
187. H. Mirzadeh, A. A. Katbab, M. T. Khorasani, R. P. Burford and G. E. Golastani, *Biomaterials*, **16**, 641 (1995).
188. H. Mirzadeh, A. A. Katbab and R. P. Burford, *Radiat. Phys. Chem*., **46**, 859 (1995).
189. H. Mirzadeh, A. R. Ekbatani and A. A. Katbab, *Iran. Polym. J.*, **5**, 4 (1996).
190. H. Mirzadeh, A.A. Katbab and R. P. Burford, *Radiat. Phys. Chem*., **41**, 507 (1993).
191. T. Kondo, *Gunma-ken Kogyo Shikenjo Kenkyu Hokoku* (Japanese), **87-92** (1999).
192. K. Du, Z. Lin and F. Xiao, *Suliao Gongye* (Chinese), **27**, 4 (1999).
193. T. Kondo, H. Kubota and R. Katakai, *J. Appl. Polym. Sci*., **74**, 2462 (1999).
194. K. Chen, *Huaxue Tongbao* (Chinese), **7**, 27 (1986).
195. R. R. Lothe, S. S. Purohit, S. S. Shaikh, V. C. Malshe and A. B. Pandit, *Bioseparation*, **8**, 293 (1999).
196. M. D. Hohol and M. W. Urban, *Polymer*, **35**, 5560 (1994).
197. Z. Oser, R. A. Abodeely and R. G. McGunnigle, *Int. J. Polym. Mater*., **5**, 177 (1977).
198. J. Chaussy, G. Escalon, P. Gianese and J. P. Roux, *Cryogenics*, **18**, 501 (1978).
199. P. Nogues, F. Dawans and E. Marechal, *Makromol. Chem.*, **182**, 843 (1981).
200. C. S. L. Baker and D. Barnard, *Adv. Elastomers Rubber Elasticity*, 175-88 Ed. J. Lal, J. E. Mark, Plenum: New York (1986).
201. Q. Xu, X. Zhang, Y. Yang and Y. Zhang, *Hecheng Xiangjiao Gongye* (Chinese), **21**, 75 (1998).
202. A. Kowalski, J. Perkowski, M. Jezierski, B. Jankowski and M. Wojtulewicz, *Przem. Chem.* (Polish), **57**, 521 (1978).
203. B. N. Misra and J. Kaul, *Indian J. Chem., Sect. A*, **22A**, 601 (1983).
204. K. Makuchi, F. Yoshii, I. Ishigaki, F. Sundardi, M. Utama, S. Kadariah, A. Zubir, Jpn Kokai Tokkyo Koho JP 01236213 (1989).
205. I. Abdullah, *Sains Malays*., **16**, 219 (1987).
206. S. H. O. Egboh and M. O. Fagbule, *Eur. Polym. J.*, **24**, 1041 (1988).
207. R. S. Lehrle and S. L. Willis, *Polymer*, **38**, 5937 (1997).
208. K. Charmondusit, S. Kiatkamjornwong and P. Prasassarakich., *J. Sci. Res.*, **23**, 167 (1998).

209. P. Nogues, F. Dawans and E. Marechal, *Makromol. Chem*., **183**, 549 (1982).

210. S. Lenka, P. L. Nayak and A. P. Das, *J. Appl. Polym. Sci*., **30**, 2753 (1985).

211. M. S. Mazam, K. Makuuchi and M. Hagiwara, *J. Rubber Res. Inst. Malays*., **31**, 214 (1983).

212. D. R. Burfield and S. C. Ng, *Eur. Polym. J.*, **14**, 799 (1978).

213. M. T. Razzak, K. Otsuhata, Y. Tabata, F. Ohashi and A. Takeuchi, *J. Appl. Polym. Sci.,* **36**, 645 (1988).

214. Y. Ikada, H. Iwata, F. Horii, T. Matsunga, M. Taniguchi, M. Suzuki, W. Taki, S. Yamagita, Y. Yonekawa and H. Honda, *J. Biomedi. Mater. Res*., **15**, 697 (1981).

215. Haddadi-asl, R. P. Burford and J. L. Garnett, *Radiat. Phys. Chem*., **44**, 385 (1994).

216. V. D. McGinniss and F. A. Sliemers, PCT Int. Appl. WO 8303419 (1983)

217. H. Mirzadeh, A. R. Ekbatani and A. A. Katabab, *Iran. Polym. J.,* **5**, 225 (1996).

218. X. S. Wang, N. Luo and S. K. Ying, *Polymer*, **40**, 4515 (1999).

219. G. H. Hsiue and W. K. Huang, *J. Appl. Polym. Sci*., **30**, 1023 (1985).

220. G. M. O. Barra, J. S. Crespo, J. R. Bertolino, V. Soldi and A. T. N. Pires, *J. Braz. Chem. Soc.*, **10**, 31 (1999).

221. J. Park, J. G. Park, C. S. Ha and W. J. Cho, *J. Appl. Polym. Sci.*, **72**, 1177 (1999).

222. A. A. Katbab, R. P. Burford and J. L. Garnett, *Radiat. Phys. Chem*., **39**, 293 (1992).

223. R. Greco, G. Maglio and P. V. Musto, *J. Appl. Polym. Sci* **33**, 2513 (1987).

224. G. G. Bohm and M. Tveekrem, *Rubber Chem. Tech*., **55**, 575 (1982).

225. V. Haddadi-asl, R. P. Burford and J. L. Garnett, *Radiat. Phys. Chem*., **45**, 191 (1995).

226. A. K. Bhowmick, P. S. Majumder and I. Banik, *Macromol. Symp*., **143**, 2, (1999).

227. J. M. Yang, M. C. Wang, Y. G. Hsu, C. H. Chang and K. S. Lo, *J. Membr. Sci*., **138**, 19 (1998).

228. [L. Slusarski, D. M. Bielinski, S. Affrossman and R. A. Pethrick, *Kautsch. Gummi Kunstst*., **51**, 429 (1998)].

229. J. C. Fernandez-Garcia, A. C. Orgiles-Barcelo and J. M. Martin-Martinez, *J. Adhes. Sci. Technol*., **5**, 1065 (1991).

230. C.A Wilkie, X. Dong and M. Suzuki, *Polym. Mater. Sci. Eng*., **71**, 296 (1994).

231. H. Y. He, Y. Zhao, K. Zhang, X. Meng, X. Ming and C. X. Zhao, *J. Fluorine Chem*., **106**, 117 (2000).

232. J. J. Yu and S. H. Ryu, *J. Appl. Polym. Sci*., **73**, 1733 (1999).

233. G. Geuskens and P. Thiriaux, *Eur. Polym. J*., **29**, 351 (1993).

234. T Okada and Y. Ikada, *J. Biomed. Mater. Res.*, **27**, 1509 (1993).

235. N. J. Hallab, K. J. Bundy, K. O'Connor, R. L. Moses and J. J. Jacobs, *Tissue Engineering*, **7**, 55 (2001).

236. E. P. J. M. Everaert, B. Van De Belt-Gritter, H. C. Van Der Mei, H. J. Busscher, G. J. Verkerke, F. Dijk, H. F. Mahieu and A. J. Reitsma, *Mater. Sci.: Mater. Med*., **9**, 147 (1998).

237. E. T. Den Braber, J. E. Ruijter, H. J. E. Croes, L. A. Ginsel and J. A. Jansen, *Cells Mater.*, **7**, 31 (1997).

238. E. T. den Braber, J. E. de Ruijter and J. A. Jansen, *J. Biomed. Mater. Res*., **37**, 539 (1997).

239. T. G. van Kooten, J. F. Whitesides and A. F. von Recum, *J.Biomed. Mater. Res.*, **43**, 1 (1998).

240. A. S. Hoffman and W. G. Kraft, *Polym Prep.* **13**, 723 (1972).

241. A. Chapiro, M. F. Millequant, A. M. J. Bonamour, Y. Lerke, P. Sadurni and D. Domurado, *Rad. Phys. Chem.* **15**, 427 (1980).

242. A. Chapiro, *Eur. Poly. J.*, **19**, 859 (1983).

243. J. P. Boelens, W. F. Tan, J. Dankert and A. J. S. Zaat, *J. Antimicrob. Chemother*., **45**, 221 (2000).

244. P. C. T. Chang, S. D. Lee and G. H. Hsiue, *J. Biomed. Mater. Res.*, **39**, 380 (1998)

245. G. H. Hsiue, S. D. Lee, P. C. T. Chang and C. Y. Kao, *J. Biomed. Mater. Res.*, **42**, 134 (1998).

246. S. D. Lee, G. H. Hsiue, C. Y. Kao and P. C. T. Chang, *Biomaterials.*, **17**, 587 (1996).

247. G. H. Hsiue, S. D. Lee and P. C. T. Chang, *Artif. Organs*, **20**, 1196 (1996).

248. M. J. Swanson and G.W. Opperman, *J. Adhes. Sci. Technol*., **9**, 385-91 (1995).

249. H. Mirzadeh, M. Khorasani and P. Sammes, *Iran. Polym. J.*, **7**, 5 (1998).

250. M. T. Khorasani, H. Mirzadeh and P. G Sammes, *Radiat. Phys. Chem*., **47**, 881 (1996).

251. M. J. Owen and S. V. Perz, *Polym. Prepr.*, **39**, 958 (1998).

252. H. Hillborg and U. W. Gedde, *Polymer*, **39**, 1991 (1998).

253. D. X. Piao, Y. Uyama and Y. Ikada, *Kobunshi Ronbunshu,* **48**, 529 (1991).

254. S. R. Gaboury and M. W. Urban, *J. Appl. Polym. Sci.*, **44**, 401 (1992).

255. J. Y. Lai, Y. Y. Lin, Y. L. Denq, S. S. Shyu and J. K. Chen, *J. Adhes. Sci. Technol*., **10**, 231 (1996).

256. S. R. Gaboury and M. W. Urban, *Polym. Mater. Sci. Eng.*, **64**, 93 (1991).

257. G. Kossmehl, W. Neumann and H. Schaefer *Makromol. Chem*., **188**, 93 (1987).

258. M. T Stewart and M. W. Urban, *Polym. Mater. Sci. Eng*., **59**, 334 (1988).

259. A. Y. Kuznetsov, V. A. Bagryansky and A. K. Petrov, *J. Appl. Polym. Sci*., **57**, 201 (1995).

260. C. A. Goss, J. C. Burmfield, E. A. Irene and R. W. Murray, *Langmuir*, **8**, 1459 (1992).

261. H. A. Willis and V.J.I. Zichy, in *Polymer Surfaces*, Ed. D. T. Clark and W. J. Feast, Wiley, New York, p.287 (1978).

262. J. J. Pireaux, M. Vermeersch, N. Degosserie, C. Gregoire, Y. Novis, M. Chtaib and R. Caudano, Springer Series in *Surface Science*, **17**, 53 (1989).

263. L. C. Sawyer and D. T. Grubb, *Polymer Microscopy*, Chapman and Hall, London, (1987).

264. R. Ynag, X. R. Ynag, D. F. Evans, W. A. Hendrickson and J. Baker., *J. Phys. Chem.* **94**, 6123 (1990).

265. O. M. Leung and M. C. Goh, *Science*, **255**, 64 (1992).

266. JP 58155331 A2 Showa, 9 pp. (1983).

267. S. Amudeswari, C. R. Reddy and K. T. Joseph, *J. Macromol. Sci. Chem*., A **23**, 805 (1986).

268. D. Briggs, *Surf. Interface Anal*., **4**, 151 (1982).

269. D. Briggs, *Polymer*, **25**, 1379 (1984).

270. C. D. Batich and R. C Wendt, *ACS Symp. Ser*., **162**, 221 (1981).

271. S. W. Park, D. H. Kim, Y. M. Kim, B. S. Park, W. S. Han and B. S. Suh, *Anal. Sci. Technol*., **7**, 301 (1994).

272. O. Kornienko, E. T. Ada and L. Hanley, *Anal. Chem.*, 69, 1536 (1997).

273. A. Takahara, X. Jiang, N. Satomi, K. Tanaka and T. Kajiyama, *Key Eng. Mater*., **137**, 79 (1998).

274. I. Koprinarov, A. Lippitz, J. F. Friedrich, W. E. S. Unger and C. Woell, *Polymer*, **38**, 2005 (1997).

275. W. E. S. Unger, A. Lippitz, C. Woll and W. Heckmann, *Fresenius' J. Anal. Chem*., **358**, 89 (1997).

276. K. Emoto, J. M. Harris and J. M. Van Alstine, *Polym. Prepr*. **38**, 555 (1997).

277. G. Steiner, V. Sablinskas, A. Hubner, C. Kuhne and R. Salzer, *J. Mol. Struct.*, **509**, 265 (1999).

278. S. L. Mcgurk, K. M. Shakesheff, M. C. Davies, A. Domb, C. J. Roberts, S. J. B. Tendler and P. M. Williams, *Proc. Int. Symp. Controlled Release Bioact. Mater.*, 24th , 947 (1997).

279. R. Murgasova, I. Capek, E. Latova, D. Berek and S. Florian, *Eru. Polym. J.*, **34**, 659 (1998).

280. H. Yasuda, A. K. Sharma and T. Yasuda, *J. Polym. Sci. Polym. Phys. Ed*. **19**, 1285 (1981).

281. C. Decker and K. Zahouily, *Macromol. Symp*., **129**, 99 (1998).

282. J. Young, *Phil. Tran.*, **95**, 82 (1805).

283. I. Langmuir, *Science*, **87**, 893 (1938).

284. A. W. Neumann and R. J. Good, *Surface Colloid Sci.*, **11**, 31 (1979).

285. A. W. Adamson, *Physical Chemistry of Surfaces*, Wiley, New York (1982).

286. D. S. Ambwani and T. Fort, Jr., *Surface Colloid Sci.*, **11**, 93 (1979).

287. A. E. Mera, M. Goodwin, O. K. Pike and K. J. Wyne, *Polymer*, **40**, 419 (1998).

288. N. J. Harrick, *J. Phys. Chem.*, **64**, 1110 (1964).

289. J. Fahrenfort, *J. Spectrochim Acta*, **17**, 698 (1961).

290. K. W. Evanson and M. W. Urban, *J. Appl. Polym. Sci*., **42**, 7 (1991).

291. F. M. Mirabella, *Appl. Spectrosc. Rev*., **21**, 45 (1985).

292. R. Kellner, G. Gidaly and F. Unger, *Adv. Biomater*., **3**, 423 (1982).

293. N. J. Harrick, *Internal Reflection Spectroscopy*; Interscience, New York (1967).

294. M. W. Urban, *Attenuated Total Reflectance Spectroscopy of Polymers: Polymer Surfaces and Interfaces Series*, ACS, Washington DC (1996).

295. Z. Chen, R. Zhang, M. Kodama and T. Nakaya, *J. Biomater. Sci., Polym. Ed.*, **10**, 901 (1999).

296. F. M. Mirabella, *J. Polym. Sci. Polym. Chem. Ed*., **20**, 2309 (1982).

297. Jr. J. A. Gardella, G. L. GorobeIII, W. L. Hopson and E. M. Eyring, *Anal Chem*., **56**, 1169 (1984).

298. J. Liu, H. Jen and Y. C. Chung, *J. Appl. Polym. Sci*., **74**, 2947 (1999).

299. D. Rabelo, F. M. B. Coutinho, C.C. R. Barbosa and S. M. Rezende, *Polym. Bull*., **34**, 621 (1995).

300. M. A. Jacqueline, R. L. Dooley and S. W. Shalaby, *J. Appl. Polym. Sci.* **76**,1865 (2000).

301. G. Goizutea, T. Chiba and T. Inoue, *Polymer*, **34**, 253 (1993).

302. D. Zang, D. H. Gracias, R. Ward, M. Gauckler, Y. Tian, Y. R. Shen and G. A. Somorjai, *J. Phys. Chem.*, B **102**, 6225 (1998).
303. G. Binnig, H. Recher, C. Gerber and E. Weibel, *Phys. Rev. Let*., **49**, 57 (1982).
304. K. H. Guenther, P. G. Wierer and J. M. Bennett, *Appl. Optics*, **23**, 3820 (1984).
305. C. Bai, J. Li, Z. Lin, J. Tang and C. Wang, *Surf. Interface Anal*., **28**, 44 (1999).
306. G. Binnig, C. F. Quate and C. Gerber, *Phys. Rev. Let*., **56**, 930 (1986).
307. N. B. Holland and R. E. Marchant, *J. Biomed. Mater. Res.*, **51**, 307 (2000).
308. P. L. Michel, E. W. Werts and H. Georges, *Langmuir*, **13**, 4939 (1997).
309. G. E. Muilenburg, *Handbook of X-ray and Ultraviolet Photoelectron Spectroscopy*, Norwalk (1979).
310. Q. Song and A. N. Netravali, *J. Adhes. Sci. Technol*., **12**, 983 (1998).
311. N. S. McIntyre, R. D. Davidson and J. R. Mycroft, *Surf. Interface Anal*., **24**, 591 (1996).
312. A. Dilks, in *Electron Spectroscopy- Theory, Techniques and Applications*, Ed. C. R. Brundle and A. D. Baker, Vol. 4, Academic Press, London (1981).
313. N. S. McIntyre, R. D. Davidson and J. R. Mycroft, *Surf. Interface Anal*., **24**, 591 (1996).
314. E. W. Merrill, N. Mahmud and S. Wan, Proc. IUPAC, *I. U. P. A. C. Macromol. Symp.*, 28th Int. Union Pure Appl. Chem.: Oxford, UK. p. 685 (1982).
315. M. M. Millard, *ACS Symp. Ser*., **199**, 143 (1982).
316. D. R. Miller and N. A. Peppas, *J. Macromol. Sci., Rev. Macromol. Chem. Phys.*, C **26**, 33 (1986).
317. D. T. Clark, *Pure Appl. Chem.*, **57**, 941 (1985).
318. A. Brown and J. C. Vickerman, *Surf. Interface Anal*., **6**, 1 (1984).
319. D. Briggs, M. J. Hearn and B. D. Ratner, *Surf. Interface Anal*., **6**, 184 (1984).
320. R. W. Odom, *Microbeam Anal*., **2**, 99 (1993).
321. L. Lianos, T. M. Duc, S. Reichimaier and J. Hammond, *Second. Ion Mass Spectrom., Proc. 9th Int. Conf.* 1993, Ed. A. Benninghoven, Wiley: Chichester, UK, p. 468 (1994).
322. D. M. Hercules, *J. Mol. Struct*., **292**, 49 (1993).
323. T. M. Duc, *Surf. Rev. Lett*., **2**, 833 (1995).
324. T. Hoshi, *Bunseki*, **5**, 414 (1999).
325. C. R. Ayre, L. Moro and C. H. Beker, *Anal. Chem*., **66**, 1610 (1994).
326. A. Benninghoven, B. Hagenhoff and E. Niehuis, *Anal. Chem*., **65**, 630A (1993).

327. R. Zenobi, *J. Mass Spectrom. Ion Processes,* **145**, 51 (1995).

328. D. C. Schriemer and L. Li, *Anal. Chem*., **68**, 250 (1996).

329. O. Kornienko, E. T. Ada, J. Tinka,; Wijesundara, B. J. Muthu and L. Hanley, *Anal. Chem.*, **70**, 1208 (1998)

330. S. Kitamura, K. Suzuki, M. Iwatsuki and C. B. Mooney, *Appl. Surf. Sci*., **157**, 222 (2000).

331. J. Mizsei, *Sens. Actuators*, B**48**, 300 (1998).

332. A. Nazarov and D.Thierry, *J. Electrochem. Soc*., **145**, 39 (1998).

333. W. A. Zissman, *Rev. Sci. Instrum*., **3**, 367 (1932).

334. L. Kelvin, *Philos. Mag.*, **46**, 82 (1898).

335. L. E. Cheran, M. L. Thompson and H. Dieter, *Analyst*, **124**, 961 (1999).

336. H. D. Liess and R. Maeckel, *J. Surf. Interface Anal*., **25**, 855 (1997).

337. G. Grundmeier, C. Reinartz, M. Rohwerder and M. Stratmann, *Electrochim. Acta*, 43, 165 (1997).

338. B. A. Cavic, M. Thompson and D. C. Smith, *Analyst*., 121, 53 (1996).

339. H. D. Liess and R. Maeckel, *J. Surf. Interface Anal*., **25**, 855 (1997).

340. G. Grundmeier, C. Reinartz, M. Rohwerder and M. Stratmann, *Electrochim. Acta*, **43**, 165 (1997).

341. B. A. Cavic, M. Thompson and D. C. Smith, *Analyst*., **121**, 53 (1996).

342. A. V. Prasad,*Ph.D Thesis,* Univ. of Pune, India (1998).

343. R. Mani, R. P. Singh, S. Sivaram, *J. Macromol. Sci.-Pure and Appl. Chem*. A**31**, 413 (1994).

344. J. L. Bolland and G. Gee, Trans. Faraday. Soc., **42**, 236 (1946).

345. P. J. Pappillo, *Mod. Plastics*, **4**, 31, (1994).

346. H. J. Hiller, Eur. Polym. J., Suppl., p. 105 (1969).

347. R. P. Singh, P. N. Thanki, S. S. Solanky and S. M. Desai, *Adv. Functional Molecules and Polymers*, Ed. H. S. Nalwa, Gordon and Bearch, Japan p. 1-53 (2000).

348. H. C. Bailey, Ind. Chem., **38**, 215 (1962).

349. M. B. Neiman, E. G. Rozantev, Y. G. Mamedora, *Nature*, **196**, 472 (1962).

350. R. Mani, *Ph. D Thesis*, Univ. of Pune, India (1995).

351. B. N. Felder, *ACS Symp. Ser*., **151**, (1981).

352. F. Gugumus, *Polym Degrd. Stab.*, **24**, 292 (1989).

353. S. M. Desai and R. P. Singh US Patent (applied 2000).

354. R. P. Singh, A.V. Prasad and J. K. Pandey, *Macromol. Chem. Phys*., **202**, 672 (2001).

355. S. M. Desai and R. P. Singh, US Patent (applied 2001)

356. P. N. Thanki and R. P. Singh, US 6284895 (2001)

357. S. M. Desai, J. K. Pandey and R. P. Singh, *Macromol Symp. Ser*., **169**, 173 (2001).

358. N. Chanunpanich, A. Ulman T, Y. M. Strzhemechny and S. A. Schwarz, *Mater Res Soc Symp Proc*, **600**, 203 (2000).

359. J. Liesegang, B. C. Senn, P. J. Pigram, E. T. Kang, K. L. Tan and K.G. Neoh, *Surf. Interface Anal.*, **28**, 20 (1999).

360. S. H. Choi, S. Y. Park and Y. C. Nho, *Radiat. Phys. Chem.* **57**,179 (2000).

361. S. H. Choi and Y. C. Nho, *Korean J. Chem. Eng.*, **16**, 725 (1999).

362. K. Ishihara, Y. Iwasaki, S. Ebihara, Y. Shindo and N. Nakabayashi, *Colloids Surf. B* **18**, 325 (2000).

363. N. Kawashima, JP 10305539 (1998)

364. P. S. Razi, R. Portier and A. Raman, *J. Compos. Mater*., **33**, 1064 (1999).

365. R. P. Singh, S. M. Desai, P. N. Thanki and S. S. Solanky, *J. Appl. Polym. Sci*., **75**, 1103 (2000).

366. G. C. Eastmond, H. Hocker and D. Klee, *Adv. Polym. Sci*, **149**, 239 (1999).

CHAPTER II

OBJECTIVES AND APPROACHES OF PRESENT INVESTIGATION

2.1 INTRODUCTION AND OBJECTIVES

Today polymers enjoy their importance in almost all fronts of human life. Polyolefins are amongst the oldest and well-accepted synthetic polymers, due to their excellent manufacturer cum user-friendly properties. Although, they have excellent bulk physical/chemical properties, are inexpensive and easy to process, yet they do not gain considerable importance as speciality materials due to their inert surface. Thus, special surface properties which polymers do not possess, such as functionality, dyeability, chemical resistance, hydrophilicity, roughness, lubricity, selective permeability, conductivity, biocompatibility etc are required for their success as specialty materials[1-4]. Surface modification of polymers has been extensively studied for decades, using conventional tools[5-9]. Although, some of these techniques are still in use but they suffer from distinct shortcomings. During the last two decades, alternative means of surface modification have been extensively explored[10-14]. Since, herculean efforts are required to synthesize polymers with distinct bulk and surface properties[15], tailoring of desired properties using surface modification techniques have become an important tool to convert the inexpensive polymers into valuable commercial products. The increasing modernization and expectancy for smart materials has, of late, sharply influenced the research in this area. Technologies such as surface engineering, which convert inexpensive materials into valuable finished goods, have become even more important in the present scenario, as material cost has become a significant factor in determining the success of any industry. The primary objective of the present study is to devise mild techniques for primary surface functionalization of elastomeric films with high degree of chemo- and topographical selectivity without causing any changes in their inherent physio-chemical properties.

Many researchers have attempted to tailor the surface properties of various polymers like polyethylene, polypropylene, polyamide, polyethylene terephthalate, polyacrylonitrile, polytetrafluoroethylene and polyethersulphone, using traditional and existing surface modification techniques[16-22]. However, there are only a few reports on the surface modification of elastomeric films of ethylene propylene diene elastomer[23], natural rubber[24], styrene butadiene styrene[25] and polydimethylsiloxane[26,27] using plasma- and photo-induced modification techniques, with hardly any systematic efforts of investigating the effects of different reaction parameters on the surface properties of these elastomers. Hence, our secondary objective was to bring about surface modification of above-mentioned elastomers in a systematic manner.

Many recent studies in this area have emphasized the need of material compatibility in the multiphase systems to provide new materials with improved properties. Surface modified PP, PE, PS, PTFE and PES have long been studied as biocompatible materials[28, 29]. However, a little attention has been paid on the development of elastomeric biomaterials[30]. Elastomers are far pertinent candidates as biomaterials due to their inherent flexibility and freedom of design. The surface modified elastomers are therefore, prospective biomaterials for a range of applications yet unimagined viz. soft cartilages, artificial nerves, blood vessels, diaphragms, flexi-valves etc. The modification of elastomeric surface was thus proposed with a view of improving their biocompatibility and examining their performance under *in vitro* conditions.

It is well known that the interaction of polymeric substrates with reactive plasmas of gases like oxygen, carbon dioxide, ammonia and sulphur dioxide generates hydrophilic groups on the substrate surface[31-33]. However, the plasma treatment of material with non-polymerizing gases has one serious drawback - on most of the polymers surfaces, the gained superior effect upon plasma treatment is usually not permanent. It disappears or diminishes significantly with the time of storage[34,35]. Although, this surface dynamics depends on polymer physio-chemical properties, temperature, storage time and many other parameters, it is a feebly understood complex phenomenon, which differs from substrate to substrate. Thus the objective of the present work is also to understand the dynamics of the elastomer surface upon storage, after treatment with reactive plasma.

Natural and synthetic polymers in common use are susceptible to photo-oxidative degradation[36] upon exposure to natural and artificial weathering. The net result of degradation is the loss in the molecular weight and macroscopic physical properties. Incorporating suitable stabilizers into the polymer matrix can efficiently prevent polymer degradation. Generally stabilizers are melt-blended in the polymer matrix for enhancing its service life. However, these stabilizers are low molecular weight organic compounds, which can be lost from the polymer by leaching, evaporation and migration under the influence of environmental conditions during their use. Chemical attachment of stabilizers to the polymer molecule offers a solution to this problem[37]. Moreover, since the degradation of a polymer commences from the surface and slowly proceeds into the matrix of the polymeric substrate, the stabilizers are therefore expected to be most potent if they are concentrated at the surface. Therefore, they should be anchored covalently to the polymer surface.

Hindered amine light stabilizer, hydroxy benzotriazoles and hindered phenols are efficient polymer stabilizers[38] that are widely used to protect polymers against thermal- and

photo-oxidative degradation. Since, vinylic light stabilizers are expected to be better choice to attain the desired thermal and photostability, the present study was also aimed at devising polymer-bound and polymerizable stabilizers.

2.2 APPROACHES

2.2.1 Photochemical surface grafting of functional monomers onto EPDM and NR films

- **2.2.1.1** EPDM films were grafted with various functional monomers using mild photochemical reactions
- **2.2.1.2** Surface selective functionalization was substantiated by ATR-FTIR and XPS study
- **2.2.1.3** The morphological changes upon surface grafting were examined using SEM and AFM techniques
- **2.2.1.4** The degree of surface modification was determined using water contact angle, optical microscopy and gravimetric measurements
- **2.2.1.5** The biocompatibility of the modified surfaces was determined by *in vitro* cell culture tests
- **2.2.1.6** Effect of reaction conditions (concentration, time, temperature etc.) on the surface grafting efficacy were studied

2.2.2 Plasma induced surface grafting of functional monomers onto EPDM and NR films

- **2.2.2.1** Surface grafting of functional monomers using mild plasma treatments
- **2.2.2.2** Evaluation of hydrophilicity and surface energy of modified substrates
- **2.2.2.3** Chemical and morphological changes were determined using XPS, ATR-FTIR, SEM and AFM
- **2.2.2.4** Comparison of surface changes brought about by photo-grafting and plasma-grafting

2.2.3 Implantation of functional groups onto EPDM films using reactive plasma

- **2.2.3.1** Functionalization of EPDM films using O_2 plasma
- **2.2.3.2** Functionalization of EPDM films using CO_2 plasma
- **2.2.3.3** Spin-coating of functional monomers with MFAs' and subsequent plasma induced surface crosslinking

2.2.3.4 Influence of storage time on migration of functional groups generated by O_2 and CO_2 reactive plasma

2.2.4 Plasma induced surface functionalization of SBS and SR films

2.2.4.1 Plasma-grafting of functional monomers onto of SBS and SR films

2.2.4.2 Functionalization of SBS and SR films using O_2 and CO_2 plasma

2.2.4.3 Influence of storage time on migration of functional groups generated by O_2 and CO_2 reactive plasma

2.2.5 Design, synthesis and performance evaluation of novel thermal and photo stabilizers

2.2.5.1 Design and synthesis of novel vinylic HALS

2.2.5.2 Design and synthesis of HALS coupled to UV absorber

2.2.5.3 Design and synthesis of copolymerizable thermal stabilizer (BHT)

2.2.5.4 Surfaces grafting of vinylic HALS onto PP, PE and SBS films and its performance evaluation against conventional melt blended stabilizers

2.3 REFERENCES

1. M. Suzuki, A. Kishida, H. Iwata and Y. Ikada, *Macromolecules*, **19**, 1804 (1986).
2. H. Iwata and T. Matsuda, *J. Membrane Sci*., **38**, 185 (1988).
3. M. Biesalski and J. Ruehe, *Macromolecules*, **32**, 2309 (1999).
4. A. M. Mayes, D. J. Irvine and L. G. Griffith, *Mater. Res. Soc. Symp. Proc*., **530**, 73 (1998).
5. D. Briggs, D. M. Brewis and M. B. Konieczko, *J. Mater. Sci*. **14**,1344 (1979).
6. I. A. Abu-Isa, *Polym.- Plast. Technol. Eng*., **2**, 29 (1973).
7. P. Blaiss, D. J. Carlsson, G. W. Csullog and D. M. Wiles, *J. Colloid Interface Sci*., **47**, 636 (1974).
8. D. Briggs and C.R. Kendall, *Polymer*, **20**, 1053 (1979).
9. C. H. Bamford and J. C. Ward, *Polymer*, **22**, 277 (1961).
10. L. Gu, A. N. Hrymak and S. Zhu, *J. Appl. Polym. Sci*., **76**, 1412 (1999).
11. C. Anders, R. Gratner, V. Steinert, B. I. Voit and S. Zschoche, *J. M. S.-Pure and Appl Chem.*, **A 36**, 1017 (1999).
12. M. Dadsetan, H. Mirzadeh and N. Sharifi-Sanjani, *J. Appl. Polym. Sci.*, **76**, 401 (2000).

13. H. Mirzadeh, A. A. Katbab, M. T. Khorasani, R. P. Burford and G. E. Golastani, *Biomaterials*, **16**, 641 (1995).
14. E. T. Kang, K. G. Neoh, J. L. Shi, K. L. Tan, D. J. Liaw, *Polym. Adv. Technol*, **10**, 20 (1999).
15. I. Noda, *Nature*, **350**,143(1991).
16. T. Richey, H. Iwata, H. Oowaki, E. Uchida, S. Matsuda and Y. Ikada, *Biomaterials*, **21**, 1057, (2000).
17. F. P. Epaillard, J. C. Brosse and T. Falher, *Macromol. Chem. Phys.*, **199**, 1613 (1998).
18. M. Y. Teng, K. R. Lee, D. J. Liaw, Y. S. Lin and J. Y. Lai, *Eur. Polym. J.*, **36**, 663 (2000).
19. B. Gupta, C. Plummer, I. Bisson, P. Frey, J. Hilborn, *Biomaterials*, **23**, 863 (2002).
20. M. Ulbricht, G. Belfort, *J. Membrane Sci.*, **111**, 193 (1996).
21. M. R. Yang and K. S. Chen, *Mater. Chem. Phys.*, **50**, 11 (1997).
22. I. Gancarz, G. Pozniak, M. Bryjak and A. Frankiewicz, *Acta Polym.*, **50**, 317 (1999).
23. P. Anelli, S. Baccaro, M. Carenza and G. Palma, *Radiat. Phys. Chem.*, **46**, 1031 (1995).
24. P. Wang, K. L. Tan, C. C. Ho, M. C. Khew and E. T. Knag, *Eur. Polym. J.*, **36**, 1323 (2000).
25. C. A. Wilkie, X. Dong and M. Suzuki, *Polym. Mater. Sci. Eng.*, **71**, 296 (1994).
26. I. F. Husein, C. Chan and P. K. Chu, *J. Mater. Sci. Letters*, **19**, 1883 (2000).
27. I. F. Husein, C. Chan, S. Qin and P. K. Chu, *J. Phys. D: Appl. Phys.*, **33**, 2869 (2000).
28. B. Pignataro, E. Conte, A. Scandurra and G. Marletta, *Biomaterials*, **18**, 1461 (1997).
29. J. H. Kim and S. C. Kim, *Biomaterials*, **23**, 2051 (2002).
30. D. Bakker, C. A. Van-Blitterswijk, W. T. H Daems, J. J. Grotte, *J. Biomed. Mater. Res.*, **22**, 423 (1988).
31. C. M. Weikart and H. K. Yasuda, *J. Polym. Sci., Part A: Polym. Chem.*, **38**, 3028, (2000).
32. F. R. Pu, R. L. Williams, T. K. Markkula and J. A. Hunt, *Biomaterials*, **23**, 2411 (2002).
33. F. P. Epaillard, B. Chevet, J. C. Brosse, *Polymer J.*, **26**, 333 (1990)
34. N. Inagaki, S. Tasaka, T. Horiuchi, R. Suyama, *J. Appl. Polym. Sci.*, **68**, 271 (1998).
35. T. Yasuda, A. K. Sharma, T. Yasuda, *J. Polym. Sci.*, A, **19**, 1285 (1981).
36. N. S. Allen, ed. *Degradation and Stabilization of Polyolefins*, Elsevier, London (1993)
37. D. J. Carlsson, D. M. Wiles, *Macromolecules*, **4**, 179 (1971)
38. S. M. Desai, J. K. Pandey and R. P. Singh, *Macromol. Symp. Ser.*, **169**, 121 (2001).

CHAPTER III

SURFACE GRAFTING ONTO EPDM FILMS

3.1 INTRODUCTION

Synthetic routes to chemically modified polymer surfaces with controllable structures continue to be an area of contemporary research having both theoretical and practical interests. As discussed in Chapter I, there is large variety of techniques for the surface modification of polymeric substrates. However, many of these techniques associate high energy, leading to detrimental effects when used for the elastomeric substrates. The energy sources commonly used in radiation grafting are high-energy radiation or ionization radiation (electron beam, X-rays and γ-rays). The two main advantages of photo-grafting over ionization radiation grafting are: 1) the modification produced by this technique is virtually restricted to the surface and 2) the energy associated with UV light is in accordance with the chemical bond energies associated with any two atoms[1]. Hence, UV radiation often has the potential to retain the properties of monomers and polymers while the other surface grafting techniques which use ionization radiation cause damage to the substrate polymer due to excessive degradation. The most widely used methods involving moderate energy (35 to105 kcal/mol) for the modification of polymer surfaces are photo-grafting and plasma-grafting/plasma treatment.

The objective of the present study is to devise placid techniques for primary surface functionalization of elastomeric films with high degree of chemo- and topographical selectivity. Additionally, the primary functional groups on the surface should be capable of generating properties like hydrophilicity, antifogging, wear-resistance, printability, dyeability and biocompatibility at the polymer surfaces. Although functionalization of the elastomer surfaces has been an interesting and challenging area of research yet, there are only few examples of modification of diene-elastomer surfaces which satisfy the rigorous criteria of chemo- and topographical selectivity[2,3]. Surface modification of EPDM using pulsed laser technique leads to high amount of subsequent homopolymerization with very thick grafted layers[4]. These drawbacks along with few more like fractal formation have been least addressed. Longer hours of photochemical grafting lead to undesirable changes in the polymer backbone as well as the topography of the substrate. However, bulk grafting of functional monomers onto elastomer backbone has been well reported[5-7]. The two versatile techniques involving initiation at low energies viz. short exposure photochemical grafting and simultaneous plasma grafting have been rarely addressed for the surface grafting of functional monomers onto the EPDM films. Simultaneous plasma-grafting is well known for its merit of

delivering functional surfaces by a solvent free process. Green chemistry avoiding the use of solvents is the need of the day, thereby making this process value added.

This chapter describes the use of two unprecedented mild techniques of surface modification viz. short exposure photochemical grafting (at 400 W) and simultaneous low-pressure cold plasma-grafting (range 40 - 75 W), for the introduction of functional monomers onto the surface of EPDM films. In the present work, the photochemical surface grafting of different functional monomers (viz. HEMA, AA, GMA, AAm and NVP) onto the surface of EPDM films have been accomplished under mild reaction conditions. A medium pressure mercury vapor lamp emitting UV-Vis radiation with wavelength > 290 nm was employed for the activation of the photosensitizers. The efficiency of different photosensitizers (viz. benzophenone, xanthone, benzil, benzoyl peroxide and AIBN) has been investigated for reactions carried out at room temperature and elevated temperature. The effect of various reaction parameters on the surface grafting efficiency has also been deeply studied. In the second approach, the surface grafting of functional monomers onto elastomeric substrates was achieved by simultaneous plasma-grafting technique, where monomer vapors were simultaneously introduced into the plasma reaction chamber. The influence of the plasma grafting conditions has also been thoroughly investigated. The functionalized surfaces obtained as a result of surface grafting were characterized by contact angle measurements, ATR-FTIR, SEM, XPS, AFM and optical microscopy techniques. The influence of the functional groups and their density on the biocompatibility (cell adhesion tests) of these surface modified films has also been investigated.

3.2 MATERIALS AND METHODS

3.2.1 Materials

All the monomers viz. 2-hydroxyethyl methacrylate (HEMA), acrylic acid (AA), N-vinyl pyrrolidone (NVP), acrylamide (AAm) and glycidyl methacrylate (GMA), procured from M/s Aldrich, USA, were purified by fractional distillation at reduced pressure using fractional distillation column. Benzophenone procured from (M/s Aldrich) was used after recrystalization. All solvents obtained from M/s E. Merck India Ltd. were of L.R. grade. EPDM obtained through the courtesy of Prof. J. Lacoste, ENSCCF, Clermont-Ferrand, France was dissolved in toluene and precipitated with acetone, followed by drying under vacuum at room temperature to a constant weight to remove the processing additives. The purified EPDM sample was characterized with ^{1}H NMR and spectra were recorded on a

'Bruker AC 200 FT-NMR' instrument (200 MHz) at 25 ºC. The EPDM terpolymer, used throughout the study comprised of ethylene: propylene: vinylidene in the proportion 55:41:4. The nitrogen and argon gases (Grade I) supplied by M/s Inox Ltd., India, were used to maintain inert reaction conditions in the photo-grafting and plasma-grafting reactions, respectively.

3.2.1.1 Preparation of EPDM films

Commercially obtained EPDM was dissolved in toluene and precipitated from acetone to remove the additives. The precipitates was thoroughly washed with fresh acetone to remove the traces of additives, followed by drying to a constant weight at room temperature in a vacuum oven. A 5 % w/v homogeneous solution of purified EPDM was prepared in analytical grade toluene. 50 ml of this solution was carefully poured in a flat-bottomed evaporation bowl (10 cm diameter) and the solvent was evaporated at room temperature to obtain EPDM films (thickness ~ 200 microns). The film, thus obtained were thoroughly washed with methanol, water, and acetone successively and dried in vacuum oven at 40 °C to remove any trapped solvent. The dried films were cut into a fixed size (4 cm × 1.5 cm) for all experiments.

3.2.1.2 Reactor design

In the present study, the surface modification of the EPDM films was carried out mainly by two methods, photo-grafting and plasma-grafting. The reactors for both the processes were tailor-made with in-house glass blowing facility.

3.2.1.2.1 Photo-grafting reactor

The Photoreactor used in all our photo-grafting reactions was a special type of Pyrex glass assembly bearing a grounded joint mouth and with a facility of bubbling nitrogen into the reaction medium, when operated at room temperature [**Figure 3.1(a)**]. A water condenser was fitted at the mouth of the reactor [**Figure 3.1(b)**], for reactions carried out at elevated temperature, in order to avoid any solvent loss. A digital thermocouple was placed at the base of the photoreactor to maintain it at a desired temperature. The photo-reactor was irradiated with an irradiation source consisting of a 400 W medium pressure mercury vapor lamp from a fixed distance (15 cm) for a fixed time under preset reaction conditions. The films (4 cm × 1.5 cm) were immersed in this photoreactor containing *solvent*, *photoinitiator* and *monomer* in a definite proportion, under nitrogen flux.

Figure 3.1 Reactor for **(a)** photo-grafting at R.T. **(b)** photo-grafting at 50 °C

(a)

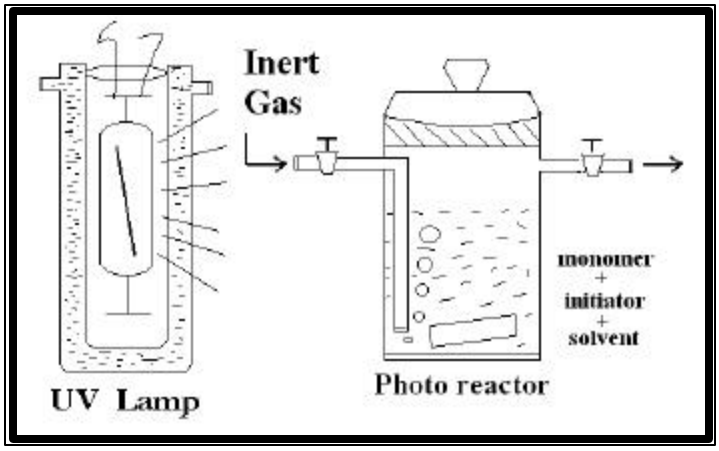

(b)

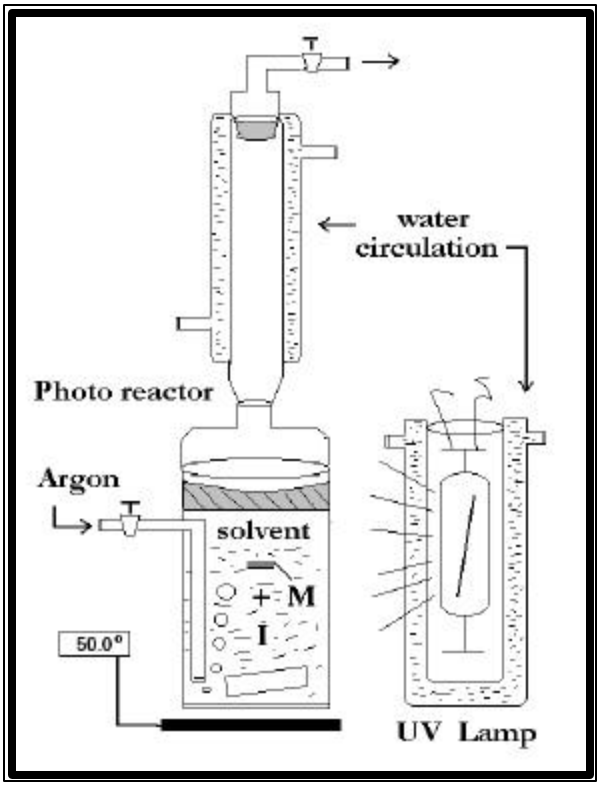

3.2.1.2.2 Plasma-grafting reactor

Experimental set-up consists of a reactor system, gas flow system and a radio frequency (RF) power source (13.56 MHz, RFX-600 from Advanced Energy) with a matching unit (ATH-50 from Astech), shielding and a vacuum system as originally designed by *Hori*[8] for plasma polymerization (**Figure 3.2**). An inductively coupled tubular type glass reactor was used to carry out the plasma polymerization of functional monomers. Initially the reactor was evacuated to 10^{-2} Torr, followed by flushing the system for 10-15 min by passing the inert gas (argon in the present study) at a high flow rate. Argon flow rate was set to 1.5-2.0 sccm and reactor pressure 0.2 Torr for carrying out plasma grafting. The monomers were heated to boil in presence of an inert carrier gas in the temperature range of 50-75 °C/ 0.2 Torr. The reactor pressure was maintained at 0.2 Torr and gas flow was 25 sccm for all experiments, unless mentioned.

3.2.1.3 Irradiation source

A medium pressure mercury vapor lamp (Mazda, Germany) was used as the irradiation source. The lamp emits polychromatic radiation of $\lambda \geq 290$ nm. The lamp was immersed in a pyrex glass jacket with cold-water circulation facility [Figure 3.1(b)] in order to maintain the system at room temperature and avoid heat transfer to the reaction.

Figure 3.2 Outline of Plasma grafting reactor used in the present study.

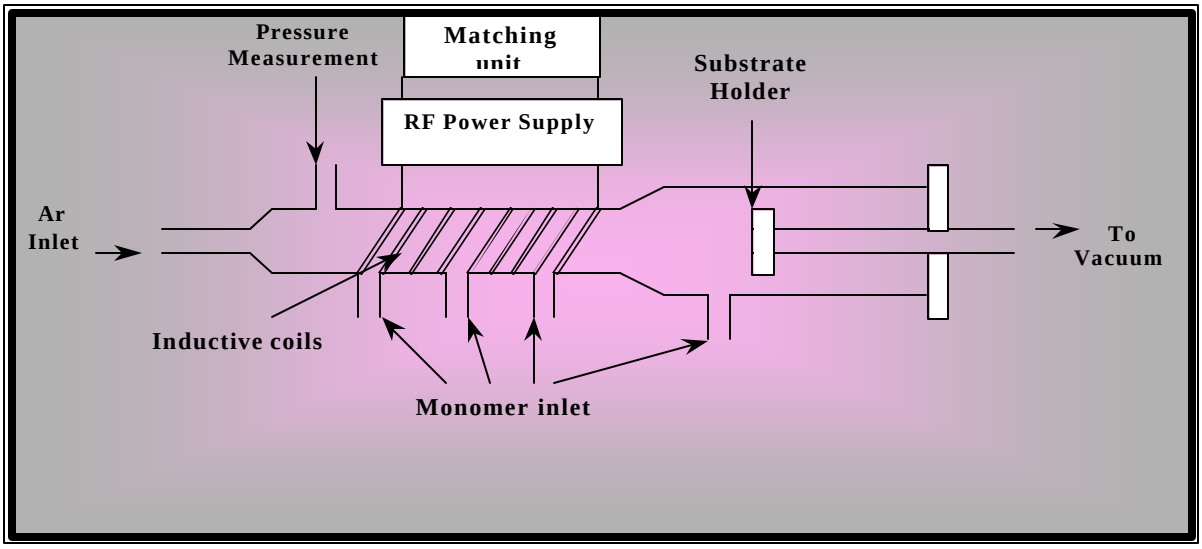

3.2.2 Experimental Methods

The surface modification of the EPDM films was accomplished by two methods involving moderate energy a) photo -grafting and b) plasma-grafting.

3.2.2.1 Photo -grafting procedure

Photo -grafting was carried out in a special type of Pyrex-glass photo-reactor irradiated with a 400 W medium pressure mercury vapor lamp from a fixed distance (15 cm) for a fixed time at *room temperature* [Figure 3.1(a)] and elevated temperature [Figure 3.1(b)]. The films (4 cm $\times$ 1.5 cm) were immersed in this photoreactor containing *solvent*, *photoinitiator* and *monomer* in a definite proportion, under nitrogen flux. The photo-grafted elastomer films in all cases were subjected to sonication, followed by soxhlet extraction in acetone/water for 12 hrs in order to remove homopolymer. These films were finally dried in a vacuum oven at 35 °C till constant weight.

3.2.2.2 Plasma-grafting procedure

The plasma reactor was evacuated to 10^{-2} Torr, followed by flushing the system for 10-15 min by passing the inert gas (argon in the present study) at a high flow rate. Argon flow rate was set to 1.5 - 2.0 sccm and reactor pressure 0.2 Torr for carrying out plasma grafting. The monomers were heated to boil in an RB in presence of carrier gas (argon) in the temperature range of 50 - 75 °C (depending upon b.p. of monomer) at 0.2 Torr. The reactor pressure was maintained at 0.2 Torr and the monomer flow was 2.5 sccm.

After the reactor pressure was stabilized, argon plasma was initiated by an RF power supply through a matching network and output power was varied from 50-75 Watts (W) and the irradiation time varied from 10-40 min. The monomer vapor was introduced after 5 min of glow discharge, through the second opening (from left) in (Figure 3.2) at distance 12 cm from the substrate in the downstream of the argon plasma (glow discharge). The monomer flow was stabilized and maintained at 2.0-2.5 sccm. After the plasma was terminated, the monomer vapor purging was continued for 10-20 min in order to utilize all the free radicals generated on the surface.

3.2.3 Characterization methods

The surface grafted EPDM films were characterized by contact angle Goniometer, ATR-FTIR, SEM, XPS, AFM and optical microscopy techniques. The change in the weight of the grafted samples was determined using microbalances: *Precisa* 205 ASCS, Switzerland and Sartorius BP 210D, Germany.

Contact angles were measured on a Rame-Hart NRL, USA contact angle Goniometer (Model 100-00 230) using freshly prepared deionized water, filtered through membrane filter. The drop volume was 2 μL. The static advancing contact angles of the water on the substrate surface were determined by 'sissile drop' method, measured within 30 sec of placing the drop at room temperature (28 ± 3 °C). The reported values are an average of minimum 7 values, measured at different places on the sample. The standard deviation in the measured value is within ± 3°.

The humidity and temperature during the conditioning of the grafted EPDM films was monitored using the hygrometer *Sipco*, USA.

ATR-FTIR spectra were recorded on a Perkin-Elmer 16 PC FTIR spectrometer. Each spectrum was recorded using 4 cumulative scans, using KRS-5 (Thallus bromide iodide) crystal with an incident angle (θ_i) of 45° as an ATR crystal element. The depth profiling study was done using the equation:

$$dp = \frac{\lambda}{2\pi n_1 [\sin^2\theta - (n_2/n_1)^2]^{1/2}}$$

where, dp is the sampling depth, n_1 = refractive index of crystal, n_2 = refractive index of the polymer, λ = wave length of incident light and θ is the angle of incident light.

Scanning electron micrographs were obtained from *Leica* SEM Stereoscan-440, Cambridge, UK. The polymeric samples, before analysis, were coated with gold in a sputter coater, in order to achieve conducting surface and were analyzed at an accelerated voltage (potential) of 10 KV.

The XPS spectra were recorded on V.G. Scientific ESCA-3MK-II spectrophotometer using MgKα (1253.6 eV) radiation (non monochromatic) X-ray source and ESCA 3000 electron spectrophotometer with twin anode, AlKα (1486.6 eV) and MgKα (1253.6 eV) to investigate the chemical changes on the surface of polymer at an atomic level. The XPS spectra were acquired at 50 eV pass energy, 5mm slit width and vacuum better than 10^{-8} Torr at take off angle of 30° and 60°.

The atomic force micrographs were recorded on the *BERLIGH* AFM in the contact mode using silicon-nitride tips.

In order to determine the thickness and homogeneity of the grafting, the cross-section of the samples were selectively stained with eosin/crystal violet and observed under *OLYMPUS* BX50 optical microscope.

3.2.3.1 Determination of graft copolymerization

Weight gain (WG): Weight gain is defined as the difference of the weight of the whole sample *(Ww)* after grafting and the initial weight of the EPDM film *(W0)* divided by the initial weight of EPDM film as shown in equation (1)

$$WG\ (\%) = \left[\left(\frac{Ww - W0}{W0} \right) \right] \times 100 \qquad \ldots\ldots\ldots\ldots (1)$$

Degree of grafting (G_d): Degree of grafting is expressed in equation (2)

$$G_d\ (mg/cm^2) = \left[\left(\frac{Wgr - W0}{W0} \right) / 2 \times SA \right] \qquad \ldots\ldots\ldots\ldots (2)$$

where, $W0$ is the initial weight of the film, Wgr is the weight of grafted film after extraction and SA is the surface area of each film.

Grafting efficiency (G_e): is expressed by the equation (3)

$$G_e\ (\%) = Wg / Wp \times 100 \qquad \ldots\ldots\ldots\ldots (3)$$

where, (Wg) is the weight of grafted polymer after extraction and (Wp) is the total weight of polymer formed (after evap oration of solvent and unreacted monomer).

3.2.4 Biocompatibility Tests

The biocompatibility of the modified and pristine EPDM films was tested by incubating the samples in a cell culture of human cervical carcinoma (SIHA) and oral carcinoma (KB) cell lines, at 37 °C, 5% CO_2, 90 % humidity in standard culture media and subsequently being monitored for cell adhesion after 24 and 48 hours of incubation using an optical microscope equipped with a camera.

3.3 RESULTS AND DISCUSSION

Different functional groups were introduced onto the surface of EPDM films depending upon the type of monomer grafted by the two mild surface modification techniques. The effects of different reaction conditions on the modification reaction were thoroughly investigated. The surface selectivity of the process was established by the surface-sensitive analytical techniques.

3.3.1 Surface photo-grafting onto EPDM films

Photochemical grafting is one of the most widely used techniques to introduce functional groups on the surface of polymeric films[9]. It is known that in a photochemical process, absorption of a photon by organic molecule (commonly called chromophore) results

in excitation of the molecule from its ground state giving rise to n-π* and π-π* transitions. The extra energy associated with the excited molecule is then dissipated by various processes, amongst which *energy transfer* is the most desirable process for grafting reactions. Absorption of UV light by a photoinitiator produces an excited singlet (S^{1*}) transition, which then releases a part of its absorbed energy to form excited triplet (T^{1*}). Before the excited triplet undergoes decay, the absorbed energy is used for photochemically induced reactions[9]. The photochemical grafting of vinylic functional monomers onto the EPDM surfaces was activated using photoinitiators viz. BP, BZ, XT, BPO and AIBN. Irradiation of photoinitiators effectively gives the triplet exited state via intersystem crossing from the initially formed singlet state. These triplets are effective in abstracting hydrogen atom from polymer surface to leave macro radicals that can initiate graft polymerization[10-12]. The photochemical reactor (due to pyrex glass) absorbs radiation below 300 nm and is thus expected to decrease the amount of homopolymerization formed during irradiation[13] since, vinyl homopolymer can be readily initiated by short wavelength UV radiation.

3.3.1.1 Reaction mechanism

The well-known mechanism of surface grafting is shown in the **scheme 3.1**, where, upon absorption of UV irradiation, the photosensitizer gets excited giving rise to the triplet-excited state from the initially formed singlet state. These triplets effectively abstract hydrogen atom from polymer surface to generate macro radicals which, upon reaction with vinylic monomer results in 'grafting from the polymer'. However, when the abstraction of hydrogen atom takes place from the monomer, 'homopolymer' is formed. This growing homopolymer chain when interacts with the polymer surface, gives rise to 'grafting onto the polymer'. By using the Pyrex glass reactor, which has a cut off limit at 300 nm, one can minimize the possibility of the later two reactions (that is homopolymer and grafting onto the polymer). All the three simultaneous reactions taking place in this process undergo the traditional 'free radical mechanism'.

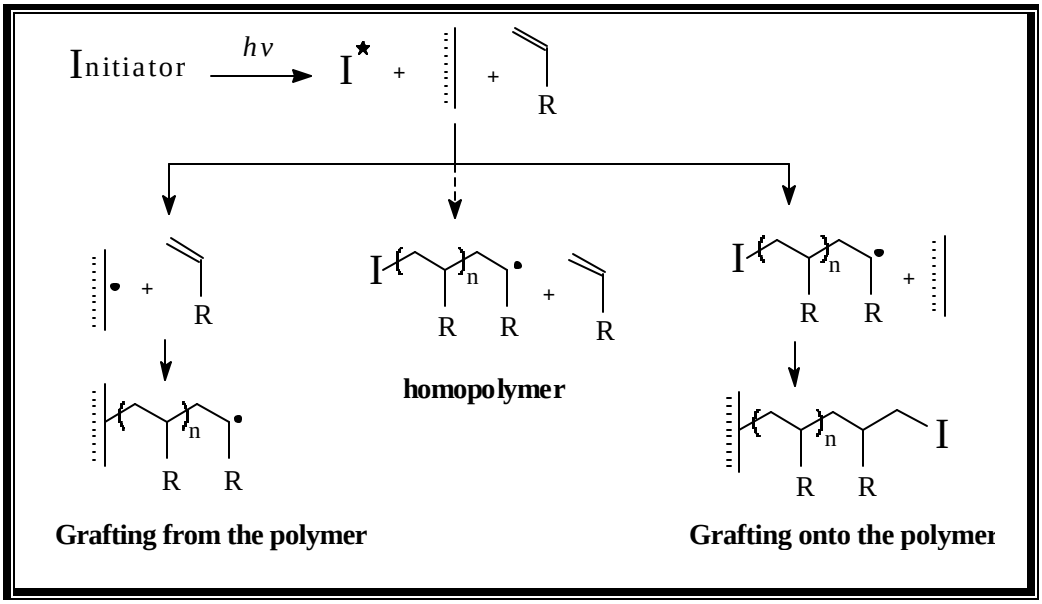

Scheme 3.1

3.3.1.2 Control experiment

The reactions were carried out according to the procedure mentioned in the **section 3.2.2.1**. Separately, in five different reactions, (0.2 M) of each photo-initiator/sensitizer (viz. BP, BZ, XT, BPO and AIBN) was taken along with a solvent mixture of acetone and toluene (44 + 3 ml) and a pair of pre-weighed EPDM films in absence of monomer in the photoreactor maintained at 50 ± 2 °C under inert conditions and irradiated for 3 hours. These films were then washed with fresh acetone, dried and characterized by ATR-FTIR, which did not show any additional peak with respect to the pristine EPDM. However, the ATR-FTIR spectra of the control experiments were taken as reference for comparing them with the photo-grafted samples. Further, there was no change in weight as well as the water contact angle of these control samples.

It was confirmed by carrying out following control experiments that the functionalities generated on the surface of EPDM were due to the photografted monomers and not due to the surface degradation induced by photo-initiations/sensitizers in the presence of UV light.

3.3.1.3 Surface photo-grafting of functional monomers

The irradiation of a pair of EPDM films (4 cm × 1.5 cm), in each photo-reactor was carried out in the presence of 0.2 M benzophenone, 1.0 M of monomer (HEMA, AA, GMA, AAm and NVP) in a solvent mixture of (44 ml acetone + 3 ml toluene) under inert reaction

condition for 1 hr at 50 ± 2 ºC. The reaction mixture was deaerated with high purity nitrogen gas for 20 minutes before commencing the reaction and the inert atmosphere was maintained throughout the reaction. A small amount of toluene was added to the reaction mixture with a view of improving the degree of grafting by swelling the surface of the film and making the polymer chains flexible. The characterization of these surface grafted films after soxhlet extraction and thorough drying revealed the following information. The **scheme 3.2** shows the photo-grafting of these functional monomers onto the EPDM films. The primary evidence of the successful accomplishment of the surface photo-grafting reaction was obtained from the results of *degree of grafting* and *contact angle measurements*, revealed in the **Figure 3.3**. The difference in the degree of grafting is attributed to the dissimilarity in the reactivity of functional monomers. The grafting efficiency (G_e) observed here is in the order HEMA>AA>GMA>NVP which is well in accordance with the % conversion of polymerization reaction (*Cp*) and grafting conversion (*Cg*) of these monomers during their photo-grafting onto LDPE[14] at 50 ºC and 2 wt % BP. The same report also revealed that the non-acrylates have a lower polymerization rate compared to the acrylates.

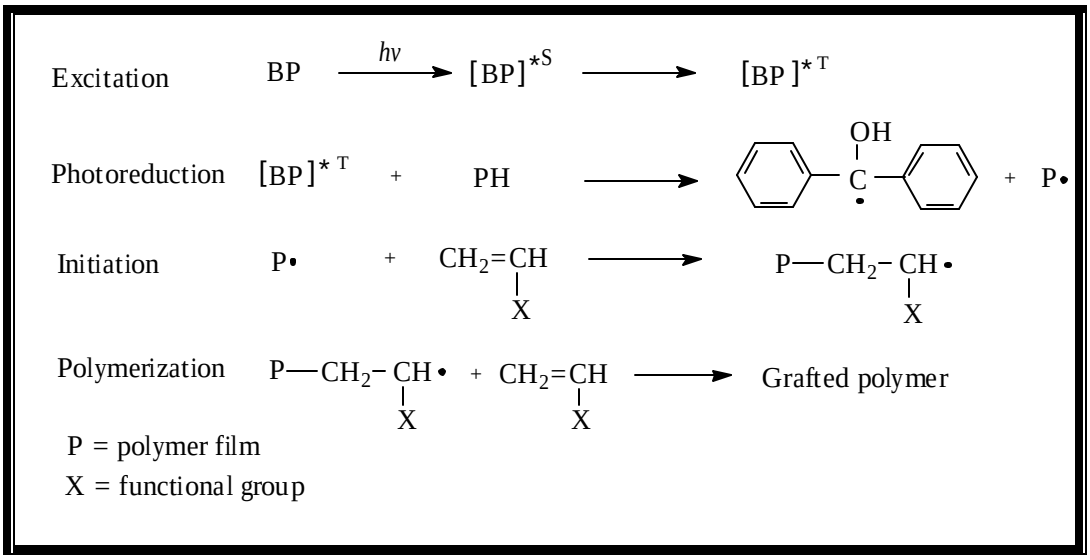

Scheme 3.2

The exceptionally low grafting of NVP is attributed to the abstraction of the more reactive hydrogen (H) from the carbon (C) adjacent to nitrogen (N) than the H-abstraction from the EPDM backbone as shown in the **Scheme 3.3**. The *degree of grafting* also depends on the affinity of the monomer towards the surface free radicals.

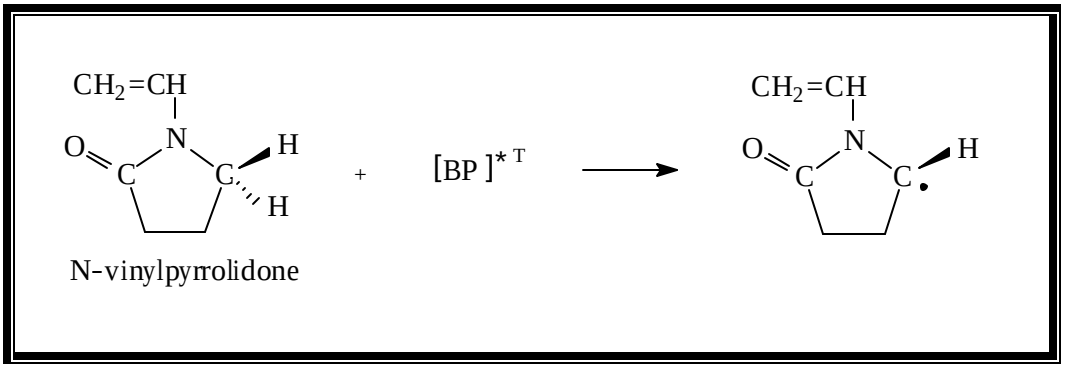

Scheme 3.3

From the **Figure 3.3**, it is understood that HEMA and AA grafted films generate highly hydrophilic surfaces. However, the hydrophilicity of the modified surfaces shows their dependence on the *degree of grafting* and the type of monomer grafted. The polymers with water contact angle (θ) < 70° are considered to exhibit good hydrophilicity and thereby biocompatibility.

The presence of respective functional groups of the grafted monomers was substantiated by spectroscopic techniques. In the ATR-FTIR spectrum, the characteristic peaks with stretching vibrations at 1720 cm^{-1} (O-C=O) & 3440 cm^{-1} (O-H) for EPDM-g-HEMA, 1663 cm^{-1} (N-C=O) for EPDM-g-NVP, 1707 cm^{-1} (COOH) for EPDM-g-AA and 3350 cm^{-1} (N-H) & 1660 cm^{-1} (N-C=O) for EPDM-g-AAm and 1728 cm^{-1} (O-C=O) & 1157 cm^{-1} (C-O-C) for EPDM-g-GMA are obvious in the **Figure 3.4**. These results are complementary to the XPS analysis performed on the surface photo-grafted films, which showed C1s, O1s and N1s binding energies (eV) of respective monomers grafted on the surface of EPDM films. Accordingly, C1s values of 285.0 (C-H), 288.8 (O-C=O), 286.2 (C-OH) and O1s values of 532.4 (C-O), 533.3 (O-C=O) for HEMA, C1s values of 286.4 (C-O), 288.5 (O-C=O) and O1s values of 532.2 (C-O) and 533.3 (C=O) for GMA, C1s values of 286.0 (C-N), 288.2 (N-C=O), N1s value of 399.8 (N-C=O) and O1s value of 532.6 (N-C=O) for NVP are observed in the **Figure 3.5**. Different morphologies arising upon photo-grafting of functional monomers are evident from the SEM images shown in the **Figure 3.6**. It can be noticed that roughness of the surface increases with the increase in the degree of grafting. Moreover, grafting of each monomer resulted in a different morphological pattern. For reactions carried out at very low monomer concentrations, grafting is often non-uniform.

Figure 3.3 Changes in the degree of grafting (G_d) and water contact angle upon photo-grafting of functional monomers (1.0 M) onto the EPDM films at 50 ºC.

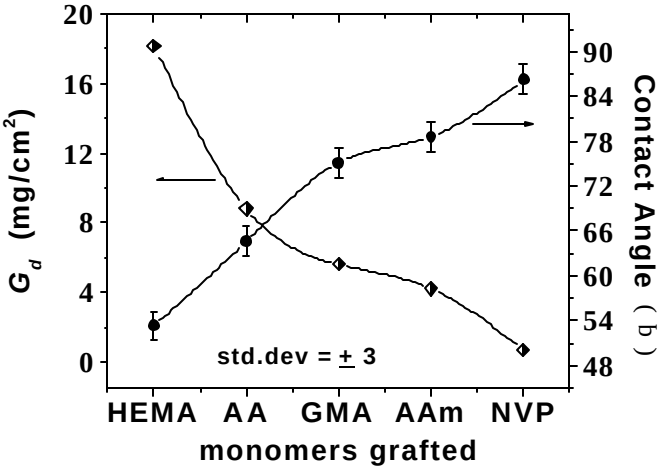

Figure 3.4 ATR-FTIR spectra of HEMA, AA, GMA, AAm and NVP photo-grafted onto the surface of EPDM films at 50 ºC.

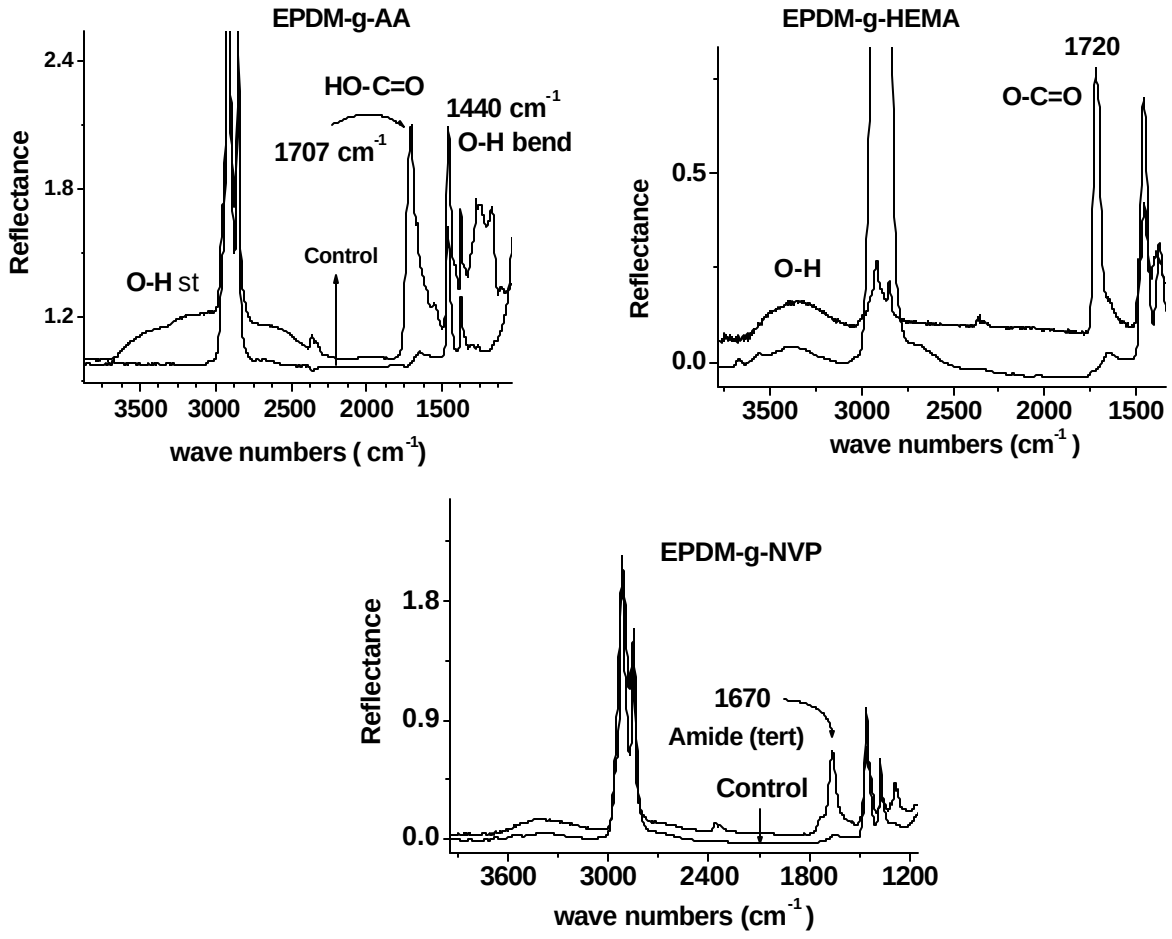

Figure 3.5 The binding energy peaks of neat and photografted EPDM in the C1s region of XPS analysis.

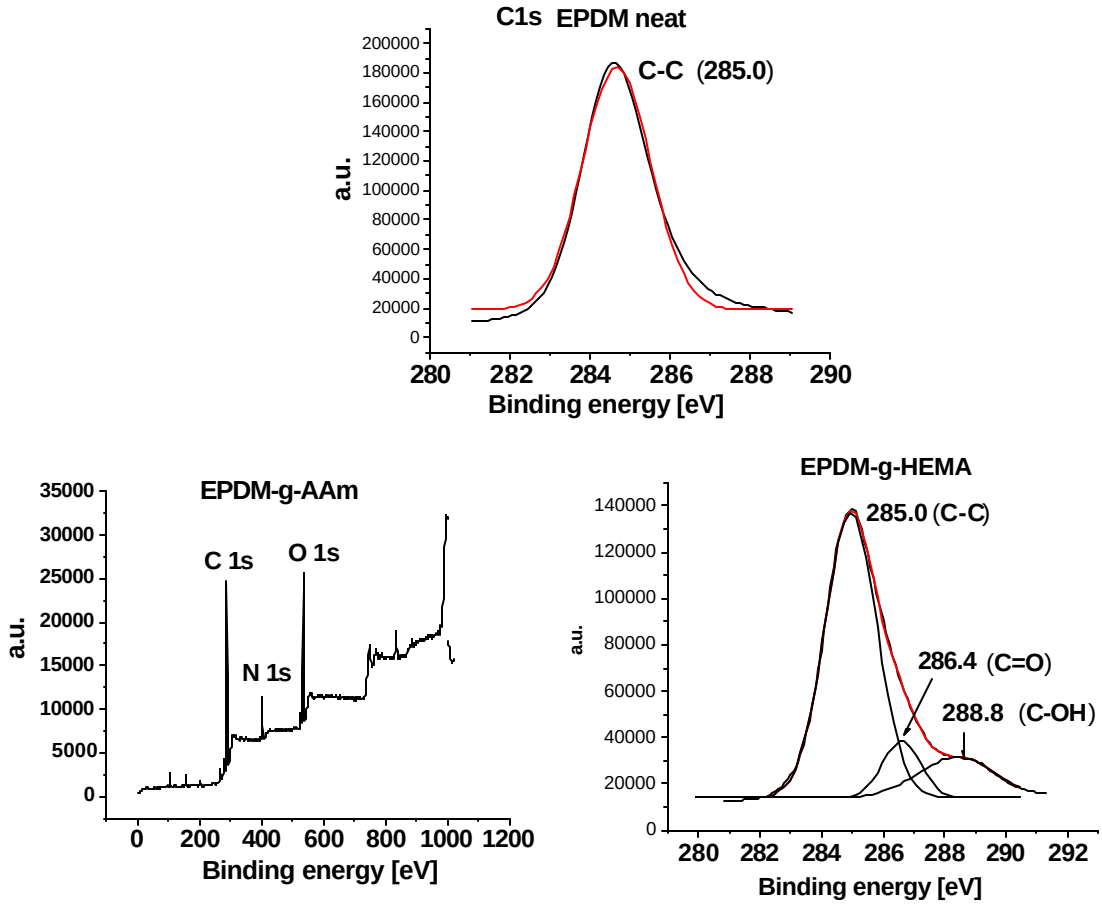

Figure 3.6 SEM images of **(a)** neat EPDM **(b)** HEMA-g- **(c)** AA-g- **(d)** GMA-g- **(e)** AAm-g- **(f)** NVP-g- photografted EPDM films.

(a) **(b)**

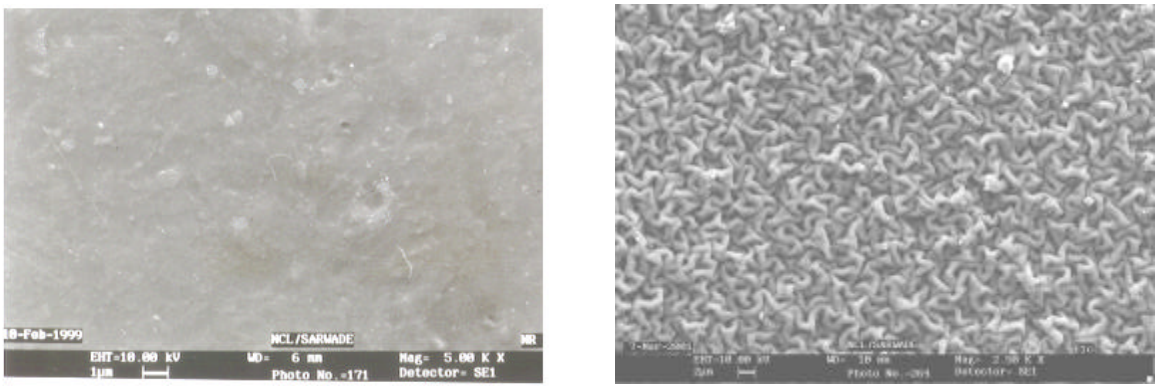

(c) **(d)**

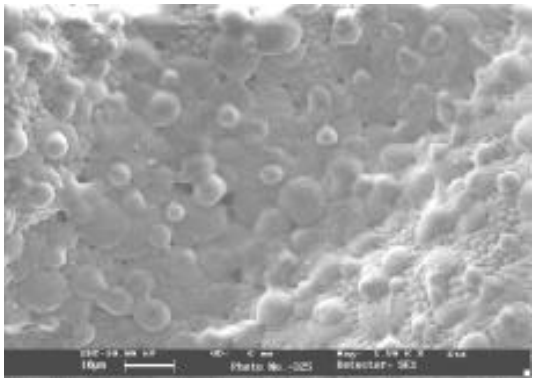

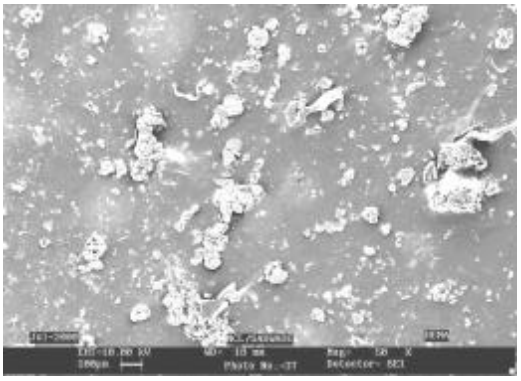

(e) **(f)**

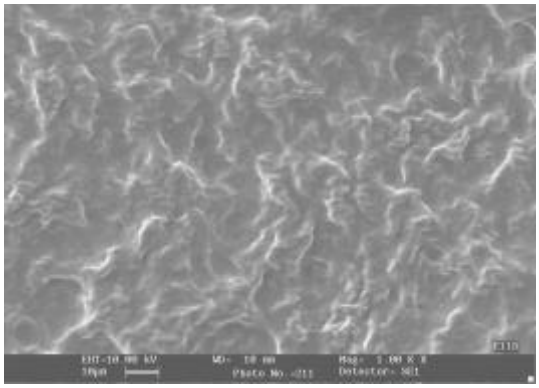

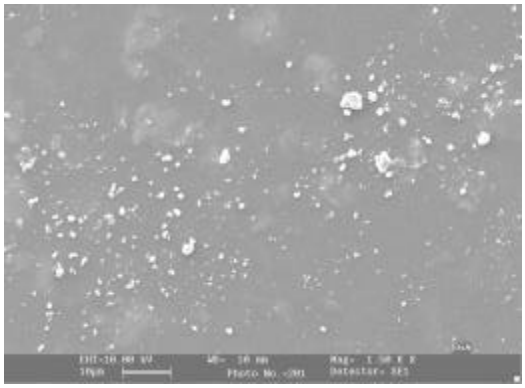

3.3.1.4 Influence of reaction conditions on surface photo-grafting

3.3.1.4.1 Effect of monomer concentration

The degree of grafting is significantly affected by the change in the monomer concentration in the reaction medium, which is evident from the **Figure 3.7 (a) and (b)**. For the two monomers viz. HEMA and AA, the G_d increases steeply with the monomer concentration, reaches a maximum value at 1.5 M and then gradually decreases with a further increase in the monomer concentration for reaction carried out at 50 ± 2 ºC. However, the same monomers show a steady rise in G_d with the concentration and levels off at 2.0 M, for grafting carried out at R.T. AAm and NVP having low monomer reactivity showed a lenient rise in the grafting yield even at higher monomer concentration for reaction carried out at room temperature. However, for photo-grafting carried out at 50 ± 2 ºC, the same monomers

showed a plateau above 1.5 M. For reactions carried out at elevated temperature, the mobility of the surface free radicals is enhanced with an additional excitation of the photosensitizer leading to better grafting yields. The dependence of water contact angle on the G_d can be clearly understood from the **Figure 3.7 (c)**.

Figure 3.7 Effect of monomer concentration on the G_d of **(a)** HEMA **(b)** AA onto EPDM films and **(c)** effect of G_d of HEMA on contact angle.

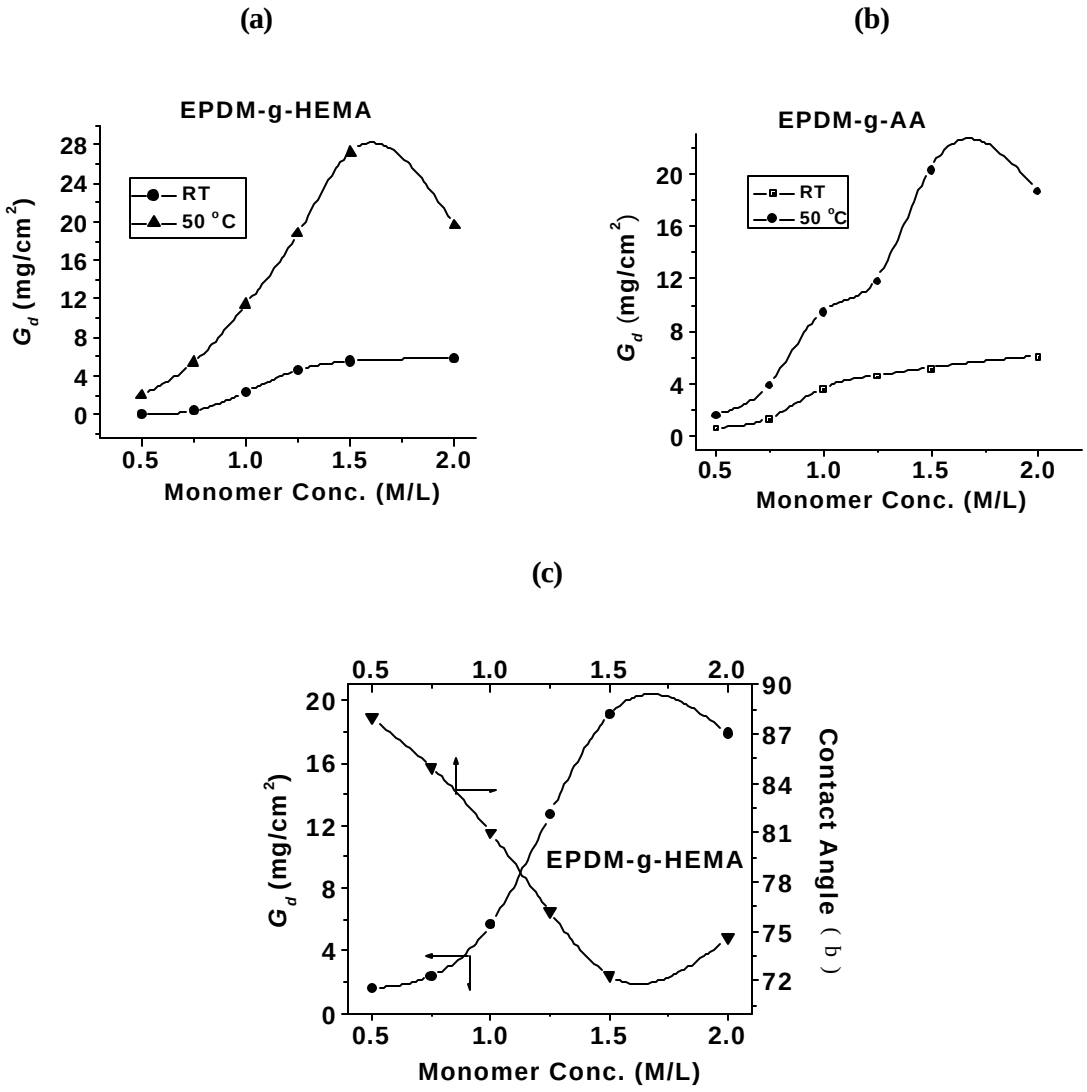

The decrease in the degree of grafting with the increase in the monomer concentration (> 1.5 M) can be attributed to the following reasons: 1) at a very high monomer

concentration, the abstraction of the H-atom by the exited photoinitiator takes place readily from the monomer instead of the polymer surface due to the high density and close proximity of monomer molecules, leading to a decrease in the efficiency to photoinitiator and thereby reducing the initiating sites on the polymer surface, 2) the abstraction of the H-atom from the monomer leads to excessive homopolymerization whereby the propagating *poly*HEMA and *poly*AA homopolymer chains undergo rapid termination via radical coupling, leading to a decrease in the grafting efficiency and 3) with the rapid homopolymer formation at higher monomer concentration, the opacity of the reaction medium increases, obstructing the UV radiations reaching the photosensitizers, resulting in less number of surface free radicals, leading to a further decrease in grafting yield. The results of ATR-FTIR spectroscopy and optical microscopy further support this explanation.

The reflectance ATR-FTIR spectra (**Figure 3.8**) of EPDM-g-HEMA intelligibly depict the effect of monomer concentration on the intensity of the hydroxyl and carbonyl groups of grafted *poly*HEMA chains present on the surface. The intensity of the respective peaks of functional groups increased with monomer concentration indicating a rise in the density of the functional groups on the film surface. The optical micrographs (**Figure 3.9**) show that the thickness of the grafted layer increases with the degree of grafting. However, the films grafted at R.T. reveal very thin grafted layers (**Figure 3.10**) of the order of few microns, which is often desired for biocompatibility applications.

Figure 3.8 ATR-FTIR spectra showing the effect of monomer concentration and reaction temperature **(a)** hydroxy peak **(b)** carbonyl peak (at 50 ºC) and **(c)** hydroxyl peak (at R.T).

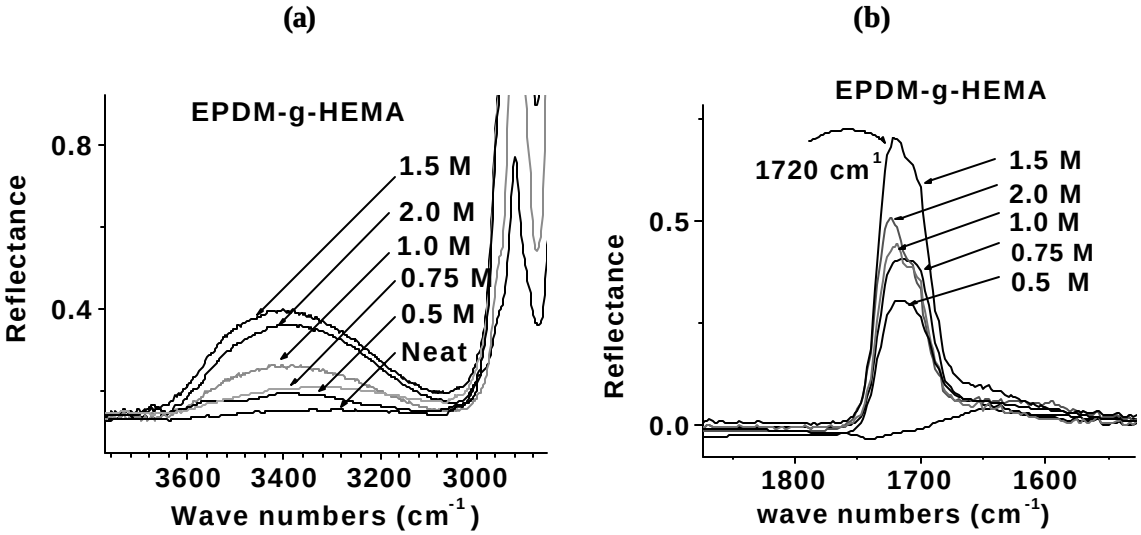

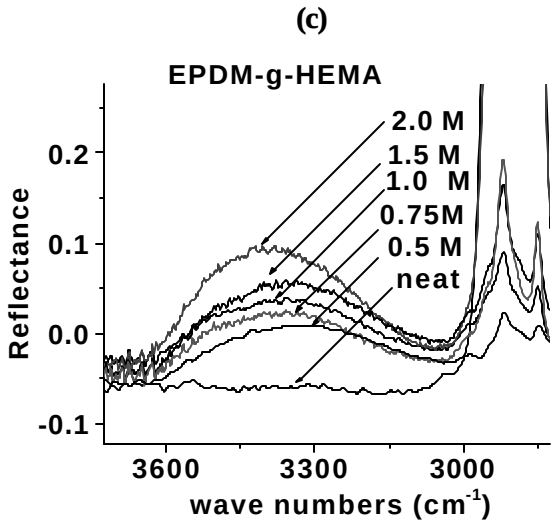

Figure 3.9 Optical micrographs of cross-section of EPDM-g-HEMA representing effect of monomer concentration on the thickness of grafted layer of HEMA for reaction carried out at 50 ºC where (a) 0.5 M (b) 1.0 M and(c) 1.5 M.

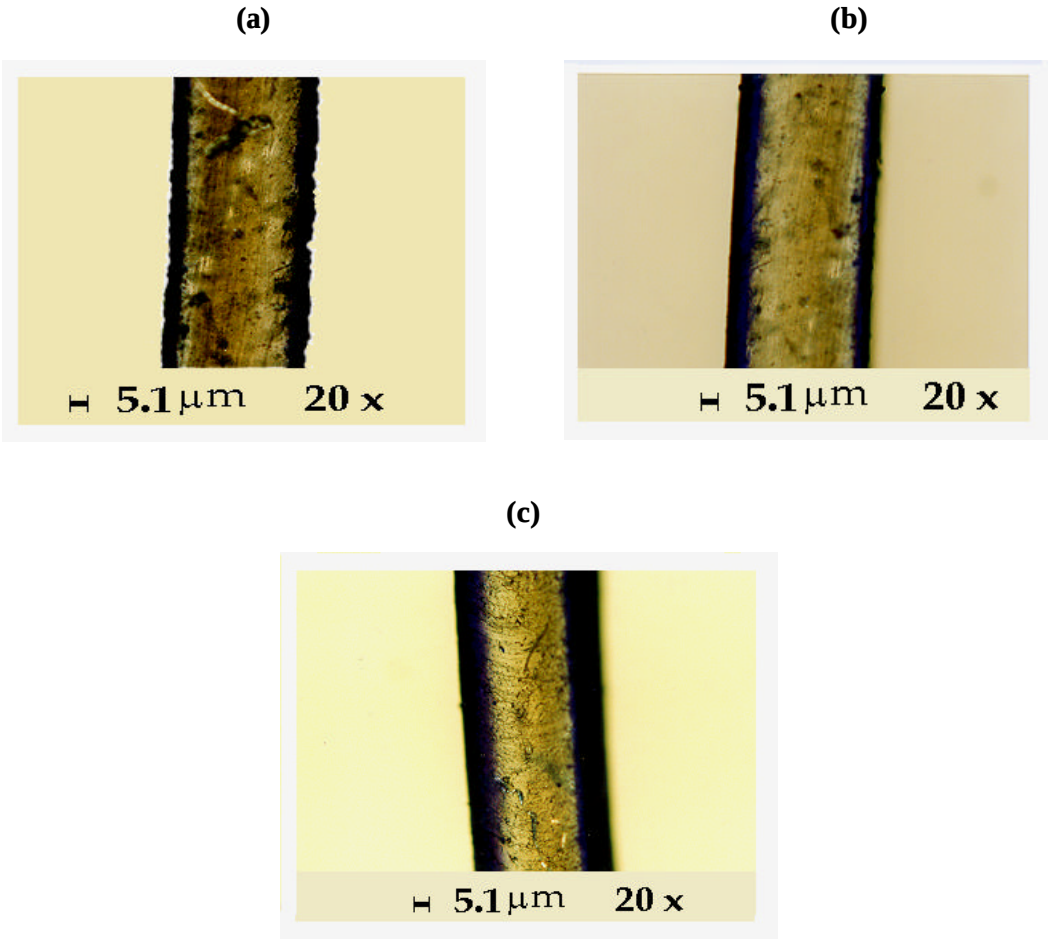

Figure 3.10 Optical micrographs of cross-section and top view of EPDM-g-HEMA films representing the effect of monomer concentration on the thickness of grafted layer of HEMA for reaction carried out at room temperature where (a) 0.5 M (b) 1.5 M.

(a)

top-view **cross-section**

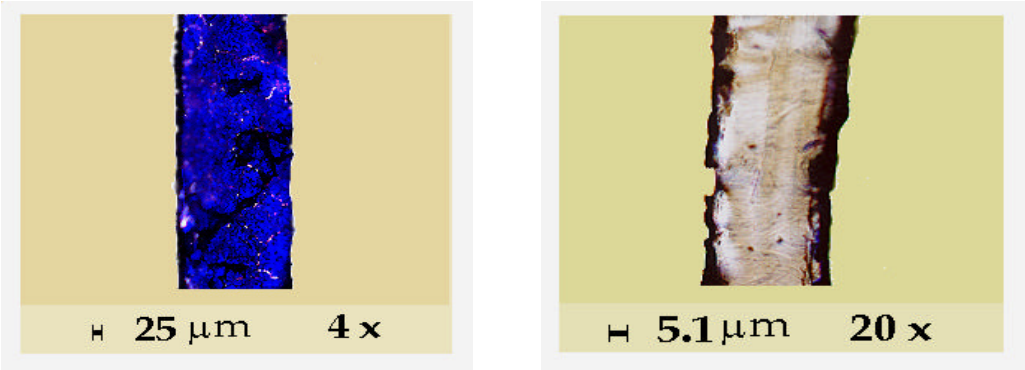

(b)

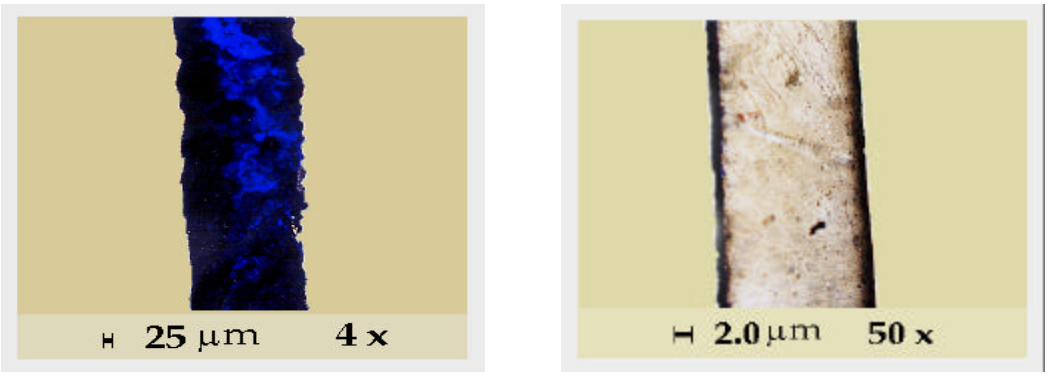

3.3.1.4.2 Effect of solvent

The irradiation of a pair of EPDM films (4 cm × 1.5 cm), in each photo-reactor was carried out in the presence of 0.2 M benzophenone, 1.0 M of monomer, HEMA and AA in each solvent under inert reaction condition for 1 hr at R.T. and 50 ± 2 ºC, according to procedure described earlier. In this study, the effect of three different solvents viz. methanol, acetone and a solvent mixture (acetone + toluene) on the surface photo-grafting of HEMA and AA onto the EPDM films has been examined. Addition of a small amount of toluene was preferred with an intention of swelling the surface of EPDM films, to allow the diffusion of monomer[15] in order to achieve better grafting yield.

The effect of solvents[16,17] in the liquid phase grafting was widely studied in the past. The accelerating function of solvents is supposed to originate either from their photosensitizing capacity[10] or swelling the polymeric substrates[18,19]. The weight gain (WG) of HEMA and AA grafted EPDM films under the influence of different solvents is compiled in the **Table 3.1**.

Table 3.1 Effect of solvent on the WG of HEMA and AA grafted onto EPDM films

Monomer	Conc. (M/L)	WG (%)					
		RT			50 ± 2 °C		
		Methanol	Acetone	Acetone + Toluene	Methanol	Acetone	Acetone + Toluene
HEMA	1.0	4.32	11.7	8.45	5.77	18.46	11.98
	1.5	7.7	16.3	12.22	9.19	23.15	16.34
AA	1.0	2.9	6.67	6.15	3.61	10.29	8.81
	1.5	5.4	10.81	8.33	7.20	15.23	12.33

Methanol as expected, proved to be a poor solvent[4] compared to acetone and mixture of acetone & toluene. The poor performance of methanol as a solvent is attributed to its high chain transfer constant, which is a very influencing factor in the graft copolymerization reactions and it is presumably governed by the inductive effect of OH. For methanol as a solvent with high chain transfer constant, a competition between reactions (**I**) and (**II**) takes place as shown in the **scheme 3.4**. If the reaction (**II**) prevails, $\bullet CH_2OH$ leads to the formation of homopolymer rather than a graft copolymer.

$$P\bullet + M \longrightarrow \text{Grafted polymer} \quad (\mathbf{I})$$

$$P\bullet + CH_3OH \longrightarrow PH + \bullet CH_2OH \quad (\mathbf{II})$$

Scheme 3.4.

In contrast to this, acetone is stable against hydrogen abstraction by $[BP]^{*T}$ therefore, $[BP]^{*T}$ can abstract hydrogen atoms from the polymer surface to initiate grafting. Although, the use of acetone gave good grafting yields, acetone being a chromophore, led to subsequent

homopolymerization under UV irradiation due to its self-sensitizing nature (E_T = 78 kcal/mole). Other researchers[10] have also observed the favorable effect of acetone as a solvent for photo-grafting reactions. Surprisingly, a negligible amount of homopolymerization, with a slightly reduced degree of grafting was observed, when reaction was carried out in a solvent mixture of acetone & toluene (44 + 3 ml). This unusual behavior is due to the photo-reduction of photoinitiator by toluene, leading to low homopolymer formation. The photoreduction reactivity of the five different types of hydrogen is shown in **Figure 3.11**.

Figure 3.11 The photoreduction reactivity of the five different types of hydrogen atoms.

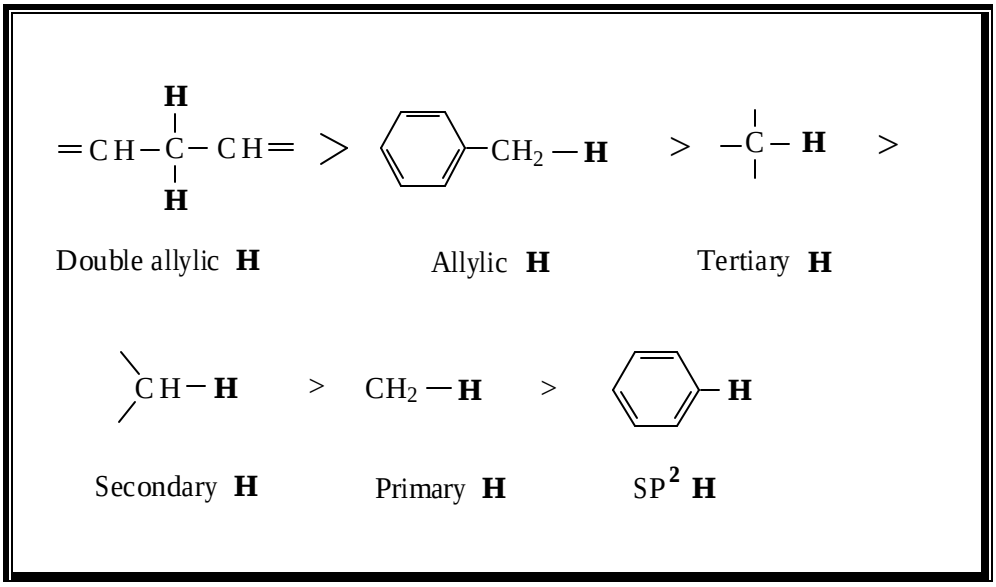

Toluene bearing an allylic H, readily donates the H-atom and causes the photoreduction of ketonic photoinitiators viz. $[XT]^{*T}$ or $[BP]^{*T}$. The resultant $C_6H_5CH_2\bullet$ radical formed has lower initiation energy (E_i) due to its stable structure and is therefore, incapable of initiating the homopolymerization of the monomer in the reaction medium. This explanation[20] is in accordance with the H-donating capacity of toluene, when present as 5 wt % additive in system comprising of 5 wt % BP at 70 °C. An additive proportion of toluene in the reaction mixture also facilitates the swelling of polymer surface helping the monomer to accommodate in the close proximity of the grafting sites. This phenomenon leads to thin grafted layers as seen in the optical micrographs **(Figure 3.12)**. But for reaction carried out at elevated temperature toluene along with monomer penetrates into the surface/sub-surface (upto ~5 microns) and gives comparatively thick grafted layer **(Figure 3.13).**

Figure 3.12 Effect of solvent (acetone + toluene) on thickness of grafted layers of HEMA onto EPDM film surface for photo-grafting carried out at R.T **(a)** 1.0 M and **(b)** 2.0 M.

(a) **(b)**

Figure 3.13 Effect of solvent (acetone + toluene) on thickness of grafted layer of HEMA (1.5 M) onto EPDM film surface for photo-grafting carried out at 50 °C.

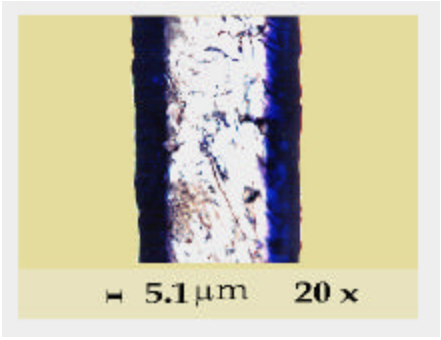

3.3.1.4.3 Effect of photoinitiator

The effect of five different photoinitiators viz. xanthone (XT), benzil (BZ), benzophenone (BP), benzoyl peroxide (BPO) and α,α'-azo bisisobutyro nitrile (AIBN), on the surface photo-grafting efficiency of HEMA and AA onto the EPDM films was also studied. The photoirradiation of a pair of EPDM films (4 cm × 1.5 cm), in each photo-reactor was carried out in the presence of 0.05 M of each photoinitiator, 1.0 M of monomer HEMA and AA, in solvent mixture (44 ml acetone + 3 ml toluene) under inert reaction condition for 1 hr at R.T. and 50 ± 2 ºC, according to procedure described in **section 3.2.2.1**.

The unimolecular fragmentation (Norrish type I, α-cleavage) of ketones into two radicals under UV radiation forms the chemical basis of photoinitiators for photo-curing

applications whereas the hydrogen abstraction by ketones (or photo-reduction) from a macromolecular hydrogen-donor under UV radiation forms the chemical basis for the photoinitiation of free radical grafting polymerization. Ample literature[14,21] is available on the photoinitiated grafting systems, however, not much systematic research work about the photoinitiators and their relevant photochemistry has been reported. Photoinitiators play a very vital role in the photografting phenomenon because, their efficiency is dependent on many components and parameters of the grafting system. The selection of photoinitiators therefore, forms the basis of the successful grafting reaction.

The **Figure 3.14** shows that the efficiency of photoinitiators is in the order XT > BP = Bz > BPO > AIBN for surface photo-grafting of HEMA and AA. The influence of photoinitiator on the grafting efficiency can also be understood from the intensity of the functional groups in the ATR-FTIR spectra of the EPDM-g-HEMA and EPDM-g-AA (**Figure 3.15** and **3.16**). The grafting efficiency of HEMA for almost all the photoinitiators is greater than AA, which is mainly dependent on the reactivity of the monomer. According to *Mayo*[22] the reactivity of the functional monomers is attributed to the electron donating ability of the substituents adjacent to the double bond. Since $-OCH_3$ is a better electron donor than OH, the ester may be expected to be more reactive than the acid. This explanation is true only for reactions of short durations but the monomers with high reactivity, readily undergo homopolymerization to give rise to macro radicals with low mobility and therefore, with a reduced reactivity with time.

Figure 3.14 Effect of photo-initiator on the grafting efficiency of HEMA and AA onto the surface of EPDM films for reaction carried out at 50 °C.

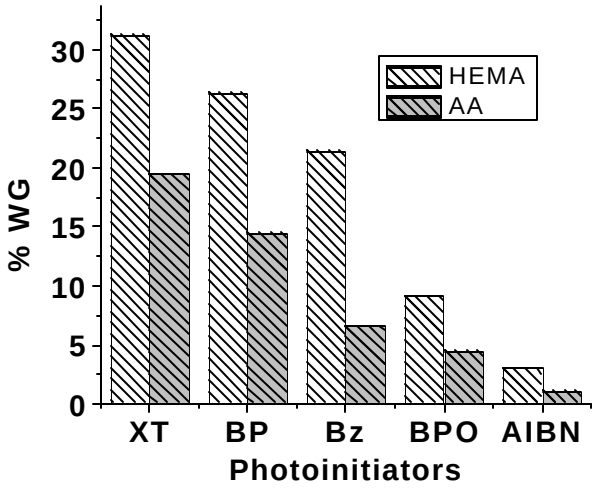

Figure 3.15 Influence of photoinitiator on the photo-grafting efficiency of HEMA in ATR-FTIR spectra.

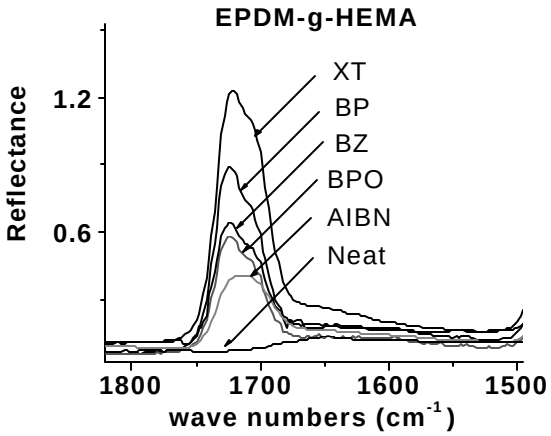

Figure 3.16 Influence of photoinitiator on the photo-grafting efficiency of AA in ATR-FTIR spectra.

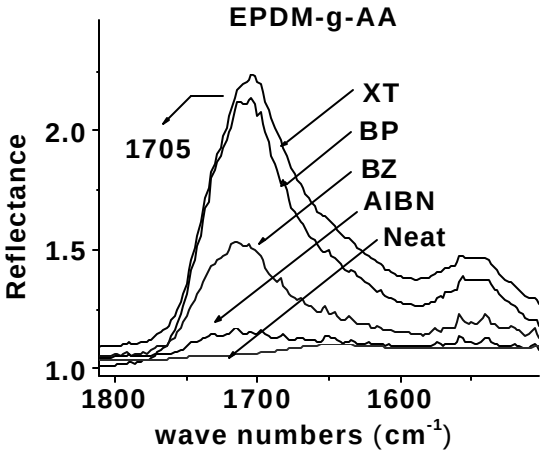

The performance and the efficiency of the photoinitiators depend on the four main factors A) stable molecular structure, B) stable ketyl radical, C) high triplet energy state and D) high UV absorption. The basic difference in the reactivity of XT & BP versus BPO & AIBN lies in their behavior in the photo-grafting conditions. Broadly it can be explained that upon UV irradiation, XT & BP act as *H-abstracting* photoinitiators whereas BPO & AIBN act as *fragmenting* photoinitiators. This behavior of the photoinitiators can be systematically explained on the basis of the **scheme 3.5**. BPO and AIBN undergo fragmentation[23] upon absorption of UV radiation or sufficient energy in the later case. The ketyl/alkyl free radical so formed being non-capable of abstracting a H-atom from the polymer backbone, initiates the formation of homopolymer (Mn) as shown in reaction **(1)** and **(2)**. This explanation is in accordance with the observation made by *Wilkie et al.*[24] and other researchers[25]. It has also been reported that hydrogen-abstracting photoinitiators[26,27] such as XT and BP are more effective compared to photo-fragmenting[28] type initiator (BPO). The grafting, if any, taking place using photo-fragmenting type initiators, mainly depends on the reactivity of the monomer/homopolymer radical[29]. Photoreduction by hydrogen abstraction from a H-donor shown in reaction **(3)** and **(4)** gives rise to a ketyl radical which may initiate homopolymerization when H-donor is a monomer and graft copolymerization when H-donor is a macromolecular free radical. This type of reactions gives rise to surface photo-grafting when H-abstraction takes place from the surface of an organic material (PH). As the polymerization proceeds, secondary and tertiary hydrogens appear on the newly formed polymer chains (grafted from the polymer surface) or homopolymer, as shown in reaction **(7)**. These hydrogens become new targets of excited photoinitiators. A secondary photoreduction then occurs with H-abstraction from the newly formed grafted polymer and newly formed homopolymer to give rise to secondary grafting as shown in reaction **(5)** and **(6)**. *Ranby et al.*[20] have recently shown that when reactions **(1)** and **(2)** are predominant, no significant photo-grafting occurs. Although reactions **(3)** and **(4)** are important, but reactions **(1)** and **(4)** also take place simultaneously. For reactions where $ki_3 > ki_4$, homopolymerization prevails but, a very thin grafted layer is still obtained. However, the amount of grafted polymer formed on the polymeric substrate may be too low to be measured gravimetrically. Only when reactions **(4)** and **(6)** prevail over all the other reactions, a thick grafted layer is obtained.

In all our experiments we observed the homopolymer formation along with surface grafting. BP being a well-known classical photoreducible agent, the homopolymerization here is attributed to the reactivity of semipinacol radicals and not fragmentation of initiator. In this process although the surface free-radicals have higher reactivity compared to the semipinacol

radical, the surface free radicals have restricted mobility. As a result the initiating reactivity of the semipinacol free radical become relatively more important. Xanthone was found to be a better grafting initiator than BP, the reasons for which may be attributed to its stable rigid structure, which prevents the fragmentation reaction[30]. Moreover, the higher triplet state energy of XT (E_T = 74 kcal/mol) than BP (E_T = 69 kcal/mol) also contributes towards its better performance. It is also known that the higher the E_T, the lower is the energy barrier required for the hydrogen abstraction (C-H, E_d = 90 kcal/mol) and higher is the grafting efficacy.

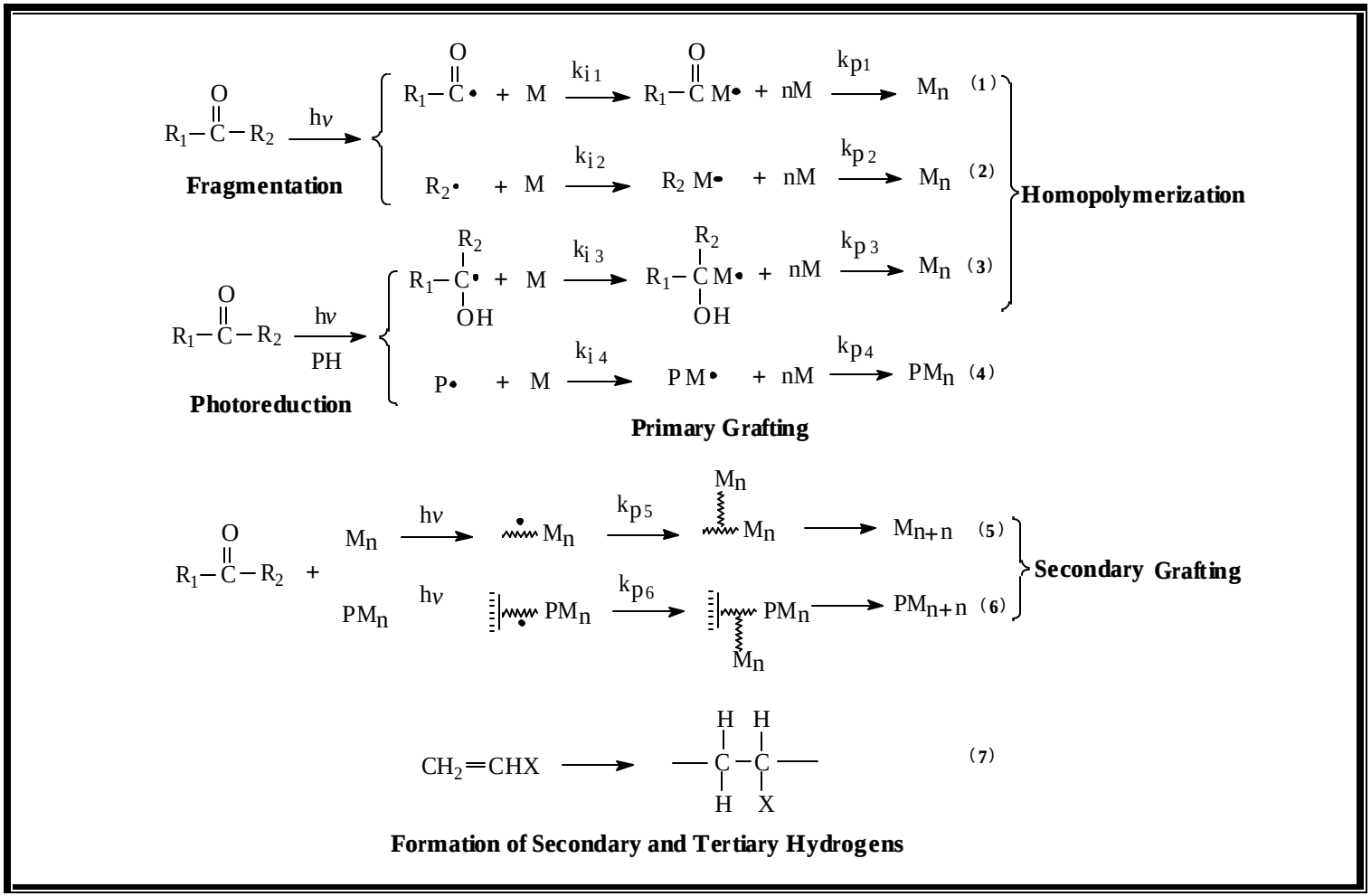
Fragmentation
Homopolymerization
Photoreduction
Primary Grafting
Secondary Grafting
Formation of Secondary and Tertiary Hydrogens

Scheme 3.5

In addition to this, the extinction coefficient for XT is ($?_{254} = 1 \times 10^4$ and $?_{313} = 3 \times 10^3$) whereas that for BP is ($?_{254} = 1.7 \times 10^4$ and $?_{313} = 50$). Although, the extinction coefficient for BP is higher at $\lambda = 254$ nm, the reaction being carried out in a Pyrex reactor with cut off level at $\lambda \geq 290$ nm, the efficiency of XT prevails. The relatively lower reactivity of BZ compared to BP is attributed to the homolytic cleavage of weak α,β-dicarbonyl bonds as in case of diketones. This homolytic cleavage results in the reaction (1) and (2), which are insignificant in bringing about surface grafting eventually. AIBN is known to have good H-abstracting capacity from organic molecules for reactions carried out at ~ 70 °C. But in our case the H-donors are macromolecules and the reactions are carried out at 50 ± 2 °C. Hence the energy may not be sufficient for the rapid homolytic cleavage of AIBN to initiate polymerization.

3.3.1.4.4 Effect of reaction temperature

The effect of temperature on the surface photo-grafting efficiency of HEMA and AA, onto the EPDM films was investigated. The photoirradiation of a pair of EPDM films (4 cm × 1.5 cm), in each photo-reactor was carried out in the presence of 0.2 M BP photoinitiator, 1.0 M of monomer HEMA and AA, in a solvent mixture of acetone and toluene (44 + 3 ml), under inert reaction condition, for 1 hr at R.T. and 50 ± 2 ºC, in the photo-grafting reactors described earlier. An advantageous effect of elevated reaction temperature on the degree of grafting (G_d) of HEMA and AA was observed. The effect of reaction temperature on the WG of the EPDM film is compiled in the **Table 3.1**. This favorable effect of reaction temperature on the grafting efficiency is the unique feature of surface photo-grafting polymerization and can be explained using the following **scheme 3.6**. Of the two initiation reactions [equation (1) and (3)] and propagation reactions [equations (2) and (4)], species (**I**) and (**II**) both have a much higher reactivity than that of the semipinacol radical. This difference in reactivity constitutes the basis of the ketone photografting system. Since, (**I**) is a surface free radical located on the solid surface and (**II**) is a macromolecular free radical anchored to the polymer substrate, the mobility and the vibrational frequency of these species are much lower than those of the semipinacol free radical and that of the homopolymer chain free radial. As a consequence, (**I**) and (**II**) show a greater sensitivity towards reaction temperature i.e. they have higher activation energy than that of reaction (3) and (4).

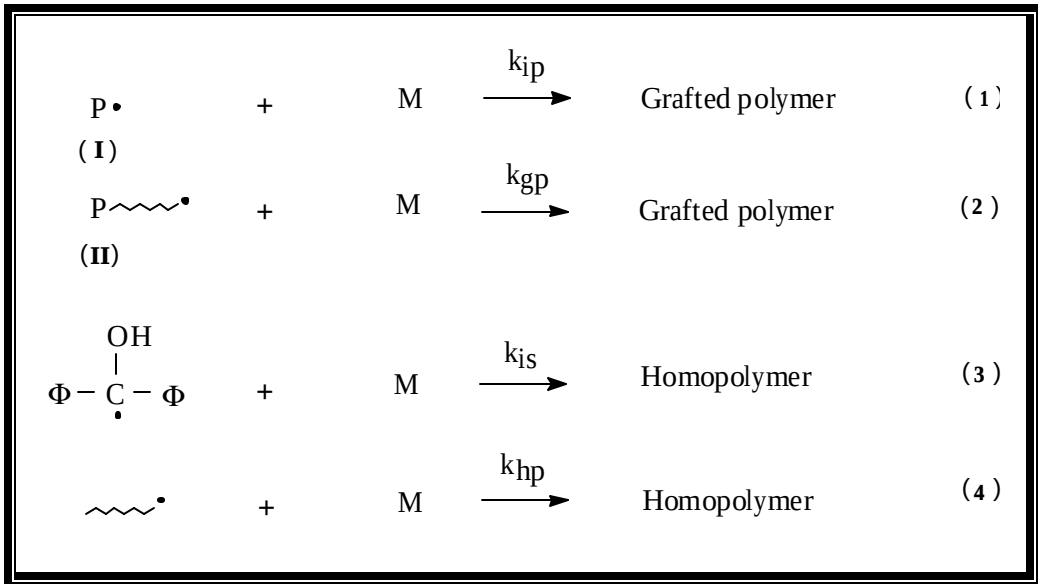

Scheme 3.6

Therefore, elevating the reaction temperature (50 ± 2 °C) increases the flexibility and mobility of these macroradicals to attack the monomer in the medium, leading to higher grafting yields[20]. For reactions, carried out at elevated temperature and monomer concentration (~ 1.0 M), higher grafting leads to thick grafted layers (~ 5 microns) (**Figure 3.17)** and reactions carried out at room temperature with same monomer concentration delivers thin grafted layers (~ 1 micron) (**Figure 3.18**).

Figure 3.17 and **3.18** Optical micro-images of cross-section of EPDM-g-HEMA revealing the influence of reaction temperature on the thickness of grafted layer of HEMA (1.0 M) for reaction carried out at 50 ºC.

Figure 3.17

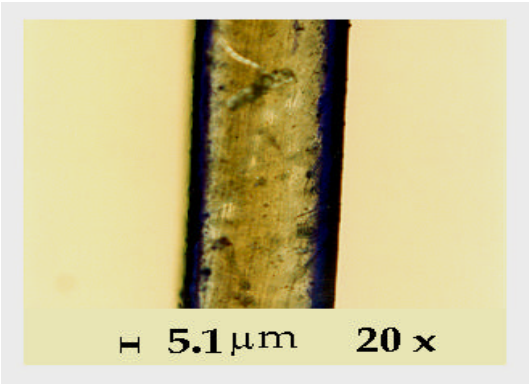

Figure 3.18

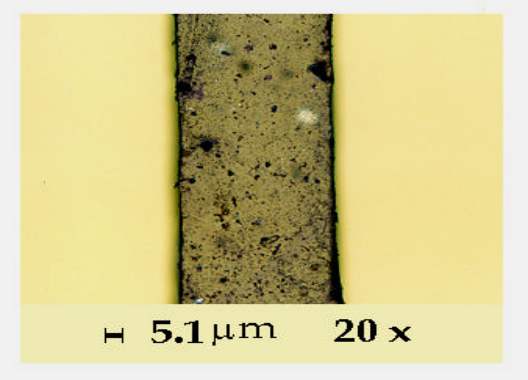

Thus, by varying the reaction temperature, one can effectively control thickness of the grafted layers. However, the choice of the monomer and type of photoinitiator has their own influence, as mentioned earlier.

3.3.1.4.5 Effect of reaction time

The effect of reaction time on the surface photo-grafting efficiency of HEMA onto the EPDM films was also investigated in the present study. The photoirradiation of a pair of EPDM films (4 cm × 1.5 cm), in each photo-reactor was carried out in the presence of 0.2 M BP photoinitiator, 1.0 M of monomer HEMA, in a solvent mixture of acetone and toluene (44 + 3 ml), under inert reaction condition, at R.T. and 50 ± 2 ºC, for different reaction time, in the photo-grafting reactors described in ***section 3.2.1.2.1***.

As is obvious from the **Table 3.2**, the G_d and G_e values increase with the reaction time. With the increase in the reaction time, the macroradicals on the surface of EPDM films gets formed under the influence of radiation and triplet-exited state of photoinitiators. The maximum grafting yield was observed for reaction time of 1 hr, beyond which the grafting yield remained constant. We assume that after 1 hr of reaction, the factors like radical coupling, restricted mobility of growing chain, homopolymerization and light scattering become detrimental. But for reaction time less than 10 min a very non-homogenous and localized grafting was observed. The SEM images of EPDM-g-HEMA for different grafting time are shown in **Figure 3.19**.

Figure 3.19 SEM images of EPDM-g-HEMA for different photo-grafting time **(a)** 30 min **(b)** 60 **(c)** 90 min **(d)** 120 min.

(a) **(b)**

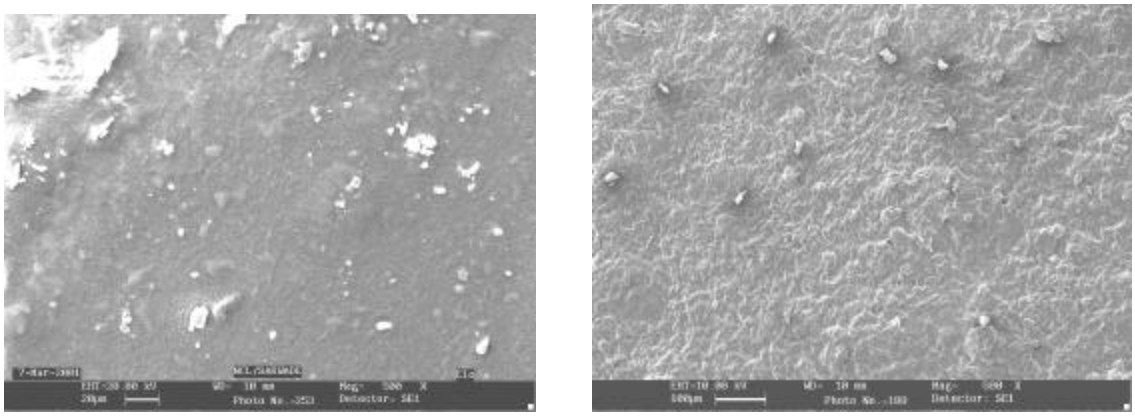

(c) **(d)**

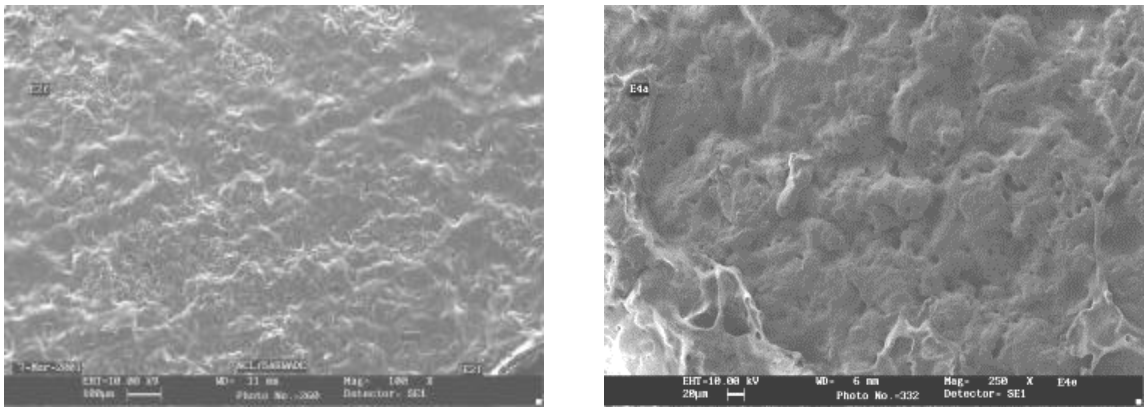

Table 3.2 Effect of reaction time on the G_d and G_e of HEMA onto the EPDM films.

Grafting time (min)	G_d *(mg/cm²)*		G_e (%)	
	RT	**50 ± 2 °C**	**RT**	**50 ± 2 °C**
15	3.3	4.1	0.8	0.66
30	5.0	8.3	0.76	1.05
60	10.0	14.2	1.03	1.36
90	13.3	20.8	1.14	1.58
120	14.1	19.1	0.89	1.16

3.3.1.4.6 Effect of homopolymer inhibitor

The effect of three different photoinitiators viz. TEGDA, EGDA and DAA on the surface photo-grafting of HEMA onto the EPDM films was investigated with a view of improving the grafting efficiency. The photoirradiation of a pair of EPDM films (4 cm × 1.5 cm), in each photo-reactor was carried out in the presence of 0.05 M BP photoinitiator, 1.0 M of monomer HEMA and AAm, 5 % v/v of an MFA, in 47 ml of acetone, under inert reaction condition, for 1 hr at R.T. and 50 ± 2 ºC, in the photo-grafting reactor described earlier.

Ever since the discovery of graft copolymerization, homopolymerization has been an associated menace and the main drawback of the radiation induced grafting systems. Metal based homopolymerization inhibitors[31-33] including Mohr's salt, $Cu(NO_3)_2$ and $FeSO_4$ have been successfully employed by various researchers to prevent homopolymerization and increase graft yield. However, the use of these inhibitors inevitably imparts colour to the substrate as observed by us. A new class of homopolymer inhibitors popularly known as multi functional acrylates (MFAs') have been successfully used by *Dworjanyn et al.*[2] as well as *Haddadi and coworkers*[34]. The multi functional acrylates, when present in additive amount, work on the principle of chain transfer from the growing macro radical chain. With the MFA present in the system, branching occurs by the attachment of the MFA onto the growing grafted substrates chains. The tail of MFA is unsaturated and hence free to initiate new chain growth via scavenging the radicals. The newly branched substrate chain may eventually terminate or cross-link by reacting with a free radical or an immobilized MFA radical.

Grafting is thus enhanced mainly through branching of grafted substrate chains. The mode of action of MFA is schematically represented in scheme 3.7.

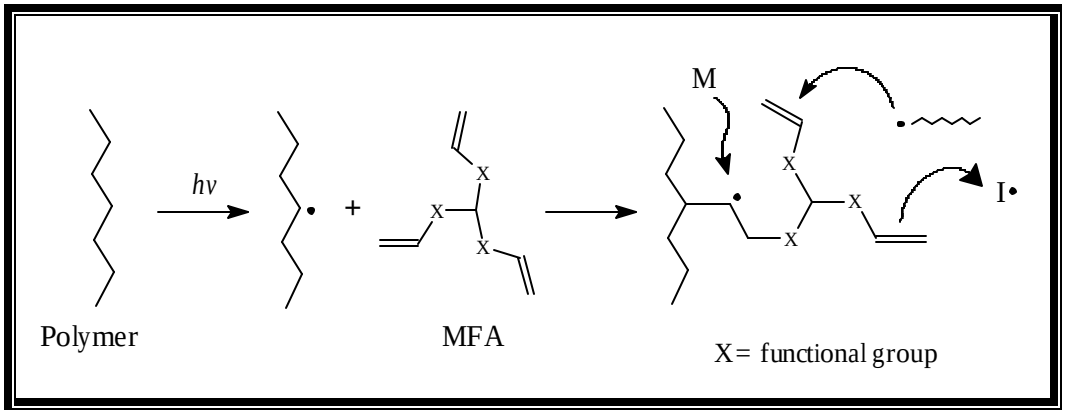

Scheme 3.7

We have used this approach to deal with the homopolymerization snag in our system. A significant drop in the homopolymerization was visually evident, with a slight decrease in the grafting yield compared to the system where acetone was used as a solvent in absence of MFA. The results are quite encouraging as evident from the **Table 3.3**. The efficacy of the multi functional acrylates was in the order TEGDA>EDGA>DAA. The difference of MFA performance may be due to the amphiphillic nature of TEGDA, leading to higher absorption of monomer into the substrate backbone. This effect termed as 'partitioning effect', determines the attraction of monomer towards the substrate surface[35].

Table 3.3 Effect of TEGDA on the homopolymer inhibition

Monomer	**M / L**	G_e (%)	
		RT	**50 ± 2 °C**
HEMA	1.0	1.22	2.0
	1.5	1.51	2.57
AAm	1.0	0.8	1.36
	1.5	1.4	1.99

3.3.2 Plasma induced surface grafting onto EPDM films

A significant amount of research has been undertaken, harnessing the versatilities of low temperature plasmas to graft functional monomers onto the surface of polymeric substrates[36]. It is known that plasma treatment of polymeric material leads to functional surfaces, however, this treatment with non-polymerizing gases has one serious drawback**:** on most of the polymer surfaces the gained superior effects are usually not permanent. It

disappears or diminishes with the storage time, due to the dynamic nature of functional surfaces[37]. The attachment of polymer chain with functional groups to the polymer surface offers an effective solution to the foresaid problem. Accordingly, solution phase post-plasma surface grafting has been thoroughly studied [38,39] for a wide range of polymers giving rise to desired functionalities on the substrate surface. However, this technique remains at a lower profile since, the success of grafting depends on combination of various reaction parameters like, plasma treatment conditions, post-grafting time, solvent, reaction temperature, monomer reactivity, density of peroxides on surface and their decomposition rate etc. Moreover, due to its complex reaction mechanism, many undesired processes like crosslinking, loss of free radicals, incomplete decomposition of peroxides, dissolution of grafted chains also take place simultaneously. In addition to this, longer reaction time (12 to 48 hrs) is mandatory for the better grafting efficiency[40]. Simultaneous vapor phase plasma-grafting thus, forms a better alternative to the post plasma-grafting technique[41]. Short reaction time, ambient temperature, solvent free grafting, homogenous modification confined to surface, lack of undesirable side-reactions are some of the merits of vapor phase plasma-grafting. The resultant functionalities generated, are found to improve hydrophilicity, hydrophobicity, adhesion property, biocompatibility and non-fouling properties of the substrate surface. Moreover, the functional groups generated are permanent and are not lost with time, but may undergo reorientation. However, the elastomers like EPDM and NR, for these purposes, have been hardly addressed[42-44]. Recently, evaluation of biocompatibility of various elastomers was under taken by *Lebret and coworkers*[45]. *Razzak et al.*[46] succeeded to some extent in improving the blood compatibility of NR by radiation induced grafting of *N*,*N*-dimethyl acrylamide and *N*,*N*-dimethyl aminoethyl acrylate.

Medical products from elastomers have found plenty of applications, ranging from surgical devices, tubings, catheters to balloons and implants. The elastomers with excellent flexibility and resistance against splitting would be more advantageous than other polymers. If improvement in body compatibility of EPDM, is accomplished, the biomedical applications of EPDM could be greatly extended. Although, plasma induced surface modification has distinct advantages, the high vacuum requirements for low-pressure plasmas, expensive treatment and difficulty in scaling up a plasma process from laboratory size to industrial continuous processes are at the top of the critic's list. But, in the present scenario with strict environmental norms, plasma treatments have an edge over the conventional wet chemistry processes, where cost of handling solvent and higher waste disposal expenses exceeded those for plasma processes. Moreover, the increasing capability of computer systems, especially with

the use of Monte-Carlo[47] codes nowadays, allow effective model calculation for cases close to real plasma processes. A solution for problems related to reactor scaling will become available with future progress in simulation techniques.

3.3.2.1 Reaction mechanism

The EPDM films when exposed to the argon plasma, generates reactive centers (mainly free-radicals) on their surface upon interaction with the highly active species (electrons, ions, radicals etc) in the plasma. The life and the density of the active species depend on the plasma power and treatment time. So, more the power/treatment time, more are the active species. When the monomer vapor is simultaneously introduced into the same chamber, the radicals generated on the surface of EPDM films ($P^{\bullet}$) readily react with the vinylic monomer ($\overset{}{=}_{x}$), leading to surface anchored functional groups as shown in the **scheme 3. 8** These monomers being chemically bonded to the polymer backbone (on the surface) cannot be removed upon mechano-physical treatments.

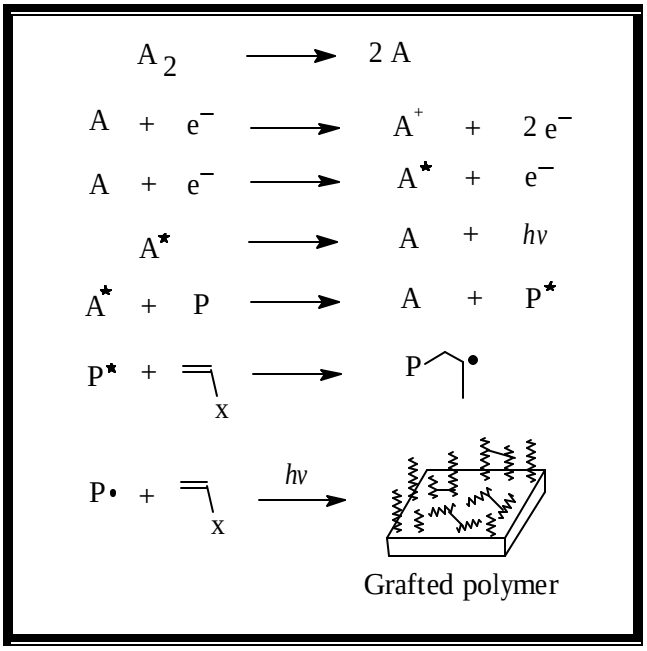

Scheme 3.8

3.3.2.2 Control experiment

In order to understand the effect of plasma treatment on the EPDM films, the pristine films were exposed to various plasma-grafting conditions (viz. treatment time, plasma power, post exposure time) in absence of monomer vapor. Each of these films was then characterized by ATR-FTIR and contact angle measurements. Almost all the films showed

the presence of carbonyl and hydroxyl groups on the surface, depending upon the treatment conditions. The spectra obtained for each condition were then taken as reference when compared with the plasma-grafting of monomers under those conditions.

3.3.2.3 Plasma-grafting of functional monomers

Plasma-grafting is a clean and solvent free technique to obtain grafted surfaces with desired functional groups. This method is known to be highly surface-selective, where modification is confined to a depth of few angstroms without altering the bulk properties. Unlike the conventional post plasma-grafting[48,49] which involves decomposition of primarily formed hydroperoxides in presence of monomer and solvent at elevated temperature, we have carried out simultaneous plasma-grafting by introducing monomer vapors along with a carrier gas in an inductively coupled plasma reactor at ambient reactor temperature, according to the detailed procedure disclosed in the ***section 3.2.1.2.2***. In the present study, four different monomers (HEMA, AA, GMA and NVP) have been employed under variable plasma-grafting conditions. The plasma power was varied from (40-75 W) and grafting time (10-50 min) with and without post-treatment exposure to monomer vapors. The post treatment exposure time allowed all the monomers in the reaction chamber to react with the surface free-radicals. The plasma-grafted films were then sonicated in water, methanol and acetone and dried in vacuum oven before characterization.

Upon applying the plasma power, excitation of the carrier gas takes place, generating active species (viz. ions, radicals and atoms) in the plasma. These active species upon interaction with the substrate, generates reactive sites (mainly free radicals) on the EPDM surface. The monomer vapors in the plasma chamber easily react with these radicals, yielding grafted surfaces as represented in scheme 3.9.

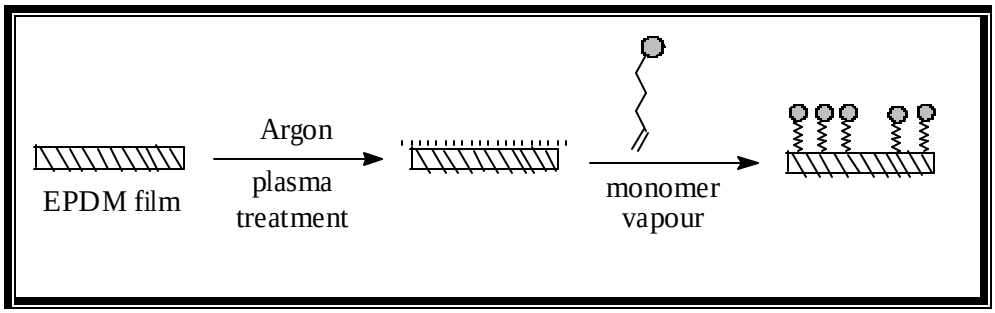

Scheme 3.9

The successful accomplishment of plasma-grafting is evident from the decrease in the water contact angle and the gravimetric changes in the EPDM films, as apparent from the **Figure 3.20.** The **Table 3.4** shows that the weight gain is much less for grafting time $\leq$ 10

minutes and plasma power ≤ 50 W. Although, the degree of grafting observed here is in the order HEMA>AA>GMA>NVP, the difference in the grafting efficiencies of the employed monomers is much less, unlike in photo-grafting. This is mainly because, the dependence of the monomer reactivity on the grafting efficiency is much less in plasma-grafting compared to that in the case of photo-grafting. Moreover, the molecular weight of all the grafted chains on a substrate is expected to be almost similar as the initiation and propagation occurs under similar reaction conditions. Chain termination[50] occurs after exposing the samples to the air. It has also been reported that the membranes modified by vapor phase plasma-grafting has many short chains on the surface, giving rise to a brush like structure[50].

Figure 3.20 Effect of plasma-grafting on G_d and contact angle measurements.

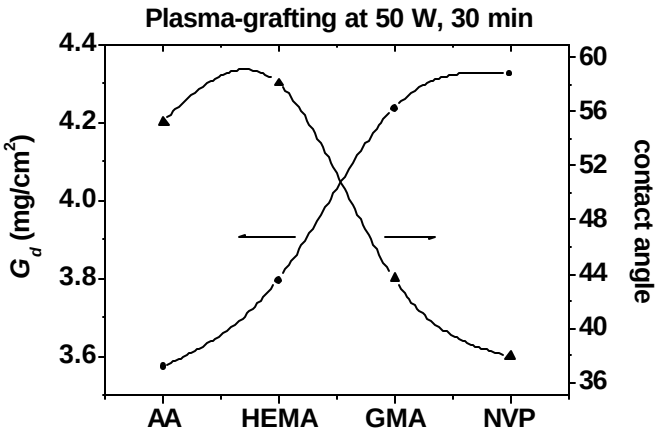

Table 3.4 Gravimetric changes in the plasma grafted EPDM films

Grafting time *(min)*	**% WG**					
	AA		**HEMA**		**NVP**	
	50 W	*75 W*	*50 W*	*75 W*	*50 W*	*75 W*
10	#	0.22	#	0.25	#	#
40	4.95	5.78	5.11	5.90	4.33	4.6

 # too small to measure gravimetrically

The use of plasma gas, distance of the substrates from the plasma edge and plasma-grafting temperature were carefully chosen after studying the optimized reaction conditions in the literature[50-52] Argon has been shown to be the best plasma medium for vapour phase grafting The distance of 12 cms from the substrate was found to be optimum, going with the fact that the increase in the distance of the substrate from the plasma edge causes lowering of

the grafting yield. *Hirotsu et al.*[53,54] reported a decrease in grafting yield for plasma induced grafting at elevated temperature. This observation was explained with an assumption that the deactivation of free radicals on the surface takes place at elevated temperature. *Johnsen et al.*[55] gave an alternative explanation for the observed temperature dependence of grafting yield, assuming that, at elevated temperature monomer tends to distill away from the sample along with the carrier gas whereas at ambient temperature (27 °C) monomer vapors condense on the substrate surface forming a thin film resulting in a higher grafting yield. The higher grafting yield of AA may be due to its comparatively lower boiling point (under reduced pressure), which favors rapid vaporization, resulting in its higher density in the reaction chamber. HEMA and GMA being high boiling monomers give slightly lower grafting yields. A similar effect of monomer, boiling point has already been reported[55].

XPS Analysis

The XPS analysis performed on the plasma grafted EPDM films showed C1s, N1s and O1s binding energies (eV) of corresponding functional monomers present on the film surface. Accordingly, C1s values of 285.0 (C-H), 288.8 (O-C=O), 286.2 (C-OH) and O1s values of 532.4 (C-O), 533.3 (O-C=O) for HEMA, C1s values of 289.2 (COOH) for AA, C1s values of 286.2 (C-O-C), 287.0 (C-O), 289.2 (O-C=O) and O1s values of 532.2 (C-O) and 533.3 (C=O) for GMA, C1s values of 286.0 (C-N), 288.2 (N-C=O), N1s value of 399.8 (N-C=O) and O1s value of 532.6 (N-C=O) for NVP are observed in the **Figure 3.21**. The values mentioned over here are with a standard deviation of 0.4 eV in the binding energy. The presence of grafted chains on the surface was further substantiated from the measurement of atomic concentration of various species, complied in **Table 3.5**. There may be a contribution of the C1s from the alkoxy/peroxide groups generated by the termination of radials by oxygen upon exposure to air after polymerization reaction but this effect is expected to be negligible compared to the total oxygen values.

Figure 3.21 Binding energy peaks in the C1s spectra of EPDM grafted with different functional monomers measured by XPS analysis.

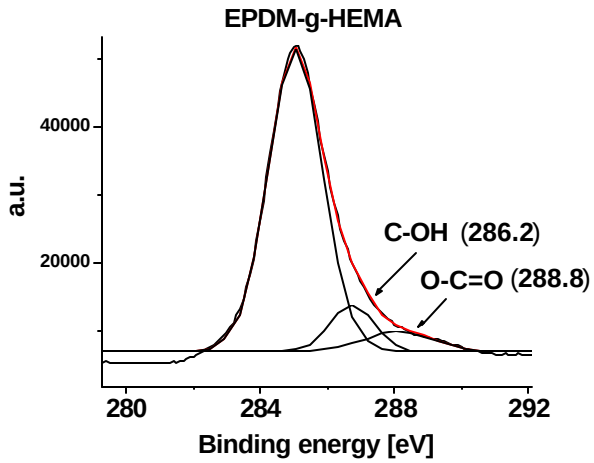

Table 3.5 The atomic concentrations of C, N and O on the plasma grafted EPDM films

Monomer grafted	Take off angle	Atomic concentration (%)			
		$C1s_1$	$C1s_2$	$N1s$	$O1s$
neat EPDM	*30°*	77.84	11.77	1.23	9.16
	60°	79.13	12.88	0.95	7.04
HEMA	*30°*	56.02	12.20	-	31.77
	60°	60.57	10.28	-	29.15
AA	*30°*	57.09	17.21	1.03	24.72
	60°	57.47	15.99	0.95	25.56
NVP	*30°*	46.97	29.82	5.13	18.08
	60°	50.48	28.66	4.67	16.19

$C1s_{1\ (C\text{-}C)} = C1s_{\ 285.0 \pm 0.2}$, $C1s_{2\ (C\text{-}O + C=O)} = C1s_{\ 286\text{-}289 \pm 0.2}$, $N1s = N1s_{\ 400.5 \pm 0.4}$, $O1s = O1s_{\ 534.5 \pm 0.4}$

A TR-FTIR spectroscopy

The presence of respective functional groups of the plasma grafted monomers, was substantiated by the characteristic peaks in the ATR-FTIR spectra with stretching vibrations at 1734 cm^{-1} (C=O) and 3440 cm^{-1} (O-H) for HEMA-g-EPDM, 1663 cm^{-1} (N-C=O) for NVP-g-EPDM, 1707 cm^{-1} (COOH) for AA-g-EPDM and 1730 cm^{-1} (O-C=O) and 1157 cm^{-1} (C-O-C) for GMA-g-EPDM, are obvious in the **Figure 3.22**. Moreover, it can be noted from the **Figure 3.23** that the intensity of the peaks for respective functional groups in the ATR-FTIR spectra are more at θ_i= 60° (d_p = 0.25 μm) than those at θ_i = 45° (d_p = 0.45 μm), indicating that density of the functional groups is more towards the surface and decreases with the sampling depth. The results of the depth profiling study are also supported by the XPS analysis.

Figure 3.22 ATR-FTIR spectra showing the peaks for respective functional groups of monomers plasma grafted onto the surface of EPDM films.

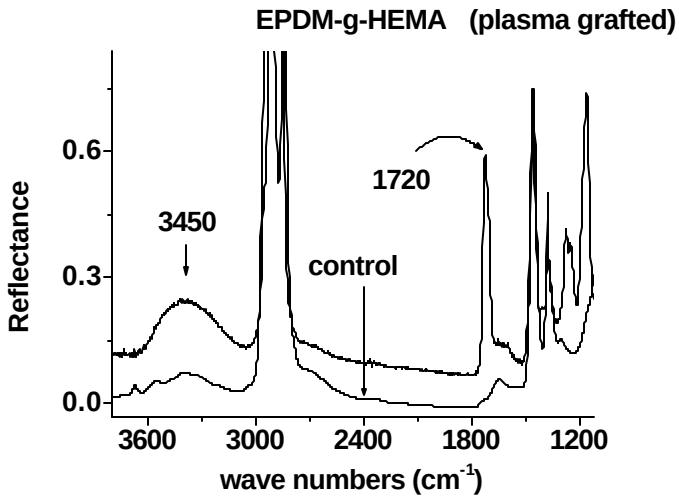

Figure 3.23 Depth profiling of functional groups on the surface of EPDM films using angle resolved ATR-FTIR.

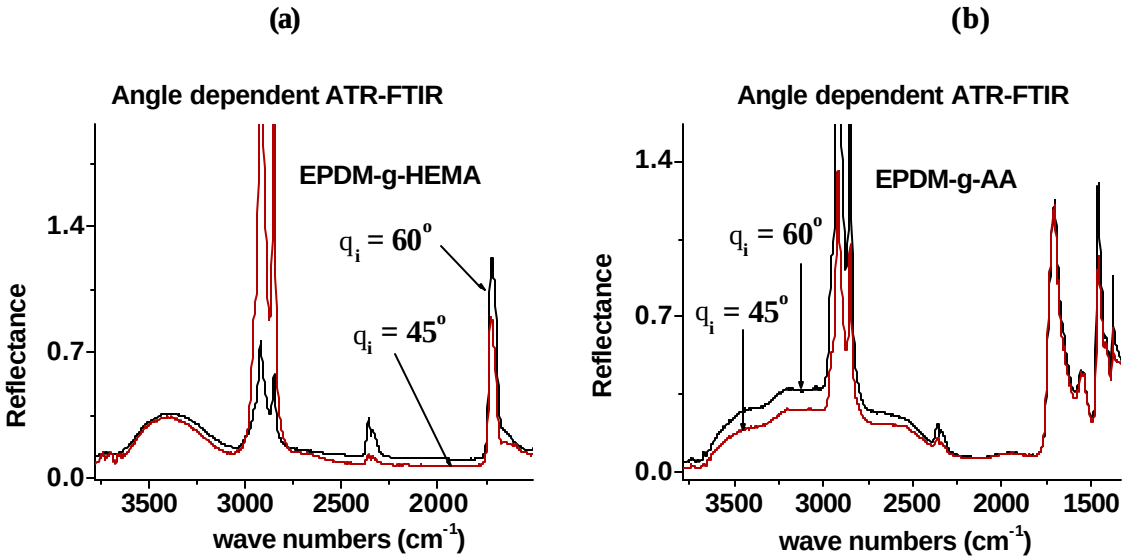

Morphology imaging by SEM and AFM analysis

The morphological investigation of the plasma grafted films indicated a uniform grafting throughout the film surface. However, the surface roughness in all cases increased compared to the pristine EPDM films. **Figure 3.24** shows the SEM micrographs of the plasma grafted EPDM films. The AFM analysis also reaffirmed that the surface roughness is less in case of plasma grafted samples compared to the photo grafted (**Figure 3.25**). This is mainly due to the controlled grafting and absence of agglomerated homopolymer chains in the former case.

Figure 3.24 SEM images of low-pressure cold plasma grafted EPDM films at 50 W for 40 minutes (a) neat (b) HEMA (c) NVP (d) AA (e) GMA.

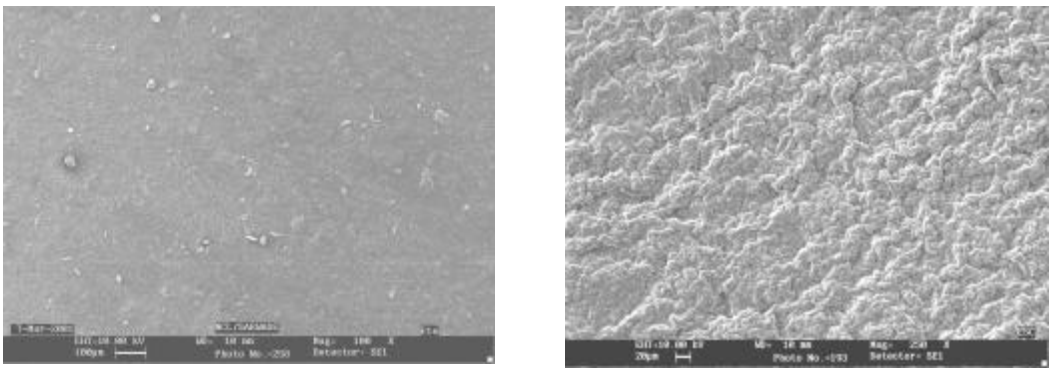

(c)

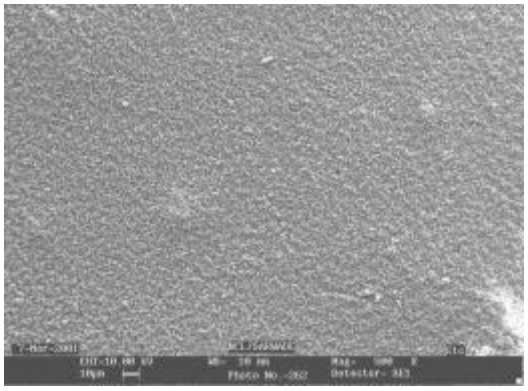

(d)

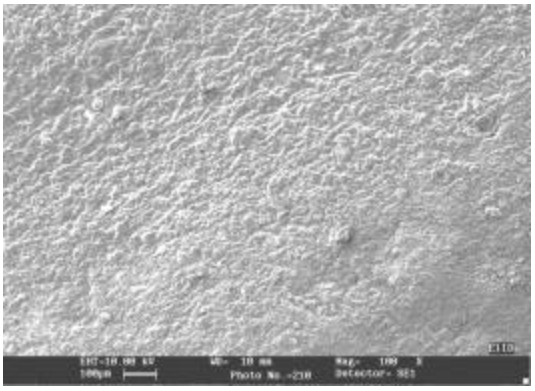

(e)

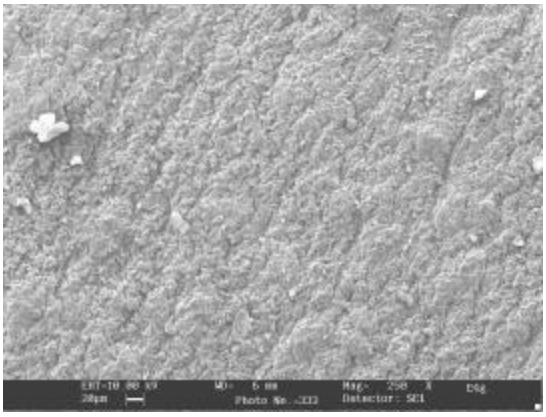

Figure 3.25 AFM images of (a) neat (b) photo- (c) plasma grafted HEMA onto EPDM.

(a)

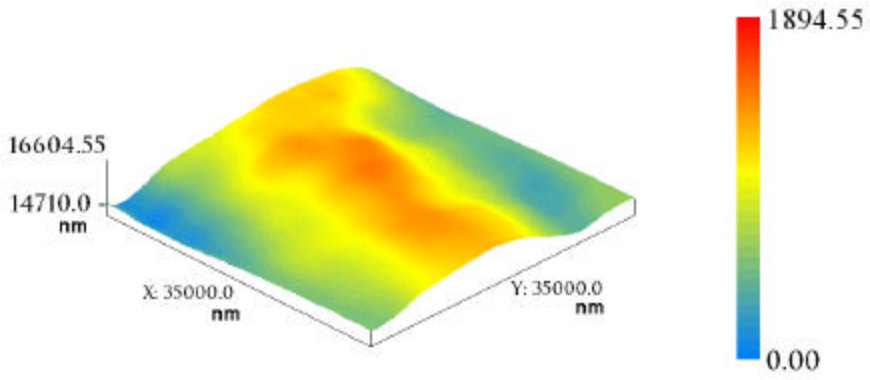

(b)

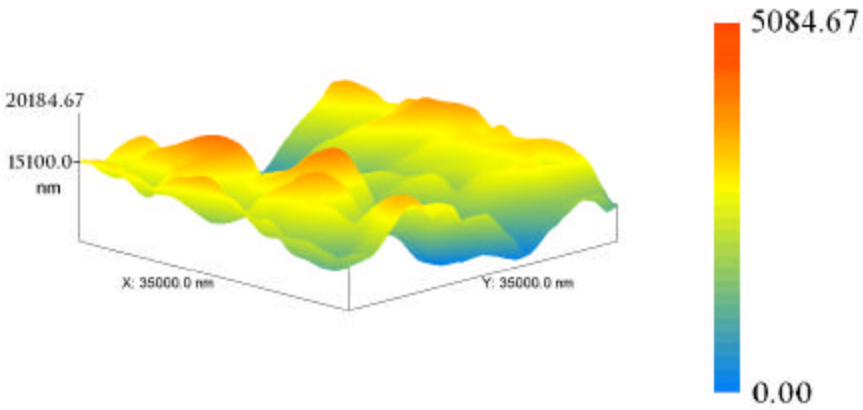

(c)

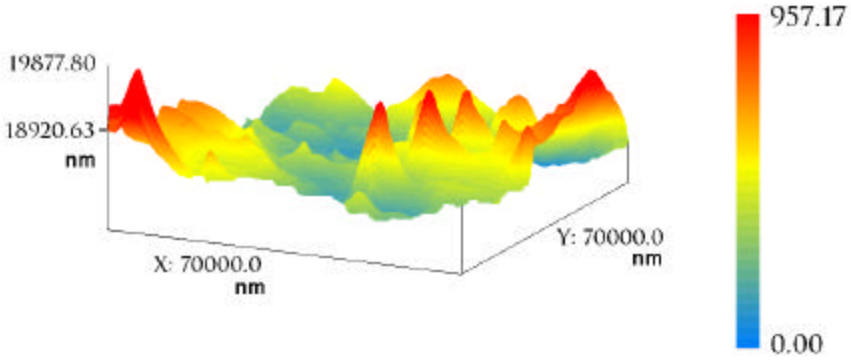

3.3.2.3.1 Effect of plasma power and grafting time

The parameters of plasma treatment and degree of grafting of three different monomers on the EPDM films have been compiled in the **Table 3.4**. Under the examined conditions, we were able to achieve degree of grafting almost 6 % WG. It is obvious from the table that the % WG increases with the increase in plasma treatment time, which is in agreement with some literature data. An increase in the plasma power beyond 75 W (30 min) had some detrimental effect on the G_d and % WG. However, there has been a discrepancy in the results reported by different researchers for the dependence of grafting yield on plasma power[56,57]. This difference may be attributed to the nature of substrate and cannot be generalized. Usually amorphous substrates undergo surface etching upon longer exposure to the plasma and the rate of etching depends on the plasma power. This might be the prime cause for the decrease in the % WG under aggressive conditions in our system. However, the ATR-FTIR spectra (**Figure 3.26**) did not show a decrease in the carbonyl peak intensity for longer irradiation time and high plasma power. *Epaillard et al.*[56] observed that for post plasma-grafting, the grafting yield increased with the plasma power and treatment time. Moreover, at high plasma power, the EPDM surface is assumed to undergo crosslinking, hindering the diffusion and interaction of the monomers with the underlying free radicals as shown in **Figure 3.27**. The surface crosslinking also hinders the orientation of the functional groups towards the polymer surface causing an increase in the hydrophobicity for samples treated with high plasma power and long exposure time.

Figure 3.26 Influence of plasma power and grafting time on the intensity of the carbonyl peaks of HEMA in the ATR-FTIR spectra of surface grafted EPDM films.

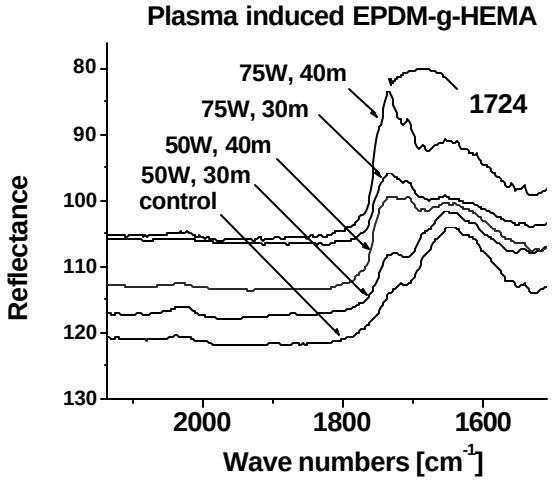

Figure 3.27 Effect of surface morphology on the monomer diffusion

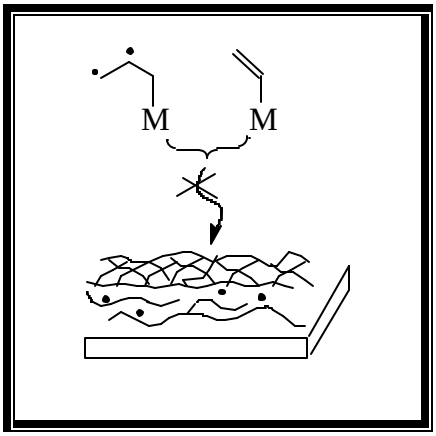

3.3.2.3.2 Effect of post exposure time

The ATR-FTIR spectra in the **Figure 3.28** shows that upon post-exposure of the plasma grafted substrates for 10 min, an increase in the intensity of the characteristic peaks was observed. Although a longer exposure (20 min) of these films did not improve the grafting yield. This indicates that a short post-exposure is favorable for exploiting all the radicals on the surface for achieving higher grafting yields. As it is already known that upon plasma treatment of polymer films, radicals are generated on their surface. Polymerizable species when present in their vicinity, readily react with these radicals to give rise to surface grafted polymer. But in the case of steric hindrance/ surface cross-linking, the monomer diffusion to the radical site may not be instantaneous. In such cases, post-exposure of the plasma treated films would allow all the radicals to react with the monomer vapor present in the chamber to give rise to higher grafting yields. The results obtained in our studies are in accordance with the above assumption. However, a similar study has not been reported yet to support this assumption.

Figure 3.28 ATR-FTIR spectra show the effect of post exposure time on the plasma grafted EPDM films **(a)** EPDM-g-HE MA **(b)** EPDM-g-NVP.

(a)

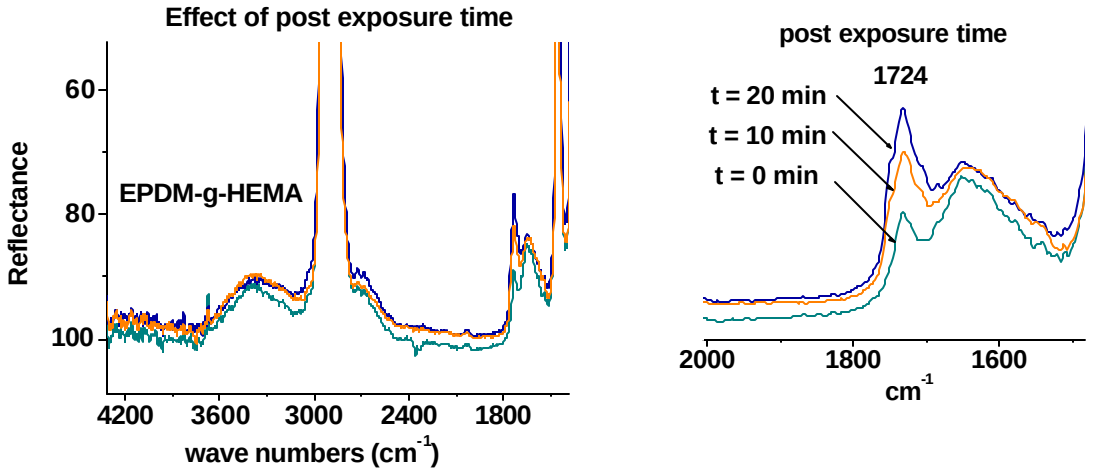

(b)

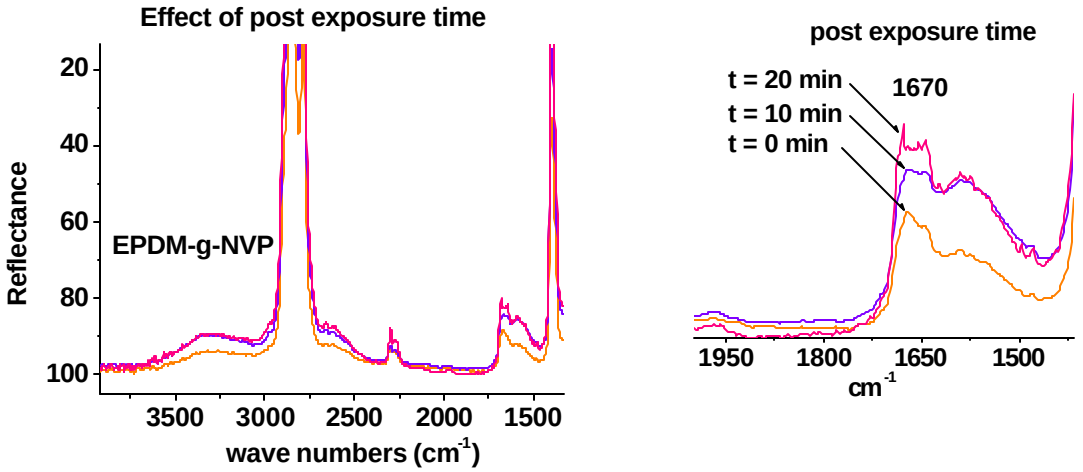

3.3.2.3.3 Effect of storage time

The functionalization of polymer surface is preferred by the grafting method over the traditional irradiation process to obtain permanently hydrophilic surfaces. In the former method, although the functional groups are chemically bound to the polymer surface, they are not permanently available at the surface[58]. Most of the researchers[59,60] claim of completely wettable and permanently hydrophilic polymer surfaces prepared by grafting techniques but it is refuted by others. The orientation of the functional groups takes place leading to a

reconstructed surface. The phenomena of reconstruction is governed by the surface dynamics (surface free-energy) under the influence of various parameters like 1) storage temperature, 2) size of the grafted chains, 3) nature of substrate, 4) T_g of the substrate, 5) density of functional groups, 6) grafting conditions and 7) surface morphology. The migration of the functional groups is represented in **Scheme 3.10**.

In the present study, it is observed that the migration of the functional groups takes place towards the sub-surface of the grafted polymer in order to minimize the surface free-energy. However, the phenomenon of re-orientation being a reversible process[60], the functional groups were not permanently lost as observed in some other cases[61]. The **Table 3.6** shows the contact angles measured by the sissile drop method for different storage time. It can be noticed that there is a minor difference in the water contact angle before and after washing the grafted films but a rapid hydrophobic recovery upon storage of these grafted films at RT is obvious from the contact angle measurements. Upon conditioning the samples at 20 °C and 64 % humidity for 2 hrs, a partial recovery of the buried functional groups at the surface of the EPDM films was observed. It is assumed that direct hydration of the substrate with water may result in almost complete recovery of hydrophobic groups. A slow orientation of the functional groups with partial hydrophobic recovery upon storage of polystyrene and polypropylene films is reported in the literature[62,63]. It was also observed that these substrates undergo a slow hydrophilic recovery upon hydrating them. Thus, in case of EPDM the rapid hydrophobic/hydrophilic recovery observed is due to the highly flexible polymer chains and free volume available unlike in PP and PS. This explanation is supported by similar mobility of functional groups observed for surface oxidized 1,4-polybutadiene[64]. A partial hydrophilic recovery was attained just within 5 min of contact with water. Therefore, the rate of re-orientation is assumed to be dependent on the T_g of the polymeric substrates.

Table 3.6 Effect of storage time on the hydrophilicity of plasma grafted EPDM films.

Monomer	Contact Angle [50 W, 30 min]						Contact angle [75 W, 40 min]					
	After grafting	After washing & drying	Stored at RT (3 hrs)	Stored at RT (24 hrs)	Stored at RT (1 week)	Hydrated at 20 °C (2 hrs)	After grafting	After washing & drying	Stored at RT (3 hrs)	Stored at RT (24 hrs)	Stored at RT (1 week)	Hydrated at 20 °C (2 hrs)
AA	32.2	37.1	46.4	63.0	81.4	69.2	29.0	33.7	37.3	43.6	49.2	42.0
HEMA	39.0	41.3	4 3.5	57.4	68.2	61.5	31.1	36.4	40.9	46.6	52.2	44.4
GMA	47.3	54.4	56.2	61.0	72.5	62.4	40.1	46.2	49.2	55.8	62.4	57.5
NVP	53.5	51.7	58.8	70.0	78.1	67.3	45.2	47.8	52.2	61.1	66.6	59.0

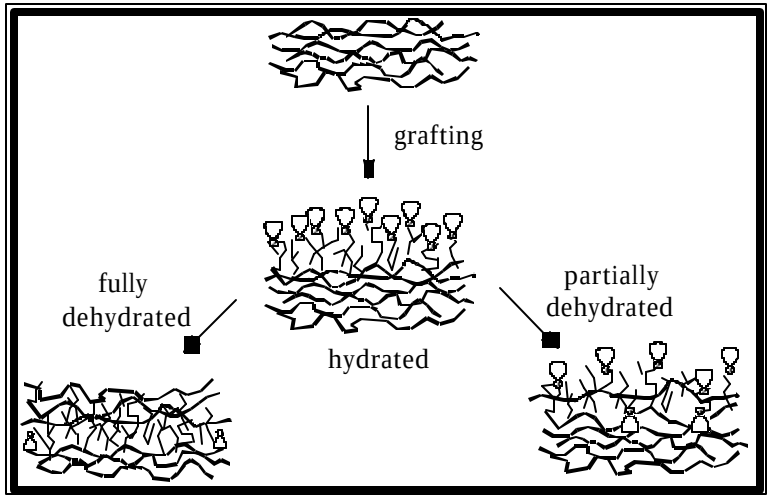

Scheme 3.10

A close examination of the **Table 3.6** also reveals that the process of re-orientation depends on the size of the grafted chain. The AA and NVP grafted EPDM films represents a faster hydrophobic recovery compared to the HEMA and GMA grafted samples. It is also understood from the results that the hydrophilicity achieved at higher plasma power and grafting time is more stable compared to that lower conditions. This behavior may be hypothesized on the basis of the surface cross-linking at higher plasma power, which hinders the migration of the functional groups towards the sub-surface[63]. Thus, the phenomenon of functional group re-orientation, although reversible, is inevitable and depends on the combined effects of various parameters mentioned above.

3.4 Biocompatibility study of surface grafted EPDM films

An ample literature is available on the surface modification of polymers to achieve biocompatibility[65]. Different techniques have been employed to generate functional surfaces. However, very few researchers have attempted to deduce the factors influencing the success and failure of these materials[45]. The present study, to some extent, highlights the factors influencing the biocompatibility of the surface modified elastomers under *in vitro* conditions. The fact that in the dehydrated state of a grafted polymer, the functional groups are not entirely located at the surface and re-orient towards the surface upon hydration, is already established[62-64]. In this scenario, if a hydrogel grafted polymeric material is implanted in the dehydrated state with an assumption that all the functional groups are available at the surface, the organism might initially interact with a very different type of surface from that, which was originally intended for the particular application. This is of concern as it has been documented that the series of events that occur within the first few seconds of implantation (eg. protein adhesion) determine the long-term success and failure of the implant. Thus, the phenomenon involving the orientation/re-orientation equilibrium plays a vial role. The elastomers bearing a low T_g show a rapid functional group re-orientation towards the surface compared to other thermoplastics and are therefore, more suitable as biomaterials.

The biocompatibility of the surface modified samples was estimated by human cell adhesion/growth. In addition to a control sample, only those samples, which showed the presence of functional groups on the surface (by ATR/XPS), were taken for the biocompatibility tests. The photo/plasma surface-grafted EPDM films were immersed in the cell-culture media in presence of SIHA (Cervical carcinoma cells) and KB (Oral carcinoma cells) in each case, incubated for 24 hrs and 48 hrs. The cell adhesion and growth were monitored under optical microscope after 24 hrs and 48 hrs of incubation (**Figure 3.29-3.30**).

Figure 3.29 Optical micrographs of KB Cell (left) and SIHA cells (right) cultured on the photografted EPDM films monitored after 48 hrs of incubation **(a)** neat EPDM **(b)** HEMA-g- **(c)** AA-g- **(d)** GMA-g- **(e)** NVP-g- EPDM.

KB Cells **SIHA Cells**

(a)

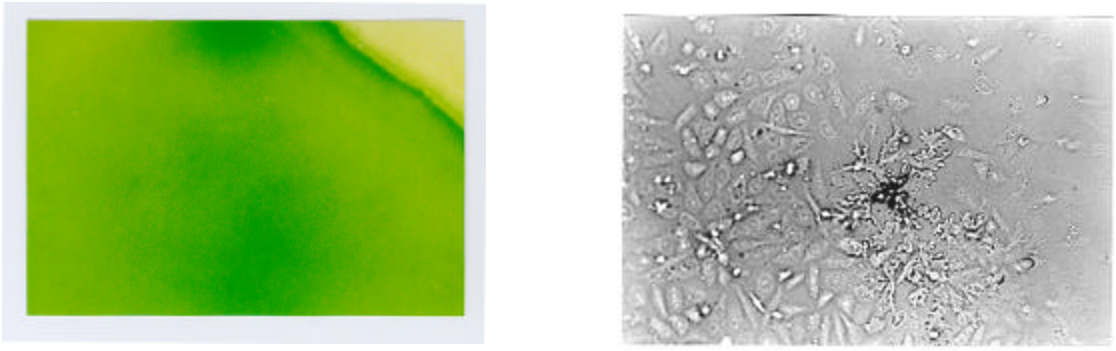

(b)

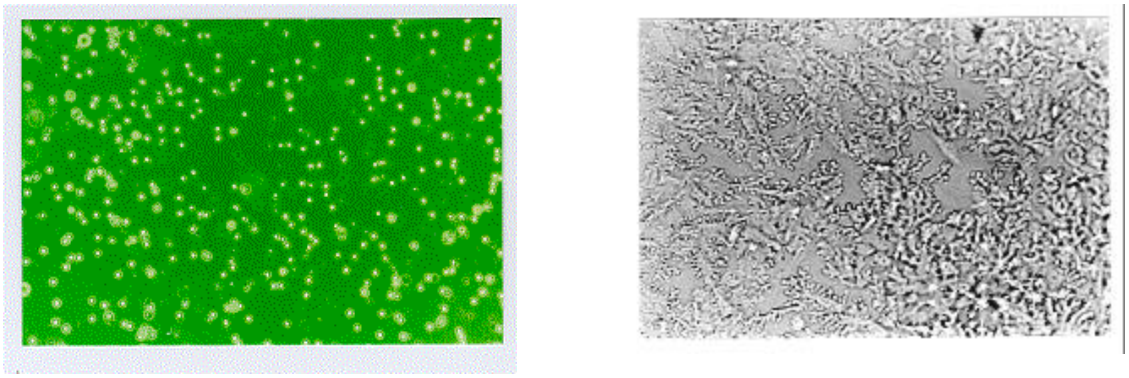

(c)

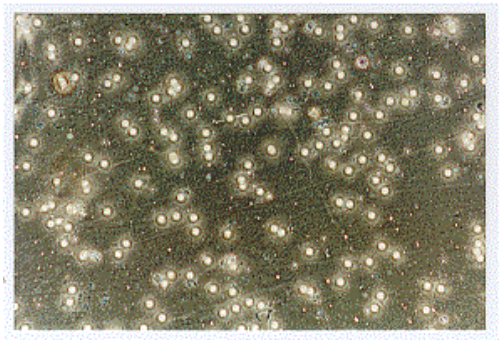

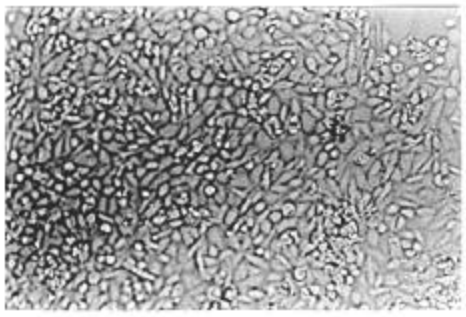

(d)

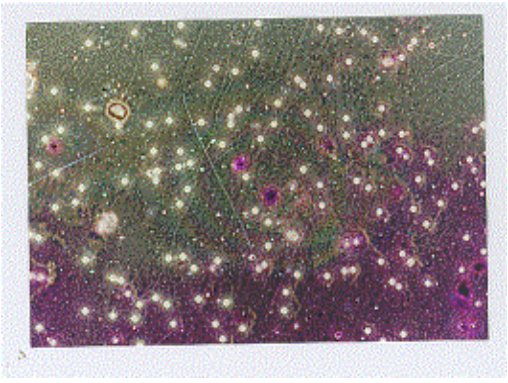

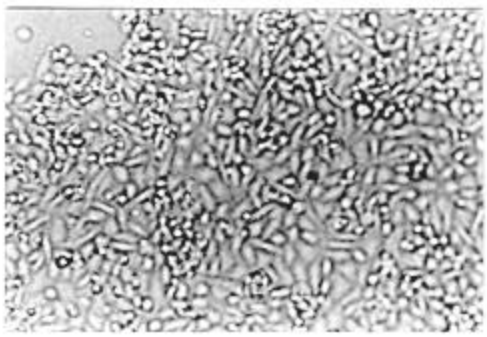

Figure 3.30 KB cell cultured on the surface of plasma grafted EPDM films after 24 hrs of incubation **(a)** HEMA **(b)** AA **(c)** GMA **(d)** NVP.

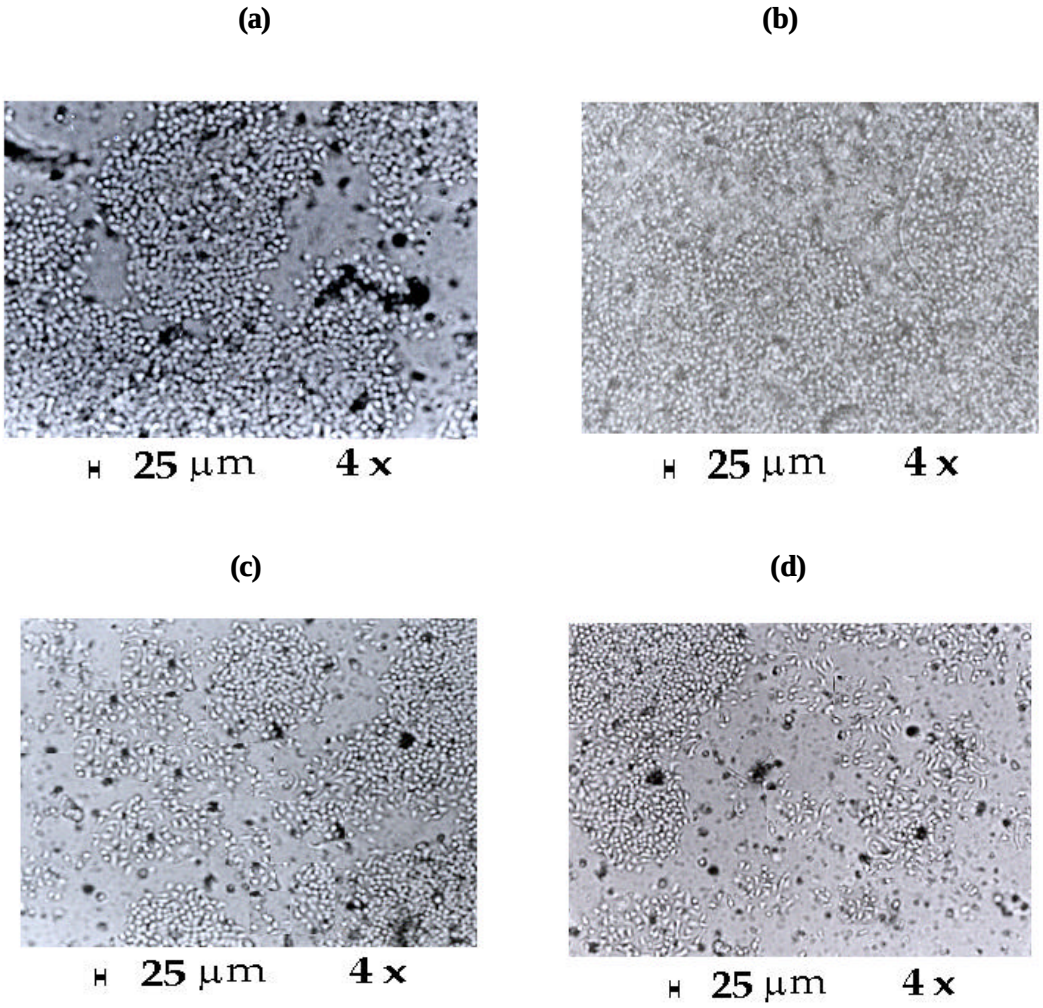

The results of KB and SIHA cell adhesion after 24 hrs of incubation tabulated in **Table 3.7** shows that HEMA (photo and plasma) grafted EPDM films demonstrate excellent cell adhesion with a high degree of uniformity through out the film surface. This substantially high biocompatibility is attributed to the uniform carpeting of *poly*HEMA chains on EPDM films (**Table 3.7**), which is again accredited to its higher grafting efficiency. The acrylic acid photo-grafted films exhibited better cell adhesion (number of cells adhered/cm^2) compared to plasma-grafted samples. The density of the cells adhered depends on the number of the freely available carboxylic acid groups, which is more in the case of photo-grafted films. However, the visual homogeneity of the cells adhered in both the cases was almost similar. Glycidyl methacrylate being moderately grafted on the EPDM surface in both the cases, exhibited

mediocre cell adhesion with less uniformity in case of photo-grafting. N-vinyl pyrrolidone having a very low grafting coefficient, was feebly grafted onto the film surface and resulted in poor cell adhesion, although its biocompatibility was good when it was plasma-grafted.

Table 3.7 Immobilizatio n of KB and SIHA cell lines on the surface of grafted EPDM films

Grafting technique	**Cell adhesion**[#]			
	HEMA	AA	GMA	NVP
Photo	★ +	★ +	• –	O –
Plasma	★ +	• +	• +	• +

[#]***Cell adhesion: Good*** ★ ***Average*** • ***Poor*** O ***Uniform*** + ***Non-uniform*** -

It is evident from the **Table 3.8**, that the growth/immobilization of both KB and SIHA cells increases upto 24 hrs of incubation for all plasma grafted and photo-grafted samples, except for NVP. The plasma-grafted samples show better adhesion/growth even after 48 hrs of incubation. Thus, cell growth/adhesion depends on the uniformity of grafting. The decrease in the adhesion, particularly of the KB cells, after 48 hrs of incubation, is attributed to their higher sensitivity towards foreign environment. Both the cell lines demonstrated a significant adhesion, however, KB cells being more sensitive, exhibited a slightly lower cell growth compared to SIHA cells. Amongst all the monomers, acrylic acid and hydroxyl ethyl methacrylate grafted samples exhib ited excellent results, however, AA was found to be the best monomer for achieving biocompatibility. The decrease in the biocompatibility of photo -grafted HEMA during the initial hours of incubation is observed. This is due to excessive homopolymerization, which leads to clustered chains on the grafted surface where functional groups (OH) are likely to be buried, thus not freely available for the bio -interactions.

Table 3.8 Dependence of Cell adhesion/growth on incubation time

Cell lines	*Cell adhesion/growth*							
	HEMA		AA		GMA		NVP	
	24 h	48 h	24 h	48 h	24 h	48 h	24 h	48 h
SIHA	↑⇑	↑⇑	↑⇑	↑⇑	↑⇑	↓⇑	↓⇑	↓⇑
KB	↓⇑	↑⇑	↑⇑	↑⇑	↑⇑	↓⇓	↓⇑	↓⇓

Increase: photo ? plasma ⇑ **Decrease:** photo ? plasma ⇓

3.5 CONCLUSIONS

The photo-grafting efficiency (*Ge*) of monomers observed here is in the order HEMA>AA>GMA> NVP. The surface of the grafted substrates examined by the SEM shows progressive roughness with the increase in the degree of grafting. A rise in the thickness of the grafted layer observed in the optical micrographs, is attributed to the multi-layer formation arising from the grafted homopolymer chains. The ketonic photo-initiators, due to their hydrogen abstraction capacity prove to be better initiating species compared to the peroxy-initiators. Multifunctional acrylates demonstrate substantial homopolymer inhibition capacity with a little influence on the grafting efficiency. Toluene as an additive suppresses the homopolymer formation and increases the grafting yield. The degree of photo-grafting increases linearly with the reaction time and temperature. The plasma grafting efficiency mainly depends on the reaction time, whereas the rate of grafting depends on the plasma power. For reaction time less than 10 minutes, grafting is almost negligible leading to poor biocompatibility. The plasma-grafted samples exhibit better cell adhesion/ growth even after 48 hrs of incubation. Thus, cell growth/adhesion depends on the uniformity of grafting and density of functional groups. In other words, hydrophilicity of the polymer surface plays a major role in determining the biocompatibility of the substrate. Both the cell lines demonstrated a significant adhesion, however, KB cells being more sensitive exhibited a slightly lower cell adhesion/growth compared to SIHA cells. Amongst all the monomers, AA and HEMA grafted samples exhibited excellent biocompatibility. However, it should be noted that the grafting yield of each monomer is different and at similar grafting yield the results might be different.

3.6 REFERENCES

1. B. Ranby, J. F. Rabek *Photodegradation, Photo-oxidation and Photostabilization of Polymers*., Interscience, New York, Chap. 1, p. 45 (1975).
2. V. Haddadi-asl, R. P. Burford and J. L. Garnett, *Radiat. Phys. Chem*., **44**, 385 (1994).
3. A. Chapiro, *Eur. Poly. J.*, **19**, 859 (1983).
4. V. Haddadi-asl, R. P. Burford and J. L. Garnett, *Radiat. Phys. Chem*., **45**, 191 (1995).
5. C. S. L. Baker and D. Barnard, *Adv. Elastomers Rubber Elasticity*, 175-188 Ed. J. Lal, J. E. Mark, Plenum: New York (1986).
6. B. N. Misra and J. Kaul, *Indian J. Chem., Sect. A*, **22A**, 601 (1983).
7. X. S. Wang, N. Luo and S. K. Ying, *Polymer*, **40**, 4515 (1999).
8. M. Hori, *J. Vac. Sci. Technol*., B 4, 500 (1986)
9. C. M. Chan, *Surface Modification and Characterization of Polymers*, Hanser Publishers (1994).
10. K. Allmer, A. Hult, B. Rånby, , *J. Polym. Sci. Polym. Chem. Educ.,* **26**, 2099 (1988).
11. Z. P. Yao and B. Rånby, *J. Appl. Polym. Sci.,* **41**, 1647 (1990).
12. C. Walling and M. J. Gibian, *J. Am. Chem. Soc.*, **87**, 3361(1965).
13. S. Edge, S. Walker, W. J. Feast, W. F. Paeynko, *J. Appl. Polym. Sci.*, **47**, 1075 (1993).
14. W. Yang and B. Ranby, *J Appl Polym Sci* , **62**, 545 (1996).
15. A. Chapiro, Radiation Chemistry of Polymer Systems, Vol. XV, Wiley, Chichester, p. 589 (1962).
16. G. Odian, M. Sobel. A. Rossi and R. Klein, *J. Polym. Sci.,* **55**, 663 (1961).
17. Y. Ogiwara, K. Torikoshi and H. Kubota, *J. Polym. Sci., Polym. Lett. Ed.*, **20**, 17 (1982).
18. H. Kubota, Y. Ogiwara, *J. Appl. Polym. Sci.,* **38**, 717 (1989)]
19. M. T. Razzak, K. Otsuhata, *J. Appl. Polym. Sci.*, **36**, 645 (1988).
20. W. Yang and B. Ranby, *J. Appl. Polym. Sci*., **62**, 533 (1996)
21. C. Walling and M. J. Gibian, *J. Am. Chem. Soc.*, **87**, 3413 (1965).
22. F. R. Mayo, F. M. Lewis and C. Walling, *J. Am. Chem. Soc*, **70**, 1529 (1948).
23. J. C., Bevington, *J. Chem. Soc. London*, **4**, 3707 (1954)
24. D. D. Jiang and C. A. Wilkie, *Eur. Polym. J.*, **34**, 997 (1998).

25. R. B. Seymour and C. E. J. Carraher, Polymer Chemistry, 3rd Edition, Dekker, NY, p 324 (1992).
26. G. S. Hammond, W. P. Baker and W. M. Moore, *J. Am. Chem. Soc.*, **83**, 2795 (1961).
27. N. J. Turro, *Modern Molecular Photochemistry*, Benjamin/Cummings, Menlo Park, CA, p. 261 (1987).
28. C. Walling and M. J. Gibian, *J. Am. Chem. Soc.,* **87**, 3413 (1965).
29. N. J. Hung and D. C. Sundberg, *J. Polym. Sci, Part A; Polym. Chem*. **33**, 2533, 2551, 2571 and 2587 (1995).
30. W. Yang and B. Ranby, *Eur. Polym. J.,* **35**, 1557 (1999).
31. A. A. Katbab, R. P. Burford and J. L. Garnett, *Radiat. Phys. Chem.*, **39**, 293 (1992).
32. A. Chapiro and P. Seidler, *Eur. Polym. J*., **1**, 9 (1965)
33. E. Collinson, F. Dainton, D. Smith, G. Trudel, S. Tazuke, *Discuss Faraday Soc*., **29**, 188 (1960).
34. P. A. Dworjanyn, B. Field, J. L. Garnett, *ACS Symp. Ser.* **38**, 1(1989).
35. C. H. Ang, J. L. Garnett, R. Levot and M. A. Long, *J. Appl. Polym. Sci,* **27**, 4893, (1982).
36. M. Y. Teng, K. R. Lee, D. J. Liaw, Y. S. Lin and J. Y. Lai, *Eur. Polym. J*., **36**, 663 (2000).
37. H. Yasuda and A. K. Sharma, *J. Polym. Sci, Polym. Phys. Ed.,* **19**, 1285 (1981).
38. F. P. Epaillard, B. Chevet and J. C. Brosse, *J. Appl. Polym. Sci*., **53**, 1291 (1994).
39. H. Chen and G. Belfort, *J. Appl. Polym. Sci*., **72**, 1699 (1999).
40. N. Inagaki, S. Tasaka and T. Inoue, *J. Appl. Polym. Sci.*, **69**, 1179 (1998).
41. N. Inagaki, S. Tasaka and Y. Horikawa, *Polym. Bulletin*, **26**, 283 (1991).
42. Y. S. Soebianto, F. Yoshii, K. Makuuch and I. Ishigaki, *Angew. Makromol. Chem*., **152**, 149, (1987).
43. A. A. Katbab, R. P. Burford, J. L. Garnett *Radiat. Phys. Chem.* **39**, 293 (1992).
44. A. A. Katbab, R. P. Burford, J. L. Garnett, *Iran. J. Polym. Sci. Technol.*, **1**, 15 (1992).
45. D. J. Chauvel- Lebret, P. Pellen-Mussi, P. Auroy and M. Bonnaure-Mallet, *Biomatierials*, **20**, 291 (1999).
46. M. T. Razzak, K. Otsuhata, Y. Tabata, F. Ohashi and A. Takeuchi, *J. Appl. Polym. Sci.*, **36**, 645 (1988).
47. M. Murat and G. S. Grest, *Macromolecules*, **22**, 4054 (1989).

48. P. Wang, K. L. Tan, C. C. Ho, M. C. Khew and E. T. Kang, *Eur. Polym. J.*, **36**, 1323 (2000).

49. M. R. Yang and K. S. Chen, *Mater. Chem. Phy.*, **50**, 11 (1997).

50. I. Gancarz, G. Pozniak, M. Bryjak and A. Frankiewicz, *Acta Polym.*, **50**, 317 (1999).

51. W. P. Lin and Y. L. Hsieh, *J. Polym. Sci., Pt. B - Polym. Phys.*, **35**, 1145 (1997).

52. N. Inagaki, Plasma surface modifcation and PlasmaPolymerization, Technomic Publishing Co. Inc., Lancaster, Basel., p.78 (1996).

53. T. Hirotsu and I. Munetoshi, *Proc. Jpn. Symp. Plasma Chem.*, **1**, 291, (1988).

54. T. Hirotsu, *Adv. Low-Temp. Plasma Chem. Technol. Appl.*, **3**, 9 (1991).

55. K. Johnsen, S. Kirkhorn, K. Olafsen, K Redford, A. Stori, *J. Appl. Polym. Sci.*, **59**, 1651 (1996).

56. F. P. Epaillard, J. C. Brosse and T. Falher, *Macromol. Chem. Phys.*, **199**, 1613 (1998).

57. N. Inagaki, S. Tasaka and T. Inoue, *J. Appl. Polym. Sci.*, **69**, 1179 (1998).

58. R. Thomas and R. Trifilet, *Macromolecules*, **12**, 1197 (1979).

59. T. Yasuda, K. Yoshida, *J. Polym. Sci., Polym. Lett. Ed.*, **26**, 2061 (1988).

60. B. Gupta, J. Hilborn, I. Bisson, P. Frey, Plasma induced graft polymerization of acrylic acid onto PET films, *J. Appl. Polym.Sci.*, (in press 2002).

61. B. D. Ratner, P. K. Weathersby and A. S. Hoffmann, *J. Appl. Polym. Sci.*, **22**, 643 (1978).

62. F. C. Loh, K. L. Tan, E. T. Kang, Y. Uyama and Y. Ikada, *Polymer*, **36**, 21 (1995).

63. H. Yasuda and A. K. Sharma, *J. Appl. Polym. Sci.*, **19**, 1285 (1981).

64. S. Khongton and G. S. Ferguson, *J. Am. Chem. Soc.*, **123**, 3588 (2001).

65. Y. Ikada, *Biomaterials*, **15**, 725 (1994).

CHAPTER IV

IMPLANTATION OF FUNCTIONAL GROUPS ONTO THE SURFACE OF EPDM FILMS

4.1 INTRODUCTION

Tailoring a polymer with properties different at its surface and in the bulk, is now-a-days one of the most important areas of research in polymer chemistry. Polyolefins are the oldest and well-accepted synthetic polymers, due to their excellent manufacturer cum user-friendly properties. Surface modification of PP and PE is most widely studied, although, olefinic elastomers are almost untouched. Many chemical and photo-physical treatments are known to bring about these changes but are often non-uniform and uncontrolled[1-3]. Amongst the alternative means of surface modification, functional group implantation using reactive gas cold-plasma treatment appears to be a rational alternative[4].

A plasma is broadly defined as "*a third state of matter consisting of charged and neutral species which include electrons, + ve ions, - ve ions, radicals, atoms and molecules*". Plasmas are generally categorized on the basis of their electron densities and electron energies. The low electron energy plasma, often called *cold plasma*, is most commonly used for the surface modification of polymers. The formation of the functional groups on a polymer surface by plasma treatment is interpreted from the action of the radicals in the plasma. In the implantation process, hydrogen atoms are first abstracted from the polymer chains located at the surface to generate free-radicals. Some of the carbon radicals in the polymer chain combine with the radicals formed in the plasma to generate functionalities of the respective gas. The other carbon radicals, when exposed to the air after the plasma treatment, are oxidized to form oxygen functionalities such as carbonyl, hydroxyl and carboxyl groups[5]. The commonly used gases for the reactive plasma treatment are oxygen, carbon dioxide, sulphur dioxide, chlorine, fluorine and ammonia. The plasmas with oxygenated gases are known to induce efficient and rapid hydrophilation of the polymer surfaces. The formation of the functional groups as a result of plasma treatment is restricted to a depth of few hundred nanometers on the polymer surface and sometimes a couple of layers[6].

Classical surface chemistry assumes that solid surfaces are rigid, immobile, at equilibrium and do not respond in any way or reorient with respect to different environments[7], although, such assumptions may be correct only for truly rigid solids or polymers with high T_g. It is often reported that functionalities generated on the polymer surface as a result of plasma implantation, are temporary and are lost with time[8]. This phenomenon is termed as 'hydrophobic recovery'. Hydrophobic recovery is usually attributed to the surface configurational change. There are actually two possibilities: (i) reversible and (ii)

permanent change. The former one is attributed to the configurational changes whereas the later one is due to the formation of oligomeric products upon surface degradation[9]. Thus, the stability of the surface state after plasma treatment is a major concern for any investigator attempting to improve wettability by plasma surface modification. Hydrophobic recovery, that is, the decrease in the surface hydrophilicity as indicated by an increase in the contact angle with the storage time, is a common example of surface instability encountered after the modification with reactive gas plasma[10,11]. Although, these surface dynamics depend on polymer physio-chemical properties, temperature, storage time and many other parameters, it is a feebly understood complex phenomenon, which differs from substrate to substrate[12,13]. Thus, the prime objective of the present study is to devise a placid technique for surface functionalization of elastomeric films with a topographical selectivity without altering their inherent physio-chemical properties with an insight into the surface dynamics from the fundamental point of view.

Surface functionalization of elastomeric substrates like silicon rubber, polyurethane and polyvinyl chloride is well documented in the form of patents[14,15] and publications[16,17]. Researchers have attempted to tailor the surface properties of various polymers like polyethylene, polypropylene, polyamide, polyethylene terephthalate, polyacrylonitrile, polytetrafluoroethylene and polyethersulphone using traditional and existing surface modification techniques[18-20]. However, there are only a few reports on the surface modification of EPDM[21], natural rubber[22] and styrene butadiene styrene[23] films using plasma-induced modification techniques, with hardly any systematic efforts to investigating the effects of different reaction parameters on the surface properties of these elastomers. Therefore, elastomeric substrate was our obvious choice.

Surface modified polymers are rapidly achieving the status of biomaterials[24]. However, a limited number of elastomers enjoy this distinction[25]. Elastomers are potential candidates for biomedical applications due to their inherent flexibility and freedom of design. Moreover, the phenomenon of functional group re-orientation being a very rapid process in case of elastomers[26a], the functionalities are readily available at the surface upon hydrating them, unlike in other thermoplastics. The surface modified elastomers are therefore, prospective biomaterials for a wide range of applications. The modification of elastomeric surface was thus proposed with a view of improving their biocompatibility and examining their performance under *in vitro* conditions.

In the present study, two reactive gases viz. oxygen and carbon dioxide are used to

obtain functional hydrophilic surface of EPDM films. The effect of reaction parameters like plasma power, gas flow, treatment time, post treatment exposure to the system gas and surface dynamics upon storage are examined carefully. In another approach, functional vinylic monomers along with functional cross-linkers were spin coated onto the surface of the EPDM films and exposed to the plasma radiation to obtain long-term hydrophilic surfaces. All the samples are analyzed using surface sensitive techniques like contact angle measurement, XPS and ATR-FTIR spectroscopy.

4.2 MATERIALS AND METHODS

4.2.1 Materials

All the monomers viz. 2-hydroxyethyl methacrylate (HEMA), N-vinyl pyrrolidone (NVP), glycidyl methacrylate (GMA), allyloxy-1,2-propanediol (AOPD), acryloyloxyethyl trimethyl ammoniumsulphate (AOETMAS) and cross-linkers; diallyl amine (DAA) and ethylene glycol dimethacrylate (EGDMA) procured from M/s. Aldrich, USA, were purified by fractional distillation under reduced pressure using fractional distillation column. Diiodomethane was procured from LOBA Chemicals. India. The nitrogen, carbon dioxide and oxygen gases (Grade I) supplied by M/s. Inox Ltd., Thane, India, were used for the plasma-treatment reactions.

4.2.1.1 Preparation of polymer films

LDPE film preparation

The LDPE pellets obtained from IPCL, Baroda, India, were dissolved in toluene and precipitated from methanol to remove the processing additives. Films were prepared by compression molding in a laboratory Carver press using the purified LDPE (density, 0.916 g/cc) at 205 $^{\circ}$C for 2 minutes and quench cooling with cold water. The films were then cut into definite size. These films were sonicated in chloroform followed by methanol and dried in vacuum oven at 40 $^{\circ}$C before use.

PP film preparation

PP pellets were also made additive free by the above mentioned procedure for LDPE purification. Films of PP were prepared by compression molding in a laboratory Carver press using purified PP pellets at 175 $^{\circ}$C for 2 minutes and quench cooling with cold water. The films were then cut into definite size. These films were sonicated in chloroform followed by methanol and dried in vacuum oven at 40 $^{\circ}$C before use.

EPDM film preparation

The detailed procedure for the preparation of EPDM films is described in the *section 3.2.1.1.*

4.2.1.2 Reactor

In the present study, the surface modification of the EPDM films is carried out mainly by plasma implantation and cross-linking of functional monomers spin coated on the surface of the EPDM films.

4.2.1.2.1 Plasma-treatment reactor

The plasma treatment of the EPDM films was carried out using MARCH (USA), RF plasma reactor (model MPA 300) operating at a frequency of 13.56 MHz. The experimental conditions were, flow rate = 5 .0 and 12.5 sscm, power = 50 - 100 W, time = 30 - 300 sec.

4.2.1.2.2 Spin coating reactor

The spin coating reactor was also built with the in-house engineering facility at the Department of Physics, University of Pune, Pune. The coating can be done from 1-8000 rpm.

4.2.2 Experimental methods

The surface modification of the EPDM films was accomplished by two methods namely, plasma treatment and plasma induced grafting.

4.2.2.1 Plasma-treatment procedure

The PE, PP and EPDM films of definite size were fixed in the plasma treatment chamber at a distance of 8 cm from the gas aperture as shown in **Figure 4.1**. The reaction chamber was evacuated to 0.2 torr and desired gas was then introduced with a definite flow. After the reaction pressure and gas flow were stabilized, a potential was applied for a fixed time from the RF generator. After the irradiation, the samples were maintained in the same gaseous atmosphere for different periods viz. 10 min and 1 hr. The samples were then immediately taken up for the contact angle measurements.

Figure 4.1 Plasma treatment reactor.

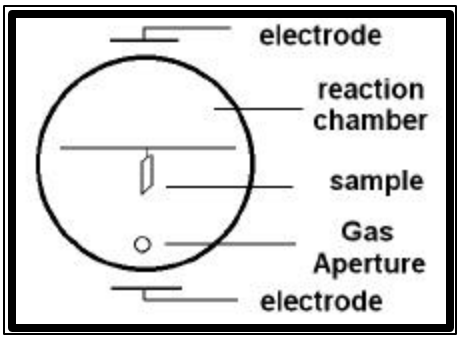

4.2.2.2 Spin coating procedure

DAA and EGDMA were used as cross-linking agents for anchoring the vinylic functional monomers onto the surface of EPDM films. A separate composition of monomer: cross-linker (3:1) was prepared and 0.5 ml of this formulation was placed on the EPDM film (4 cm × 1.5 cm) and spin-coated at 5000 rpm for 3 min to form a micro-coating.

4.2.2.3 Plasma induced grafting

The spin coated EPDM films bearing a monomer and cross-linker in (3:1) proportion were placed in the plasma reactor and irradiated for 300 sec in oxygen plasma to facilitate rapid cross-linking of the vinylic monomers at the film surface. The films were taken up for the weight gain measurements after irradiation and also after washing.

4.2.3 Characterization methods

The surface modified EPDM films were characterized by contact angle goniometer, ATR-FTIR and XPS. The change in the weight of the grafted samples was determined using microbalances: *Precisa* 205 ASCS, Switzerland and Sartorius BP 210D, Germany, with a standard deviation of 0.05 mg.

The water and diiodomethane contact angles were measured on a Rame-Hart NRL, USA contact angle Goniometer (Model 100-00 230) using freshly prepared deionized water, filtered through membrane filter. The drop volume was 2 μL. The static contact angles of the water on the substrate surface were determined by 'sissile drop' method, measured within 30 sec of placing the drop at room temperature (27 ± 3 °C). The reported values are an average of minimum 7 values, measured at different places on the sample. The standard deviation in the measured value is within ± 3°. The details of ATR-FTIR, XPS and SEM are described in *section 3.2.3.*

Surface free-energy calculation

The surface free-energy was calculated using the Fowkes equation[26b] for the total work of adhesion (W_{SL}):

$W_{SL} = W^{d}_{SL} + W^{nd}_{SL}$

where, W^{d}_{SL} is the work of adhesion due to dispersive interactions and W^{nd}_{SL} work of adhesion due to nondispersive interactions. The adhesion work corresponds to the expression: $W_{SL} = \gamma_S + \gamma_L - \gamma_{SL}$ and $W_{SL} = \gamma_L (1 + \cos\theta)$

moreover,

$W^{d}_{SL} = 2(\gamma^{d}_{L} \gamma^{d}_{S})^{1/2}$ and $W^{nd}_{SL} = 2(\gamma^{nd}_{L} \gamma^{nd}_{S})^{1/2}$

therefore,

$\gamma_{L1} (1 + \cos\theta) = 2(\gamma^{d}_{L1} \gamma^{d}_{S})^{1/2} + 2(\gamma^{nd}_{L1} \gamma^{nd}_{S})^{1/2}$

$\gamma_{L2} (1 + \cos\theta) = 2(\gamma^{d}_{L2} \gamma^{d}_{S})^{1/2} + 2(\gamma^{nd}_{L2} \gamma^{nd}_{S})^{1/2}$

where, L_1 is water and L_2 is diiodomethane.

using this equation we have calculated γ^{d}_{S} and γ^{nd}_{S} for the polymer film

γ_{total} (mJ m^{-2}) = $\gamma^{d}_{S} + \gamma^{nd}_{S}$

4.2.4 Biocompatibility Tests

The biocompatibility of the modified and pristine EPDM films was tested by the procedure disclosed in *section 3.2.4*.

4.3 RESULTS AND DISCUSSION

4.3.1 Functional group implantation using O_2 and CO_2 plasma

Oxygenated gases used for the plasma treatment are known to generate hydroxyl, carbonyl and carboxyl functionalities, thereby increasing the polarity of the treated surfaces[27] . The mechanism of polymer surface modification by reactive gas plasma can be differentiated as oxidation and degradation, where degradation is further categorized into etching and cross-linking. Polymers giving rise to volatile products undergo etching whereas those producing non-volatile oligomers often undergo surface cross-linking. Thus, there is no general mechanism of plasma modification of polymers as such, since they behave distinctly in each plasma, under variable conditions. **Scheme 4.1** and **4.2** show the modification of PP upon carbon dioxide and oxygen plasma treatment.

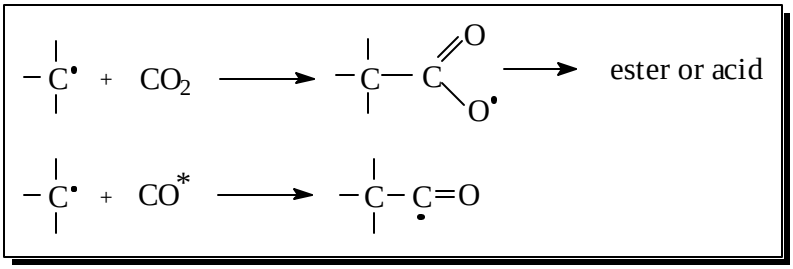

Scheme 4.1

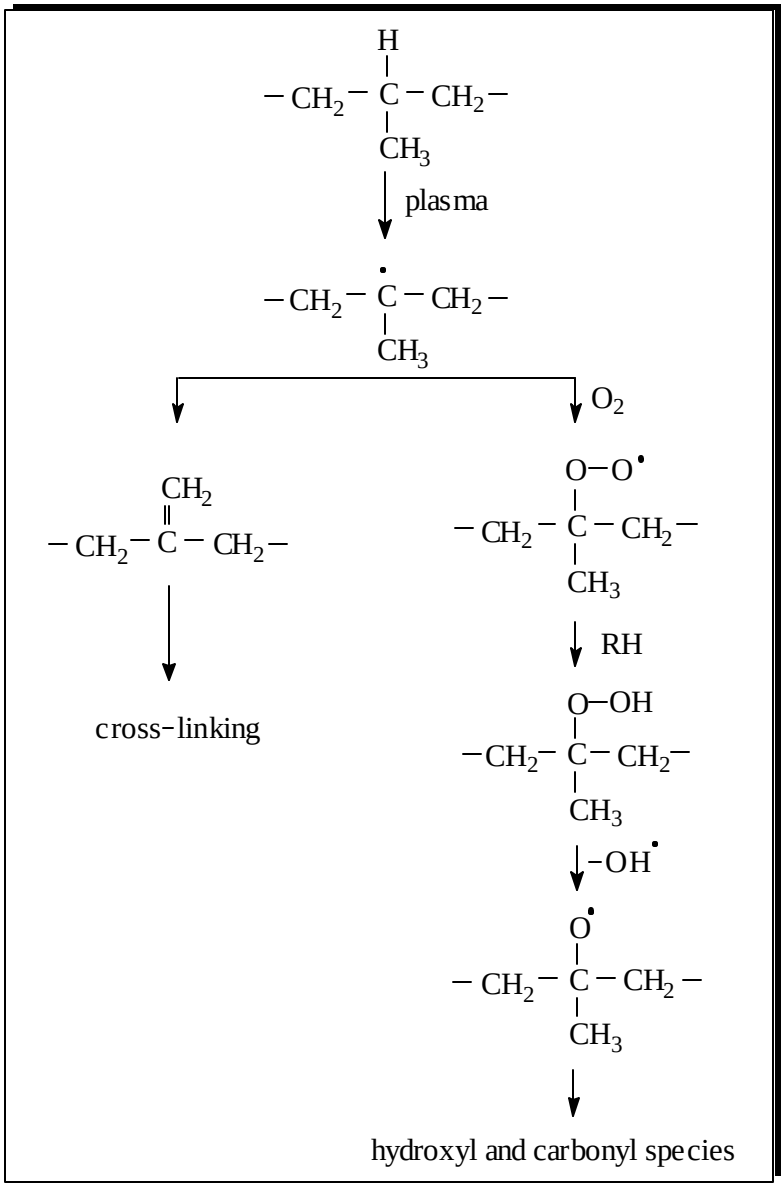

Scheme 4.2

It can be noticed that the functionalization of PP under oxygen plasma is a complex process and gives rise to hydroxyl and carbonyl species whereas carbon dioxide plasma predominantly

generates carbonyl and carboxyl species on the polymer surface[28]. This explanation is supported by the XPS spectra in **Figure 4.2 (a)** and **(b)**. The plot in **Figure 4.3** represents the changes in the surface energy of the functionalized polyolefin films. The ATR-FTIR spectra did not show any difference between the untreated and moderately treated samples. The reason is that the modified layer is not thick enough to induce detectable changes in ATR spectra[29].

Figure 4.2 XPS spectra of **(a)** O_2 and **(b)** CO_2 plasma treated PP films.

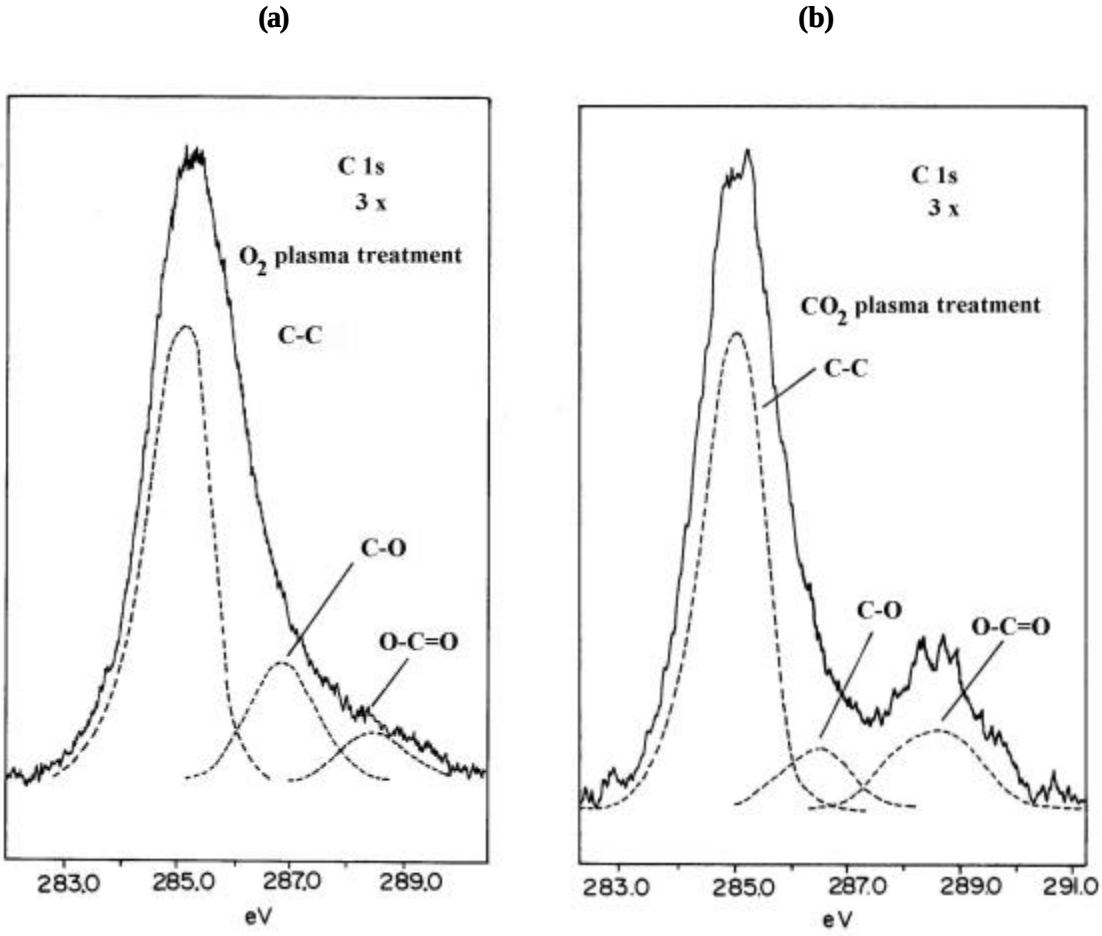

4.3.1.1 Effect of plasma power and irradiation time

The water contact angle (θ) measurements of PP, PE and EPDM films treated with oxygen and carbon dioxide plasma are compiled in the **Table 4.1** and **Table 4.2**, respectively. The θ values clearly reveal an increase in the hydrophilicity of the surfaces treated with both the plasmas. However, a close observation of the θ values for low plasma power and small treatment time also reveals that surface of PP undergoes rapid hydrophilization compared to

EPDM and PE. This effect is due to the spontaneous elimination of tertiary hydrogens from the polymer chains located at the surface during the first few seconds of the treatment. Once all the *tert*-H atoms are eliminated, the functionalization of these polyolefins is assumed to be sterically controlled whereas amongst the *sec*-H atoms, those that are sterically less hindered, are easily knocked off. A close look into the contact angle measurement also depicts that the surface hydrophilicity at low plasma power increases with treatment time, but at high plasma power, hydrophilicity decreases with the treatment time irrespective of the system gas. This indicates that either surface cross-linking or etching takes place simultaneously. *Charlesby*[30] has reported that PP and PE undergoes cross-linking under high-energy radiation. The thermodynamically favored orientation of functional groups takes place with the loss of functional groups from the interface. Moreover, it can also be noticed that hydrophilicity achieved using carbon dioxide plasma is better than that obtained by oxygen plasma. This is in accordance with a previous report[31]. This may be due to the higher cross-linking and degradation at the polymer surface in case of the oxygen plasma. In addition to this, the peroxides generated on the polymer as a result of oxygen plasma treatment are bound to undergo decomposition, leading to a cross-linked surface. The proposed hypothesis is schematically expressed in the **scheme 4.3**. At very high plasma power, the chain scission at the polymer surface takes place, giving rise to dangling hydrocarbon chains or low molecular weight oligomers[32]. The initially generated functional groups are assumed to be buried below these chains of low surface free-energy. Thus, a decrease in the hydrophilicity is observed upon irradiating the polymer films at higher plasma power for a longer time. The formation of gel, with small amount of insoluble mass upon dissolution of the plasma treated (100 W, 300 sec) polyolefin samples in toluene reaffirmed the cross-linking during the treatment.

Figure 4.3 Surface free-energy changes in O_2 plasma treated polyolefin films.

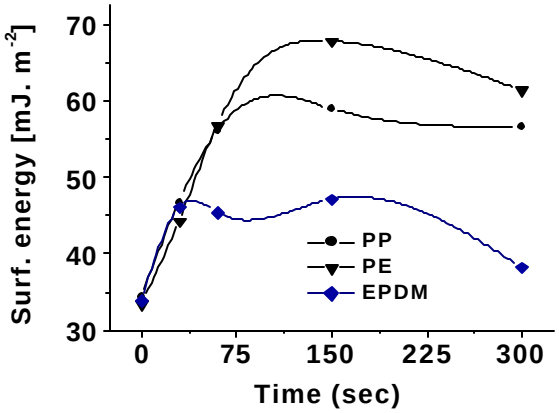

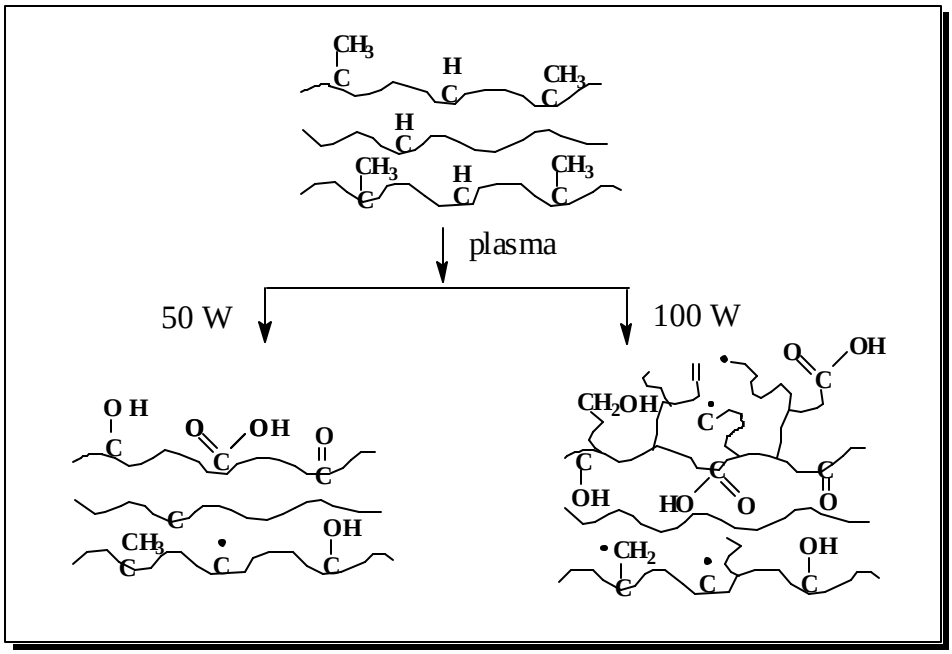

Scheme 4.3

4.3.1.2 Effect of gas flow rate and post-treatment exposure to the system gas

It is known that all the plasma treatment parameters have their distinct influence on the modifications brought about at the polymer surface. The surface energy of the treated polymer varies with the flow rate of the system gas. The effect of the oxygen and carbon dioxide flow rate on the surface free- energy of the EPDM films is represented in the **Figure 4.4 (a)** and **(b)**. It is observed that at low gas flow rate (i.e. 5.0 sscm) the hydrophilicity achieved is better than that at higher gas flow rate (i.e. 12.5 sscm). The two possibilities for the detrimental effect at higher flow rate are, the decrease in the reactive species due to rapid recombination of the active species in the plasma and subsequent etching of the polymer surface, giving rise to volatile/non volatile degradation products[34]. However, there is no precise tool other than contact angle measurement to determine the chemical modifications brought about at the θ interface.

Table 4.1 Water contact angle of O_2 plasma treated polyolefin films

Irradiation time (sec)	**water contact angle** (°)								
	PP			**PE**			**EPDM**		
	50 W	**75 W**	**100 W**	**50 W**	**75 W**	**100 W**	**50 W**	**75 W**	**100 W**
30	59.0	54.4	61.6	69.0	59.2	56.8	64.0	55.3	64.0
60	52.2	41.4	35.8	41.3	40.1	36.2	62.6	56.5	50.0
150	44.4	37.0	43.8	28.5	24.0	35.1	61.5	53.6	40.2
300	38.2	40.4	45.5	27.0	33.7	43.0	66.0	70.8	80.2

Table 4.2 Water contact angle of CO_2 plasma treated polyolefin films.

Irradiation time (sec)	**water contact angle** (°)								
	PP			**PE**			**EPDM**		
	50 W	**75 W**	**100 W**	**50 W**	**75 W**	**100 W**	**50 W**	**75 W**	**100 W**
60	34.0	38.4	43.2	44.7	41.4	54.5	57.6	58.1	58.6
150	57.1	44.6	58.8	53.9	49.0	41.5	54.3	55.0	52.5
300	56.9	46.5	52.2	51.5	43.0	44.9	54.4	55.0	58.7

We have also studied the effect of post-exposure of the treated films to the system gas. After the plasma treatment with a particular gas the polyolefin films were maintained under the environment of the system gas for different time. The objective of the post-exposure was to utilize all the radicals generated on the polymer surface for the reaction with the system gas rather than with the atmospheric oxygen. It is well-known that exposure of the polymer films to the atmosphere, immediately after the plasma treatment, leads to the reaction between the surface free radicals and atmospheric oxygen, giving rise to functionalities other than those of the system gas. An advantageous effect of the post-treatment exposure can be understood from the **Figure 4.5**, which shows the XPS spectra of the plasma modified EPDM films. The increase in the intensity of the carbonyl and hydroxyl species in the XPS spectra of CO_2 and O_2 plasma treated films undoubtedly justifies our assumption. The contact angle measurements are also in accordance with the results of XPS analysis.

Figure 4.4 Effect of gas flow rate on the surface energy of plasma-treated polyolefin films.

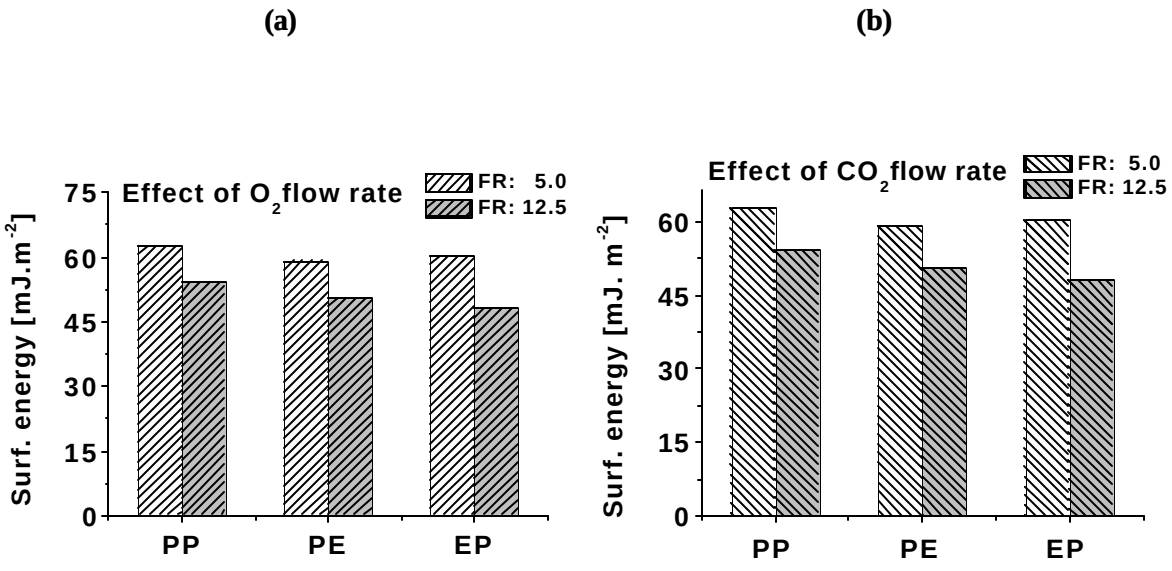

Figure 4.5 XPS spectra show the effect of post exposure time (T=0 min and T=10 min) on enhanced surface functionality of O_2 and CO plasma treated EPDM films.

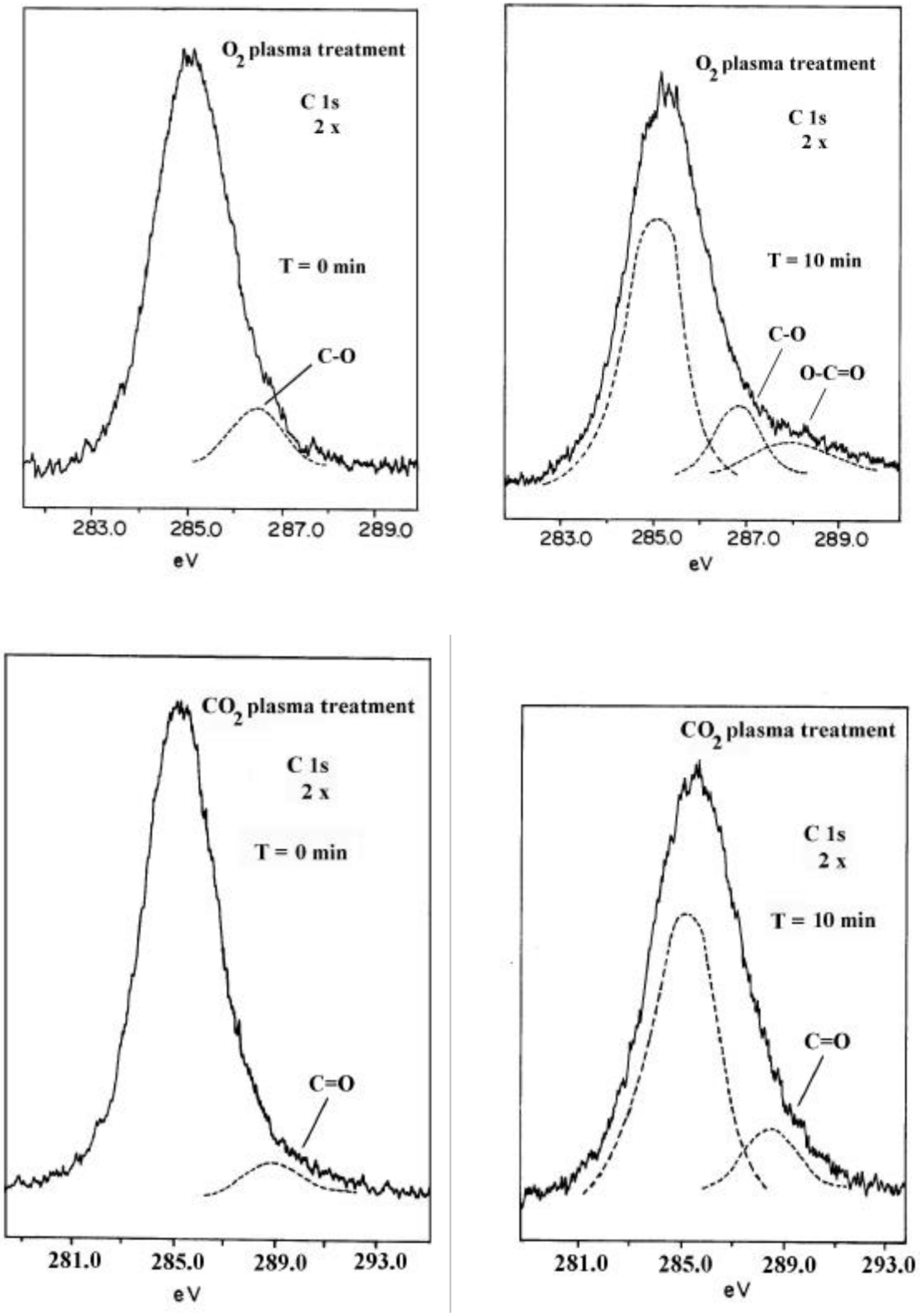

4.3.1.3 Surface re-construction during storage

The importance of polymer surface dynamics to its surface properties was realized by the medical community a couple of decades back[35]. The terms like *re-orientation*, *re-structuring*, *re-construction* and *hydrophobic recovery* have been used time to time by different researcher[36,37] studying the decrease in wettability of the functionalized surfaces with the storage time. In few cases attempts have been made to determine the mechanism of recovery process[10, 38]. One of the most common observation is that, while the chemically modified polymer surface bearing grafted chains is stable at room temperature in contact with air, the plasma modified polymer surfaces are dynamic in nature even at room temperature and undergo hydrophobic recovery in contact with air or vacuum[10,39]. Apart from the demand of surface thermodynamics for a minimum free-energy, the physical properties of the polymer also play a major role in governing the surface re-construction. The **Table 4.3** shows the effect of storage time at R.T. (24 % humidity) and re-orientation of the functional groups upon conditioning at 20 °C (58-66 % humidity) on the hydrophilicity of the polyolefin film surface. It can be seen from the table that EPDM undergoes rapid re-orientation compared to PP and PE. At the same time the hydrophilicity regained is faster in EPDM than in the other two thermoplastics. *Ferguson et al.*[40] in their study on re-orientation in oxidized polybutadiene have shown that the entropic forces associated with rubber elasticity, influence the process of re-construction. According to them, since the interfacial region of polybutadiene-oxy contains a small number of polar groups relative to the total number of non-polar groups, the migration of the polar groups to the polymer / water interface likely requires extension of polymer chain out of their entropically preferred, random coil conformations. In case of PE and PP, the possible mechanisms of hydrophobic recovery are: rotational motion of polymer segments bearing polar groups, slippage of chain segments or diffusion of polymer segments containing functional groups into the bulk of the polymer[41]. *Ferguson et al.* [41] has also suggested that the surface motions in case of glassy polymers is attributed either to the increase in the free volume caused by the enrichment of chain ends at the surface or to a reduction in entanglement density at the surface. According to *Yasuda and Mishra*[10], the slow decay in the hydrophilicity of the oxygen plasma treatment PP is due to the difference in the polarity at the surface and in the bulk. They found that the hydrophilicity in oxygen plasma treated PP was completely lost after 20 days of the treatment, however, the similarly treated surface of *plasma polymerized* PP, which had much higher degree of crosslinking, lost its wettability much more slowly. Reports also suggest that re-construction is initially driven by minimization of the interfacial free-energy. A slower process-probably driven simply by the dilution of

concentrated interfacial functionalities by diffusion into the polymer sub-surface and then results in further re-construction[38]. All these processes causing re-construction appear to take place faster in EPDM. Elastomers, in this case posses the most dynamic surfaces, which readily reorient in response to the changes in their environment. This orientation of the elastomeric chains is favored by their inter-chain free-volume and highly flexible coiled structure. However, the main driving force for the dynamic nature of the polymer surface molecules is the tendency of the surface to decrease its surface/interfacial free energy[36,39,42,43]. The rate of surface re-structuring depends on the nature of the polymer, temperature and polarity of the environment[9]. From the tabulated data, it can be seen that this rate varies from a few minutes in case of EPDM to a few hours and days in case of thermoplastics (PE and PP). Some researchers have also observed these variations in the rate of re-structuring for different types of polymers[44,45]. It is understood from **Table 4.3** that hydrophobic recovery increases with the temperature. This is due to the fact that with the increase in temperature the molecular motion becomes more rapid. Further, even those motions that require more energy start operating causing a decrease in the hydrophilicity of the modified surface. Moreover, the hydrophobic recovery in all the three polymers is not complete even after one month of storage. This indicates that the movement of the polymer segments bearing the functionalities is probably restricted, which might be due to the cross-links formed during the plasma treatment or entanglement of the polymer chains bearing the functional groups. It is documented that the polyethylene molecules, present at the surface undergo cross-linking mainly due to the UV irradiation generated during the plasma treatment[46]. Another possible explanation for the incomplete re-construction is on the basis of the relation between interfacial thermodynamics and T_g of the polymer. Full re-construction can be achieved only above the bulk T_g of the polymer; at R.T removal of all hydrophilic functionalities from the surface would be restricted by the remainder of the segments embedded within the glassy interior of the polymer[41]. In case of EPDM, a part of the diene segments readily undergo cross-linking under the influence of plasma. The cross-linked surface-network hinders the free rotation of the functional groups towards the bulk[47]. *Yasuda et al.* [10] described the hydrophobic recovery of different polymers at room temperature, a result of rotation of polymer chains at surface.

Table 4.3 Effect of storage time and conditioning on the water contact angle of oxygen plasma treated polyolefin films

Irradiation time (sec)	**water contact angle#** (°)											
	PP				**PE**				**EPDM**			
	Storage time (0 min)	Storage time (3 hrs)	Storage time (24 hrs)	Hydrated (2 hrs)	Storage time (0 min)	Storage time (3 hrs)	Storage time (24 hrs)	Hydrated (2 hrs)	Storage time (0 min)	Storage time (3 hrs)	Storage time (24 hrs)	Hydrated (2 hrs)
150	37.0	40.9	48.5	44.3	24.0	29.6	36.2	30.4	53.6	58.5	70.3	60.6
300	40.4	41.5	44.8	42.0	33.7	35.5	39.7	38.6	70.8	74.1	76.9	73.0

 # films treated at 75 W, in O_2 plasma

We further suggest that, since the mobility of the flabby chains especially in EPDM is more than the whole polymer chain, the surface of EPDM films probably becomes enriched with these unmodified chains, which screen the polar functional groups from water. In addition to this, since the surface polar moieties with overlying water interact via hydrogen bonding and dipole-dipole interactions, these short-range interactions operate effectively only when water is in direct contact with the polar group. A monolayer or bilayer of hydrocarbon chains can effectively screen these interactions and thus water cannot sense the buried polar groups[48]. However, the thickness and number of hydrocarbon layers are not known in this case. It is known from the literature[49] that a 5 $^{\circ}$A thick PE layer is sufficient enough to screen the underlying carboxylic acid groups.

4.3.2 Plasma induced surface grafting onto EPDM films

This section describes an unusual method of surface grafting of functional monomers onto the EPDM films. It is now well-known that the functionalities generated upon plasma treatment on the EPDM films are not permanently available at the surface due to the exceptional flexibility of elastomer chains and dynamic nature of the polymer surface. However, the functionalities generated as a result of chemical modification can lead to permanently hydrophilic/polar surfaces. Moreover, it is also established that surface cross-linking restricts the free rotation of the functional groups towards the sub-surface. Taking the advantage of these drawbacks of cross-linked surfaces, we have successfully accomplished the deliberate cross-linking of functional monomers and multi-functional acrylates (cross-linking agents) on the EPDM surface.

4.3.2.1 Reaction mechanism

The mechanism of grafting functional monomers using reactive gas plasma is shown in **scheme 4.4**. A thin layer of monomer and cross-linker is formed on the surface of the EPDM film upon spin coating. When this micro-coated film is exposed to reactive gas plasma, the vinyl groups present on the surface readily undergo crosslinking with each other as well as with the pendant dienes of the EPDM. The idea employed here is similar to *plasma immobilization* reported earlier[50,51]. The technique used by the researchers then involved coating of a thin layer of unsaturated surfactant having specific functional group onto the surface of a polymeric substrate (PP, PE and PBD). Subsequently, the substrate was treated with argon plasma by which a part of the coated surfactant was covalently coupled to the polymer surface. In case of PP and PE the secondary and tertiary radicals formed upon plasma treatment reacted with the unsaturated surfactant whereas in case of PBD opening of the double bond resulted in the immobilization of the surfactant via cross-linking, a process

similar to the vulcanization of the diene rubber. The results of the gravimetric analysis and contact angle measurements are compiled in the **Tables 4.4 - 4.6**. It is understood from the results that EGDMA is a better cross-linker compared to DAA for obvious reasons like higher reactivity and polarity. The ATR-FTIR spectra in the **Figure 4.6** show the presence of surface anchored functional monomers and cross-linkers.

It can also be observed from the gravimetric results that each monomer when solely coated on the polymer surface does not undergo effective anchoring, which may be due to the less number of vinylic moieties.

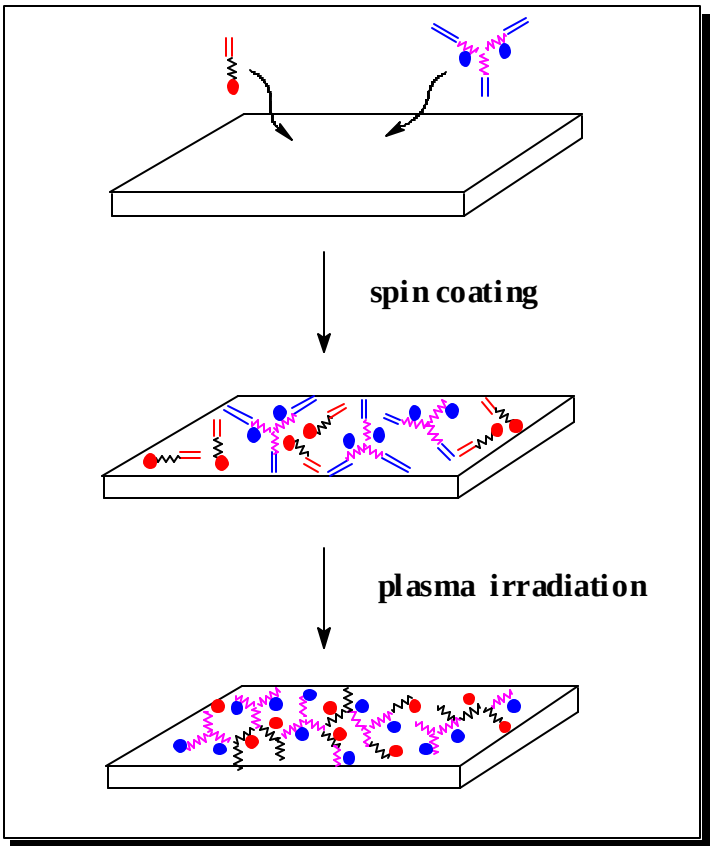

Scheme 4.4

Monomers when present along with either of the cross-linkers undergo efficient cross-linking resulting in significant number of hydrophilic groups to generate long-term wettable surfaces[30]. It is also obvious that the wettability of the modified surfaces increase with the degree of grafting. Oxygen being easily converted into its biradical state in the plasma was used as system gas to facilitate the cross-linking of the coated monomers and MFA with the film surface. The use of oxygen as system gas additionally contributes to the hydrophilicity of the EPDM surface.

Figure 4.6. ATR-FTIR spectra of plasma induced surface grafted monomers and MFA.

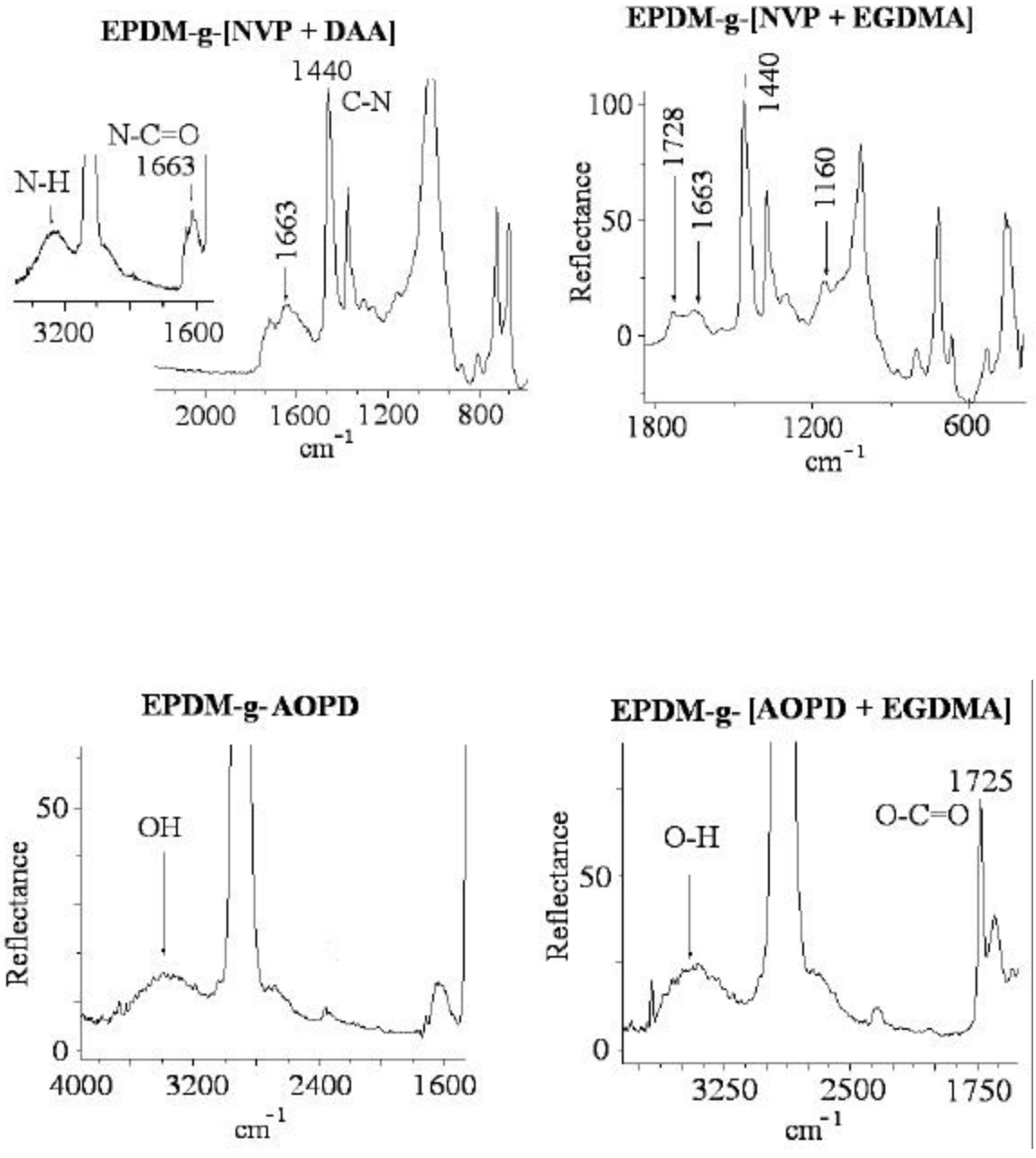

Table 4.4 *Gd* and contact angle of spin coated and surface grafted functional monomers

Monomer	G_d^B (mg/cm^2)	G_d^A (mg/cm^2)	θ^A ($^\circ$)
AOETMAS	1.16	0.60	41.0
AOPD	0.46	0.1	51.2
HEMA	0.34	0.16	54.6
GMA	0.40	0.12	66.1
NVP	0.82	0.50	55.0

Table 4.5 *Gd* and contact angle of grafted functional monomers and cross-linker (DAA)

Monomer + DAA	G_d^B (mg/cm^2)	G_d^A (mg/cm^2)	θ^A ($^\circ$)
AOETMAS	1.35	0.90	36.8
AOPD	0.86	0.55	47.2
HEMA	0.64	0.56	49.6
GMA	0.50	0.60	48.1
NVP	0.89	0.66	51.5

Table 4.6 *Gd* and contact angle of grafted functional monomers and cross-linker (EGDMA)

Monomer + EGDMA	G_d^B (mg/cm^2)	G_d^A (mg/cm^2)	θ^A ($^\circ$)
AOETMAS	1.40	1.04	30.0
AOPD	1.06	0.86	33.2
HEMA	1.02	0.64	45.6
GMA	1.20	0.78	44.8
NVP	1.04	0.61	47.0

A= after washing, B = before washing and θ = water contact angle

4.3.2.2 Effect of storage time

A favourable effect of anchoring the functional groups on the EPDM films surface via cross-linking is clearly reflected in the **Table 4.7,** which is self-explanatory. As discussed in the *section 4.3.1.3*, the cross-links present at the polymer surface have a significant influence on the mobility of the functional groups. A small increase in the water contact angle with

storage time may be due to the orientation of those functional groups generated by the oxygen plasma. However, upon conditioning the samples at low temperature (20 °C and 58 % humidity), the surface hydrophilicity is regained. This reaffirms the migration of only those functionalities that are developed as a result of oxygen plasma. *Whitesides et al.*[38] in their study have deduced that the process of re-construction is slow when the interfacial functional groups are large and polar. Thus, the structure of interfacial groups significantly influence the rate of re-construction.

Table 4.7 Effect of storage time on the hydrophilicity of surface modified EPDM films

Monomer + EGDMA	**water contact angle** (°)				
	Storage time (0 min)	Storage time (24 hrs)	Storage time (1 week)	Storage time (4 weeks)	Conditioning (12 hrs)
AOPD	33.2	36.7	38.8	40.0	34.1
GMA	44.8	49.1	50.9	51.5	47.0
NVP	47.0	51.7	54.9	55.4	46.3

4.4 BIOCOMPATIBILITY STUDY OF SURFACE MODIFIED EPDM FILMS

The ultimate objective of our study was to develop biocompatible surfaces of elastomers. It is assumed that dynamic nature of elastomers has restricted their use as biomaterials. The functional groups those are generated onto the elastomer surface are not permanently available at the air-polymer interface. From our study we have deduced that the functional groups generated on any polymer surface by whichever method are not fully available at the interface at a given point of time, particularly if the surfaces are not rehydrated/conditioned in a humid environment before use. An interesting observation is that the functional groups oriented towards the sub θ interface in elastomers, reorient faster towards the interface than those for other thermoplastics like PE and PP, which is attributed to the higher flexibility of their polymer chains. For a polymeric material to be a successful biomaterial, the reactions taking place during the first few minutes of implantation play a vital role in determining their long-term success. The processes like cell clustering, blood clotting, platelet adhesion and protein adsorption operate as soon as the biomaterials are implanted.

When a dehydrated surface-functionalized polymer is implanted into a biological system assuming that all the functional groups are available at the interface, a totally different surface is actually interacting with the components of this system, leading to unfavorable side reactions. Therefore, elastomers with their dynamic surfaces are expected to be better alternatives.

It can be seen from the optical micrographs (**Figure 4.7** and **4.8**) of cell adhesion study that the difference in the number of cells adhered on hydrated and dehydrated PP is more than that in case of EPDM although, the cell adhesion observed after 12 hrs of incubation is similar for hydrated PP and EPDM. The difference in the cell adhesion on the hydrated and dehydrated surfaces may be due the different types of interaction of the cells with the surfaces. This indicates that functional group re-orientation is a faster process in elastomers compared to thermoplastics. The qualitative biocompatibility study on AOPD plasma grafted EPDM films showed that the cell adhesion was in the order AOPD < AOPD + DAA < AOPD + EGDMA. This is attributed to the capacity of the cross-linked network to capture the functional groups on the EPDM surface. Thus, immobilization of the functional groups at the polymer-air interface significantly influences performance of the biomaterials.

Figure 4.7 a) dehydrated PP **b)** dehydrated EPDM after 12 hrs of incubation in KB cell culture

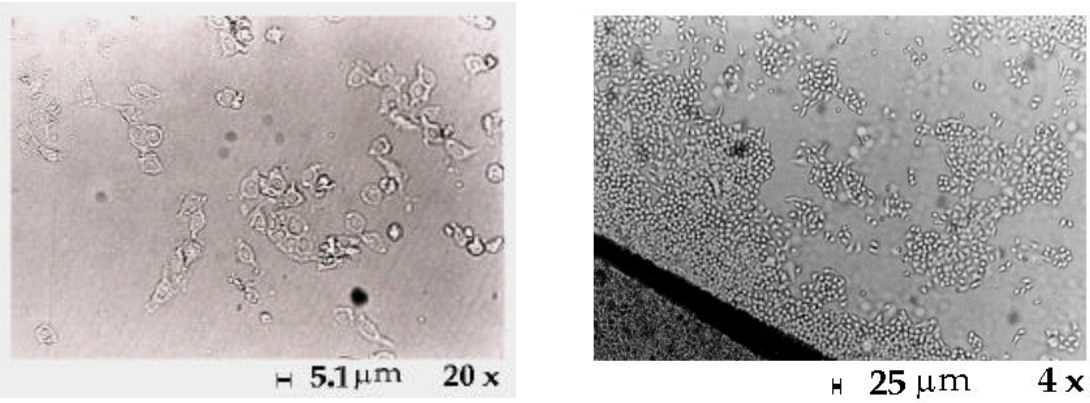

(a) **(b)**

Figure 4.8 a) hydrated PP **b)** hydrated EPDM after 12 hrs of incubation in KB cell culture

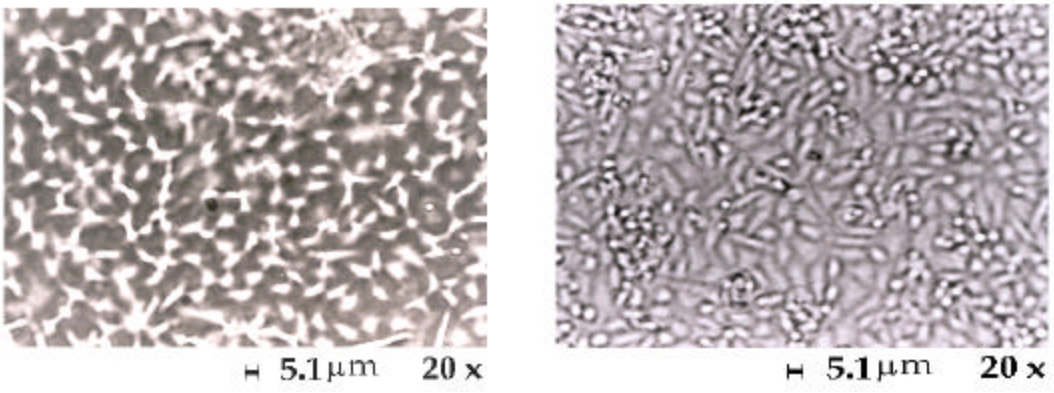

(a) **(b)**

4.5 CONCLUSIONS

The plasma treatment using reactive gases like oxygen and carbon dioxide generates OH/OOH and C=O functionalities onto the surface of the polyolefin films. Exposure of polymer films to low power plasma for short irradiation time generates functional groups respective to the system gas but exposure to high plasma power for long time causes surface cross-linking and etching, which significantly decreases the surface hydrophilicity. Hydrophobic recovery due to surface re-construction is a slow process in thermoplastics, which is attributed to the lower mobility of the polymer chains and rotation of only functional groups and not the polymer chain bearing them. EPDM elastomer surface re-construction is a rapid process and is an outcome of very high mobility of the flexible elastomer chains. Hydrophobic recovery may also be due to the screening of the polar functional groups by the hydrocarbon chains. Restricted mobility of the functional groups on a cross-linked surface can be used as a tool to permanently immobilize functional groups at the polymer-air interface. By using this technique, functional groups can be permanently made available at the elastomer surfaces, which further helps in improving their biocompatibility.

4.6 REFERENCES

1. G. Oster, G. K. Oster and H. J. Moroson, *J. Polym. Sci.*, **34**, 671 (1959).
2. F. Garbassi, E. Occhiello and F. Polato, *J. Mater. Sci.*, **22**, 207 (1987).
3. S. H. O. Egboh and M. O. Fagbule, *Eur. Polym. J.*, **24**, 1041 (1988).
4. N. Inagki, Plasma surface modification and plasma polymerization, Technomic publishing Co., Lancaster, USA (1996).
5. M. Kawabe, S. Tasaka and N. Inagaki, *J. Appl. Polym. Sci*., **78**, 1392 (2000).
6. F. P. Epaillard, B. Chevet and J. C. Brosse, *Makromol. Chem*., **192**, 1589 (1991)
7. D. J. Williams, Polymer Science and Engineering, Prentice-Hall Inc., Englewood Cliffs, New Jersey (1971).
8. E. Occhiello, M. Morra, G. Morini, F. Garbassi and P. Humphrey, *J. Appl. Polym. Sci*, **42**, 551 (1991).
9. C. M. Weikart, H. K. Yasuda, *J. Polym. Sci., Part A: Polym. Chem.*, **38**, 3028 (2000).
10. H. Yasuda, A. K. Sharma and T. Yasuda, *J. Polym. Sci.*, A **19**, 1285 (1981).
11. M. Morra, E. Occiello, F. Garbassi, *J. Adhes. Sci., Technol*., **7**, 1051 (1973).
12. M. Mora, E. Occiello, F. Garbassi, *Langmuir*, **5**, 872 (1989)
13. I. Gancarz, G. Pozniak and M. Bryjak, *Eur. Polym. J.* **36**, 1563 (2000).
14. H. Beatrice, F. Amihay and G. Ralph, US 5578073 (1996).
15. D. D. Lee and W.T. Conner US 5,543,019 (1996).
16. L. Thiele, *Acta Polymerica*, **30**, 323 (1979).
17. W. Breuers, D. Klee, H. Hocker, C. Mittermayer, *J. Mater Sci., Mater. Med*., **2**, 106 (1991).
18. F. P. Epaillard, G. Legeay and J. C. Brosse, *J. Appl. Polym. Sci.*, **44**, 1513 (1992)
19. M. Y. Teng, K. R. Lee, D. J. Liaw, Y. S. Lin and J. Y. Lai, *Eur. Polym. J.*, **36**, 663 (2000).
20. B. Gupta, C. Plummer, I. Bisson, P. Frey, J. Hilborn, *Biomaterials*, **23**, 863 (2002).
21. P. Anelli, S. Baccaro, M. Carenza and G. Palma, *Radiat. Phys. Chem*., **46**, 1031 (1995).
22. P. Wang, K. L. Tan, C. C. Ho, M. C. Khew and E. T. Knag, *Eur. Polym. J*., **36**, 1323 (2000).
23. C. A. Wilkie, X. Dong and M. Suzuki, *Polym. Mater. Sci. Eng.*, **71**, 296 (1994).
24. D. Klee and H. Hocker, *Adv. Polym. Sci.*, **149**, 1, (1999).

25. D. L. Leake, E. Cenni, D. Cavedagna, S. Stea, G. Ciapetti, A. Pizzoferrato, *Biomaterials*, **10**, 441 (1989).
26. a) S. Khongton and G. S. Ferguson, *J. Am. Chem. Soc*., **123**, 3588 (2001), b) F. M. Fowkes, *Ind. Eng. Chem*., **56**, 40 (1964).
27. H. V. Boenig, Plasma Science and Technology, Carl Hanser, Munchen (1982).
28. N. Inagaki, Plasma Surface Modification and Plasma Polymerization, p.78 Technomic publishing Co., Lancaster, USA (1996).
29. F. Garbassi, M. Mora, E. Occhiello, L. Barino and R. Scordamaglia, *Surf. Interface. Anal*., **14**, 585, (1989).
30. A. Charlesby, Atomic Radiation and Polymers, Chapter 28, p 412, Pergamon Press, New York (1960).
31. F. P. Epaillard, B. Chevet, J. C. Brosse, *Eur. Polymer J.*, **26**, 333 (1990).
32. L. Reich and S. S. Stivale, Elements of Polymer Degradation, Chapter 1, p. 1, McGraw-Hill, New York (1971),
33. N. Inagaki, Plasma Surface Modification and Plasma Polymerization, p.23 Technomic publishing Co., Lancaster, USA (1996).
34. A. J. Muller, J. L. Freijoo, C. A. Villamizar and P. E. Vasquez, *Metal Finishing*, **84**, 57 (1986).
35. F. J. Holly and M. F. Refojo, *J. Biomed. Mater. Res*., **9**, 315 (1975).
36. B. Gupta, J. Hilborn, C. Hollenstein, C. J. G. Plummer, R. Houriet and N. Xanthopoulos, *J. Appl. Polym. Sci*., **78**, 1083 (2000).
37. S. Khongtong and G. S. Ferguson, *J. Am. Chem. Soc*., **123**, 3588 (2001).
38. S. R. Holmes-Farley, R. H. Reamey, R. Nizzo, T. J. Mc Carthy, G. M. Whitesides, *Langmuir*, **3**, 799 (1987).
39. K. B. Lewis and B. Ratner., *J. Colloid. Interface. Sci*., **159**, 77 (1993).
40. D. H. Carey and G. S. Ferguson, *J. Am. Chem. Soc.*, **118**, 9780 (1996).
41. H. Rouse, P. L. Twaddle and G. S. Ferguson, *Macromolecules*, 32, 1665 (1999) (and reference therein)
42. G. S. Fergusson and G. M. Whitesides, In Modern Approaches to Wettability: Theory and Practical, Ed. M. E. Schrader and G. I. Loeb., Plenum Press, New York, p. 143-177 (1992).
43. R. J. Good, *J. Coll. Interf. Sci*., **59**, 398 (1977).
44. D. F. Lawson, *Rubber Chem. Tech*., **60**, 102 (1987).
45. E. Occhiello, M. Mora, P. Cinquina and F. Garbassi, *Polymer*, **21**, 895 (1992).

46. H. Yasuda, *J. Macromol. Sci. Chem*., A **10**, 383 (1976).

47. Y. Yao, X Liu, Y. Zhu., *J. Appl. Polym. Sci.*, **48**, 57 (1993).

48. S. Balamurugan, Surface Modification of Polyolefins by Chemical and Plasma Methods, University of Pune, Chapter 7, p. 208 (1998).

49. E. B. Troughton, C. D. Bain, G. M. Whitesides, R. G. Nuzzo, D. L. Allara and M. D. Porter, *Langmuir*, **4**, 365 (1988).

50. J. P. Lens, J. G. A. Terlingen, G. H. M. Engbers and J. Feijen, *J. Polym. Sci., Polym. Chem*., **36**, 1829 (1998).

51. J. G. A. Terlingen, J. Feijen and A. S. Hoffman, *J. Biomater. Sci., Polym. Ed*, **4**, 31 (1992).

CHAPTER V

SURFACE GRAFTING ONTO NATURAL RUBBER FILMS

5.1 INTRODUCTION

The past decade has witnessed a tremendous surge in the interest regarding techniques for material surface preparation and modification. After thoroughly exploring the surface modification of thermoplastics (viz. PP, PE and PS) in the past four decades, the interest of the scientific community is now focused at the surfaces of diene elastomers[1-3]. Researchers previously believed that elastomers aren't suitable candidates for surface modification mainly due to their highly dynamic surfaces but with time and genuine research inputs this perception has proved false[4]. However, systematic studies are still required to understand the complex mechanisms of surface modification in case of elastomers. Significant efforts have gone into the bulk modification of NR via graft copolymerization[5,6]. The traditional systems involved the use of free-radical and redox initiators to bring about functionalization of the NR[7,8]. Medical products prepared from natural rubber have found extensive applications, ranging from surgical gloves, tubings, catheters to balloons etc. However, the blood compatibility of devices made up of NR is poor compared to those made out of silicone and polyurethanes. The excellent elasticity, flexibility and resistance against splitting of NR would be more advantageous than those of other polymers. If improvement in blood/body compatibility of NR could be accomplished, the biomedical applications of NR could be greatly extended. Not many but few genuine attempts have been made to improve the blood compatibility of NR[9-11].

In the present study natural rubber was preferred as a substrate due to its low cost and free abundance in the Indian subcontinent. Moreover, we found that a systematic research related to the surface modification of NR has not been done yet. In fact, only few articles on the surface modification of natural rubber have appeared till now[3,4,10]. One of the main reasons for this is the tedious procedure for the preparation of self-standing thin films of natural rubber. The films of natural rubber readily crimp due to their excellent elasticity and very strong adhesive nature. During the present study we have developed a very simple and consistent technique for the preparation of NR thin films. Photo-grafting and plasma-grafting techniques are preferred for the surface modification of the NR films for obvious merits like moderate energy and surface selectivity. Surface modification of NR using pulsed laser technique leads to high amount of subsequent homopolymerization with very thick grafted layers[12,13]. These drawbacks along with few more like fractal formation have been least addressed in the past.

The objective of the present study is to determine the suitability of two versatile techniques involving initiation at low energies viz. short exposure photochemical grafting and simultaneous plasma-grafting for the generation of desired functionalities onto the surface of the NR films without altering their native properties. Additionally, the functional groups anchored onto the surface should be capable of generating properties like hydrophilicity, dyeability and biocompatibility of the NR films. Green chemistry avoiding the use of solvents is the need of the day, thereby making the plasma-grafting process value added. The present chapter describes the use of two unprecedented mild techniques of surface modification viz. short exposure photochemical grafting (at 400 W) and simultaneous low-pressure cold plasma-grafting (between 40 - 75 W), for the introduction of functional monomers onto the surface of NR films. In the present work, the photochemical surface grafting of different functional monomers (viz. hydroxyethyl methacrylate, acrylic acid and acrylamide) onto the surface of NR films has been accomplished and the efficiency of different photoinitiators (viz. benzophenone, hydrogen peroxide and xanthone) has been investigated for reactions carried out at variable temperature. The effect of various reaction parameters on the surface grafting efficiency has also been thoroughly studied. In the second approach, the surface grafting of functional monomers onto these elastomeric substrates was achieved by simultaneous plasma-grafting technique, where monomer vapors were simultaneously introduced into the plasma reaction chamber. The influence of the plasma grafting conditions has also been thoroughly investigated. The functionalized surfaces obtained as a result of surface grafting were characterized by contact angle measurements, ATR-FTIR, SEM, XPS, AFM and optical microscopy techniques. The influence of the functional groups and their density on the biocompatibility (cell adhesion tests) of these surface modified NR films has also been investigated.

5.2 MATERIALS AND METHODS

5.2.1 Materials

The monomers viz. 2-hydroxyethyl methacrylate (HEMA), acrylic acid (AA) and acrylamide (AAm) procured from M/s. Aldrich, USA, were used after purification. All solvents obtained from M/s. E. Merck India Ltd. were of L.R. grade. The photoinitiators obtained from E. Merck, India, were used as received. Natural rubber was obtained from Kottayam, Kerala, India, by the courtesy of Prof. Sabbu Thomas. It was purified by dissolving in toluene and precipitating with acetone, followed by drying under vacuum at room

temperature to a constant weight. The nitrogen and argon gases (Grade I) supplied by M/s. Inox Ltd., India, were used for photo-grafting and plasma-grafting reactions.

5.2.1.1 Preparation of NR films

A 1.5 % w/v homogeneous solution of purified NR was prepared in analytical grade toluene and 125 ml of this solution was carefully poured (avoiding air bubbles) in a flat-bottomed evaporating bowl (10 cm diameter) containing 2.0 % NaCl solution in distilled and filtered water. This bowl covered with perforated aluminium foil was kept in dark and the toluene was evaporated at room temperature to obtain NR films (thickness ~ 200 microns). The films thus formed were carefully removed and immediately kept in acetone to avoid crimping, followed by a thorough wash with methanol, water and acetone successively. The films were dried in vacuum oven at 40 °C to remove any trapped solvent. The dried films were cut into a fixed size (4 cm × 1.5 cm) and stored in deep freezer till use.

5.2.1.2 Reactor design

In the present study, the surface modification of the NR films was carried out mainly by two methods, short exposure photo-grafting and simultaneous plasma-grafting. The reactors for both the processes were tailor-made with in-house glass blowing facility.

5.2.1.2.1 Photo-grafting reactor

The details of the photografting reactor are described in the Chapter 3, *section 3.2.1.2.1.*

5.2.1.2.2 Plasma-grafting reactor

The experimental set-up and the details of plasma-grafting assembly are described in the Chapter 3, *section 3.2.1.2.2*

5.2.1.3 Irradiation source

A medium pressure 400 W mercury vapor lamp (Mazda, Japan) was used as the irradiation source. The lamp emits polychromatic radiation of $\lambda \geq 290$ nm. The lamp was immersed in a pyrex glass jacket with cold-water circulation facility [Figure 3.1(b)] in order to maintain the system at room temperature and avoid heat transfer to the reaction.

5.2.2 Experimental methods

The surface modification of the NR films was accomplished by two methods involving moderate energy **a)** photo-grafting and **b)** plasma-grafting.

5.2.2.1 Photo-grafting procedure

Photo-grafting was carried out in a special type of pyrex-glass photo-reactor irradiated with a 400 W medium pressure mercury vapor lamp from a fixed distance (15 cm) for a fixed time at room temperature [Figure 3.1(a)] and elevated temperature [Figure 3.1(b)]. The films (4 cm × 1.5 cm) were immersed in this photoreactor containing *solvent*, *photoinitiator* and *monomer* in a definite proportion, under nitrogen flux. The photo-grafted NR films in all cases were subjected to sonication, followed by Soxhlet extraction in acetone/water for 12 hrs in order to remove homopolymer. These films were finally dried in a vacuum oven at 35 °C till constant weight.

5.2.2.2 Plasma-grafting procedure

The plasma reactor was evacuated to 10^{-2} Torr, followed by flushing the system for 10 - 15 min by passing the inert gas (argon in the present study) at a high flow rate. Argon flow rate was set to 1.5 - 2.0 sccm and reactor pressure 0.2 Torr for carrying out plasma grafting. The monomers were heated to boil in a RB in presence of carrier gas (argon) in the temperature range of 50 - 75 °C (depending upon b.p. of monomer) at 0.2 Torr. The reactor pressure was maintained at 0.2 Torr and the monomer flow was 2.5 sccm.

After the reactor pressure was stabilized, argon plasma was initiated by an RF power supply through a matching network and output power was varied from 50 - 75 W and the irradiation time varied from 10 - 40 min. The monomer vapor was introduced after 5 min of glow discharge, through the second opening (from the left) in the Figure 3.2 at distance 12 cm from the substrate in the downstream of the argon plasma (glow discharge). The monomer flow was stabilized and maintained at 2.0 - 2.5 sccm. After the plasma was terminated, the monomer vapor purging was continued for 10 - 20 min in order to utilize all the free radicals generated on the surface.

5.2.3 Characterization methods

The surface grafted NR films were characterized by contact angle Goniometer, ATR-FTIR, SEM, XPS, AFM and optical microscopy techniques. The change in the weight of the grafted samples was determined using microbalances: *Precisa* 205 ASCS, Switzerland and Sartorius BP 210D, Germany. The details of all these analytical instruments are revealed in Chapter 3, *section 3.23*.

5.2.3.1 Determination of graft copolymerization

Weight gain (WG): Weight gain is defined as the difference of the weight of the whole sample *(Ww)* after grafting and the initial weight of the NR film *(Wo)* divided by the initial weight of NR film as shown in equation (1)

$$WG\ (\%) = \left[\left(\frac{Ww - Wo}{Wo} \right) \right] \times 100 \qquad \ldots\ldots\ldots\ldots (1)$$

Degree of grafting (G_d): Degree of grafting is expressed in equation (2)

$$G_d\ (mg/cm^2) = \left[\left(\frac{Wgr - Wo}{Wo} \right) / 2 \times SA \right] \qquad \ldots\ldots\ldots\ldots\ldots (2)$$

where Wo is the initial weight of the film, Wgr is the weight of grafted film after extraction and SA is the surface area of each film.

Grafting efficiency (G_e): is expressed by the equation (3)

$$G_e\ (\%) = Wg / Wp \times 100 \qquad \ldots\ldots\ldots\ldots\ldots (3)$$

where (Wg) is the weight of grafted polymer after extraction and (Wp) is the total weight of polymer formed (after evaporation of solvent and unreacted monomer).

5.2.4 Biocompatibility tests

The biocompatibility of the modified and pristine NR films was tested by incubating the samples in a cell culture of human oral carcinoma (KB) cell lines, at 37 °C, 5% CO_2, 90 % humidity in standard culture media and subsequently being monitored for cell adhesion after 24 and 48 hours of incubation using an optical microscope equipped with a camera.

5.3 RESULTS AND DISCUSSION

Different functional groups viz. hydroxyl, carboxyl, ester, amide and bromide were introduced onto the surface of NR films depending upon the type of monomer grafted by the two mild surface modification techniques. The effect of different reaction conditions on the surface modification was thoroughly investigated.

5.3.1 Surface photo-grafting onto NR films

A typical photo-grafting system in our experiments has BP, XT and H_2O_2 as photoinitiators and HEMA, AA and AAm as functional monomers. The selected photointiators have their λ_{max} in the range of the radiation emitted by the UV lamp i.e. 290 - 400 nm. The photochemical grafting reaction is carried out in a Pyrex reactor since it absorbs

all the radiation below 290 nm responsible for the homopolymer formation[14]. *Ranby et al.*[15] in their recent findings have reported that the dissolved oxygen in the reaction system is responsible for the induction period caused by the scavenging/quenching reactions with the photoinitiator thus, significantly retarding the graft copolymerization. Hence, all the experiments in the present study are conducted under inert atmosphere. All the reactions are found to proceed via typical photo-grafting mechanism.

5.3.1.1 Control experiment

The control reactions were carried out according to the procedure mentioned in the **section 3.2.2.1**. In individual reaction, (0.2 M) of each photo-initiator (viz. BP, XT and H_2O_2) was taken along with a solvent and a pair of pre-weighed NR film in absence of monomer in the photoreactor maintained at 50 ± 2 °C under inert conditions and irradiated for a specific period. These films were then washed with fresh acetone, dried and characterized by ATR-FTIR, which did not show any significant change with respect to the pristine NR. However, the ATR-FTIR spectra of the control experiments were taken as reference for comparing them with the photo-grafted samples. Further, there was no change in weight of these samples. It was confirmed by carrying out following control experiments that the functionalities generated on the surface of NR films were due to the photografted monomers and not due to the surface degradation induced by photo-initiations/sensitizers in the presence of UV light.

5.3.1.2 Reaction mechanism

The mechanism of surface grafting onto natural rubber is shown in the **scheme 5.1**. Upon absorption of UV radiation, the photoinitiator gets excited giving rise to the triplet-excited state from the initially formed singlet state. These triplets effectively abstract hydrogen atom from polymer surface to generate allyl macro radicals which, when reacts with vinylic monomer results in 'grafting from the polymer'. However, when the abstraction of hydrogen atom takes place from the monomer, 'homopolymer' is formed. This growing homopolymer chain when attacks the unsaturation on the polymer back-bone, gives rise to 'grafting onto the polymer'. However, the possibility of homopolymerization arises only under specific reaction conditions. Moreover, *Sundberg et al.*[16] have shown that the grafting via double bond addition is not a major reaction. Thus, photo-grafting predominantly takes place 'from the polymer'.

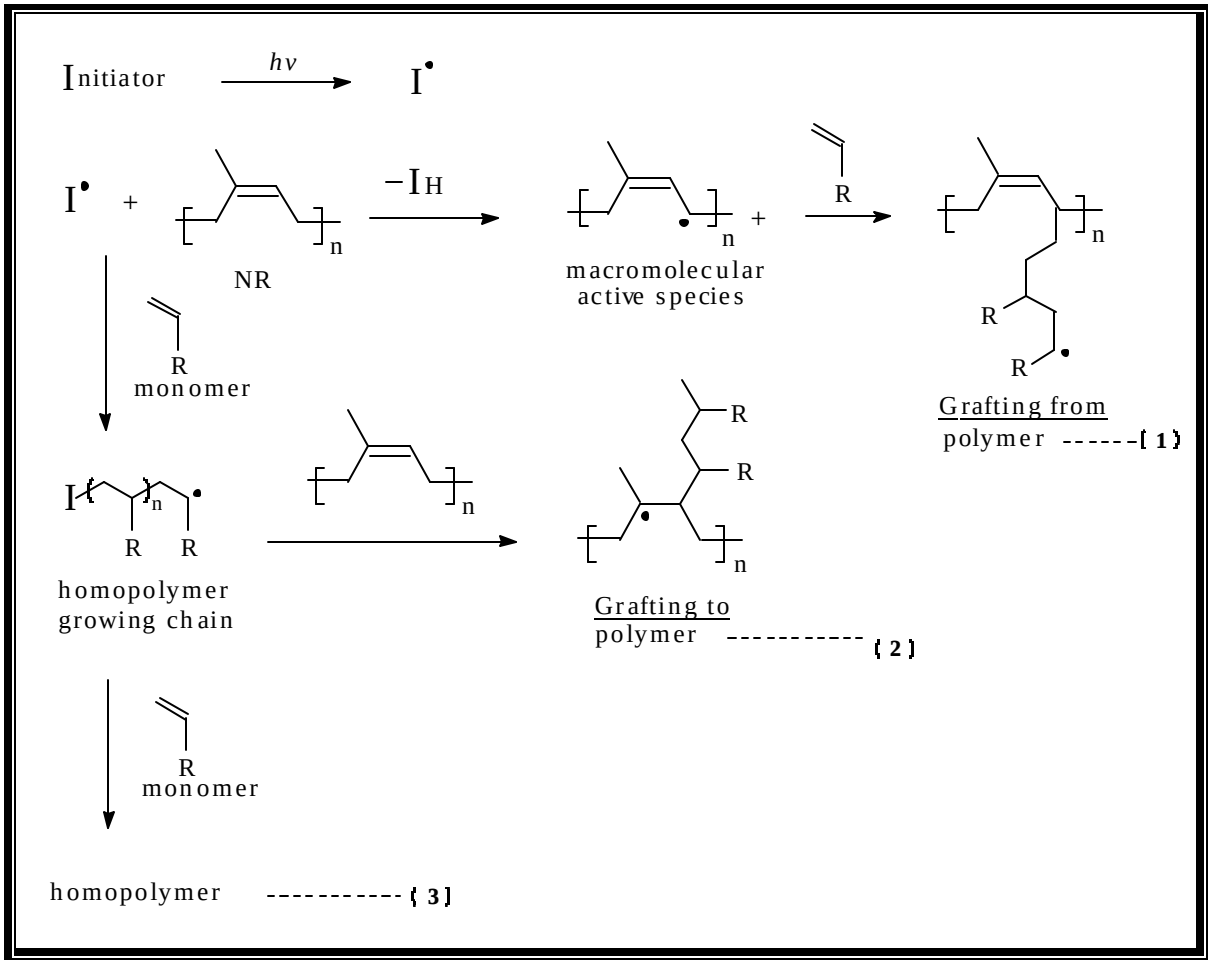

Scheme 5.1

5.3.1.3 Photo-grafting of functional monomers

The irradiation of a pair of NR films (4 cm × 1.5 cm), in each photo-reactor was carried out in the presence of 0.2 M benzophenone, 1.0 M of monomer (HEMA, AA and AAm) in 47 ml acetone under inert reaction condition for 1 hr at 50 ºC. The reaction mixture was de-aerated with high purity nitrogen gas for 20 minutes before commencing the reaction and the inert atmosphere was maintained throughout the reaction. The characterization of these surface grafted films after Soxhlet extraction and thorough drying revealed the following information. The primary evidence of the successful accomplishment of the surface photo-grafting reaction was obtained from the results of *degree of grafting* and *contact angle measurements*, revealed in the **Figure 5.1**. The difference in the degree of grafting is attributed to the dissimilarity in the reactivity of functional monomers. The grafting efficiency (G_e)

observed here is in the order HEMA > AA > AAm. The *degree of grafting* also depends on the affinity of the monomer towards the surface free-radicals. From the **Figure 5.1**, it is also understood that HEMA and AA grafted films generate significantly hydrophilic surfaces. However, the hydrophilicity of the modified surfaces shows their dependence on the *degree of grafting* and the type of monomer grafted.

Figure 5.1 Effect of surface photo-grafting of functional monomers onto NR films

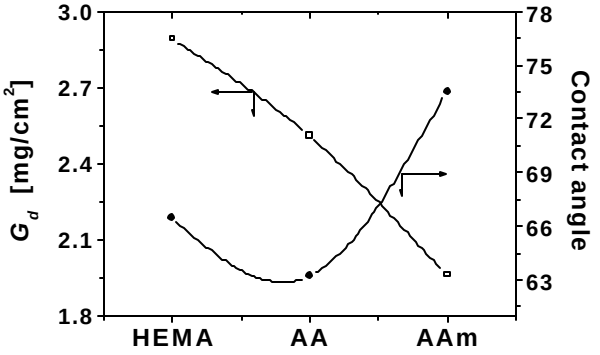

The presence of respective functional groups of the grafted monomers was substantiated by spectroscopic techniques. In the ATR-FTIR spectrum, the characteristic peaks with stretching vibrations at 1725 cm^{-1} (C=O) and 3440 cm^{-1} (O-H) for NR-g-HEMA, 1704 cm^{-1} (COOH) for NR-g-AA and 3350 cm^{-1} (N-H) and 1660 cm^{-1} (N-C=O) for NR-g-AAm are obvious from the **Figure 5.2.** These results are supported by the XPS analysis, which shows the peaks corresponding to the binding energies of C1s, O1s and N1s of respective monomers grafted onto the surface of NR films. Accordingly, C1s values of 285.0 (C-H), 288.8 (O-C=O), 286.2 (C-OH) and O1s values of 532.4 (C-O), 533.8 (O-C=O) for HEMA, C1s values of (COOH) of 289.2 and O1s values of 533.0 (C-O) for AA, C1s values of 286.2 (C-N), 288.2 (N-C=O), N1s value of 399.9 (N-C=O) and O1s value of 532.4 (N-C=O) for AAm are observed in the **Figure 5.3**. The **Figure 5.4** reveals the morphology of NR-g-HEMA.

Figure 5.2 ATR-FTIR of photo-grafted NR films.

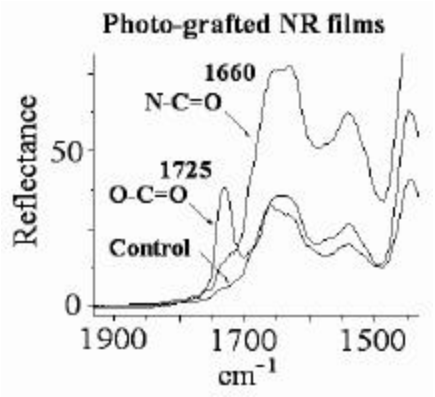

Figure 5.3 XPS spectra showing C1s and O1s binding energies corresponding to the functional groups in the HEMA and AA grafted EPDM films.

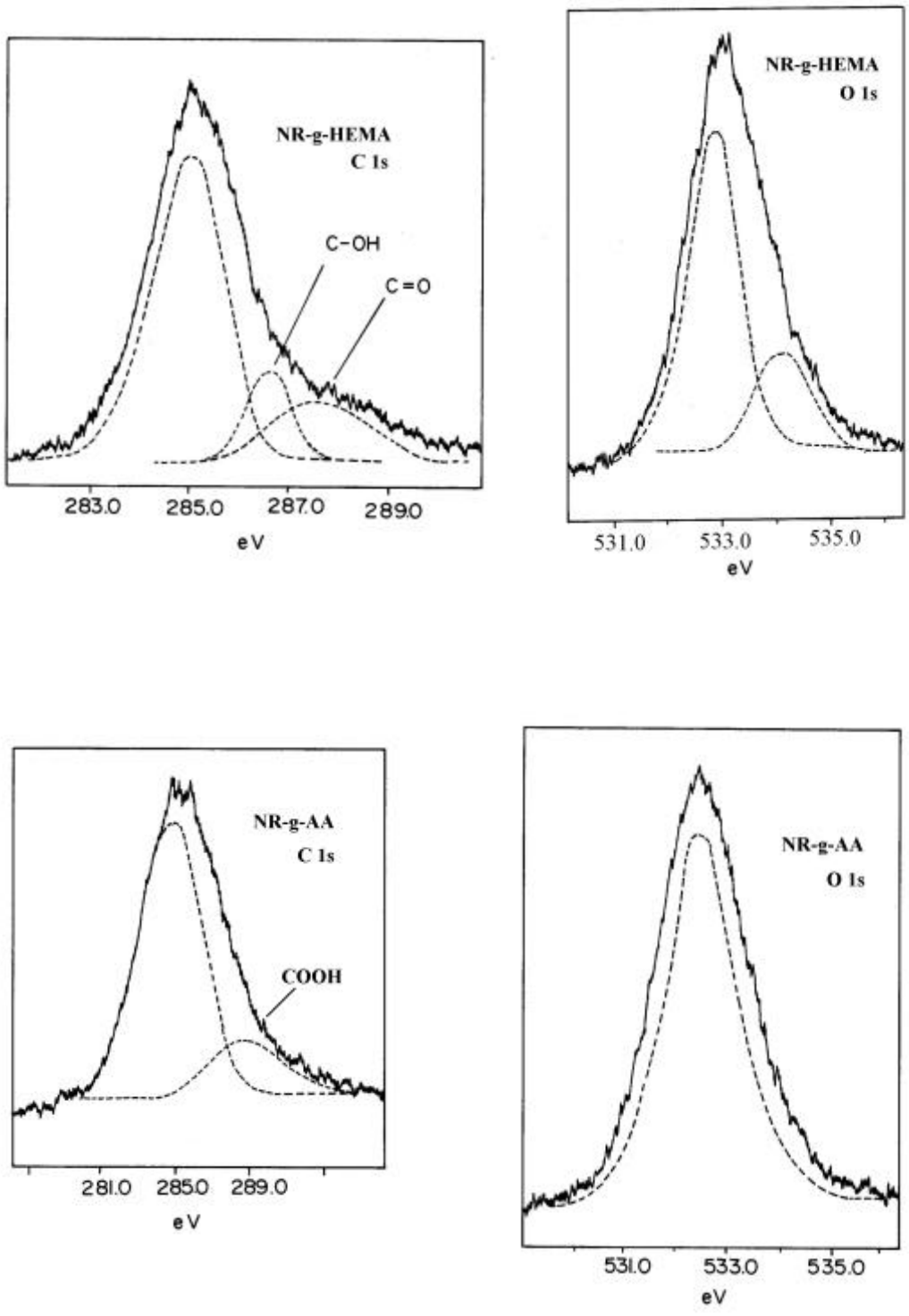

Figure 5.4 The surface roughness as seen in the SEM image of NR-g-HEMA.

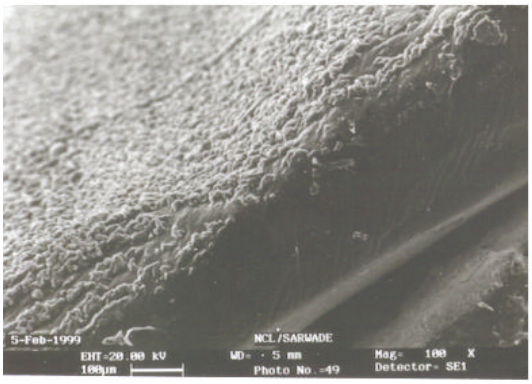

5.3.1.3.1 Effect of monomer concentration

The degree of grafting is significantly affected by the change in the monomer concentration in the reaction mixture as is evident from the **Figure 5.5**. For the two monomers studied viz. HEMA and AAm, the G_d increases sharply with the monomer concentration. For HEMA, which is a highly reactive monomer, the grafting yield reaches a maximum value at 1.25 M and then gradually levels off with a further increase in the monomer concentration for reaction carried out at 50 ºC. However, it was found that at higher monomer concentration a very high amount of homopolymer was formed in the reaction vessel. For AAm the G_d increases upto 2.0 M in the reaction medium and then gradually decreases. The higher limiting value of monomer concentration in this system is due to the comparatively lower reactivity of AAm.

Figure 5.5 Effect of monomer concentration on contact angle and G_d for NR-g-HEMA.

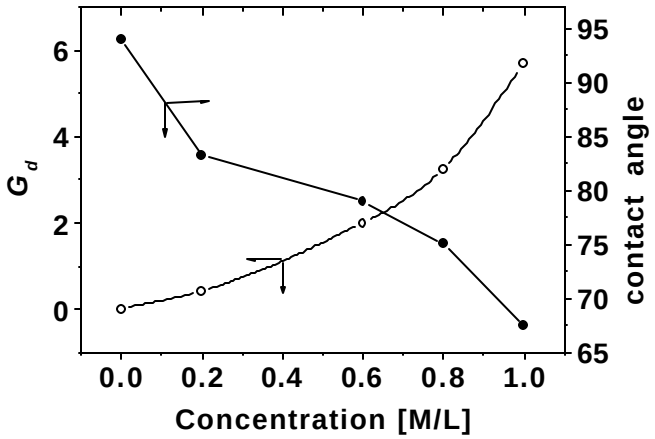

The reflectance ATR-FTIR spectra (**Figure 5.6**) of NR-g-HEMA clearly depict the intensity of the carbonyl groups of grafted *poly*HEMA chains as a function of monomer concentration. The intensity of the ester peak increased with monomer concentration indicating a rise in the density of the carbonyl groups on the film surface. The optical micrographs in the **Figure 5.7 (a)** and **(b)** reveal the dependence of grafted layer thickness on the monomer concentration.

Figure 5.6 Increase in the intensity of the ester peak with the HEMA concentration in the reaction mixture a) neat NR, b) 0.2 M, c) 0.6 M, d) 0.8 M and e) 1.0 M.

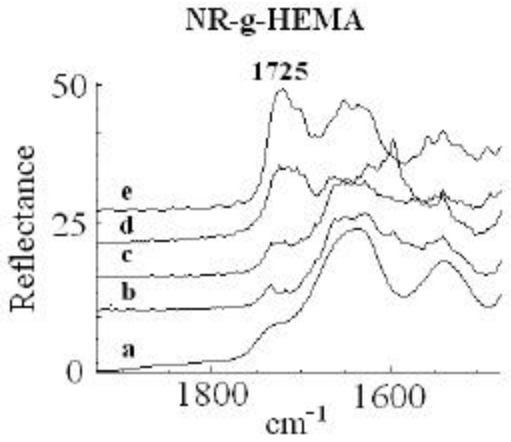

Figure 5.7 Optical micro-images of NR-g-HEMA: Effect of HEMA concentration in reaction medium.

(a) 1.0 M/L

(b) 1.25 M/L

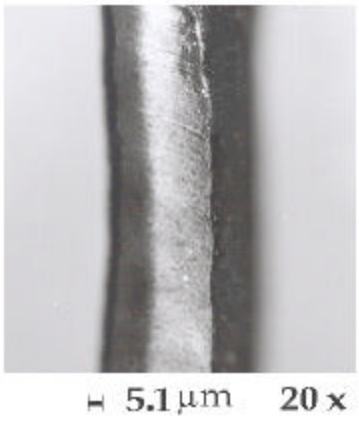

The decrease in the degree of grafting with the increase in the monomer concentration (> 1.5 M) is attributed to the reactions (**2**) and (**3**) shown in the scheme 5.1. The reaction (**2**) proceeds with a very slow rate due to the exceptionally high stability of tertiary free radicals. Moreover at high monomer concentration, the photoreduction of the photoinitiator readily takes places via H-abstraction from the monomer instead of the polymer surface due to the high density and close proximity of monomer molecules leading to a decrease in their efficiency. In addition to this, the growing homopolymer chains undergo rapid termination via radical coupling, leading to a decrease in the grafting efficiency. Also with the rapid homopolymer formation at high monomer concentration, the clarity of the reaction medium decreases, hindering the UV radiations reaching the photosensitizers, leading to a further decrease in the grafting yield [17].

5.3.1.3.2 Effect of solvent

In this study, the effect of three different solvents viz. methanol, acetone and water on the surface photo-grafting of HEMA onto the NR films has been examined. The effect of solvents on liquid phase grafting is widely studied for different polymers[18-20]. The efficiency of the solvents determined from the degree of grafting of HEMA onto the NR films is in the order: acetone > water > methanol. Acetone when used as a solvent acts as a sensitizer, which is capable of abstracting hydrogen atom from the polymer backbone/ monomer to form graft copolymer or homopolymer. Moreover, since acetone is stable against hydrogen abstraction by excited photoinitiator (e.g. BP^{*3}), BP^{*3} can abstract hydrogen only from the polymer backbone to yield graft copolymer. Thus, the accelerating effect of solvents is supposed to originate either from their photosensitizing capacity[21] or swelling the polymeric substrates[22,23] but in the case of acetone, the former one rules.

Methanol proved to be a poor solvent compared to acetone and water. The poor performance of methanol as a solvent is attributed to its high chain transfer constant, which is a very influencing factor in free radical graft copolymerization reactions. Methanol[24,25] has also been reported to negatively affect grafting of AAm and acrylonitrile onto PE and PP. In contrast to this, alcohols have been found to improve the grafting efficiency of functional monomers onto the cellulose. The explanation for this advantageous effect is the favorable interaction of the alcohols with the hydroxyl groups of the cellulose, where alcohols tend to swell the cellulose and accommodate the monomers in the proximity of the grafting site[26]. In case of NR, no such interaction with methanol occurs. On the other hand, methanol is a non-solvent for NR, so the possibility of the grafting due to swelling is also eliminated. Water

having a zero chain transfer constant[27] emerges to be a better solvent compared to methanol, although influence due to swelling does not play any role in this case.

5.3.1.3.3 Effect of photoinitiators

The effect of three different photoinitiators viz. benzophenone (BP), xanthone (XT), and hydrogen peroxide (H_2O_2) on the surface photo-grafting efficiency of HEMA was investigated. The photoirradiation of a pair of NR films (4 cm × 1.5 cm), in each photo-reactor was carried out in the presence of a photoinitiator, 1.0 M of HEMA, under inert reaction conditions for 1 hr at R.T. and 50 ± 2 ºC, according to procedure described in section 3.2.2.1.

The photo-reduction (or hydrogen abstraction) by organic ketones from a macromolecular hydrogen-donor under the influence of UV light forms the chemical basis of photoinitiation for free radical grafting polymerization. In early investigations, hydrogen peroxide has been used as a photoinitiator for free radical polymerization of acrylonitrile[28]. Hydrogen peroxide has a weak O-O linkage with about 34 kcal/mol bond energy and can readily undergo homolytic bond cleavage to yield hydroxy radicals[29]. Ample literature is available on the photoinitiated grafting systems, but with very few systematic studies involving their efficiency and relevant photochemistry[30,31]. The **Figure 5.8** shows that the efficiency of photoinitiators is in the order H_2O_2 > XT > BP for surface photo-grafting of HEMA. The influence of photoinitiator on the grafting efficiency can also be understood from the intensity of the functional groups in the ATR-FTIR spectra of the NR-g-HEMA. The grafting efficiency of HEMA for almost all the photoinitiators was found to be greater than that for AA, which is mainly dependent on the reactivity of the monomer. The effect of the monomer reactivity on grafting efficiency has been discussed in details in the Chapter 3.

The performance and the efficacy of the photoinitiators depend on four main factors **a**) stable molecular structure, **b**) stable ketyl radical, **c**) high triplet energy state and **d**) high UV absorption. The basic difference in the reactivity of XT & BP versus H_2O_2 lies in their behavior in the photo-grafting conditions. Broadly, it can be explained that upon UV irradiation, XT & BP act as *H-abstracting* photoinitiators whereas H_2O_2 acts as *fragmenting* photoinitiators. *Merz and Waters*[32] were the first to suggest that $^{\bullet}OH$ can be used to graft vinyl monomers onto polymer backbone. *Mishra*[26] suggested that the $^{\bullet}OH$ formed in the solution can abstract hydrogen atom from the polymeric backbone to leave sites on which grafting can occur. It is also known that H_2O_2 undergoes fragmentation via homolytic cleavage upon absorption of sufficient energy. The hydroxy free radicals so formed initiates all the three

reactions shown in **scheme 5.1**, simultaneously, out of which, the reaction (**3**) is incapable in bringing about any surface-grafting. From reaction **(1)** and **(2),** it is difficult to determine the predominant one. The highly reactive hydroxyl radicals generated up homolytic cleavage of H_2O_2 undergoes two reactions 1) allylic H-atom abstraction from the NR backbone to initiate graft copolymerization and 2) interaction with the monomer to generate growing homopolymer radical which can back attack the C=C of NR to yield a graft copolymer. This explanation is in accordance with the observation made by *Wilkie et al.*[33] and coworkers[34]. It has also been reported that hydrogen-abstracting photoinitiators[35,36] such as XT and BP are more effective compared to photo-fragmenting type initiator (H_2O_2). However, this is in contrast to our observations in the present system. H_2O_2 was found to yield very good surface grafting for reaction time ≤ 30 min at room temperature. We propose that the grafting, taking place using photo-fragmenting type initiators also depends on the reactivity of the monomer and mobility of homopolymer radical[37].

Xanthone was found to be a better grafting initiator than BP, the reason for which may be attributed to its stable rigid structure, which prevents the fragmentation reaction[38]. Moreover, the higher triplet state energy of XT (E_T = 74 kcal/mol) than BP (E_T = 69 kcal/mol) also contributes towards its better performance. It is also known that the higher the E_T, the lower is the energy barrier required for the hydrogen abstraction (C-H, E_d = 90 kcal/mol) and higher is the grafting efficacy. In addition to this, the extinction coefficient for XT is ($\varepsilon_{254} = 1 \times 10^4$ and $\varepsilon_{313} = 3 \times 10^3$) whereas that for BP is ($\varepsilon_{254} = 1.7 \times 10^4$ and ε_{313} = 50). Although, the extinction coefficient for BP is higher at λ = 254 nm, the reaction being carried out in a Pyrex reactor with cut off level at 290 nm, the efficiency of XT prevails.

Figure 5.8 Effect of photo-initiator on *WG* of NR-g-HEMA.

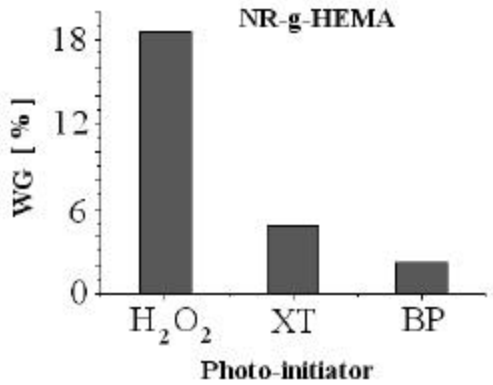

5.3.1.3.4 Effect of reaction temperature

The effect of reaction temperature on the surface photo-grafting efficiency of HEMA and AA, onto the NR films was also investigated. The photoirradiation of a pair of NR films (4 cm × 1.5 cm), in each photo-reactor was carried out in the presence of 0.2 M XT, acetone, 1.0 M of HEMA for 1 hr at R.T. and 50 ± 2 ºC, in the photo-grafting reactors described earlier. In another set of experiments, 0.25 % v/v H_2O_2 and water were used keeping rest of the parameters same.

The effect of reaction temperature on the G_d of the NR film is compiled in the **Table 5.1**. For BP the favourable effect of increasing the reaction temperature is obvious from the tabulated results but for H_2O_2 a very high amount of homopolymerization took place instead of grafting. An advantageous effect of elevated reaction temperature on the degree of grafting G_d was observed for all three monomers. This favorable effect of reaction temperature on the grafting efficiency is the unique feature of surface photo-grafting and is already explained using the scheme 3.6 in Chapter 3. As seen in the **Figure 5.9**, there are four main constituents of the free-radical photografting system: [1] polymer macro-radical, [2] radical on the grafted chain, [3] ketyl radical and [4] homopolymer radical. Out of these four species, [1] and [2] have high reactivity but low mobility/flexibility whereas [3] and [4] have low reactivity and high mobility. Moreover, since species [1] and [2] are responsible for the graft copolymerization, they show higher sensitivity towards the reaction temperature.

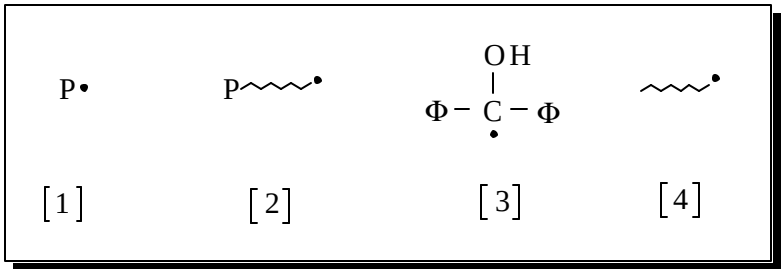

Figure 5.9

At room temperature, the mobility and flexibility of macromolecular free radical is much less compared to the semipinacol free radical and the homopolymer chain free-radical. By elevating the reaction temperature, the mobility of the macroradicals on the substrate backbone increases which in turn attacks the monomer in the reaction medium, leading to higher grafting yields[17]. It has also been observed that by varying the reaction temperature, one can effectively control thickness of the grafted layers.

Table 5.1 Effect of reaction time on the G_d of HEMA onto the NR films

Grafting time (min)	G_d *(mg/cm²)*			
	XT		H_2O_2	
	RT	**50 ± 2 °C**	**RT**	**50 ± 2 °C**
15	0.0	0.0	0.08	0.63
30	0.39	0.85	0.11	1.07
45	1.46	2.11	2.45	8.75
60	1.89	4.63	32.66	39.30
120	4.82	9.40	29.4	20.56

5.3.1.3.5 Effect of reaction time

The effect of reaction time on the surface photo-grafting efficiency of HEMA onto the NR films was also investigated in the present study. The photoirradiation of a pair of NR films in each photo-reactor was carried out in the presence of 0.2 M BP and 0.25 v/v H_2O_2 as photoinitiator, 1.0 M of HEMA, under inert reaction condition at R.T. and 50 ºC and R. T. respectively for different reaction times in the photo-grafting reactors described earlier.

As it is obvious from the **Table 5.1**, the G_d values increase with the reaction time upto a critical point, for reactions carried out with different photoinitiators at different temperatures. It is assumed that with the increase in the reaction time, the macroradicals on the surface of NR gets formed under the influence of radiation and triplet-excited state of photoinitiators. For BP, maximum grafting yield was observed for reaction time of 1.5 hrs beyond which the grafting yield remained constant, but homopolymerization increased. The increase in the homopolymerization is probably due to the chain transfer from the growing graft chain to the monomer. We also assume that after 1.5 hr of reaction, the factors like radical coupling, restricted mobility of growing chain, homopolymerization and light scattering become detrimental to the graft yield. But for reaction time less than 10 min, a very non-homogenous and localized grafting was observed. For H_2O_2 as a photoinitiator maximum grafting yield was obtained just within 45 min at room temperature. This high rate of grafting is attributed to the highly reactive hydroxy radicals[29]. For reaction time beyond one hour, very thick grafted layers were formed on the surface of NR films, which may be attributed to the secondary grafting initiated from the grafted chains anchored onto the

surface of NR films. The SEM images of NR-g-HEMA for different grafting time are shown in **Figure 5.10**.

Figure 5.10 Effect of grafting time on the morphology of the NR-g-HEMA films: **a)** 15 min, **b)** 60 min and **c)** 120 min.

(a) **(b)**

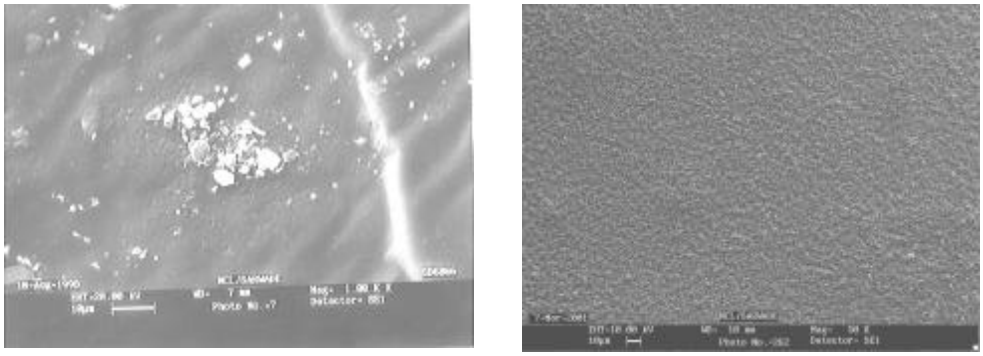

(c)

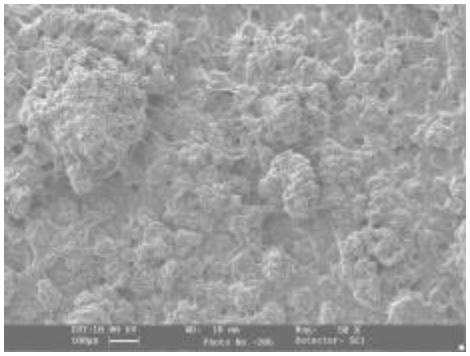

5.3.2 Plasma induced surface grafting onto NR films

The plasma induced anchoring of functional monomers onto the polymer surface is an effective tool to achieve tailor made surfaces. A significant amount of research has been undertaken, harnessing the versatilities of low temperature plasmas to graft functional monomers onto the surface of polymeric substrates[39,40]. Sufficient literature is now available on the surface modification of polymeric substrates facilitated by different types of plasmas[41]. Although, post plasma treatment grafting provides an effective solution to achieve homogenous grafting, the associated shortcomings like longer reaction time (12 to 48 hrs), elevated reaction temperature and use of solvent limits its applications[42]. Simultaneous vapor phase plasma-grafting with merits like short reaction time, ambient temperature, solvent free grafting, homogenous surface modification, form a better alternative to the post plasma-grafting technique[43]. The lack of sufficient literature on plasma-grafting onto NR encouraged

us to under take this research [44,45]. After the pioneering work of *Razzak et al.*[46] improving the blood compatibility of NR some more attempts have recently been made to develop natural rubber latex with functionalized surfaces[47,48].

5.3.2.1 Reaction mechanism

The reaction mechanism of simultaneous plasma-grafting is the same as described in *section 3.3.2.1* in Chapter 3. The NR films upon interaction with highly active species (electrons, ions, radicals etc) in the argon plasma, generates reactive centers (mainly free-radicals) on their surface. In the case of saturated polyolefins, hydrogen abstraction leads to radical formation whereas in case of unsaturated polymer C=C opens up, to render polymer surface with free-radicals[49]. When the monomer vapor is simultaneously introduced into the same chamber, the radicals generated on the surface of NR films ($P^{\bullet}$) readily react with the vinylic monomer ( ), leading to surface linked functional groups as shown in **scheme 5.2**.

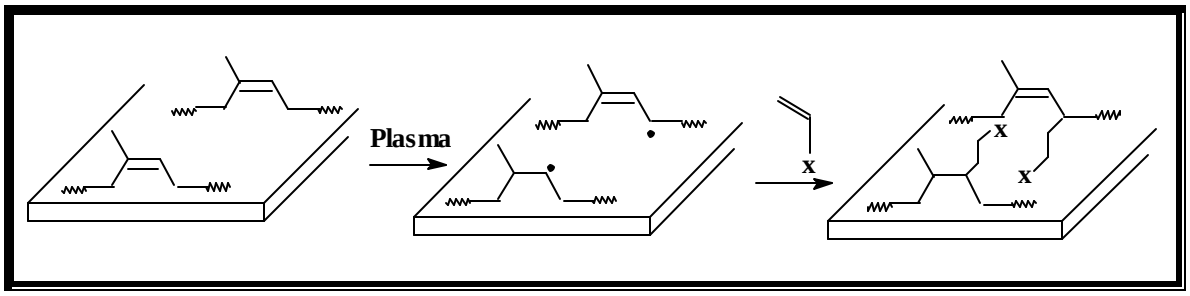

Scheme 5.2

5.3.2.2 Control experiment

In order to understand the effect of plasma treatment on the NR films, the pristine films were exposed to various plasma-grafting conditions (viz. treatment time, plasma power, post exposure time) in the absence of monomer vapor. Each of these films was then characterized by ATR-FTIR and contact angle measurements. Almost all the films showed the presence of small amount of carbonyl and hydroxyl species on their surface, depending upon the treatment conditions. The spectra obtained for each condition were then taken as reference when compared with the plasma-grafted samples.

5.3.2.3 Plasma-grafting of functional monomers

Plasma-grafting is a highly surface-selective technique to obtain tailored surfaces with desired functional groups. The modification achieved by this technique is confined to a depth of few microns without altering the bulk properties. Unlike the conventional post plasma-

grafting[50,51] which involves decomposition of primarily formed hydroperoxides in presence of monomer and solvent at elevated temperature, we have carried out simultaneous plasma-grafting by introducing monomer vapors alongwith a carrier gas in an inductively coupled plasma reactor at ambient reactor temperature, according to the detailed procedure disclosed in the ***section 3.2.1.2.2***. In the present study, three different monomers (HEMA, AA and allyl bromide) have been employed under variable plasma-grafting conditions. The plasma power was varied from (40 - 75 W) and grafting time (10 - 50 min) with and without post-treatment exposure to monomer vapors. All the plasma-grafting parameters were selected on the basis of optimized conditions reported in the literature[52,53]. The post treatment exposure time allowed all the monomers in the reaction chamber to react with the surface free-radicals. The plasma-grafted films were then sonicated in water, methanol and acetone and dried in vacuum oven before characterization.

The successful accomplishment of plasma-grafting is evident from the decrease in the water contact angle and the appearance of characteristic peaks of functional groups in the ATR-FTIR spectra. The ATR-FTIR spectra did not show any significant peaks of functional groups for grafting time ≤ 10 minutes and plasma power ≤ 50 W. Although, the contact angle measurements performed on these films showed an increase in the hydrophilicity as compared to the pristine films. This discrepancy is mainly because of the extremely thin grafted layer generated upon plasma-grafting for short reaction times, which are beyond the sensitivity of ATR-FTIR technique. It has also been reported that the membranes modified by vapor phase and simultaneous plasma-grafting, have many short chains on the surface, giving rise to a brush like structure[52].

XPS Analysis

The XPS analysis performed on the plasma grafted NR films showed C1s, O1s and Br 3d binding energies (eV) of corresponding functional monomers present on the film surface. Accordingly, C1s values of 285.0 (C-H), 288.8 (O-C=O), 286.4 (C-OH) and O1s values of 532.4 (C-O), 533.3 (O-C=O) for HEMA, C1s values of 289.2 (COOH) O1s values for AA, C1s values of 286.3 (C-Br), 286.6 (C-O) and Br3d value of 70.4 (C-Br) for allyl bromide were observed. **Figure 5.11** shows the peaks corresponding to the C-Br and Br 3d binding energies in the XPS spectra of NR-g-allyl bromide. In all the spectra recorded, there may be a contribution of the C1s from the alkoxy/peroxide groups generated by the termination of radicals by oxygen upon exposure to air after polymerization reaction but this effect is expected to be negligible compared to the total oxygen values.

Figure 5.11 XPS spectra of NR-g-allyl bromide by plasma-grafting.

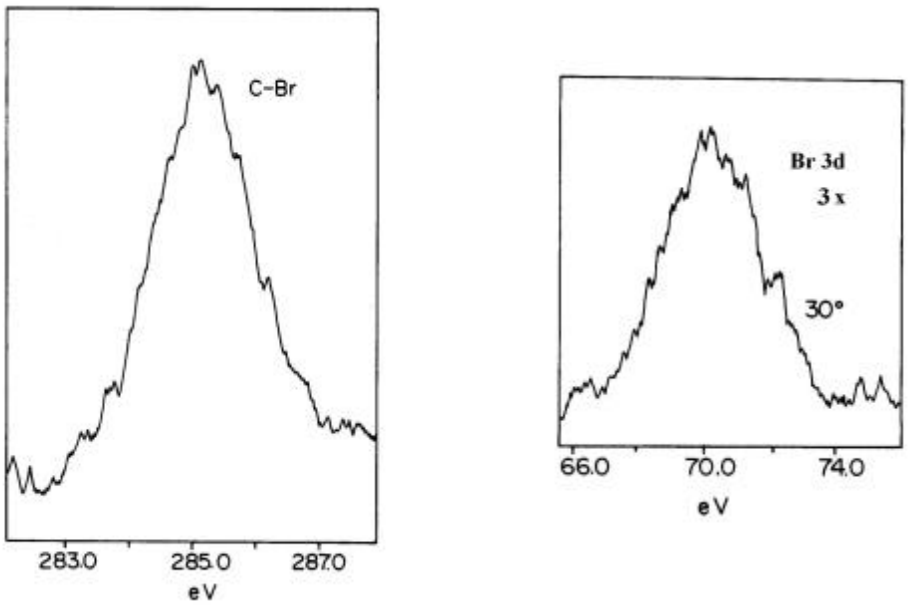

ATR-FTIR spectroscopy

The presence of respective functional groups of the plasma grafted monomers were substantiated by the characteristic peaks in the ATR-FTIR spectra with stretching vibrations at 1734 cm^{-1} (C=O) and 3440 cm^{-1} (O-H) for NR-g-HEMA, 1704 cm^{-1} (COOH) for NR-g-AA and 684 (C-Br) for NR-g-allyl bromide, which are obvious in the **Figure 5.12**. Moreover, it can be noticed from the **Figure 5.13** that the intensity of the peaks for respective functional groups in the ATR-FTIR spectra are higher at θ_i= 60° (d_p = 0.25 μm) than those at θ_i = 45° (d_p = 0.45 μm), indicating that density of the functional groups is more towards the surface and decreases with the sampling depth. The results of the depth profiling studies are in accordance with the XPS analysis performed at different grazing angles.

Figure 5.12 ATR-FTIR spectra of allyl bromide plasma-grafted onto NR film.

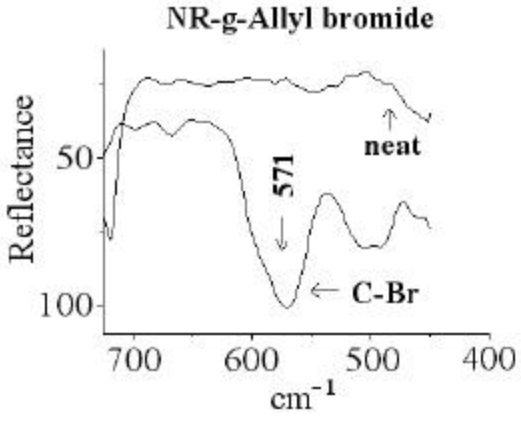

Figure 5.13 ATR-FTIR spectra of NR-g-HEMA taken at different incident angles.

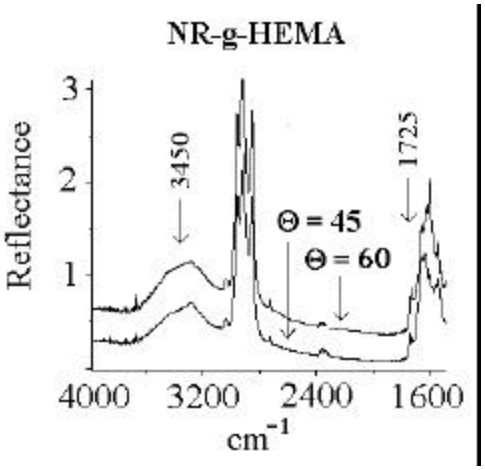

Morphology imaging by SEM and AFM analysis

The morphological investigation of the plasma-grafted films indicated a uniform grafting throughout the film surface. However, the surface roughness in all cases increased compared to the pristine NR films. **Figure 5.14** shows the SEM micrographs of the plasma grafted NR films. The AFM analysis also reaffirmed that the surface roughness is less in case of plasma grafted samples compared to the photo grafted (**Figure 5.15**). This is mainly due to the controlled grafting and absence of agglomerated homopolymer chains.

Figure 5.14 SEM image of HEMA plasma grafted onto NR film.

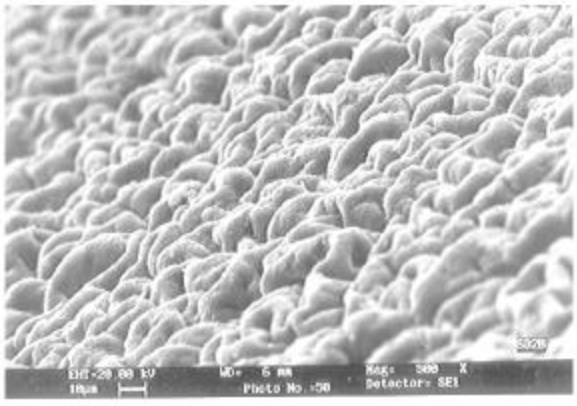

Figure 5.15 AFM images of **(a)** photo-grafted and **(b)** plasma-grafted NR films.

(a)

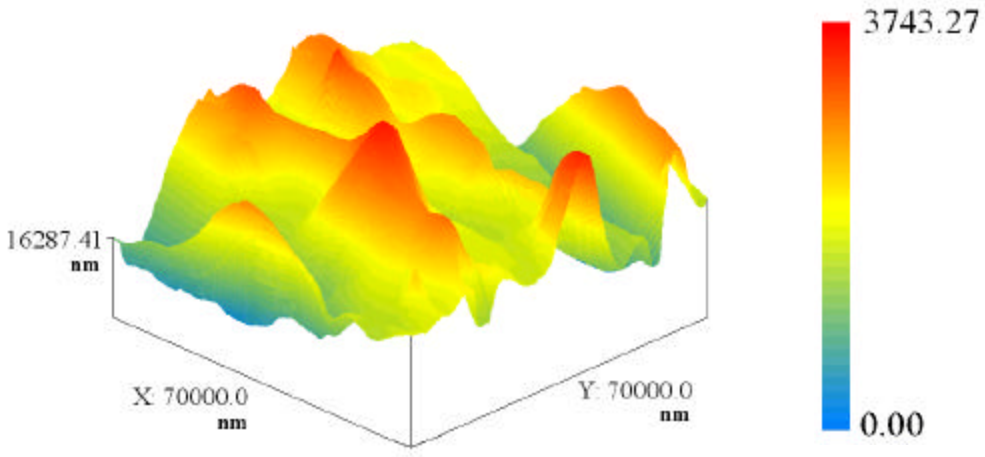

(b)

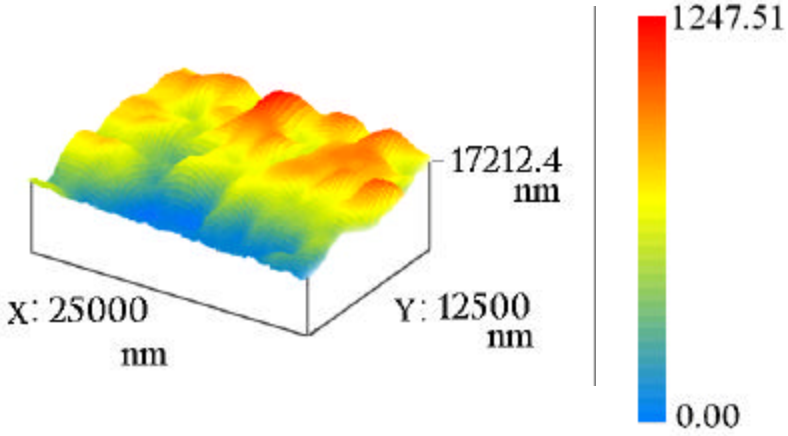

5.3.2.3.1 Effect of reaction parameters on surface grafting

The influence of plasma power and grafting time on the NR films is apparent from the ATR-FTIR spectra (**Figure 5.16**). NR being a highly amorphous polymer is susceptible to etching and surface cross-linking when irradiated at high plasma power for a longer time[54]. Hence, it is difficult to gravimetrically estimate the exact grafting yield as a function of treatment time and plasma power. However, a satisfactory amount of hydrophilicity is achieved for reactions carried out under mild conditions. An increase in the plasma power beyond 75 W and irradiation time over 20 min had some detrimental effect on the surface hydrophilicity. It was observed that for grafting attempted beyond 75 W led to a significant decrease in the C=C peak in the ATR-FTIR spectra, which suggests surface crosslinking. This was followed by an increase in the water contact angle, which is an additional indication of

the increased hydrophobicity. The generation of the cross-links is further supported by the gel formation upon dissolution of the treated NR in toluene. It is assumed that surface cross-linking hinders the diffusion and interaction of the monomers with the underlying free radicals. Moreover, the previously generated functional groups are possibly buried below the cross-linked network[55]. The favorable effect of post treatment exposure to the monomer vapors was established by the increase in the intensity of the characteristic peaks in the ATR-FTIR spectra, which is supported by the XPS analysis (**Figure 5.17**). It can be noticed that the intensity of the Br 3d peak is more for the sample with post grafting exposure time of 10 min, compared to the sample without any post exposure to the monomer vapors.

Figure 5. 16 ATR-FTIR spectra showing the effect of plasma power and grafting time.

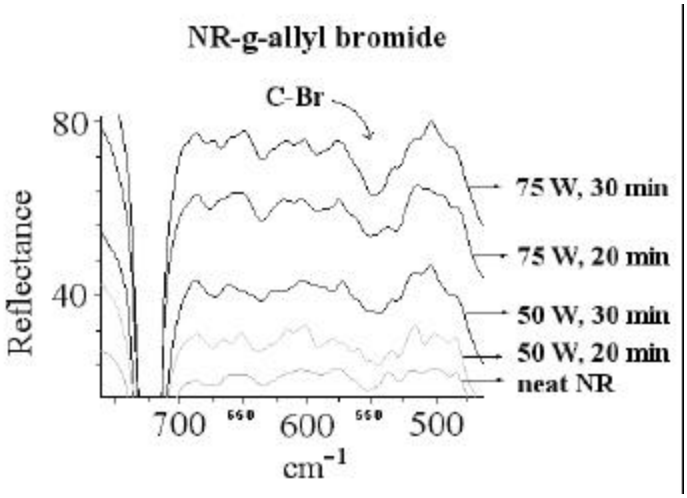

Figure 5.17 Effect of post plasma exposure time on grafting efficiency of NR-g-ally bromide.

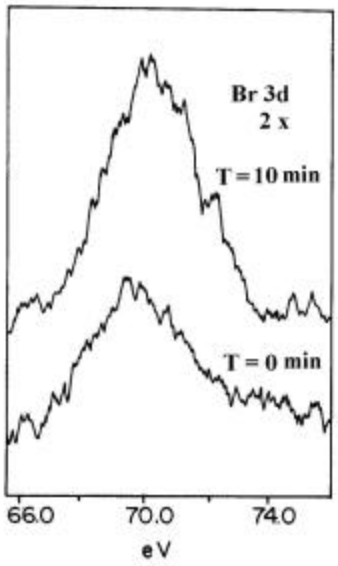

5.4 BIOCOMPATIBILITY STUDY OF SURFACE GRAFTED NR FILMS

The excellent flexibility and resistance against splitting of NR has attracted the attention for the development of biomaterials. The hydrophobicity of NR has limited its applications to surgical devices and medico-tubings. If the biocompatibility of NR is achieved it can find many more applications including blood transfusion tubes and implants. In the present study, we have tried to determine the biocompatibility of surface functionalized NR by *in vitro* cell adhesion test. From the biocompatibility test it was found that plasma and photo-grafted HEMA and AA gave better cell adhesion compared to the pristine NR films, however, plasma grafted films showed the highest efficiency. One possible reason is that, since the photografted samples gave thick grafted layers, the functional groups in the dehydrated state are assumed to be buried in the agglomerated grafts and require more time to reorient to the surface. Moreover, the interaction of the cells with the feebly functionalized interface leads to poor compatibility and thereby moderate cell adhesion. In contrast to this for plasma modified samples having thin grafted layers, the functional groups even if oriented towards the sub-surface reorient rapidly towards the surface in the culture media leading to better cell adhesion. Another possible explanation is that during the plasma treatment the surface of NR becomes crosslinked leading to hindered rotation of the functional groups towards the sub-surface and thus hydrophilicity of the modified surfaces is retained for a longer time favoring better cell adhesion. The cell adhesion and growth were monitored under optical microscope after 24 hrs and 48 hrs of incubation.

This substantially high biocompatibility is attributed to the uniform carpeting of *poly*HEMA chains on NR films (**Table 5.2**), which is again accredited to its higher grafting efficiency. The acrylic acid photo-grafted films exhibited better cell adhesion (number of cells adhered/cm^2) compared to plasma-grafted samples. The density of the cells adhered depends on the number of the freely available carboxylic acid groups, which is more in the case of photo-grafted films.

Table 5.2 Adhesion of KB cell lines on the surface of functionalized NR films after 48 hrs of incubation.

Grafting Technique	**Cell adhesion**[#]	
	HEMA	AA
Photo	★ •	★ +
Plasma	★ +	★ +

[#] ***Good*** ★ ***Average*** • ***Uniform*** +

5.5 CONCLUSIONS

The photo-grafting efficiency (*Ge*) of monomers observed here is in the order HEMA > AA > NVP. The surface of the grafted substrates examined by the SEM shows progressive roughness with the increase in the degree of grafting. A rise in the thickness of the grafted layer is also observed in the optical micrographs, which is attributed to the multi-layer formation arising from the grafted homopolymer chains. The ketonic photo-initiators, due to their hydrogen abstraction capacity proved to be better initiating species compared to the peroxy-initiators. Although, hydrogen peroxide gave very high grafting yield, the reaction being uncontrolled led to very thick grafted layers, undesirable for biocompatibility. The degree of photo-grafting increases linearly with the reaction time and temperature and gradually falls beyond a certain limit due to unfavorable reactions like chain transfer, radical coupling and homopolymerization. The plasma grafting efficiency mainly depends on the reaction time, whereas the rate of grafting depends on the plasma power. For reaction time less than 10 minutes, grafting is very less. The plasma grafting generated thin grafted layers with functional groups available at the interface. The plasma-grafted samples exhibited better cell adhesion/ growth compared to the photo grafted ones. Thus, cell growth/adhesion depends on the uniformity of grafting and density of functional groups. In other words, hydrophilicity of the polymer surface plays a major role in determining the biocompatibility of the substrate.

5.6 REFERENCES

1. D. H. Carey and G. S. Ferguson, *Macromolecules*, **27**, 7254 (1994),
2. H. Mirzadeh, A. A. Katbab, M. T. Khorasani, R. P. Burford, E. Gorgin and A. Golestani, *Biomaterials*, **16**, 641 (1995).
3. D. J. Lamb, J. F. Anstey, C. M. Fellows, M. J. Monteiro, R. G. Gilbert, *Biomacromolecules*, **2**, 518, (2001).
4. M. T. Razzak, K. Otsuhata, Y. Tabata, F. Ohashi and A. Takeuchi, J. Appl. Polym. Sci., **36**, 645 (1988).
5. W. Arayapranee, P. Prasassarakich and G.L.Rempel *J. Appl. Polym. Sci*., **83**, 2993 (2002).
6. D. Y. Lee, N. Subramaniam, C. M. Fellows and R. G. Gilbert, *Journal of Polymer Science, Part A: Polymer Chemistry*, **40**, 809, (2002).
7. S. H. O. Egboh and M. O. Fagbule, *Radiat. Phys. Chem.*, **24**, 1041 (1988)
8. N. M. Claramma, N. M. Methew and E. V. Thomas, *Radiat. Phys. Chem*., **33**, 87 (1989).
9. R. Yoda, *J. Biomater. Sci. - Polym. Ed.*, **9**, 561 (1998),
10. M. T. Razzak, K. Otsuhata, Y. Tabata, F. Ohashi and A. Takeuchi, *J. Appl. Polym. Sci*., **38**, 829 (1989)
11. N. V. Kislinovskaja, I. D. Khodzhaeva, S. P. Novikova and N. B. Dobrova, *Int. J. Polym. Mater*., **17**, 131 (1992).
12. V. Haddadi-ASL, R. P. Burford and J. L. Garnett, *Radiat. Phys. Chem*., **45**, 191 (1995).
13. A. A. Katbab, R. P. Burford and J. L. Garnett, *Radiat. Phys. Chem.*, **39**, 293 (1992).
14. S. Edge, S Walker, W. J. Feast and W. F. Pacynko, *J. Appl. Polym. Sci*., **47**, 1075 (1993).
15. W. Yang and Ranby, *J. Appl. Polym. Sci*., **62**, 533 (1996)
16. N. J. Huang and D. C. Sundberg, *J. Polym. Sci. Part A, Polym. Chem*., **33**, 2587 (1996).
17. W. Yang and Ranby, *J. Appl. Polym. Sci*., **62**, 545 (1996)
18. G. Odian, M. Sobel. A. Rossi and R. Klein, *J. Polym. Sci*., **55**, 663 (1961).
19. P. J. Burchill, D. M. Pinkerton and R. H. Stacewicz, *J. Macromol. Sci. Chem*., A **14**, 79 (1980).

20. I. K. Mehta, D. S. Sood and B. N. Mishra, *J. Polym. Sci., Part A: Polym. Chem*., **27**, 53 (1989).
21. K. Allmer, A. Hult, B. Rånby, , *J. Polym. Sci. Polym. Chem. Educ.*, **26**, 2099 (1988).
22. H. Kubota, Y. Ogiwara, *J. Appl. Polym. Sci*., **38**, 717 (1989).
23. M. T. Razzak, K. Otsuhata, *J. Appl. Polym. Sci.*, **36**, 645 (1988).
24. S. Tazuke and H. Kimura, *J. Polym. Sci., Polym. Lett. Ed*., **16**, 497 (1978).
25. I. K. Mehta, S. Kumar, S. G. Chanman and B. N. Mishra, *J. Appl. Polym. Sci*., **41**, 1171 (1990).
26. M.K Mishra, J. M. S. – Rev. Macromol. Chem. Phys. C **22**, 471 (1983)
27. V. Stannett, *Radiat. Phys. Chem*., **18**, 215 (1981).
28. H. Miyama, N. Harumiya and A. Takeda, *J. Polym. Sci., Polym. Chem. Ed.*, **16**, 943 (1972).
29. M. K. Mishra and Y. Yagchi, Handbook of Radical Vinyl Polymerization, Marcel Dekker Inc., New York, (1998).
30. W. Yang and B. Ranby, *J Appl Polym Sci.*, **62**, 545 (1996).
31. C. Walling and M. J. Gibian, *J. Am. Chem. Soc*., **87**, 3413 (1965).
32. J. H. Merz and W. A. Waters, *J. Chem. Soc*., **5**, 15 (1949).
33. D. D. Jiang and C. A. Wilkie, *Eur. Polym. J*., **34**, 997 (1998).
34. R. B. Seymour and C. E. J. Carraher, Polymer Chemistry, 3rd Edition, Dekker, NY, p 324 (1992).
35. G. S. Hammond, W. P. Baker and W. M. Moore, *J. Am. Chem. Soc*., **83**, 2795 (1961).
36. N. J. Turro, *Modern Molecular Photochemistry*, Benjamin/Cummings, Menlo Park, CA, p. 261 (1987).
37. N. J. Hung and D. C. Sundberg, *J. Polym. Sci, Part A; Polym. Chem*. **33**, 2533, 2551, 2571 and 2587 (1995).
38. W. Yang and B. Ranby, *Eur. Polym. J*., **35**, 1557 (1999).
39. T. Hirotsu, *Adv. Low-Temp. Plasma Chem. Technol. Appl*., **3**, 9 (1991).
40. K. Johnsen, S. Kirkhorn, K. Olafsen, K Redford, A. Stori, *J. Appl. Polym. Sci*., **59**, 1651 (1996).
41. C. M. Chan, *Surface Modification and Characterization of Polymers*, Hanser Publishers (1994).
42. M. R. Yang and K. S. Chen, *Mater. Chem. Phy*., **50**, 11 (1997).

43. I. Gancarz, G. Pozniak, M. Bryjak and A. Frankiewicz, *Acta Polym*., **50**, 317 (1999).
44. M. Yan, *Reactive and Functional Polymers*, **45**, 137 (2000).
45. N. V. Kislinovskaja, I. D. Khodzhaeva and S. P. Dobrova, *Int. J. Polym. Mater*., **17**, 131 (1992).
46. M. T. Razzak, K. Otsuhata, Y. Tabata, F. Ohashi and A. Takeuchi, *J. Appl. Polym. Sci.,* **38**, 829 (1989).
47. P. Wang, K. L. Tan, C. C. Ho, M. C. Khew and E. T. Kang, *Eur. Polym. J*., **36**, 1323 (2000).
48. S. H. Y. Cheo, P. Wang, K. L. Tan, C. C. Ho, E. T. Kang, *J. Mater. Sci.: Mater. Med.*, **12**, 377 (2001).
49. N. J. Huang and D. C. Sudenberg, *J. Polym. Sci., Part A: Polym. Chem.,* **33**, 2587, (1995).
50. M. Yan, *Reactive and Functional Polymers* **45**, 137 (2000).
51. K. Kildal, K. Olafsen and A. Stori, *J. Appl. Polym. Sci*., **44**, 1893 (1992).
52. K Olafsen, A. Stori and D. A. Tellefsen, *J. Appl. Polym. Sci.*, **46**, 1673 (1992).
53. N. Inagaki, Plasma Surface Modification and Plasma Polymerization, Technomic Publishing Co. Inc., Lancaster, Basel., p.78 (1996).
54. N. Inagaki, Plasma Surface Modification and Plasma Polymerization, Technomic Publishing Co. Inc., Lancaster, Basel., p.89 (1996).
55. A. Charlesby, Atomic Radiation and Polymers, Chapter 28, p 412, Pergamon Press, New York (1960).

CHAPTER VI

SURFACE MODIFICATION OF SILICON RUBBER AND STYRENE BUTADIENE STYRENE FILMS

6 .1 INTRODUCTION

In the recent years, elastomers have spun major interest in different specialty applications. Amongst the existing elastomers, silicone rubber and styrene butadiene styrene have a well-defined backbone structure. While the backbone network is responsible for the bulk properties, in many applications, the elastomer surfaces need to be modified in order to achieve desirable surface energy or functionality. Tailoring a polymer with properties different at its surface and in the bulk, is nowadays one of the most important areas of research in polymer chemistry. Amongst the different surface modification techniques[1] plasma treatment employing reactive gases is the most controlled means of achieving desired interfaces. Plasma treatment can bring about surface modification of polymers by three different methods: a) functional group implantation, b) simultaneous grafting and c) post-treatment grafting. In the implantation process, hydrogen atoms are first abstracted from the polymer chains to generate radicals within the polymer chains located at the surface. Some of these carbon radicals in the polymer chain combine with the radicals formed in the plasma to form functionalities of the respective gas. The other carbon radicals, when exposed to the air, form oxidized species on the surface[2]. The formation of the functional groups as a result of plasma treatment is restricted to a depth of few hundred nanometers on the polymer surface[3]. It is well known that functionalities generated on the polymer surface as a result of plasma implantation are temporary and are lost with time irrespective of the T_g of the polymer[4]. *Urban et al.*[5] has proved from their study that the assumption that surface cross-linking increases with plasma treatment is not always true. This behavior of polymer surfaces treated with the reactive plasmas is studied over here.

In comparison to thermoplastics, there are only few references disclosing the systematic study on the surface modification of elastomers[6-8], except for silicone rubber. In the past few years efforts have been made to modify the surface of SEBS, SBS and SR by grafting techniques[9,10]. Amongst these, the most widely studied technique is the surface photografting[11,12]. A few attempts have also been made to improve the surface properties via plasma immersion ion implantation technique[13]. Breaking the monopoly of thermoplastics, researchers are now switching over to explore the biocompatibility of unattended conventional elastomers[14-16]. During the biocompatibility test performed in the recent past, some misconceptions about the biocompatibility of a material has been exposed. In one such study *Lee et al.*[9] found that excessive grafting leads to a decrease in the corneal epithelial cell adhesion. They found that surface of SR films grafted with 150 $\mu gm/cm^2$ *poly*HEMA gave

better cell adhesion compared to 1650 $\mu gm/cm^2$ for reasons not mentioned. The modification of elastomeric surface is thus undertaken with a view of improving their biocompatibility and examining their performance under *in vitro* conditions. In the present study, two reactive gases viz. oxygen and carbon dioxide are used to obtain functional hydrophilic surface of SR and SBS films. The effect of reaction parameters is carefully examined. Moreover, the functional monomers viz. HEMA, AA and NVP are also plasma grafted onto the surface of these films. All these samples are analyzed using surface sensitive techniques like contact angle measurement, XPS and ATR-FTIR spectroscopy. The causes of the hydrophobic recovery have also been revealed.

6.2 MATERIALS AND METHODS

6.2.1 Materials

All the monomers viz. 2-hydroxyethyl methacrylate (HEMA), acrylic acid (AA) and N-vinyl pyrrolidone (NVP) procured from M/s Aldrich, USA, were used after purification. The argon, nitrogen, carbon dioxide and oxygen gases (Grade I) supplied by M/s Inox Ltd., Thane, India, were used for the plasma-treatment reactions. The silicone rubber was received by the courtesy of GE Silicones, India, which contains 21% fumed silica filler and linear PDMS into the vinyl terminated PDMS. The styrene butadiene styrene terpolymer was obtained from Shell Ltd., USA and ATV-prene, India. The butadiene : styrene content in Shell sample was (81:19) and in ATV-prene was (77: 23).

6.2.1.1 Preparation of elastomer films

SR film preparation

A 3.3 % w/v homogenous solution of silicone rubber was prepared in chloroform. To this solution 0.15 % w/v benzoyl peroxide was added as a cross-linking agent. A 25 ml of this homogenized solution as carefully poured in a petri dish (10 cm diameter). The solvent was evaporated naturally at room temperature. The films were then cured in a vacuum oven for 3 - 4 hrs at 90 - 100 °C. The films thus obtained were thoroughly washed with methanol to remove impurities and decomposed BPO. The thickness of films obtained was approximately 125 microns.

SBS film preparation

A homogenous solution of 2.5 % w/v SBS was prepared in dichloromethane. 25 ml of this solution was carefully poured in a petri dish (8 cm diameter). The solvent was evaporated naturally at R.T. to obtain thin films of SBS. These films were then dried in

vacuum oven at 45 °C to remove any trapped solvent. The thickness of the films was approximately 150 microns.

6.2.1.2 Reactor

The details of the plasma grafting and plasma treatment reactor are given in the Chapter 4, *section 4.2.1.2*.

6.2.2 Experimental methods

The surface modification of the SR and SBS films was accomplished by two methods a) plasma treatment and b) plasma grafting. The details of which are given in *section 4.2.2.*

6.2.3 Characterization methods

The surface modified elastomer films were characterized mainly by contact angle goniometer, ATR-FTIR and XPS techniques. The details of all these techniques are given in *section 4.2.3.* The contact angle measurements are an average of seven measurements taken at different places on the treated sample.

6.2.4 Biocompatibility test

The biocompatibility of the modified and pristine SR and SBS films was tested by method mentioned in *section 4.2.4*.

6.3 RESULTS AND DISCUSSION

6.3.1 Functional group implantation using O_2 and CO_2 plasma

The plasma treatment of the SR and SBS films generated highly hydrophilic surfaces, as expected. Interestingly, the hydrophilicity achieved on both these films was better than that obtained for EPDM films. The static water contact angle measurements taken by the sessile drop method for the oxygen and carbon dioxide plasma treated SR and SBS films are aggregated in the **Table 6.1** and **6.2**. From the table, it can be noticed that just 60 secs of oxygen plasma treatment of both the films generated highly hydrophilic surfaces. For the carbon dioxide plasma treated films, the hydrophilicity initial attained was slightly less compared to the oxygen plasma treated films. The composition of the polymer backbone also plays a vital role in determining the surface properties. It was observed that the ATV-prene samples produced higher hydrophilicity compared to the SHELL samples. This indicates that the unsaturation at the polymer surface is one of the major influencing factors. The contact angle results are very well supported by the XPS analysis, which shows a significant increase

in the C-O and C=O species on the surface of the plasma treated films. **Figures 6.1** and **6.2** show the XPS spectra of the plasma treated SR and SBS films. The asymmetry in the spectra corresponds to the C1s peaks at 286.5, 287.7 & 289.2 eV. However, for small treatment time at low plasma power the ATR-FTIR spectra in the **Figure 6.3** did not show any significant change in the surface functionality. This is due to the lack of sensitivity of this technique to identify functionalities present at the interface[17]. This further reaffirms that only the interface of the polymer is modified during the plasma treatment under controlled conditions.

Figure 6.1 XPS spectra of CO_2 and O_2 plasma treated SBS films.

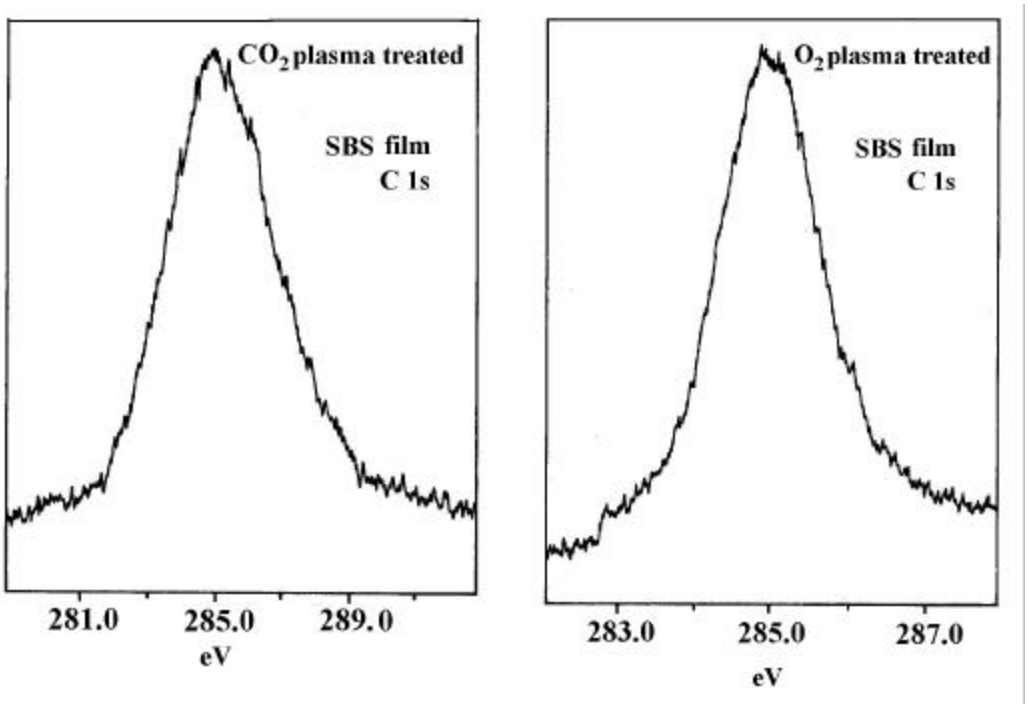

Figure 6.2 XPS spectra of O_2 plasma treated SR films.

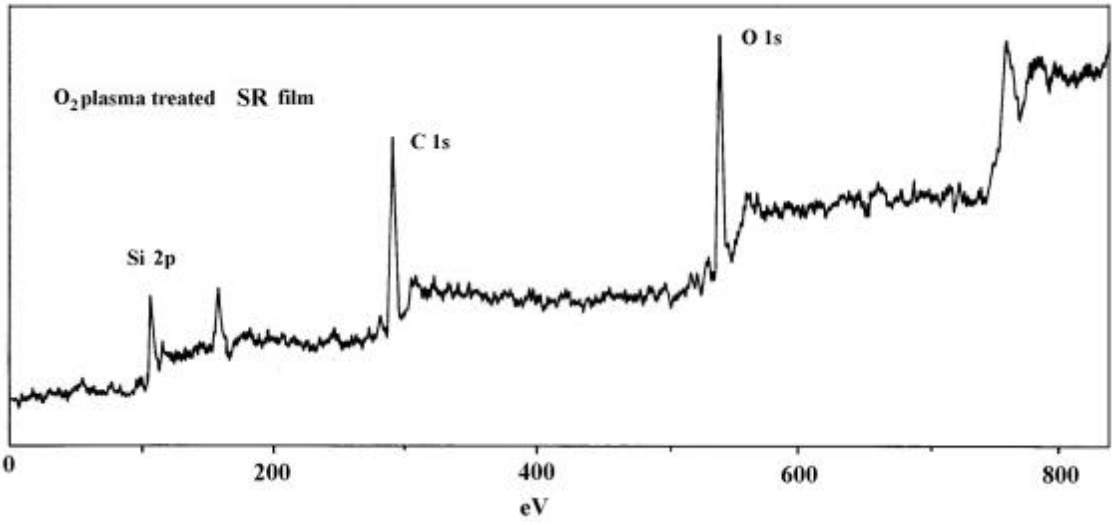

Table 6.1 Oxygen plasma treatment of elastomer films for 60 seconds.

Plasma power	**Water contact angle** (°)		
	SR	**SBS**	**EPDM**
50 W	28.0	48.4	62.6
75 W	22.2	42.4	56.5

Table 6.2 Carbon dioxide plasma treatment of elastomer films for 60 seconds.

Plasma power	**Water contact angle** (°)		
	SR	**SBS**	**EPDM**
50 W	37.6	57.0	57.6
75 W	32.2	42.0	58.1

Figure 6.3 ATR-FTIR spectra of O_2 plasma treated SR and SBS films.

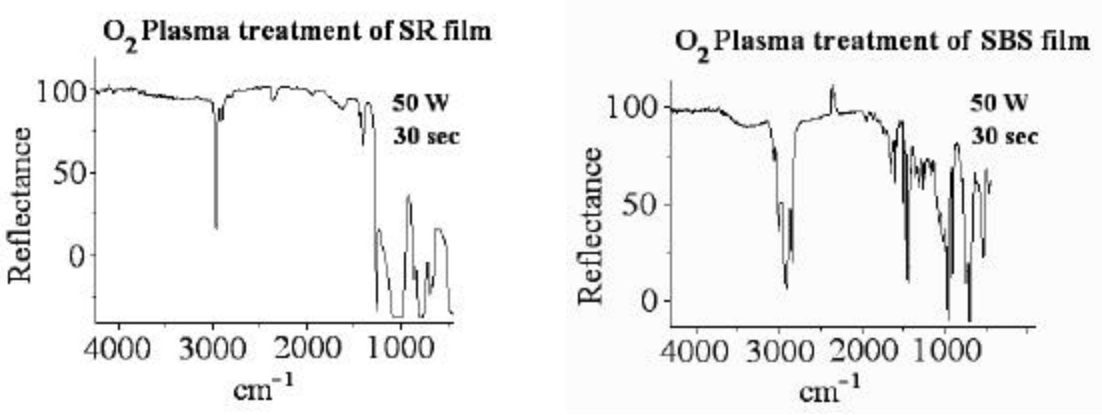

6.3.1.1 Effect of plasma power and irradiation time

The water contact angle measurements of SR and SBS films treated with oxygen and carbon dioxide plasma are compiled in the **Table 6.3** and **6.4,** respectively. From the table, it is obvious that the SR films undergo excellent hydrophilization amongst all the samples treated under the identical conditions. Moreover, the surface hydrophilization of silicone rubber requires a very little time. The plasma treatment conditions i.e. 75 W and 150 sec gives the best hydrophilicity for oxygen plasma treatment. It is also observed that hydrophilicity increases with the treatment time and then falls for irradiation time longer than 150 seconds. It is believed that the process of degradation dominates once the sample is continuously irradiated for a longer time. *Yasuda et al.*[18] has shown that SR being less susceptible to weight loss degradation favors the formation of non-volatile oligomers upon O_2 plasma treatment.

From the table it can also be understood that irradiation time has a more detrimental effect than the plasma power, for, treatments with high plasma power with short irradiation time gave better hydrophilicity than the treatments with low plasma power for long irradiation times. Thus, a combination of plasma power and treatment time should be optimized in order to achieve exceptional hydrophilicity of the treated surfaces. The carbon dioxide plasma treated SR films also show a fairly good surface hydrophilicity. The best hydrophilicity is achieved for the 50 W and 150 secs. *Urban et al.*[5] has reported that continuous irradiation of silicone rubber films at higher plasma power, causes the delinking of the reinforced silica and aggregation of the silica fillers towards the surface.

Table 6.3 Effect of O_2 plasma treatment parameters on the hydrophilicity of the films.

Irradiation time (sec)	**Water contact angle** (°)					
	SR			**SBS**		
	50 W	**75 W**	**100 W**	**50 W**	**75 W**	**100 W**
30	40.6	27.1	23.3	53.6	46.0	38.5
60	28.0	22.5	19.0	48.4	42.4	27.2
150	21.2	13.5	21.4	46.8	23.6	18.3
600	40.5	24.0	29.1	51.4	52.8	62.1

The formation of short segments of silicone elastomer as a result of chain scission has also been mentioned in the same report. These segments also undergo oxidation during the treatment and are said to form a layer of approximately 10 microns over the sample surface. This is the reason why the longer plasma treatment time reveals functional groups in the ATR-FTIR spectra shown in the **Figure 6.4**. It is evident from the Table 6.3 that the SBS films upon plasma treatment show a relatively slow hydrophilization but the hydrophobic recovery is quicker compared to the SR films. The possible reason for this behavior is the higher surface cross-linking. Moreover, the degradation in SBS leads to either volatile products or dangling hydrocarbon chains unlike in SR. It is reported by *Morra et al.*[4] that polystyrene upon plasma treatment undergoes cross-linking and reduces the efficiency of the hydrophobic recovery. This is in contrast to our observation. But it is believed that the cross-linking hinders the orientation phenomenon and restricts the free-movement of either of the groups.

Figure 6.4 ATR-FTIR spectra of O_2 plasma treated SR and SBS films.

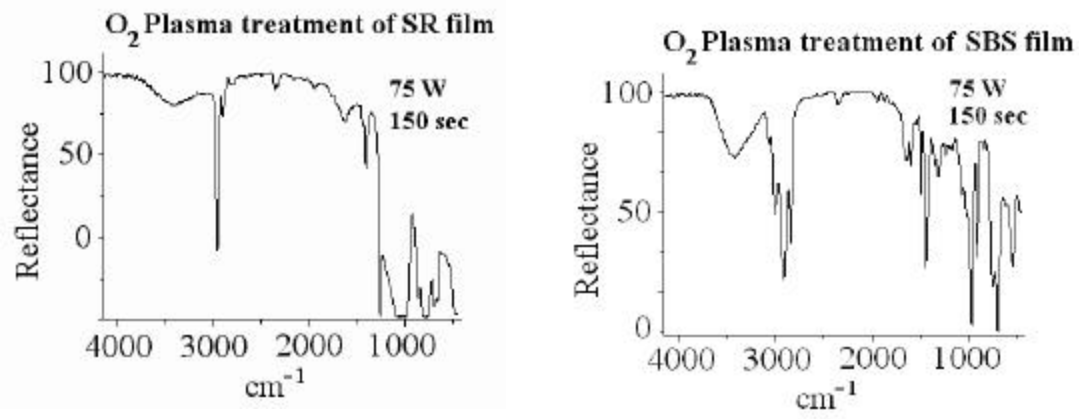

Table 6.4 Effect of CO_2 plasma treatment parameters on the hydrophilicity of the films

Irradiation time (sec)	**Water contact angle** (°)					
	SR			**SBS**		
	50 W	**75 W**	**100 W**	**50 W**	**75 W**	**100 W**
60	37.6	32.2	26.0	57.0	42.0	34.6
150	18.0	43.3	28.6	40.3	30.7	28.2
600	18.1	30.3	33.0	41.3	37.5	38.9

6.3.1.2 Effect of post-treatment exposure to the system gas

The effect of post-exposure of the treated elastomer films to the system gas is studied for different exposure time. It was assumed that during the plasma treatment, all the radicals generated on the polymer surface do not react immediately with the reactive species in the plasma. If the samples are exposed to the atmosphere immediately after plasma treatment, the radicals present on the surface react with the components of air to give rise to undesired functionalities[19]. In order to avoid these undesired reactions the films were maintained in the system gas for different times to access the effect of post exposure on the surface functionality. The contact angle measurements and XPS analysis substantiates our assumption of enhanced functionality upon post exposure to the system gas. It was observed that post exposure of 10 min is sufficient to allow all the surface free-radicals to react with the system gas. A further exposure time did not bring about any significant increase in the surface functionality or hydrophilicity. The increase in the intensity of the carbonyl species in XPS

spectra upon post exposure of the plasma treated films to the system gas, clearly supports our assumption. This effect of post exposure is revealed in the **Figure 6.5**.

Figure 6.5 The XPS spectra of SR films treated with CO_2 gas plasma showing: effect of post exposure time on the surface functionality.

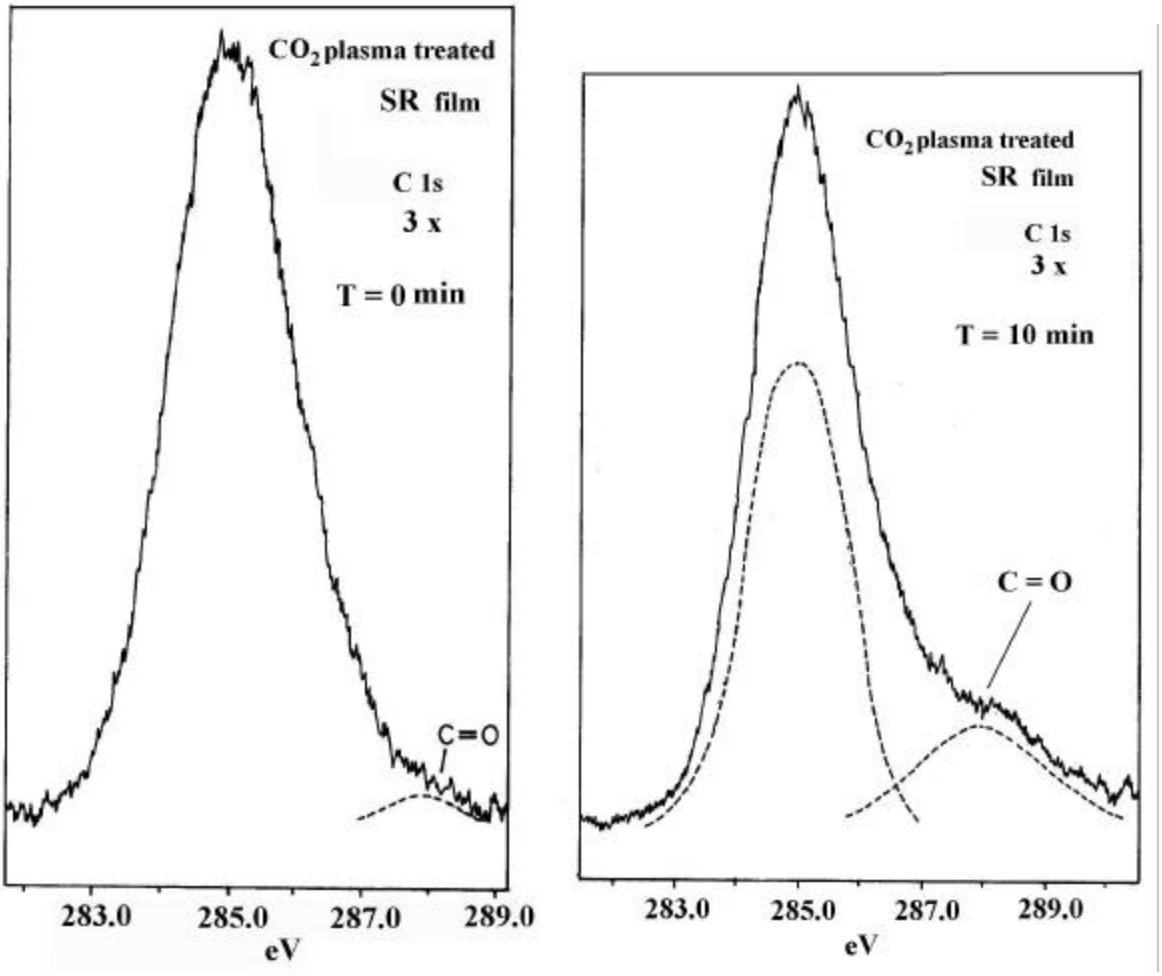

6.3.2 Plasma-grafting onto SR and SBS films

Now it is established that the surfaces modified by plasma treatment gradually lose the gained hydrophilicity with the storage time. Although, this loss is not permanent, the hydrophilicity diminishes with time as observed in different polymers[20]. The phenomenon of hydrophobic recovery is swift and reversible in the case of elastomers as compared to that in thermoplastics. Moreover, the plasma treatment generates only a small variety of functional groups on the treated surfaces, most of them are either hydroxy or carbonyl derivatives[21]. It is, therefore, necessary to graft selective functional monomers to achieve desired functionalities on the polymer surface. **Figures 6.6** and **6.7** show the ATR-FTIR spectra of HEMA and

NVP grafted onto the surface of SR and SBS films, respectively. The characteristic peaks of hydroxyl (3450 cm^{-1}), ester (1725 cm^{-1}) and tert-amide (1670 cm^{-1}) are evident in the spectra.

Figure 6.6 and **6.7** Plasma grafted SR and SBS films

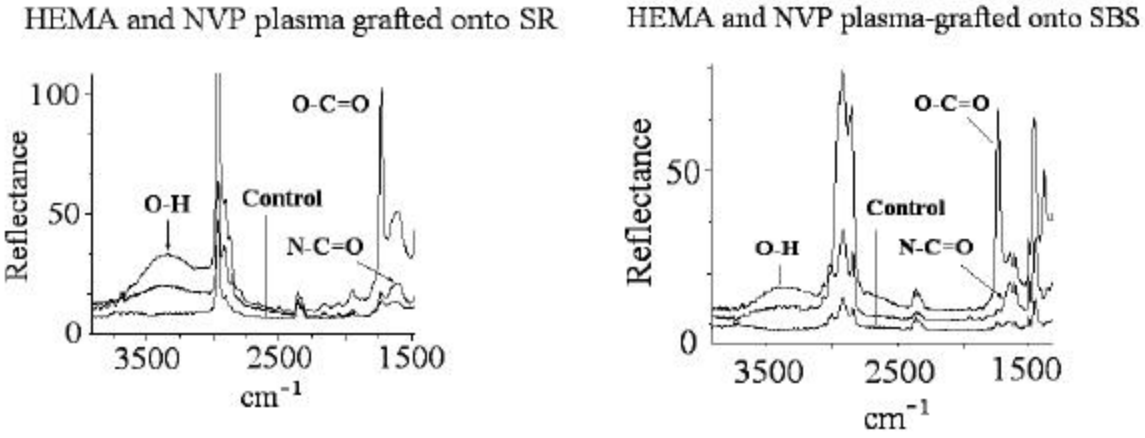

6.3.2.1 Effect of plasma power and grafting time

A linear rise in the surface functionality and hydrophilicity with an increase in the plasma power and plasma treatment time is evident from the **Table 6.3** and **6.4**. The hydrophilicity and functionality levels off above treatment at 75 W for 30 min. It is assumed that beyond this treatment, the phenomena like cross-linking, chain scission and etching of the grafted layers become very prominent. As a result, there is no further improvement in the surface properties. Upon comparison of the water contact angle with the plasma grafted EPDM, it can be noticed that the hydrophilicity achieved in the case of SBS is faster than that achieved for EPDM under similar conditions. This is attributed to the higher unsaturation in the SBS backbone, which facilitates the radical formation and hence grafting. The increase in the intensity of stretching vibrations of O-H at 3500 cm^{-1} and COOH at 1707 cm^{-1} with the plasma power is evident from the ATR-FTIR of SBS-g-AA (**Figure 6.8**). It should be noted that the intensities of both these peaks for SR-g-AA are relatively less (**Figure 6.9**). The low plasma grafting efficiency of the SR films is due to the lack of active hydrogens in the SR backbone. Moreover, the primary alkyl radicals are less efficient in bringing about surface grafting. In a unsaturated polymer, there are large number of active allylic hydrogen atoms which can be easily abstracted [22]. This reaffirms our hypothesis that the unsaturation at the polymer surface favorably influences the plasma grafting efficiency of functional monomers.

Figure 6.8 Effect of plasma power on the plasma grafting of AA onto SBS

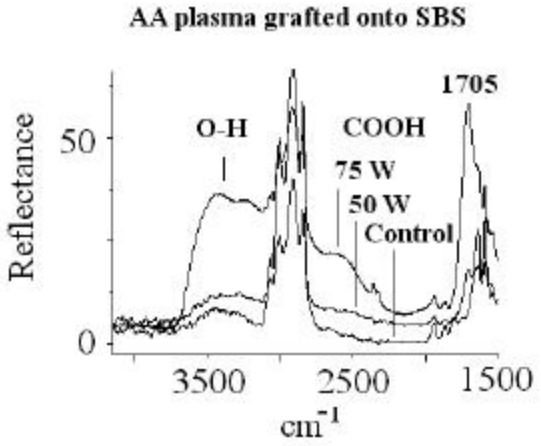

Figure 6.9 Effect of plasma power on the plasma grafting of AA onto SR

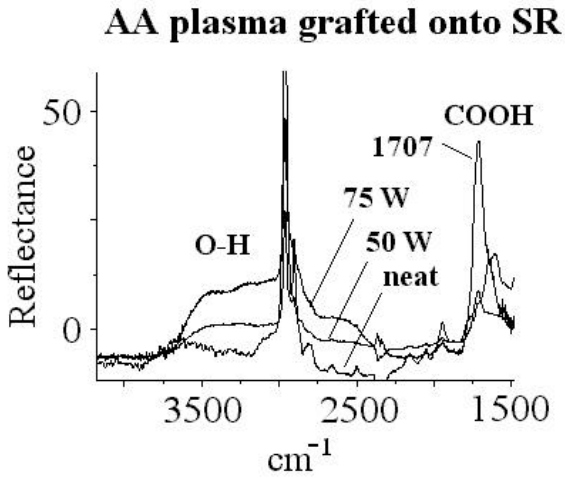

6.4 BIOCOMPATIBILITY STUDY OF SURFACE MODIFIED EPDM FILMS

The optical micrographs of cell adhesion test are shown in **Figure 6.10**. The biocompatibility test revealed that the plasma grafted SR films offered better cell adhesion compared to plasma treated the samples. One possible reason is the less/localized hydrophilicity at the film interface in case of treated samples. Amongst the HEMA and AA grafted films, the later generated better biocompatible surface. This may be due to the specific

interactions between the carboxylic acid groups and the cells. In case of SBS, plasma grafted and plasma treated films offered good biocompatibility. The cell adhesion was homogenous throughout the film surface.

Figure 6.10 Optical micro-graphs of **a)** neat **b)** CO_2 plasma treated **c)** AA plasma grafted onto SR films.

(a)

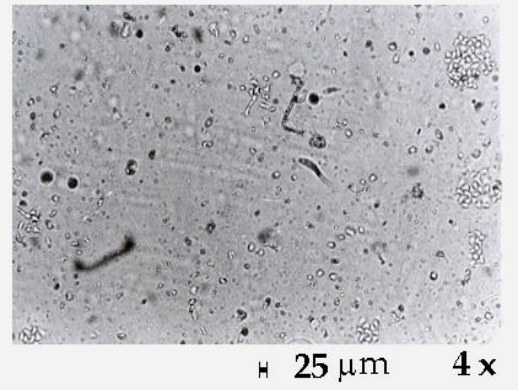

(b)

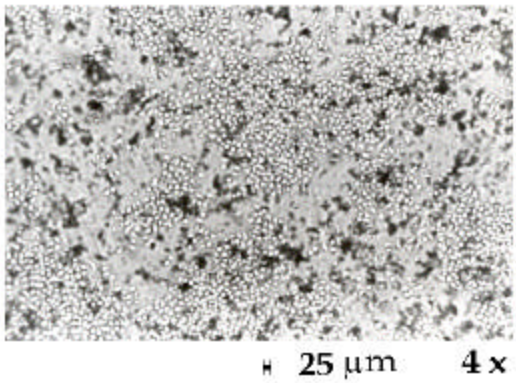

(c)

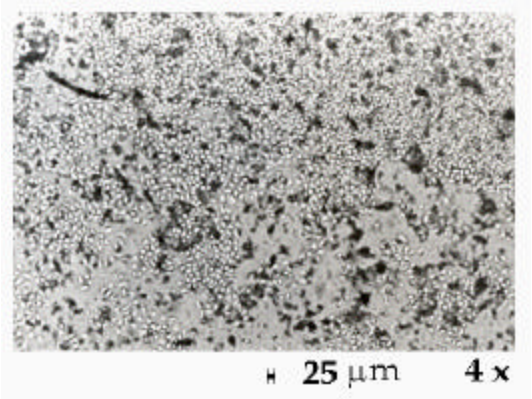

6.5 CONCLUSIONS

Exposure of polymer films at lower plasma power for short irradiation time generates functional groups respective to the system gas but exposure at high plasma power for longer time, causes surface cross-linking, chain scission and etching, which decreases the surface hydrophilicity. ATR-FTIR spectroscopy is not a very efficient tool to detect functional groups located at the film interface. The water contact angle measurements clearly reflect the surface profile. The functionalities generated on the surface depend on the type of the system gas used. Hydrophobic recovery observed in the elastomeric samples is due to the exceptional mobility of the elastomer chains. Vapor phase plasma grafting is an effective method of generating desired functionalities at the polymer-air interface. The unsaturation at the polymer surface favors the rapid hydrophilization due to the easily abstractable allylic H-atoms. Hydrophilicity is not the only criteria of achieving biocompatibility. The type of functional groups also determines the extent of biocompatibility of the polymeric materials.

6.6 REFERENCES

1. C. M. Chang, *Surface Modification and Characterization of Polymers*, Hanser Publishers, (1994).
2. M. Kawabe, S. Tasaka and N. Inagaki, *J. Appl. Polym. Sci.*, **78**, 1392 (2000).
3. F. P. Epaillard, B. Chevet, J. C. Bro sse, *Makromol. Chem*., **192**, 1589 (1991).
4. M. Morra, E. Occhiello and F. Garbassi, *Die Angew Makromol. Chem.*, **189**, 125 (1991).
5. M. K. Urban and M. T. Stewart, *J. Appl. Polym. Sci.*, **39**, 265 (1990).
6. F. P. Epaillard, G. Legeay and J. C. Brosse, *J. Appl. Polym. Sa.*, **44**, 1513 (1992).
7. P. Wang, K. L. Tan, C. C. Ho, M. C. Khew and E. T. Knag, *Eur. Polym. J*., **36**, 1323 (2000).
8. P. Anelli, S. Baccaro, M. Carenza and G. Palma, *Radiat. Phys. Chem*., **46**, 1031 (1995).
9. S. D. Lee, G. H. Hsiue, C. Y. Kao and P. C. T Chang, *Biomaterials*, **17**, 587 (1996).
10. J. J. Yu and H. Ryu, *J. Appl. Polym. Sci*., **73**, 1733 (1999).
11. D. Ruckert, G. Geuskens, P. Fondu and S. Van Erum, *Eur. Polym. J*., **31**, 431, (1995).
12. D. Ruckert and G. Geuskens, *Eur. Polym. J*., **32**, 201 (1996).
13. I. F. Husein, C. Chan, S. Qin and P. K. Chu, *J. Phy. D: Appl. Phys.*, **33**, 2869 (2000).
14. C. A. Wilkie, X. Dong and M. Suzuki, *Polym. Mater. Sci. Eng.*, **71**, 296 (1994).
15. P. Wang, K. L. Tan, C. C. Ho, M. C. Khew and E. T. Knag, *Eur. Polym. J*., **36**, 1323 (2000).
16. J. M. Yang, M. C. Wang, Y. G. Hsu, C. H. Chang and S. K. Lo, *J. Memb. Sci*., **138**, 19, (1998).
17. F. Garbassi, M. Morra, E. Occhiello, L. Barino and R. Scordamaglia, *Surf. Interface. Anal.*, **14**, 585 (1989).
18. C. M. Weikart and H. K. Yasuda, *J. Polym. Sci., Part A: Polym. Chem*., **38**, 3028 (2000)
19. J. D. Andrade, Polymer Surface Dynamics, Plenum Press, New York (1988).
20. H. K. Yasuda, A. K. Sharma and T. Yasuda, *J. Polym. Sci.*, A **19**, 1285 (1981).
21. N. Inagaki, Plasma Surface Modification and Plasma Polymerization, Technomic Publishing Co. Inc., p.28 (1996).
22. W. Yang and B. Ranby, *J. Appl. Polym. Sci*., **62**, 545 (1996).

CHAPTER VII

DESIGN, SYNTHESIS AND PERFORMANCE EVALUATION OF NOVEL POLYMER STABILIZERS

7.1 INTRODUCTION

Most of the polymers are susceptible to degradation by oxygen under an additional influence of UV light or heat. The net result of degradation is the loss in the molecular weight and macroscopic physical properties[1]. This oxidative-degradation can be partially prevented by melt blending the polymers with appropriate stabilizers that ensure the desired polymer properties throughout its service life. Antioxidants like hindered phenols are found to be effective in preventing oxidative degradation[2]. The most widely used antioxidants are the derivatives of 2,6-ditert-butyl-p-cresol (BHT), which act as chain terminating agents by reacting with the alkyl peroxy radicals ($ROO^{\bullet}$) or alkyl radicals ($R^{\bullet}$). However, their low molecular weight, high mobility and rapid volatility from the polymer matrix are main drawbacks[3]. Attempts have been made to overcome this problem by designing high molecular weight stabilizers by linking them to long saturated hydrocarbon chains[4,5]. But, stabilizers with low mobility are often found to under perform against their capacity. Thus, we have designed and synthesized diol-functionalized BHT that can be used to synthesize nylon and polyurethane bearing pendant BHT moieties. Nylons and polyurethane are most widely used polymers for the out door applications and are thus prone to undergo rapid oxidative-degradation influenced by light and heat. We assume that diol functionalized BHT-antioxidant would enhance the service life of these polymers.

The photo-stabilization of polymer involves retardation or elimination of destructive photochemical processes in polymers. UV absorbers, antioxidants and radical scavenger are widely used stabilizers to prevent photo-oxidative degradation in variety of polymers[6,7]. The most efficient UV absorbers include *o*-hydroxy phenyl benzotriazoles and *o*-hydroxy phenyl-s-triazines. This class of stabilizers bear intermolecular hydrogen bonded phenol moiety, which helps in converting incident UV-energy into less harmful form heat[8]. The compatible and mobile stabilizers usually prove to be the best choice in attaining the desired stability. Most of these stabilizers are commercially available and are successfully employed, single and/or in combination with other stabilizers for the polymer stabilization. Researchers have even attempted to study the combined effect of screeners, quenchers, ultraviolet absorbers and thermal stabilizers[9,10]. Depending upon the type of combination, the effect of the stabilizers can be synergistic and antagonistic. The efficacy of the stabilizer depends on many factors viz. type of combination, proportion of additive, compatibility with the polymer and molecular weight of the stabilizer. Hindered amine light stabilizer (HALS) and benzotriazole based UV absorbers are known to work in synergism and there is no literature on the synthesis of the

coupled derivatives of HALS and UV absorbers. Keeping in mind, all the above-mentioned requirements, we have designed and synthesized a novel photostabilizer: HALS coupled to an UV absorber.

During the past decade, the chemistry of synthesis of stabilizers and their mechanism has been extensively studied [11] and the interaction between polymer and the stabilizer at molecular level has been elucidated. Since the degradation of a polymer commences from the surface and slowly proceeds into the bulk of the polymeric substrate, the stabilizers are therefore expected to be most potent if they are anchored at the surface. With an objective to enhance the stabilizing efficiency of HALS, a vinylic HALS; 1,2,2,6,6-pentamethyl piperidinyl-4-acrylate (PMPA) is designed, synthesized, surface grafted and evaluated for the photo-stabilization of SBS, PE and PP.

Thus, in the present study we have synthesized three novel photo-stabilizers from existing commercial light stabilizers. The vinylic photostabilizer (PMPA) is photo-grafted onto the surface of polypropylene, polyethylene and styrene rubber butadiene styrene thin films. The photostabilizing efficacy of the surface anchored stabilizers against the conventional melt blended stabilizers is evaluated.

7.2 MATERIALS AND METHODS

7.2.1 Materials

The styrene butadiene styrene thermoplastic elastomer [SBS block copolymer] and unstabilized oil extended used in the present investigation were supplied by M/s ATV projects India Ltd., Nagothane, India. While ENICHEM and SHELL are their competitor's SBS samples. The contents of styrene and butadiene are given in **Table 7.1**. Commercial samples of isotactic polypropylene (i-PP, Koylene S30330), low density polyethylene (LDPE, Indothene 16MA400) were obtained from Indian Petrochemicals Corp. Ltd., Baroda, India. The stabilizers: 2,6-di-tert-butyl-4-methylphenol [BHT], 2-(2′-hydroxy-5-methylphenyl) benzotriazole [Tinuvin P] and tris(nonylphenyl)phosphite [Irgafos TNPP] were obtained from M/s Hindustan Ciba-Geigy Ltd., Bombay. The reagents 2,2,6,6-tetramethyl-4-piperidinol, 4-dimethyl aminopyridine, tetrabutyl ammonium fluoride, tert-butyl dimethylsilylchloride, benzophenone and acryloyl chloride were procured from Aldrich Chemicals. Maleic anhydride obtained from E. Merck, India, was recrystallized from chloroform. Triethyl amine was obtained from Ranbaxy Laboratories Limited, India and dichloromethane from S.d. Fine Chemicals Limited, India.

Table 7.1: Polybutadiene contents in different grades of SBS rubber.

Sample	PB (mole %)	Styrene (mole %)
ATV-prene	77	23
ATV-oil	78	22
ENICHEM	82	18
SHELL	81	19

7.2.2 Methods

7.2.2.1 Sample preparation

SBS film preparation

Films of unstabilized oil-extended [ATV-oil], stabilized oil-extended SBS [ATV-prene], ENICHEM and SHELL samples of SBS rubbers were prepared by solution casting. The pellets of the copolymer were dissolved in dichloromethane (1.5 % w/v) at room temperature and different concentrations (0.15 and 0.3 wt %) of the stabilizers were incorporated in ATV-oil solution. The solution was homogenized and casted on glass plates, evaporated the solvent and dried under vacuum till constant weight. The unstabilized films of SBS were also prepared by the same method, except for the addition of stabilizer.

PE and PP film preparation

Minimax, *ATLAS*, U.S.A, blender was used for blending 0.2 wt % of 2,2,6,6-tetrametyl-4-piperidinol with LDPE and *i*-PP for the accelerated weathering study. Thin films (~100 μm thickness) were prepared by pressing the polymer pallets (containing stabilizer) in a preheated Carver press (M/s Carver, USA) at 205 °C and 175 °C, respectively, by applying 150 kg/cm^2 platen pressure for 2 min, followed by quenched cooling with cold water circulation.

7.2.2.2 Performance evaluation of stabilized polymer films

The polymer films bearing stabilizers were exposed to UV light (4×400 W MPM UV lamps) supplying $\lambda \geq 300$ nm, under controlled temperature (45-50 °C), in photo-irradiation chamber SEPAP 12/24, procured from M/s. Le Materiel Physico Chimique, Neuilly, France, for accelerated weathering study. The details of the equipment are described elsewhere[12]. The films were examined for the structural changes using FTIR spectroscopy and morphological changes by scanning electron microscope (*Leica*, Cambridge, Stereoscan 440 model).

7.2.3 Analysis

Spectroscopy

FTIR measurements of the synthesized molecules were carried out with a Perkin Elmer 16 PC Spectrophotometer (supplied with ATR accessory). ^{1}H and ^{13}C-NMR spectra were obtained for samples dissolved in $CDCl_3$ at 25 $^{\circ}C$ on a 'Bruker AC 200 FT-NMR' instrument at a frequency of 200 MHz. The purity of the compound was determined by Gas Chromatography (Auto System XL Gas Chromatograph, Perkin Elmer).

Gravimetry

Gravimetric analysis was used to calculate the amount of HALS on the polyolefin film after surface grafting of the stabilizer. The concentration of HALS ($mole/cm^2$) present on the surface of the film was calculated from the increase in the weight of the polyolefin films.

7.2.4 Experimental

7.2.4.1 Synthesis of vinylic HALS (Scheme 7.1)

7.2.4.1.1 Synthesis of 1,2,2,6,6-pentamethyl-4-piperidinol (a)

1,2,2,6,6-pentamethyl-4-piperidinol was synthesized from 2,2,6,6-tetramethyl-4-piperidinol following a reported procedure[13]. 2,2,6,6-tetramethyl-4-piperidinol (3.55 g, 0.02 mol), 37 % formalin (3.3 ml) and 1 ml formic acid were taken in a 25 ml round bottom flask (RB) fixed with a reflux condenser. The contents were heated over a steam bath for 5 h. The reaction mixture was made basic using 1.0 M potassium hydroxide and the product was extracted with diethyl ether (5 × 15 ml) and dried over anhydrous sodium sulphate. The ether extract was evaporated to get the product, which was purified by sublimation at 88 $^{\circ}C$ under reduced pressure (0.05 mm). The white sublime weighed 3.5 g. Yield 92 %, m.p. 72-74, Lit: m.p. (73 - 74 $^{\circ}C$).

^{1}H NMR (δ ppm) : 1.0 (s, 6 H), 1.1 (s, 6 H), 1.25-1.4 (t, 2H), 1.75-1.85 (dd, 2H),
(200 MHz, $CDCl_3$) 2.45 (s, 3H) ($N-CH_3$).
FTIR (cm^{-1}) : 3525-3145 (broad), O-H stretching, 1048 (C-N) stretching.

7.2.4.1.2 Synthesis of 1,2,2,6,6-pentamethyl piperidinyl-4-acrylate (PMPA) (b)

1,2,2,6,6-pentamethyl piperidinyl-4-acrylate (PMPA**)** was synthesized under strictly inert and dry reaction conditions. 1,2,2,6,6-pentamethyl piperidinyl-4-acrylate (PMPA**)** was synthesized from 1,2,2,6,6-pentamethyl-4-piperidinol (**a**).

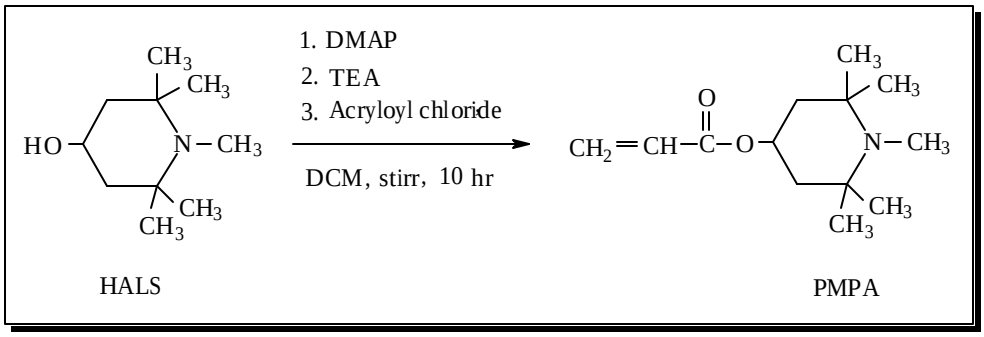

Scheme 7.1

1,2,2,6,6-pentamethyl-4-piperidinol (1.0 M) was taken in a two neck RB along with 4-dimethylaminopyridine (0.4 mol equiv.) [DMAP], dry dichloromethane (10 ml/gm), triethyl amine (1.5 mol equiv.) [TEA]. This reaction mixture was initially stirred for 10 min followed by the addition of acryloyl chloride (1.2 mol equiv.) at 0-4 °C with stirring. The reaction mixture was allowed to stir at room temperature for approximately 10 hrs. This reaction mixture was then quenched in ice water and the product was extracted in dichloromethane (4 × 25 ml). The combined extract was given (2 × 20 ml) washes of saturated sodium bicarbonate solution and finally dried over anhydrous magnesium sulfate. The solvent was evaporated under vacuum at 38 °C over a rotavapor. The product was in the form of pale yellow viscous liquid. The TLC didn't show any spot of either the starting material or the catalyst (DMAP) after the workup. The yield of 1,2,2,6,6-pentamethy piperidinyl-4-acrylate was 1.11 gm (85 %). The product was found to be 98.7 % pure by Gas chromatography.

^{1}H NMR (δ ppm) (200 MHz, $CDCl_3$) (**Figure 7.1**)	(**a**) 5.75 (d, 1H), (**b**) 6.4 (d, 1 H), (**c**) 6.2 (q, 1 H), (**d**) 5.15 (m, 1H), (**e**) 1.8 (dd, 2H), (**f**) 1.5 (dd, 2 H), (**g**) 1.1 (s, 6 H) axial, (**h**) 1.2 (s, 6 H) equatorial, (**i**) 2.2 (s, 3 H) N-CH_3.
FTIR (cm^{-1}) (**Figure 7.2**)	1730, vinyl ester, 1636, C=C stretching and 985, C-H bending.

Figure 7.1 ^{1}H NMR of 1,2,2,6,6-pentamethyl piperidinyl acrylate.

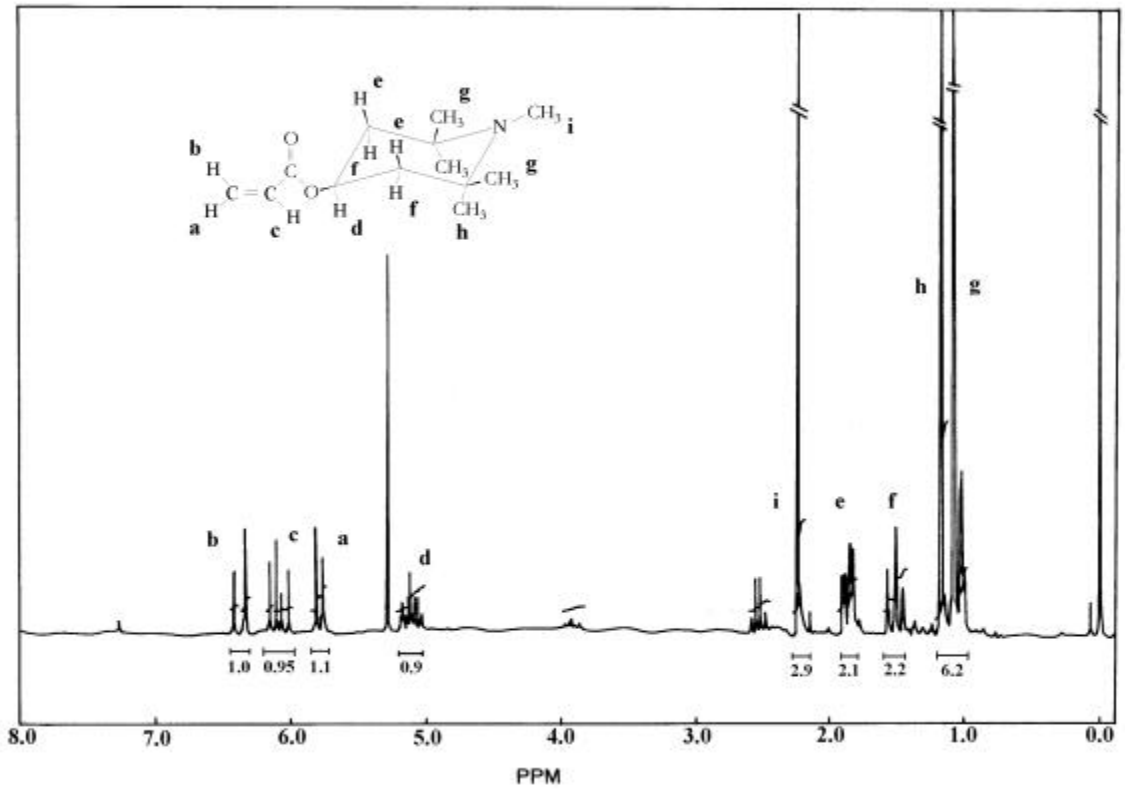

Figure 7.2 FTIR of 1,2,2,6,6-pentamethyl piperidinyl-4-acrylate.

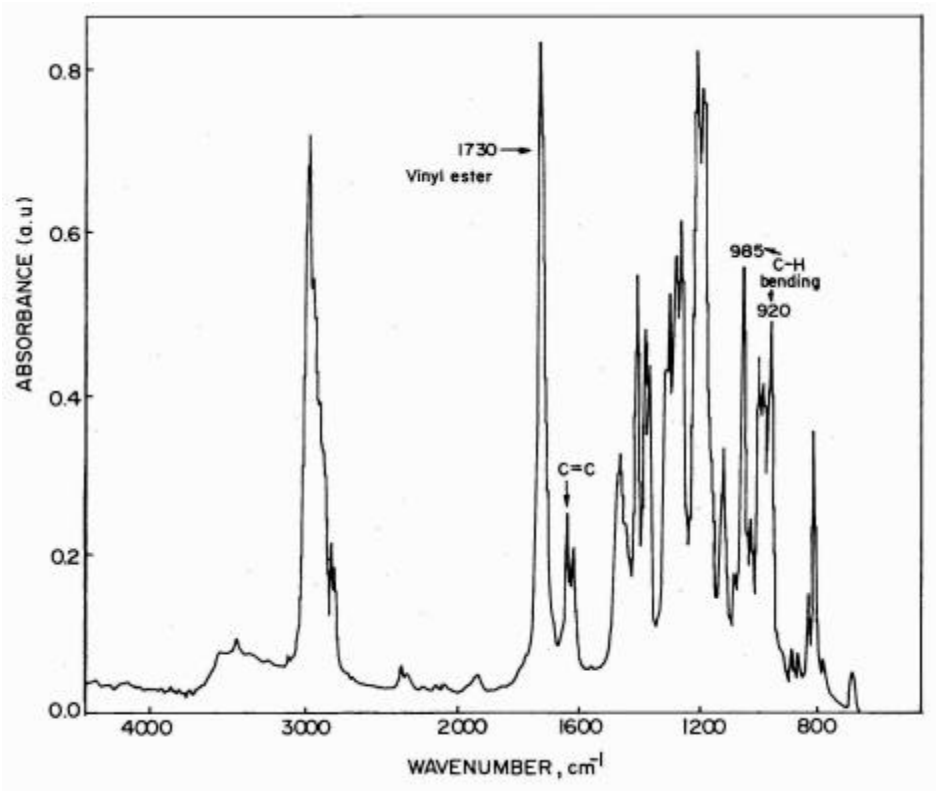

7.2.4.2 Synthesis of a HALS coupled to UV absorber

The synthetic route to the foresaid stabilizer is schematically represented in the **Scheme 7.2**.

7.2.4.2.1 Synthesis of 2-(2'-hydroxy-5'-bromomethyl phenyl) benzotriazole (Step-I)

2-(2'-hydroxy-5'-bromomethyl phenyl) benzotriazole was prepared by the bromination of 2-(2'-hydroxy-5'-methyl phenyl) benzotriazole (Tinuvin P) [14]. In a 500 ml three necked round-bottomed flask (***a***), 5.0 gm (0.0223 mol) of 2-(2'-hydroxy-5'-methyl phenyl) benzotriazole and 100 mg of AIBN were taken and dissolved in 150 ml of dry carbon tetrachloride. In a separate conical flask 4.18 gm (1.5 ml, 0.03 mol) of bromine was dissolved in 75 ml of dry carbon tetrachloride and solution was transferred to a cylindrical addition funnel with a pressure equalizing tube. Three-necked round-bottomed flask with the solution of (***a***) was kept in an oil-bath at temperature 47 $^{\circ}$C. Nitrogen was continuously bubbled through the solution to maintain an inert atmosphere. Cylindrical funnel containing bromine solution was mounted on the three-necked round-bottomed flask. Solution was continuously stirred with the help of magnetic stirrer. Bromine solution was added, drop-wise from the addition funnel to the flask in a span of 4-5 hours till all the solution was poured out. Heating was then stopped and the final reaction mixture was allowed to gradually cool to room temperature. Product was separated by solvent evaporation. Finally, the product was purified by recrystalization from acetone. The yield of 2-(2'-hydroxy-5'-bromomethyl phenyl) benzotriazole was 5.5 g (80 %) m.p. 169-171 $^{\circ}$C.

^{1}H NMR (δ ppm) (**Figure 7.3)**	(**a**) 7.90-8.05 (q, 2H), (**b**) 7.45- 7.60 (q, 2H), (**c**) 11.45-11.55 (s, 1H), (**d**) 7.15-7.25 (d, 1H), (**e**) 7.35-7.45 (d, 1H), (**f**) 8.45-8.53 (d, 1H), (**g**) 4.5-4.7 (s, 2H)
FTIR (cm^{-1}) (**Figure 7.4**)	3450, O-H stretching, 1258, CH_2 wagging, 1222, C-O stretching, 684 and 571, C-Br stretching.

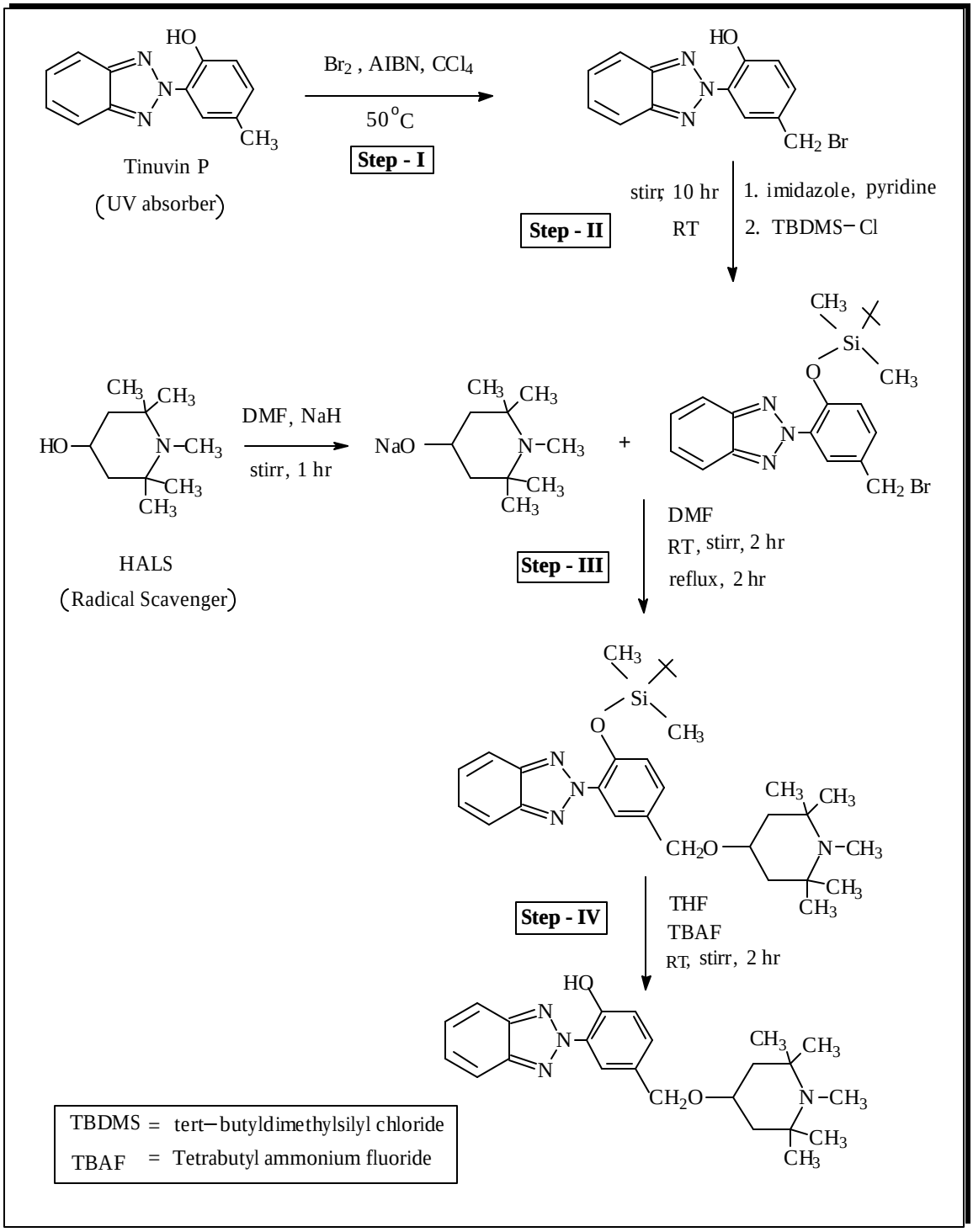
Tinuvin P
(UV absorber)
Br2 , AIBN, CCl4
50°C
Step - I
stirr, 10 hr
RT
Step - II
1. imidazole, pyridine
2. TBDMS−Cl
HALS
(Radical Scavenger)
DMF, NaH
stirr, 1 hr
Step - III
DMF
RT, stirr, 2 hr
reflux, 2 hr
Step - IV
THF
TBAF
RT, stirr, 2 hr
TBDMS = tert−butyldimethylsilyl chloride
TBAF = Tetrabutyl ammonium fluoride

Scheme 7.2

7.2.4.2.2 Synthesis of 2-(2'-tert-butyldimetylsilyloxy-5'-bromomethylphenyl) benzotriazole (Step-II)

2-(2'-tert-butyldimetylsilyloxy-5'-bromomethylphenyl) benzotriazole was synthesized strictly under dry and inert reaction conditions. In a 50 ml capacity RB, 2-(2'-hydroxy-5'-bromomethyl phenyl) benzotriazole (3.0 gm, 0.00986 mol) was taken along with imidazole (2.1 gm, 0.0295 mol), closed the RB with rubber septum and applied an inert atmosphere using argon gas balloon. In RB flask, 10 ml of dry pyridine was added and then the reaction mixture for 20-60 min. The reaction mixture becomes very thick and difficult to stir. To this mixture, tert-butyl dimethylsilylchloride (5.2 gm, 0.0345 mol) was added under inert condition and continued agitating the reaction mixture for 10-14 hrs. After checking the TLC for the completion of the reaction, the pyridine from the RB was evaporated to dryness under vacuum. The contents of the RB were consequently dissolved in 15 ml dichloromethane. The insoluble mass, mainly pyridinium hydrochloride, was filtered off and the mother liquor was evaporated under vacuum to give (a semi crystalline rust colored compound) 2-(2'-tert-butyl-di-metylsilyloxy-5'-bromomethylphenyl) benzotriazole. The crude product weighed 3.30 gm to give 80 % yield. The crude compound was purified by column chromatography, employing a solvent system of 4:6 ethyl acetate: petroleum ether. The yield of the pure compound was 76 % and its m.p. 162-164 $^{\circ}$C.

^{1}H NMR (δ ppm) **(Figure 7.5)**	(**a**) 0.05-0.1 (s, 6H) (**b**) 1.1-1.25 (s, 9H) (**c**) 7.15-7.2 (d, 1H), (**d**) 7.3-7.45 (dd, 1H), (**e**) 8.45-8.55 (d,1H), (**f**) 4.5-4.7 (s, 2H), (**g**) 7.8-8.15 (dd, 2H), (**h**) 7.5-7.75 (dd, 2H).
FTIR (cm^{-1}) (**Figure 7.6**)	3300, O-Si stretching, 1258, CH_2 wagging, 1590, C=N, 1220, Si-CH_3, 672 and 571, C- Br stretching.

7.2.4.2.3 Synthesis of 2-[2'-tert-butyldimetylsilyloxy-5'-methyleneoxy ((1", 2", 2", 6", 6"-pentamethyl-4"- piperidinyl) phenyl)]benzotriazole (Step-III)

This compound was synthesized strictly under dry and inert reaction conditions. The compound 2-(2'-tert-butyl-di-metylsilyloxy-5'-bromomethylphenyl)benzotriazole (2.1 gm, 0.00501 mol) was taken in one 25 ml capacity RB (**A**) and dissolved with 8 ml dry *N*,*N*-dimethyl formamide (DMF) under Argon atmosphere with stirring. In an another two necked RB **(B)**, 1,2,2,6,6-pentamethyl-4-piperidinol (1.0356 gm, 0.00601 mol) and sodium hydride (0.3 gm, 0.01252 mol) were taken and dissolved in 6 ml dry DMF with stirring under Argon

atmosphere. This reaction mixture was agitated for almost 1 hr and then cooled to 4-8 °C. To this reaction mixture (**B**), the contents of the RB (**A**) were gradually added over a period of 30-60 min. This reaction mixture was further agitated for 2 hrs followed by refluxing the same for an additional period of 2 hrs. The contents of the RB were cooled to room temperature and further agitated for 4 hrs at room temperature. The solvent in the RB was evaporated under reduced pressure and the solid mass in the RB was dissolved in 15 ml water and repeatedly extracted with dichloromethane (4 × 10 ml). Dichloromethane was then evaporated under vacuum at 38 °C over a rotavapor to give pale yellow colored crystalline product 2-[2'-tert-butyldimetylsilyloxy-5'-methyleneoxy ((1", 2", 2", 6", 6"-pentamethyl-4"-piperidinyl) phenyl) benzotriazole. The TLC showed very little amount of unreacted starting material. The crude yield was 2.22 gms (87 %). The product was purified by recrystalization technique using polar solvents like ethanol or acetone to get (83 %) yield of pure product.

FTIR (cm^{-1})	3700-3300, Si-O, stretching, 1220, C-O, stretching, 1048, C-N, stretching

7.2.4.2.4 Synthesis of 2-[2'-hydroxy-5'-methyleneoxy((1", 2", 2", 6", 6"-pentamethyl – 4"- piperidinyl) phenyl)]benzotriazole (Step-IV)

This step involves the deprotection of the phenolic -OH group upon cleavage of O-Si bond. The compound 2-[2'-tert-butyldimetylsilyloxy-5'-methyleneoxy ((1", 2", 2", 6", 6"-pentamethyl-4"-piperidinyl)phenyl)] benzotriazole (2.0 gm, 0.003937 mol) was taken in an RB with tetrabutyl ammonium fluoride [4.71 ml, (1.0 M solution in THF)] and agitated the reaction mixture at room temperature for 1-3 hrs under anhydrous conditions, followed by addition of 10 ml water and extracted the product in DCM (4 × 10 ml). The combined extract was dried with anhydrous magnesium sulfate after neutralization with anhydrous potassium carbonate. Evaporating the solvent gave a lemon yellow crystalline product, 2-[2'hydroxy-5'-methyleneoxy((1",2",2",6",6"-pentamethyl-4"-piperidinyl)phenyl)benzotriazole with a crude yield of 1.39 gms (90 %).

^{1}H NMR (δ ppm) (500 MHz, $CDCl_3$) (**Figure 7.7**)	2.2-2.4 (**a**) (s, 3H), 1.21-1.24 (**b**) (s, 6H), 1.15-1.20 (**c**) (s, 6H), 1.25-1.45 (**d**)(dd, 2H), 1.75-2.1 (**e**) (dd, 2H), 3.8-4.1 (**f**) (s, 2H), 7.15-7.2 (**g**) (d, 1H), 7.2-7.25 (**h**), (d, 1H), 11.4-11.5 (**i**) (s, 1H), 7.8- 8.15 (**j**) (dd, 2H), 7.5-7.75 (**k**) (dd, 2H), 7.35-7.45 (**m**) (dd, 1H)
FTIR (cm^{-1}) (**Figure 7.8**)	3250, O-H stretching, 1375, C-OH bending, 1258, CH_2 wagging, 1222, C-O stretching, 1070, C-O-C stretching, 1048, C-N stretching.

Figure 7.3 ^{1}H NMR of 2-(2'-hydroxy-5'-bromomethyl phenyl) benzotriazole.

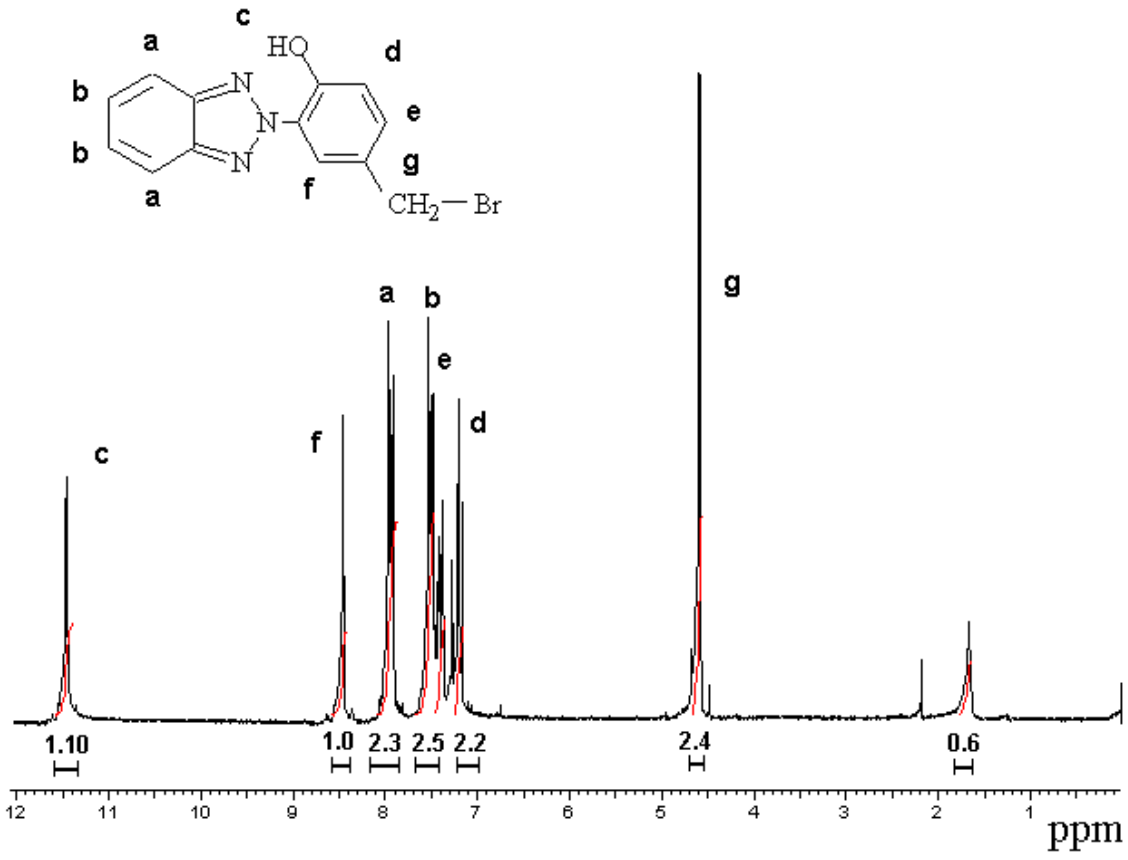

Figure 7.4 FTIR spectrum of 2-(2'-hydroxy-5'-bromomethyl phenyl) benzotriazole.

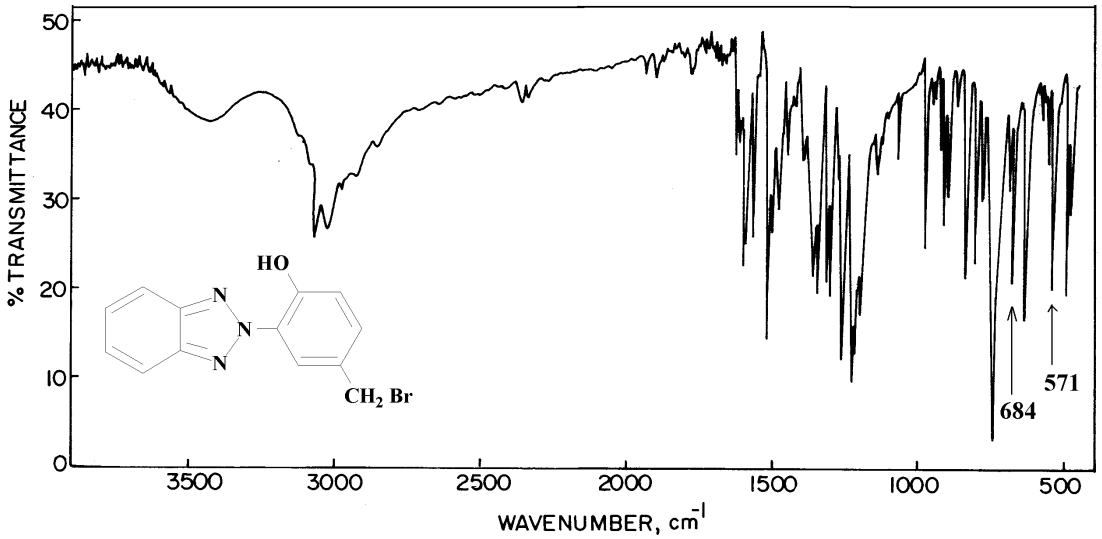

Figure 7.5 [1]H NMR of 2-(2'-tert-butyldimetylsilyloxy-5'-bromomethylphenyl) benzotriazole.

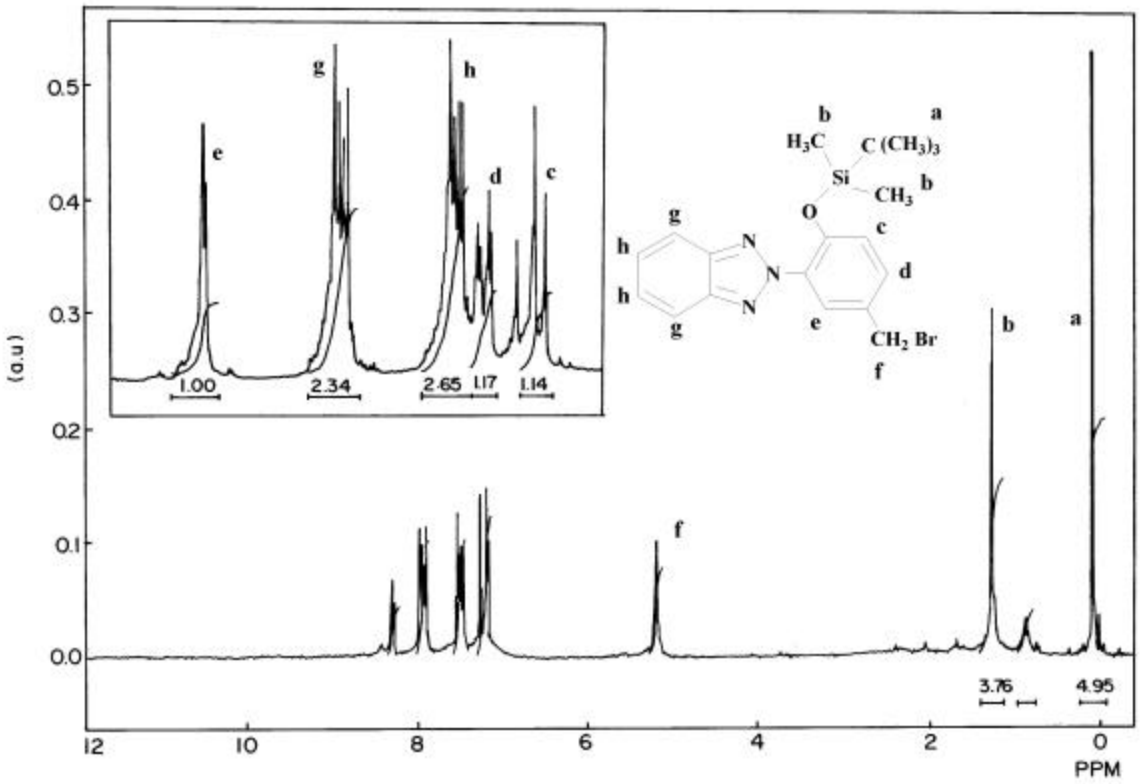

Figure 7.6 FTIR of 2-(2'-tert-butyldimetylsilyloxy-5'-bromomethylphenyl) benzotriazole.

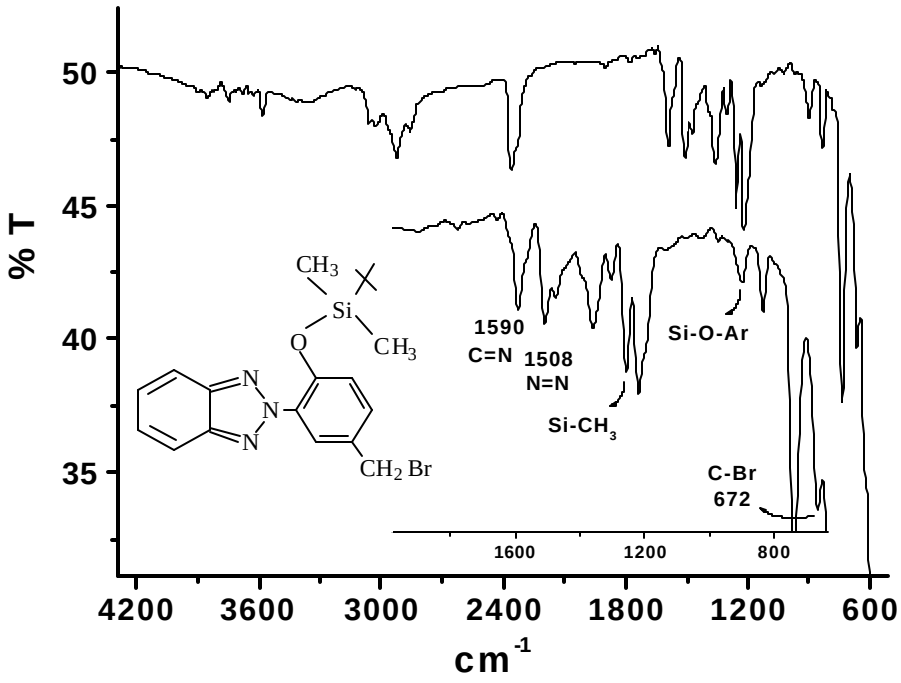

Figure 7.7 ^{1}H NMR of 2-[2'-hydroxy-5'-methyleneoxy ((1", 2", 2", 6", 6"-pentamethyl-4"-piperidinyl) phenyl)]benzotriazole.

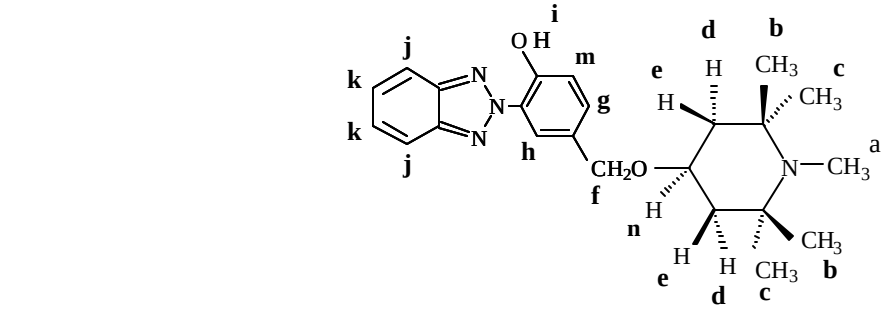

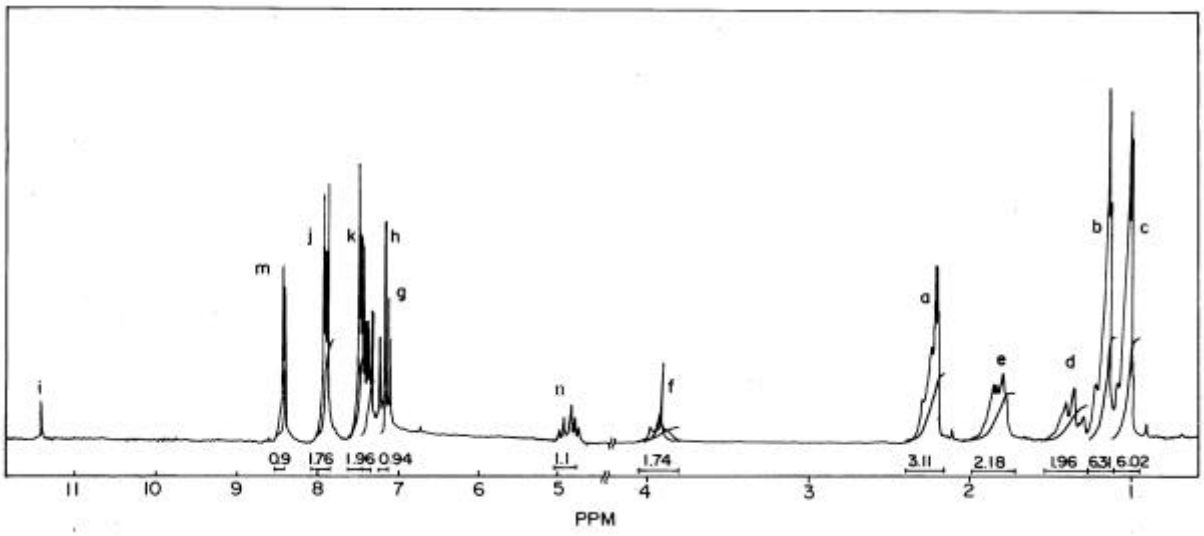

Figure 7.8 FTIR of 2-[2'-hydroxy-5'-methyleneoxy((1", 2", 2", 6", 6"-pentamethyl-4"-piperidinyl) phenyl)]benzotriazole.

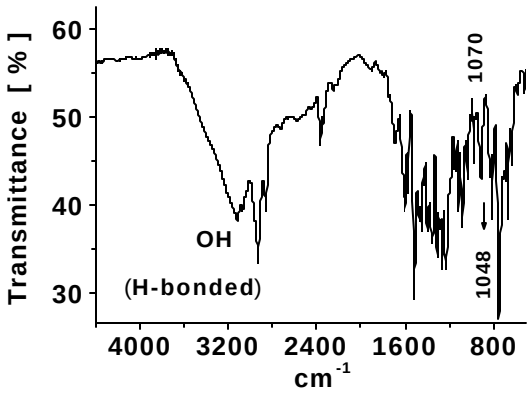

7.2.4.3 Synthesis of diol functionalized BHT

7.2.4.3.1 Synthesis of 3,5-di-*tert*-butyl-4-hydroxy benzylbromide

The synthetic route to the desired product is out lined in the **Scheme 7.3**.

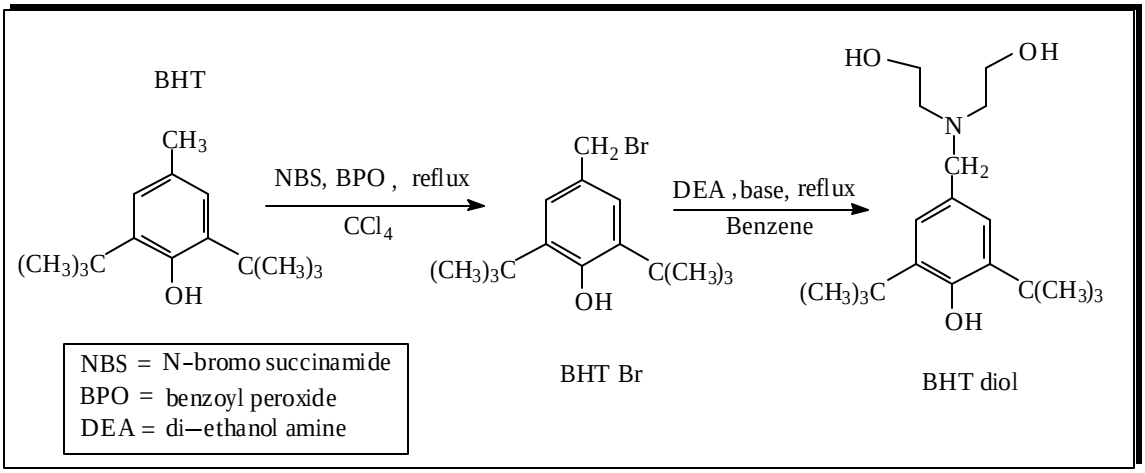

Scheme 7.3

3,5-ditert-butyl-4-hydroxy benzyl bromide was prepared from the bromination of 2,6-ditert-butyl-4-methyl phenol. In a 250 ml three-necked round bottomed flask, 2.5 g (0.0113 mol) of 2,6,-ditert-butyl-4-methyl phenol and dissolved in 25 ml of dry carbon tetrachloride. In a separate conical flask, (0.3 ml, 1.05 mol equiv.) of bromine was dissolved in 25 ml of dry carbon tetrachloride and solution was transferred to a cylindrical funnel with pressure equalizing tube. Three-necked round-bottomed flask containing solution of 2,6-ditert-butyl-4-methyl phenol was kept in oil-bath with temperature 85 °C. Nitrogen was bubbled through

the solution for creating inert atmosphere. Cylindrical funnel containing bromine solution was mounted on the three-necked round-bottomed flask. Solution in the flask was continuously stirred with the help of magnetic stirrer. Bromine solution was added, drop-wise from funnel to the flask for a span of 3-4 hours till all the solution was poured out. After the heating was stopped, the reaction mixture was allowed to cool to the room temperature. Product was separated by solvent evaporation. The product obtained was a viscous yellow liquid, which was absolutely pure and was identified from the ^{1}H NMR and FTIR. The product was found to be unstable upon longer exposure to air and was stored under argon atmosphere for further use. The yield of 3,5-ditert-butyl-4-hydroxy benzyl bromide was 3.15 g (> 90 %).

^{1}H NMR (δ ppm) (**Figure 7.9**)	4.45 - 4.55 (**a**) (s, 2H), 7.2 – 7.25 (**b**) (s, 2H), 1.4 -1.6 (**c**) (s, 18 H), 5.3 - 5.35 (**d**) (s, 1H)
FTIR (cm^{-1})	3600-3200, O-H stretching, 1222, C-O stretching/ O-H bending, 684 and 571, C-Br stretching

7.2.4.3.2 Synthesis of 3,5-di*tert*-butyl-4-(bis-N-(2-hydroxyethyl)aminomethylene) phenol)

This step involves elimination of hydrogen bromide to give the desired product. In a two neck RB, 3,5-ditertbutyl-4-hydroxy benzylbromide (515 mg, 0.0017 mol), diethanol amine (3.14 gm, 1.1 mol equiv.) were taken alongwith 25 ml distilled benzene. The reaction mixture was refluxed under inert atmosphere for 6 hrs. Upon cooling the contents of the RB, the product crystallized out in the form of sharp long colorless needles. The solvent was then removed by decantation and the crystals were repeatedly washed with fresh benzene. Product was identified by ^{1}H-NMR and FTIR.

^{1}H NMR (δ ppm) (500 MHz, $CDCl_3$) (**Figure 7.10**)	7.35 – 7.45 (**a**) (s, 2H), 4.05 - 4.2 (**b**) (t, 4H), 3.35 - 3.5 (**c**) (t, 4H) 4.45 - 4.55 (**d**) (s, 2H), 7.25 – 7.3 (**e**) (d, 2H), 1.4 -1.6 (**f**) (s, 18 H), 5.45- 5.5 (**g**) (s, 1H).
FTIR (cm^{-1}) (**Figure 7.11**)	3600-3250, O-H stretching, 1220, C-O (stretching) and O-H (bending) phenol, 1050, C-O (stretching) and O-H (bending) alcohol

Figure 7.9 ^{1}H NMR of 3,5-di*tert*-butyl-4-hydroxy benzyl bromide.

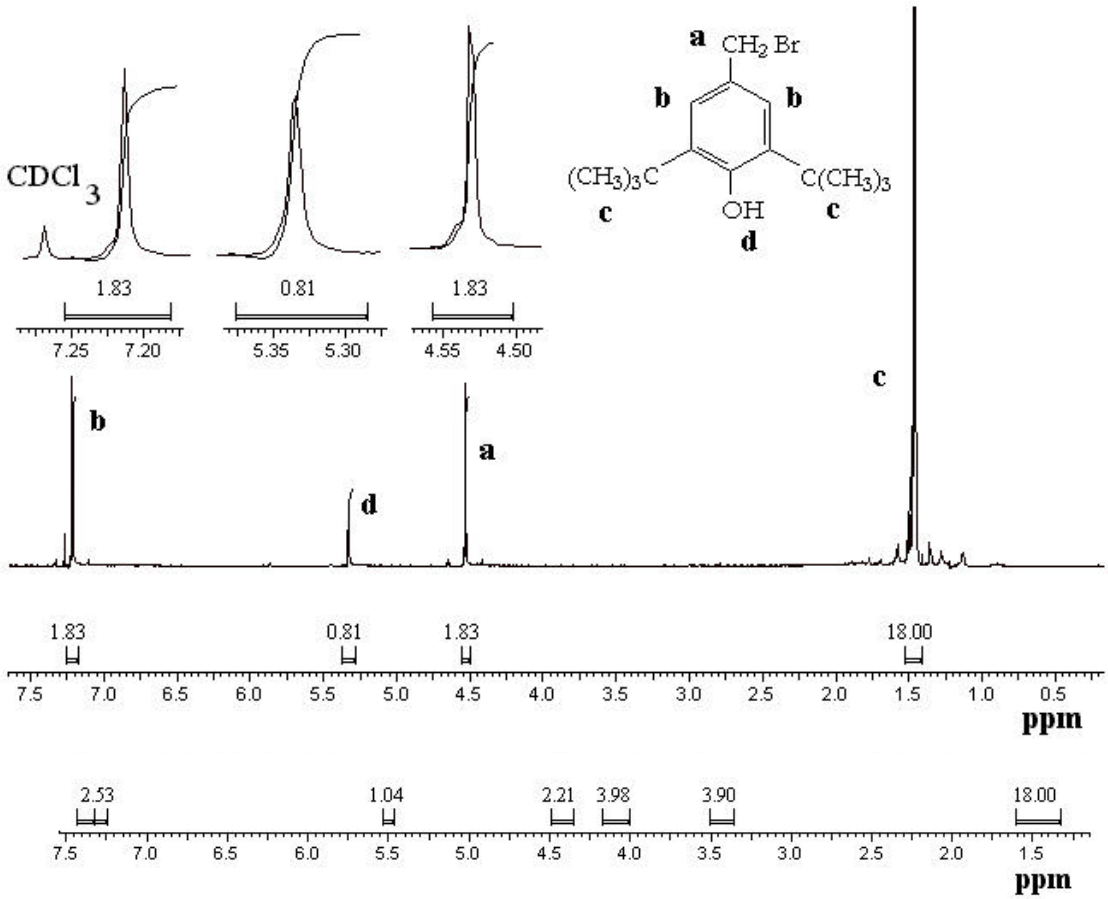

Figure 7.10 ^{1}H NMR of 3,5-di*tert*-butyl-4-(bis-N-(2-hydroxyethyl)aminomethylene) phenol).

Figure 7.11 FTIR of 3,5-di*tert*-butyl-4-(bis-N-(2-hydroxyethyl)aminomethylene) phenol).

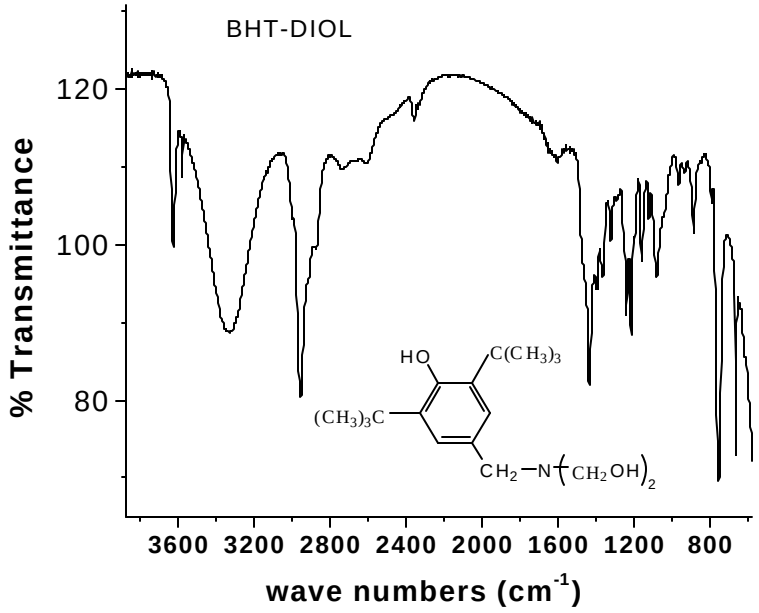

7.2.4.4 Synthesis of SBS-, iPP- and LDPE-g-HALS (Scheme 7.4)

7.2.4.4.1 Surface-grafting of PMPA on Styrene butadiene styrene (SBS) film

A pair of unstabilized thin film of styrene butadiene styrene thermoplastic elastomer was taken in a specially designed photoreactor, with acetone (30 ml), benzophenone (0.2 M) and PMPA (0.166 M) under nitrogen atmosphere and irradiated ($\lambda \geq 290$ nm) for 1 hr at 55-60 °C. The films were soxhlet extracted in methanol for 6 hrs and then dried under vacuum.

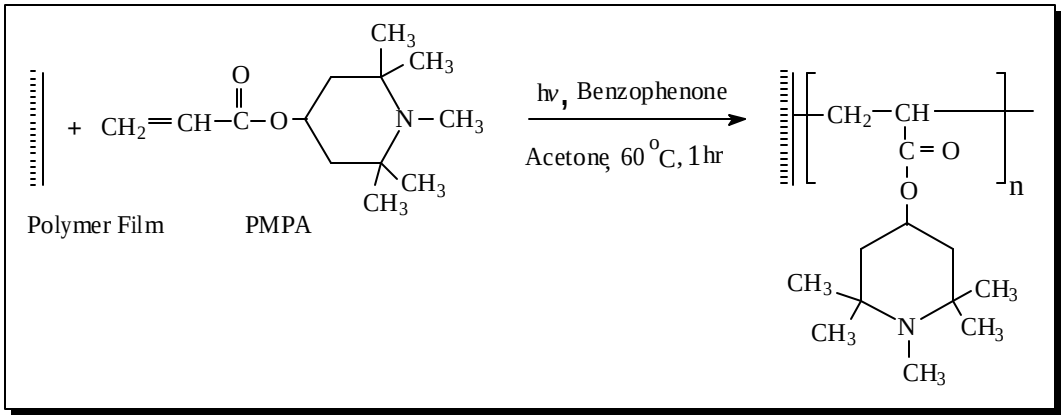

Scheme 7.4

7.2.4.4.2 Surface photo-grafting of PMPA onto polyolefin films

The films of LDPE and i-PP were taken in a specially designed photo-reactor (mentioned in Chapter 3, *section 3.2.2.1*) with 42 ml of acetone, 0.4 M benzophenone and allowed to stand under nitrogen atmosphere for 1½ h, added (0.27 M) PMPA with 7 ml of acetone and thoroughly deareated with nitrogen for 10 min. The films were UV irradiated for 1 hr at 60 ± 2 °C under nitrogen atmosphere followed by extraction in methanol for 6 hrs and dried under vacuum at room temperature till constant weight.

7.2.4.4.3 Preparation of polyolefin surface bearing succinic anhydride groups

The LDPE and i-PP films were taken in a photo-reactor (pyrex glass) with 25 ml dry acetone, (2.0 M) pure maleic anhydride and (0.29 M) benzophenone at 60 °C under UV irradiation ($\lambda \geq 290$ nm) for 2 hrs using 400 W medium pressure mercury vapor lamp. The reaction was carried out under nitrogen atmosphere. After the completion of reaction, these films were soxhlet extracted at reflux temperature with acetone for 8 hrs in order to remove physically adhered/ homopolymerized maleic anhydride. The films were dried at room

temperature under vacuum till constant weight. A control experiment was carried out to prove that the generation of characteristic peak is due to grafting and not due to the photo-degradation caused by the UV irradiation used for the photo-grafting. The same procedure was followed in case of i-PP films also.

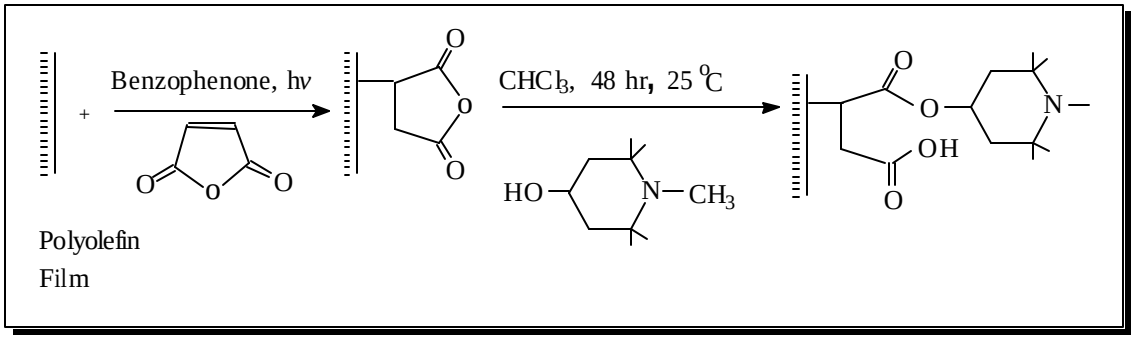

Scheme 7.5

7.2.4.4.4 Preparation of polyolefin surface-bound HALS

Surface modified LDPE films (3 x 1 cm^2) bearing succinic anhydride (SA) group were reacted with (0.016 M) PMPO in dry chloroform for 48 hrs at room temperature with occasional stirring. FTIR spectroscopy was used to monitor the completion of reaction. The film was soxhlet extracted with chloroform for 5 hrs to remove any unreacted HALS.

7.2.4.4.5 Control Experiment

The virgin films of LDPE and i-PP were taken in the pre-mentioned photo-reactor with 42 ml of acetone, (0.4 M) benzophenone without PMPA, thoroughly de-aerated with nitrogen for 10 min followed by UV irradiation for 1 hr at 60 ± 2 °C under nitrogen atmosphere, washed the films with methanol and dried under vacuum at room temperature till constant weight. These films were then taken up for the determination of structural changes by ATR-FTIR spectrophotometer. The control samples did not show any changes compared to the ATR-FTIR spectra of the virgin samples.

7.3 RESULTS AND DISCUSSION

The stabilizing efficacy of PMPA is studied for two different classes of polymers against conventionally melt blended photostabilizers. The discussion section is sub-divided into two parts for the sake of convenience.

7.3.1 Photo-stabilizing efficiency of PMAP-g-SBS

Since SBS rubber contains an unsaturated rubber mid-block, the degradation mechanism may resemble to that of polybutadiene[15] (**Scheme 7.6**) and styrene butadiene rubber[16] to some extent but it is expected to be more complex as SBS rubber is a triblock copolymer. The degradation of SBS arises from the generation of free radicals by U.V. light causing undesirable reaction of double bonds in polybutadiene segment. The initial photo-oxidation[17] of polybutadiene block initiates the rapid degradation of polystyrene segment. The photo-oxidation of styrene block leads to yellowing. The hydroperoxide, alcohol and hydroxyl groups formed due to photo-oxidative degradation are observed in the hydroxyl region whereas the acidic, carboxyl and ketonic groups are identified in the carbonyl region of FTIR spectra. The ^{13}C NMR spectrum of the photo-oxidized SBS rubber[17,18], showed the resonance peaks at 71.2 and 58.5 ppm which were assigned to alcohol and epoxides, respectively.

The photo-oxidative degradation of the four different unstabilized SBS samples (ATV-oil, ATV-prene, ENICHEM and SHELL) revealed that the degradation of ATV samples were faster compared to ENICHEM and SHELL samples, which is obvious from the hydroxyl and carbonyl peak evolution in the FTIR spectra of the irradiated samples (**Figure 7.12** and **7.13**). Since, the ATV-oil sample showed highest rate of degradation, it was further taken up for the efficiency evaluation of surface grafted-PMPA against melt-mixed conventional stabilizers. The ATV-oil films containing 0.3 % w/w of stabilizer (BHT, Tinuvin P, Irgafos TNPP) each, were U.V. irradiated along with 0.32 % w/w surface grafted PMPA. A very broad hydroxy region (3700-3200 cm^{-1}) with a maximum at 3400 cm^{-1} appeared in the FTIR spectra and the carbonyl region (1850-1600 cm^{-1}) showed several overlapping bands (**Figure 7.14** and **7.15**). These broad bands often contain absorptions at 1715, 1722 and 1740 cm^{-1} assigned to carboxylic acid, ketone and ester, respectively. The area under the carbonyl region increases with the increase in the irradiation time. **Figure 7.15** shows that the PMPA grafted film gives the best stabilization of ATV-oil sample. The rate of hydroxyl and carbonyl absorption for different photo-irradiated samples plotted against irradiation time, presented in the **Figures 7.16 and 7.17** show that amongst the unstabilized samples ENICHEM offer the best stabilization. On the other hand, amongst the ATV-oil samples stabilized with different stabilizers, PMPA grafted ATV-oil film showed minimum hydroxyl/carbonyl group formation, indicating that it is the better stabilizer compared to BHT, Tinuvin P and Irgafos

TNPP. This remarkable stabilization capability of PMPA may be due to its availability at the surface, from where the degradation commences.

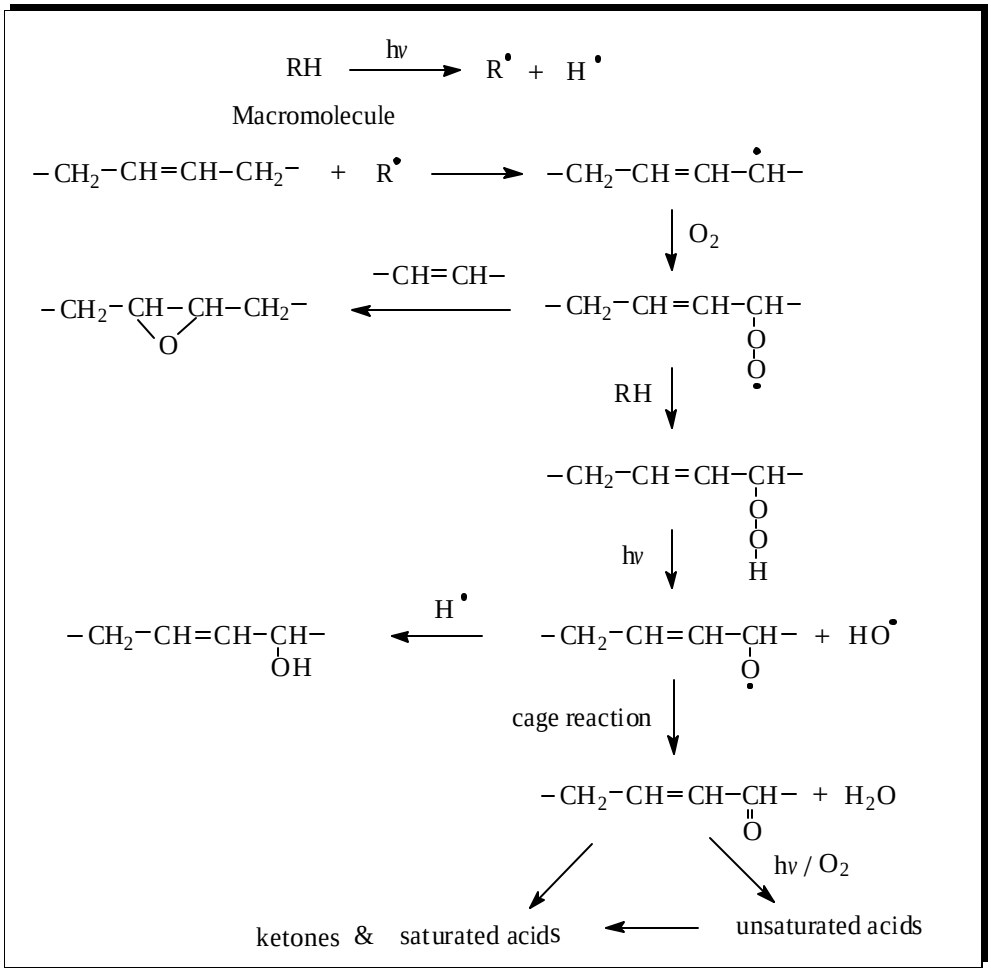

Scheme 7.6

7.3.2 Photo-stabilizing efficiency of iPP and LDPE-g-PMPA

The polyolefin (PO) surface modification was characterized using ATR-FTIR spectroscopy. In the IR overlay spectra (**Figure 7.18**), the pristine LDPE film is denoted by **A** whereas a sharp peak at 1735 cm^{-1} in film **B** is due to the carbonyl group (ester) of the grafted 1,2,2,6,6-pentamethylpiperidinyl-4-acrylate (PMPA). The characteristic peaks at 1868 and 1789 cm^{-1} emerge from the vibrational frequencies of succinic anhydride group anchored on the film **C**, due to the grafting of maleic anhydride. The complete disappearance of peaks at 1868 and 1789 cm^{-1} in **D** confirms that the succinic anhydride groups present on the films have completely reacted with 1,2,2,6,6-pentamethyl-4-piperidinol (PMPO). The presence of some carboxylic acid/ carboxylate on the surface results in the appearance of bands at 1500

cm^{-1} and 1600 cm^{-1} in the ATR-FTIR spectrum, which is due to the ring opening of succinic anhydride upon reaction with PMPO (**Scheme 7.7**). The concentration of different HALS on the surface of LDPE and *i*-PP films determined by gravimetric analysis are given in (**Table 7.2**). It is clear from the table that the concentration of HALS on the polymer surface is significantly high when PMPA is grafted on the polyolefins. Moreover, the effective concentration of HALS in case of PO-g-SA-PMPO may even be still less since the weight gain is attributed to the combined effect of SA and PMPO moieties, unlike that for PO-g-PMPA.

Table 7.2. Concentration of HALS on the iPP and LDPE film surface.

Sample	Conc. in $\mu mol/cm^2$
LDPE -g-PMPA	1.11
LDPE-g-SA-PMPO	0.98
i-PP-g-PMPA	0.74
i-PP-g-SA-PMPO	0.66

Since, it is almost impossible to control degree of grafting, the studies are carried out with closest possible concentration of stabilizer. The photo-stabilization efficiencies of PMPA and SA-PMPO in i-PP and LDPE were studied from carbonyl group formation at 1740 cm^{-1} (**Figure 7.19**). The area under carbonyl peak was plotted against the irradiation time (**Figure 7.20**) and their performance was compared with those prepared by melt blending. The **Figure 7.20** shows that the unprotected polyethylene developed a drastic increase in carbonyl absorbance just within the initial hours of irradiation. The LDPE-g-PMPA and LDPE-g-SA-PMPO films showed a remarkable photo-stability compared to the polymer stabilized with melt blended 2,2,6,6-teramethyl-4-piperidinol (HALS). Since the stabilizer is not homogeneously dispersed into the system in case of melt blending, it offers a poor stability to the substrate as compared to the surface anchored HALS. *Ranby et al*.[11] have demonstrated an effective stability of i-PP against U.V.-initiated degradation by grafting the i-PP surface with glycidyl methacrylate followed by chemical attachment of HALS to the oxirane group.

It can be clearly noticed from **Figure 7.21** that the photo-stability offered by PMPA is maximum. It is assumed that in case of polymer grafted with SA-PMPO, the free carboxyl group may act as a chromophore and sensitize the degradation thus, decreasing the efficiency of the stabilizer, which is not so in case of PMPA. A similar trend was observed when the change in the hydroxyl peak intensity in the FT- IR spectrum was measured with the irradiation time. The fact is well established that the degradation of a polymer commences

from its surface and proceeds towards the bulk of the substrate. When the availability of the photo-stabilizer is extended to the degradation site, the rate of degradation is minimized. Being a monomeric HALS, PMPA is directly attached to the surface of the polymer without any pre-grafting by a functional monomer. These are the reasons for which PMPA outperforms all other melt blended conventional photo-stabilizers.

Figure 7.12 FTIR spectral changes in the hydroxyl region for various hours irradiated ATV-prene (—), ENICHEM (-----), SHELL (**.....**) and ATV-oil (--•--) samples.

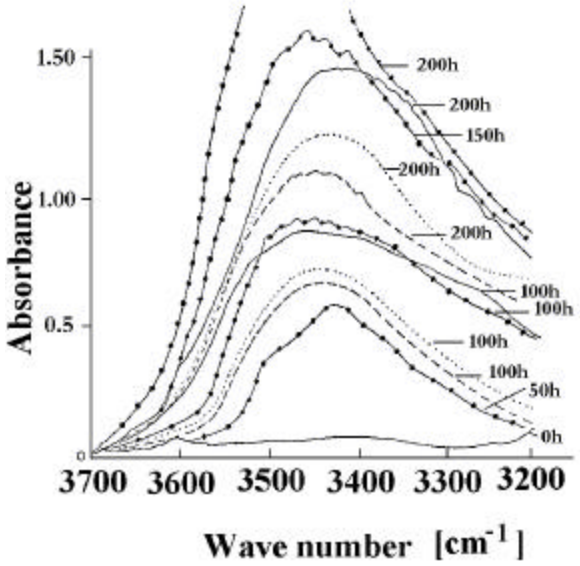

Figure 7.13 FTIR spectral changes in the hydroxyl region for various hours irradiated ATV-prene (—), ENICHEM (-----), SHELL (.....) and ATV-oil (--•--) samples.

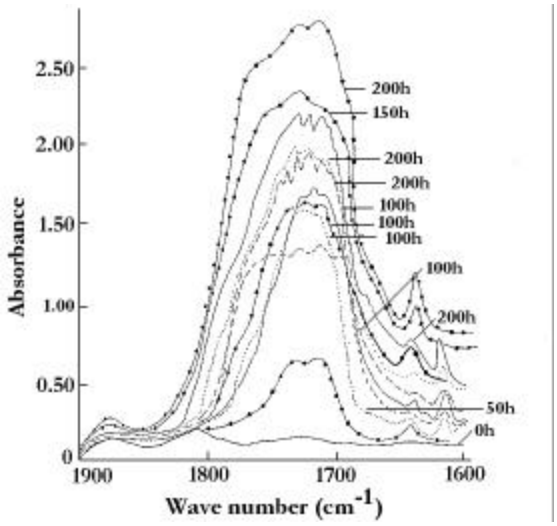

Figure 7.14 FTIR spectral changes in the hydroxyl region for various hours irradiated ATV-oil in presence of 0.3 wt % each of BHT(—), Irgafos TNPP (-----), Tinuvin P (**.....**) and 0.32 wt % of grafted PMPA (–•–•–).

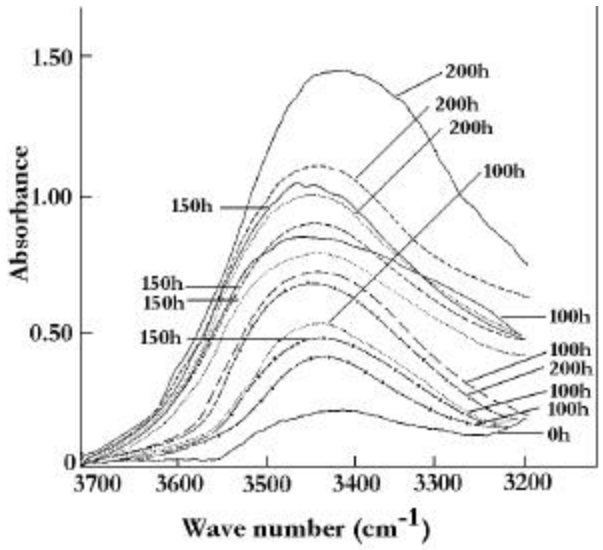

Figure 7.15 FTIR spectral changes in the hydroxyl region for various hours irradiated ATV-oil in presence of 0.3 wt % each of BHT(—), Irgafos TNPP (-----), Tinuvin P (**.....**) and 0.32 wt % of grafted PMPA (–•–•–).

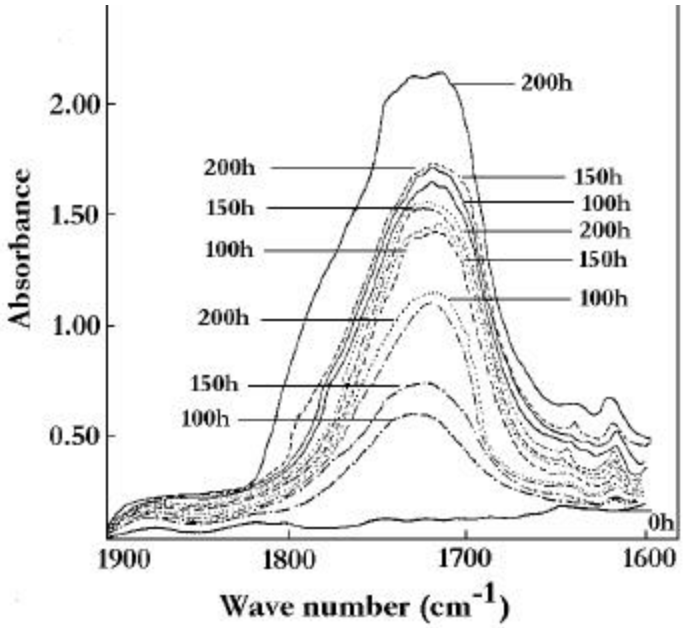

Figure 7.16 FTIR spectral changes in the hydroxyl region for various hours irradiated ATV-prene (–? –), ENICHEM (--•--), SHELL (–¦–), and ATV-oil (–••--) in presence of 0.3 wt % each of BHT(—), Irgafos TNPP (-----), Tinuvin P (•••••) and 0.32 wt % of grafted PMPA (--•--•--).

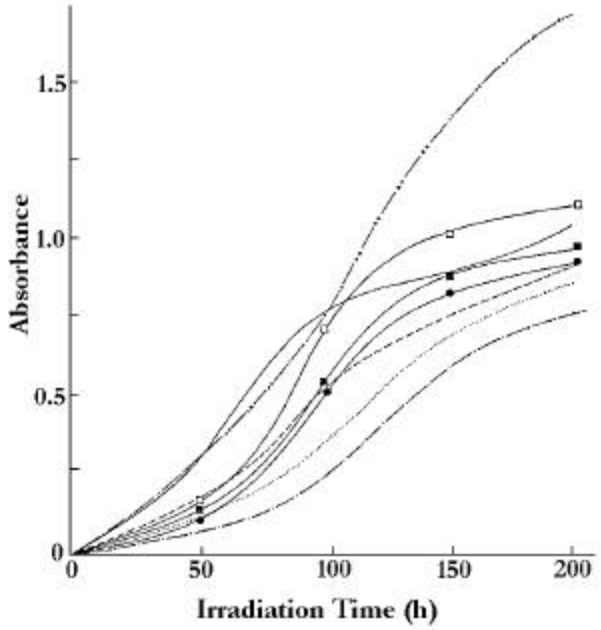

Figure 7.17 FTIR spectral changes in the hydroxyl region for various hours irradiated ATV-prene (–? –), ENICHEM (--•--), SHELL (–¦–), and ATV-oil (–•·--) in presence of 0.3 wt % each of BHT(—), Irgafos TNPP (-----), Tinuvin P (•••••), and 0.32 wt % of grafted PMPA (–•--•–).

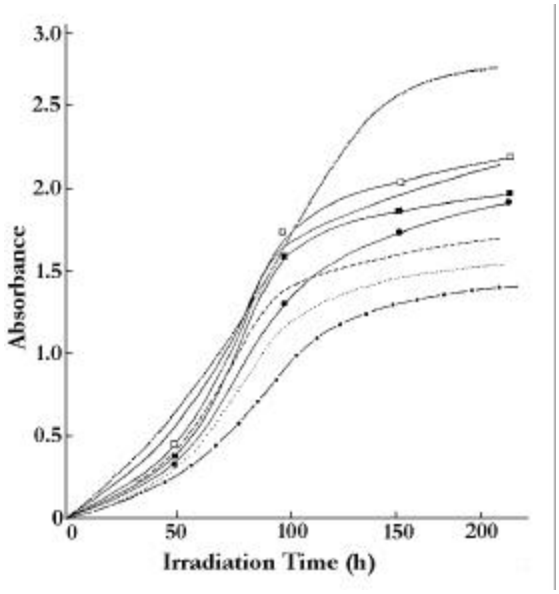

Figure 7.18 ATR-FTIR spectra of **A**) neat LDPE **B)** LDPE-g-PMPA **C)** LDPE-g-MA and **D)** LDPE-g-succinic anhydride-HALS.

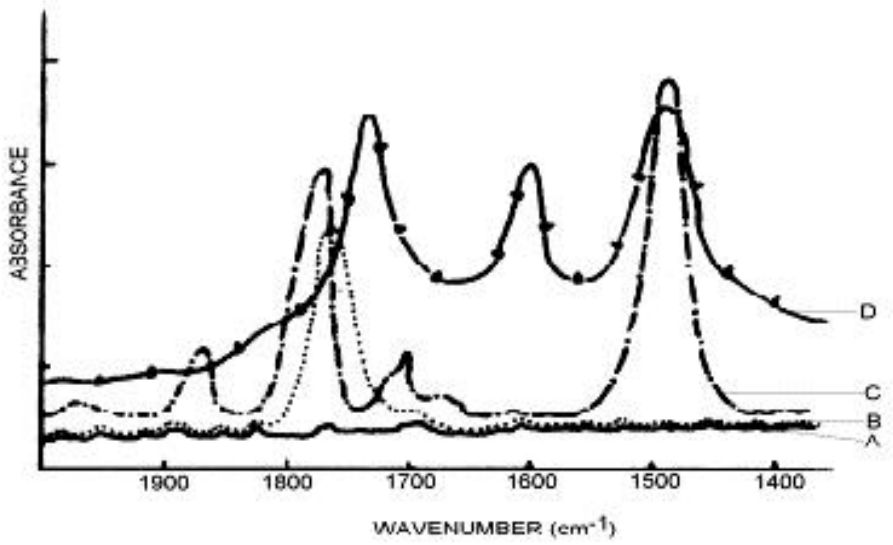

Figure 7.19 Photostabilizing efficiency of surface-grafted HALS in LDPE films. Here (■) is polymer-g-PMPA, (●) is polymer-g-SA-PMPO, (▼) is polymer-blend TMPO and (▲) denotes the unstabilized polymer film.

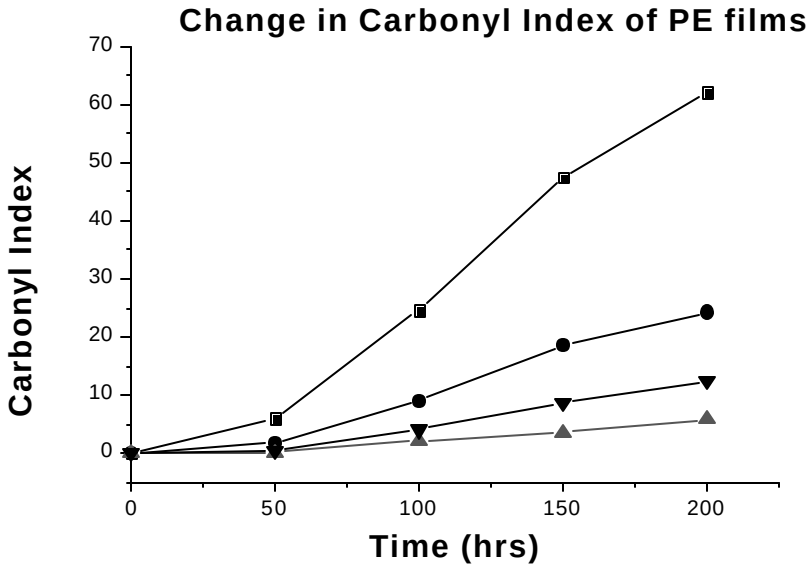

Figure 7.20 Photostabilizing efficiency of surface-grafted HALS in i-PP films. Here (■) is polymer-g-PMPA, (●) is polymer-g-SA-PMPO, (-▼-) is polymer-blend TMPO and (-▲-) denotes the unstabilized polymer film.

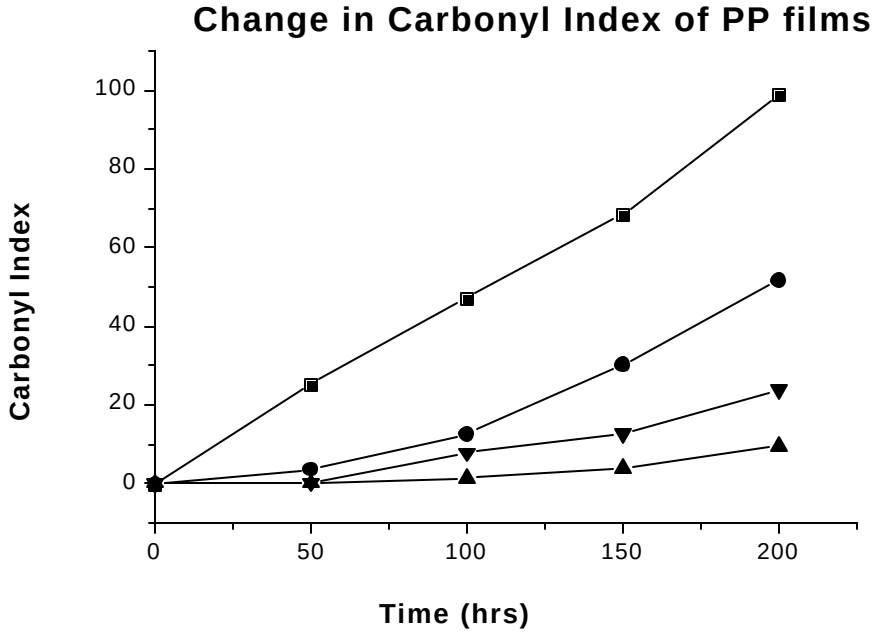

Figure 7.21 FTIR overlay spectra of photo -irradiated LDPE films.

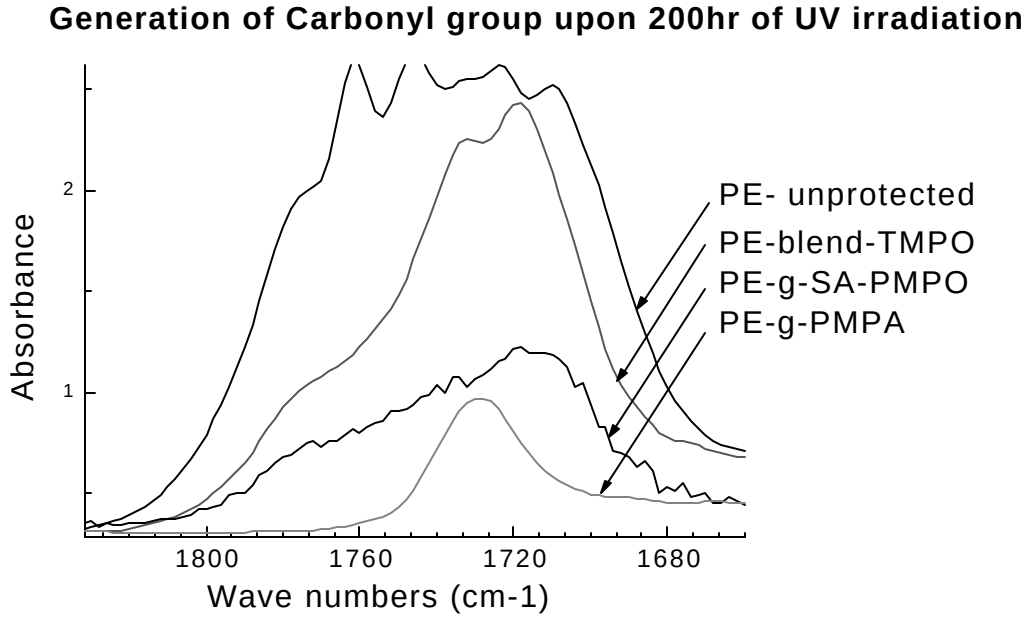

7.4 CONCLUSIONS

Three novel and highly potential photostabilizers have been devised. Upon evaluation of efficiency, hindered amine light stabilizers exhibited better photo-stability compared to the other melt blended conventional stabilizers. Amongst the HALS, polymer bound photo-stabilizers showed extra-ordinary stabilization capacity. Surface grafted PMPA proved to be the best stabilizer amongst all the stabilizers used for the study. This is attributed to the higher concentration of HALS at the degradation site, when directly anchored to the polymer surface. Moreover, PMPA showed excellent stabilization capacity and compatibility for two different classes of polymers studied.

7.5 REFERENCES

1. J. F. Rabek, in *Comprehensive Chemical Kinetics*, Ed. C. H. Bamford and C. F. Tripper, Elsevier, Oxford, Vol. 14, p. 265 (1974).
2. L. R. Dugan, Jr., *Kirk-Othmer Encyclopedia of Chemical Technology*, Wiley-Inter-science, New York, Vol. 2, p. 588 (1963).
3. R. P. Singh, *Prog. Polym. Sci.*, 17, 251 (1992).
4. S. Costanzi, C. Neri, Carlo, WO 2000018833 (2000).
5. T. Konita, H. Watanabe, T. Hayashi, Y. Konishi, S. Kijima, JP 03149287 (1991).
6. D. J. Carlsson, T. Suprunchuk, D. M. Wiles, *J. Appl. Polym. Sci*, **16**, 615, (1972).
7. O. Cicchetti, *Adv. Polym. Sci*., **7**, 70, (1970).
8. H. J. Hiller, *Eur. Polym. J. Suppl*., **105** (1969).
9. J. M. Pena, N. S. Allen, M. Edge, C. M. Liauw, B. Valange, *Polym. Degrad. Stab*., **72**, 259 (2001).
10. A. Onishi, JP 71 38,687 (1971).
11. B. Ranby and J. F. Rabek, *Photodegradation, Photo-oxidation and Photostabilization of Polymers*, Chap10, Interscience, New York, p. 407 (1975).
12. A. V. Prasad, *Photo-oxidative degradation of heterophasic EP copolymers*, Ph. D thesis, University of Pune, India (1999).
13. R. Mani, *A Study of Thermal and Photodegradation and Stabilization of Polyolefins*, Ph. D thesis, University of Pune, India (1994).
14. P. N. Thanki and R. P. Singh US 6284895 (2001).
15. C. Adam, J. Lacoste and G. Dauphin, *Polym. Commn*., **32,** 317 (1991).
16. R. P. Singh, R. Mani, S. Sivaram, J. Lacoste and D. Vaillant, *J. Appl. Polym. Sci*., **50**, 1871 (1993).
17. R. P. Singh, R. A. Raj, A. Vishwa Prasad, S. Sivaram, J. Lacoste and J. Lemaire, *Polym. Intern.*, **36**, 309 (1995).
18. R. V. Gemmer and M.A. Golub, *J. Polym. Chem. Ed*., 16, 2985 (1978).

CHAPTER VIII

SUMMARY AND FUTURE SCOPE

8. 1 SUMMARY AND CONCLUSIONS

The present study was initiated with a primary objective of modifying the surface of elastomers with chemo- and topographical selectivity, without causing any changes in their inherent physio-chemical properties. Although, surface modification of polymers is not a new area of research, elastomers have been very little explored. Our study was mainly focused on the surface modification using photo-grafting and plasma-grafting techniques. The influence of surface modification on the properties of elastomers was deduced from their dyeability, biocompatibility and photo -stability.

From our study, we found that the reactivity of the monomer plays a major role in determining the success of the surface grafting. Monomers with low reactivity either donot get grafted onto the polymer surface or form a non-uniform grafted layer. Amongst the monomers studied, the reactivity of monomers was in the order HEMA > AA > GMA > NVP. Other reaction parameters also have a significant influence on the grafting efficiency. For reactions carried out at room temperature, monomers give thin and uniform grafted layer less than 1 micron. A favorable effect of elevated reaction temperature (i.e. 50 ºC) is observed for low reactivity monomers like NVP whereas highly reactive monomers like HEMA form thick grafted layer of approximately 5 microns. For surface grafting carried out using reactive monomers and at elevated temperature subsequent homopolymerization also takes place, which is the primary shortcoming of photografting technique. By using the multi functional acrylates, homopolymer formation is substantially reduced. The multifunctional acrylate (MFA) works on the principle of chain transfer from the growing grafted chain. The reaction solvent also determines the success of surface grafting. Solvents with high chain transfer constant are not suitable to achieve good grafting efficacy. Acetone for this purpose is the most suitable solvent. Interestingly, we found that additions of a small amount of H-donating solvent, toluene in our case, significantly reduced the homopolymerization and facilitated efficient surface grafting. One of the most influencing factor is the choice of photoinitiator. From our study we found that ketonic H-abstracting photoinitiators are better than the photo -fragmentation type initiators. The main reason is that the photo-fragmentation type initiator is incapable of generating a free-radical on the polymer backbone and leads to homopolymerization. Amongst the photoinitiators examined, the efficacy observed was XT > BP > Bz > BPO > AIBN. The degree of grafting also increased linearly with the increase in the reaction time. However, it attained a plateau after a critical point, beyond which we assume that the reactions like radical coupling, chain transfer and homopolymerization play a

detrimental role. In the present study we have developed an elegant technique for the preparation of NR thin films.

The other technique that was utilized for achieving our aim was plasma induced surface modification. Here, the surfaces of the elastomers were modified by plasma treatment and plasma induced grafting. Oxygen and carbon dioxide were used for this purpose. It was found that the oxygen plasma treated films predominantly generated hydroxy/ hydroperoxy groups on the films surface whereas the carbon dioxide plasma treated films yields carbonyl and carboxyl species on the modified surfaces. The plasma treatment conditions and reaction parameters greatly influence the degree of surface modification. The substrates studied are PP, PE, EPDM, SBS and SR. In this study, PP and PE were taken up to compare the results with the EPDM and to understand the influence of each component on the surface properties and underlying mechanisms. It was found that the hydrophilicity of the plasma treated films increased with the increase in the plasma power and plasma treatment time. However, treatment at high plasma power i.e. above 75 W and treatment time above 150 sec causes a loss in the attained hydrophilicity. This loss is known as the hydrophobic recovery. Some of the causes of hydrophobic recovery are surface etching, surface cross-linking, chain scission and dangling hydrocarbon chains and formation of a layer of non-volatile oligomers. The functional groups generated under mild plasma treatment conditions are either lost or screened by any of the above-mentioned effects. Moreover, it is also observed the functionality attained at the air polymer interface is lost with the storage time. The migration of the functional groups is due to the nature of the polymer surface to attain minimum surface free-energy. The orientation of the functional groups towards the subsurface is very fast in elastomers. This is attributed to the high mobility of the elastomer chains and inter-chain free volume. Moreover, upon hydrating the elastomer surface, the lost hydrophilicity is readily retained. Thus this orientation and reorientation process is very fast in the elastomers. From our study, we learnt that the presence of surface cross-links hinders the migration/orientation of the functional groups. We utilized this demerit of cross-linked surfaces to achieve long-term hydrophilic surfaces by deliberately cross-linking functional monomers with functional cross-linkers onto the surface of EPDM films under the influence of oxygen plasma. The results are encouraging and supporting the assumption.

The application of the modified surfaces was determined by performing the biocompatibility tests. It is found that the surface hydrophilicity and functionality plays a prime role in determining the biocompatibility of the polymer films. The type of functional groups implanted also determines the success of the material. The rapid reorientation of the

functional groups back to the interface also influences the cell adhesion in the elastomeric films. In the present study we have also synthesized some novel vinylic stabilizers and evaluated their photostability against conventional melt blended stabilizers by grafting them onto the surface of PP, PE and SBS films. It was found the PMPA, a vinylic HALS, performs best when located at the surface of polymer film. The reason is that degradation of any polymer initiates from the surface and proceeds into the matrix. Photostabilizer, when located at the surface, effectively retards the degradation process. Thus, it gives the best stabilization. It is well known that polymers with hydrocarbon backbone are highly hydrophobic and difficult to stain but we could attain a very good dyeability of these polymer surfaces after surface modification. Thus, our work focuses on both fundamental and applied aspects of surface chemistry.

8.2 FUTURE SCOPE

Looking at the present scenario, it would be right to say that polymers have become an irresistible element of human life. With the emerging novel applications of the polymers their importance in our society is continuously increasing. Though, there is a wide scope for the synthesis of new polymers, scientists today are looking forward to develop novel applications of the existing polymers. In this situation, the properties of polymer surface play a vital role. By tailoring the desired properties of the polymer surface, it would be possible to develop a wide range of applications of the existing polymers. However, an in depth knowledge of the polymer and its surface associated processes is required to bring about these changes. The progress in the field of surface modification and characterization shall lead to the development of next generation materials like micro-electronic devices and biomimetic systems.

SYNOPSIS

The thesis entitled **Surface Modification of Diene Elastomers via Radiation Grafting of Functional Monomers** is divided into eight chapters

Polymers are important commercial materials and constitute one of the fast moving frontiers of daily life. Polymers enjoy their importance in a wide range of applications conventionally from packaging, protective coatings, adhesion, friction & wear, composites, home-appliances, to the most recent ones in bio-materials, micro-electronic devices, high performance membranes etc. Although, polymers have excellent bulk physical/chemical properties, are inexpensive and easy to process, yet they do not gain any considerable importance as commercial specialty products due to their inert surface. Thus, special surface properties which polymers do not possess, such as functionality, chemical resistance, hydrophilicity, roughness, lubricity, selective permeability, conductivity, biocompatibility are required for their success as specialty materials[1-4].

Surface properties are of especial concern because the interaction of any polymer with its environment mainly occurs at the surface. Since it is almost impossible to synthesize polymers with distinct bulk and surface properties, tailoring of these properties using surface modification[5,6] techniques have become an important tool to convert the inexpensive polymers into valuable commercial products. The need for developing engineered interfaces is underscored by the above mentioned prerequisites of surface properties.

Many researchers have attempted to tailor the surface properties of various polymers using traditional and existing surface modification techniques[7]. However, there are only a few reports on the surface modification of elastomers viz. ethylene propylene diene elastomer[8], natural rubber[9], styrene butadiene styrene[10] and silicon rubber[11] using plasma- and photo-induced modification techniques. Advances have been made in recent years to render chemical and morphological properties of surface in a desired way with negligible change in the polymer bulk properties. Many recent studies[12] in the field of polymers have emphasized the need of material compatibility in the multiphase systems to provide new materials with improved properties. Surface modified polypropylene, polyethylene, polystyrene, polytetrafluoroethylene and polyether sulphone have long been studied as biocompatible materials[13,14], however, a little attention has been paid on the development of elastomeric biomaterials[15,16] . Elastomers are far pertinent candidates as biomaterials due to their inherent

flexibility and freedom of design. The surface modified elastomers are therefore, prospective biomaterials for a range of applications yet unimagined viz. soft cartilages, artificial nerves, blood vessels, diaphragms, flexi-valves etc. The modification of the polymer surface is thus proposed depending upon the type of its application.

The following changes at the polymer surface have been used to enhance the surface properties:

- Generation of special functional groups at the surface, which can be used for secondary functionalization.
- Increase the surface free energy of polymers.
- Increase hydrophilicity thereby improving dyeability and paintability.
- Improve adhesion of cells and microorganisms to obtain bio - functional surfaces.
- Improve the chemical and wear resistance.

The conventional methods[7] of surface modification viz. flame treatment, high-energy radiation, corona treatment, chemical etching and so lution grafting often suffer from different shortcomings, making them trivial. In recent years, a variety of technologies have been proposed for improving surface properties of polymers, amongst these; surface-initiated grafting is a rather new technology, which offers versatile means for providing existing polymers with desired surface properties. Photochemical[17] and plasma-grafting[18] are the most efficient methods of surface modification, being studied for last one and a half-decade, yet they have not been thoroughly explored. Since, a polymer tends to react distinctly with each surface modification technique, it leaves a wide scope for in-depth explorations and novel applications.

Objectives of the present study

The objectives of present study are:

1. To carryout surface modification of ethylene propylene diene elastomer (EPDM) and natural rubber (NR) thin films via plasma- and photo- induced grafting of different functional biomonomers and to explain the effect of various reaction parameters on the grafting efficiency and their biocompatibility.
2. To achieve surface hydrophilicity of EPDM, styrene butadiene styrene (SBS), silicone rubber (SR) thin films by implanting different functional entities using oxygen and carbon dioxide plasma irradiation and to explain the underlying mechanism.

3. To understand the surface dynamics involving the migration of different functional groups generated upon plasma irradiation.
4. The correlate and explain the changes in the morphology of the grafted films rendered by different grafting techniques.
5. To apply the knowledge of surface modification to the development of biocompatible elastomeric substrates.
6. Synthesis and performance evaluation of novel photo-stabilizers involving surface photo-grating.

Outline of the thesis

Chapter I

This introductory chapter explores with a discussion of various types of surface modification techniques for polymeric substrates. This chapter meticulously delivers a comprehensive literature incorporating the significant work done by prominent scientists in this area. The general background on the mechanisms of photo-grafting and plasma-induced surface modification has also been discussed. The existing and emerging applications of this work are also presented.

Chapter II

The objective and scope of the present investigation are described in this chapter.

Chapter III

This chapter deals with the surface modification of ethylene propylene diene elastomer thin films via plasma- and photo- induced grafting of different functional biomonomers. The effect of various reaction parameters is also discussed in details. The functional groups generated on the film surface upon grafting are evaluated using ATR-FTIR and ESCA spectroscopic techniques. The surface hydrophilicity is determined by water contact angle measurements and staining technique. The surface morphology/topography of the modified surfaces are investigated using microscopic imaging techniques. The thickness of the grafted layers is determined using optical microscopy. The biocompatibility of the grafted surfaces is also determined.

Chapter IV

This chapter discusses the results of plasma induced surface modification of EPDM using implantation technique. The two gases used for this purpose are oxygen and carbon dioxide. The effects of different reaction parameters viz. grafting time, plasma power and post exposure are evaluated and a suitable explanation has been put forward. A comparative study of EPDM with PP and PE substrates has also been carried to understand the role of back-bone chemistry. The biocompatibility of the modified surfaces is determined from the human cell adhesion tests.

Chapter V

This chapter presents the results of surface modification of natural rubber thin films via photo- and plasma-induced grafting of different functional biomonomers. The effect of various reaction parameters is also discussed in details. The functional groups generated on the film surface upon grafting are evaluated using ATR-FTIR spectroscopy. The surface hydrophilicity is determined by water contact angle measurements and staining techniques. The surface morphology and topography of the modified surfaces are investigated using microscopic imaging techniques. The thickness of the grafted layers is determined using optical microscopy. The biocompatibility of the grafted surfaces is also determined.

Chapter VI

Plasma-induced surface modification of two more elastomers viz. Styrene butadiene styrene and silicon rubber has also been studied. The effects of different reaction parameters viz. grafting time, plasma power and post exposure on the surface functionalization are explained with justification. The functional groups generated on the film surface upon grafting are evaluated using ATR-FTIR and ESCA spectroscopic techniques. The surface morphology/topography of the modified surfaces is investigated using microscopic imaging techniques. The surface hydrophilicity is determined by water contact angle measurements. The biocompatibility of the modified surfaces is determined from the human cell adhesion tests.

Chapter VII

This chapter deals with the synthesis of novel photo-stabilizers, namely 1,2,2,6,6-pentamethylpiperidinyl-4-acrylate (PMPA) and 2-[2'-hydroxy-5'-methyleneoxy((1", 2", 2", 6", 6"-pentamethyl –4"- piperidinyl) phenyl)]benzotriazole. These molecules are characterized using FTIR, NMR and GC techniques. Most of the polymers are susceptible to degradation by oxygen under an additional influence of UV light or heat. This consequent

oxidative-degradation can be partially prevented by melt blending the polymers with appropriate stabilizers. Low molecular weight stabilizers being mobile are easily lost from the polymer through evaporation, migration and extraction. Since the degradation of a polymer commences from the surface and slowly proceeds into the bulk of the polymeric substrate, the stabilizers are therefore expected to be most potent if they are anchored at the surface. Keeping this in view, PMPA is photo-grafted onto the surface of PE, PP and SBS films. The efficacy of this photo-stabilizer is tested against commercially available photostabilizers.

Chapter VIII

This chapter summarizes the results and describes the salient conclusions of the study. Additional thoughts for further research are also expressed.

APPENDIX - I

The studies on surface initiated grafting via atom transfer radical polymerization and surface grafting facilitated by cross-linkers is in progress.

REFERENCES

1. M. Suzuki, A. Kishida, H. Iwata and Y. Ikada, *Macromolecules*, **19**, 1804 (1986).
2. H. Iwata and T. Matsuda, *J. Membrane Sci*., **38**, 185 (1988).
3. H. Kubota and A. Sugiura, *Polym. Inter.* **34**, 313 (1994).
4. A. M. Mayes, D. J. Irvine and L. G. Griffith, *Mater. Res. Soc. Symp. Proc*., **530**, 73 (1998).
5. Isao Noda, *Nature*, **350**, 143 (1991).
6. Y. Ikada, *Adv. Polym. Sci*., **137**, 1 (1998).
7. Chan C M , *Polym.* Surf. Modification & Characterization, Hanser Publishers (1994).
8. R. P. Burford, *Rad. Phy. Chem*., **41**, 507 (1993).
9. M. T. Razzak, K. Otsuhata, Y. Tabata, F. Ohashi and A. Takeuchi, J. Appl. Polym. Sci, **36**, 645 (1988).
10. R. P. Singh, S. M. Desai, S. S. Solanky and P.N. Thanki, J. Appl. Polym. Sci., **75**,1103 (2000).
11. A. Chapiro, *Eur. Poly. J*., **19**, 859 (1983).
12. S. M. Desai and R. P. Singh, Adv. Polym. Sci., (accepted 2001).
13. N. Angelova and D. Hunkeler, *Tibtech*, **17**, 409 (1999).
14. R. N. Satuffer, *J. Bone Joint Surg*., **64A**, 983 (1982).
15. K. M. Defife, M. S. Shive, K. M. Hagen, D. L. Clapper, J. M. Anderson, *J. Biomed. Mater. Res.*, **44**, 298(1999).
16. D. J, Chauvel-Lebert, P. Pellen-Mussi, P. Auroy and M. Bonnaure-Mallet, *Biomaterials*, **20**, 291 (1999).

17. Y. Ogiwara, H. Kubota and Y. Hata, *J. Poly. Sci. Poly. Lett. Ed., J. Polym. Sci., Polym. Lett. Ed.,* **23**, 365 (1985).

18. N. Inagaki, *Plasma Surface Modification and Plasma Polymerization*, Technomic Publishing Company Inc. USA (1996).

LIST OF PUBLICATIONS

1. R. P. Singh, S. M. Desai, S. S. Solanky and P. N. Thanki, "Photo-oxidation and Stabilization of Styrene-Butadiene-Styrene Rubber", *J. Appl. Polym. Sci.,* **75**, 1103 (2000).
2. S. M. Desai, J. K. Pandey and R. P. Singh, "A novel additive for Polyolefins photostabilization: Hindered Amine Light Stabilizer", *Macromol. Symp. Ser.* **169**, 121 (2001)
3. R. P. Singh, P. N. Thanki, S. S. Solanky and S. M. Desai, Photodegradation and Stabilization of Polymers in a book entitled "*Advanced Functional Molecules and Polymers*", Vol.**4,** pg 1-55 (2001) *Gordon and Breach Science Publishers,* Tokyo, Japan.
4. R.P. Singh, S. M. Desai, S. Sivaram and K. Kishore "A Novel Synthesis of Polystyrene peroxide with controlled peroxy linkages at room temperature (*Macromol. Chem. Phy.* accepted March 2002)
5. S. M. Desai and R. P. Singh, Surface Modification of Polyethylene, *Advances in Polymer Science, Springer Verlag Pub.,* Chap. **9** (accepted, March 2002).
6. R. P. Singh, S. M. Desai and G. Pathak, Thermal Decomposition kinetics of the photo-oxidized Nylon 66 (*J. Appl. Polym. Sci*., accepted April 2002)
7. S. M. Desai, D. Bodas, M. Patole and R. P. Singh, Tailor made functional surfaces: elastomers as potential biomaterials-I. (comm. to *Biomaterials*, Dec. 2001)
8. R. P. Singh, S. M. Desai, J. K. Pandey, S. S. Solanky, A. N. Patwa, Synthesis of new polymeric hindered amine light stabilizers: Performance evaluation in styrenic polymers (comm. *J. Polym. Sci., Polym. Chem.,* June 2002)
9. S. M. Desai D. Bodas, M. Patole, K. R. Patil and R. P. Singh, "Effect of surface dynamics on the efficiency of biomaterials: elastomers as potential biomaterials-II (under preparation)
10. S. M. Desai, D. Bodas, A. Siankar and R. P. Singh, Comparison of surface-grafting efficiencies of biomonomers onto EPDM and NR: elastomers as potential biomaterials-III (under preparation)
11. S. M. Desai, S. S. Solanky, A. B. Mandale and R. P. Singh, Controlled grafting of AA brushes onto i-PP Films via surface initiated ATRP (under preparation).

LIST OF PATENTS

1. Process for the preparation of novel vinylic hindered amine light stabilizer (filed **US Patent**, CSIR Ref No. NF-22/2001).
2. Novel Photo-stabilizer: A HALS coupled to an UV absorber (**PCT-Patent,** CSIR Ref. No. NF-291/2001).
3. Novel intermediates in the preparation of Photo-stabilizer: A HALS coupled to an UV absorber (**US Patent,** CSIR Ref. No. NF-291/2001).
4. Process for the preparation of Novel Photo-stabilizer: A HALS coupled to an UV absorber (**US Patent,** CSIR Ref. No. NF-291/2001).
5. Diol functionalized antioxidant (to be filed).